Acta Morphologica Hungarica

VOLUME 36, NUMBERS 1–2, 1988

Akadémiai Kiadó, Budapest

ACTA MORPH. HUNG. HU ISSN 0236–5391

ACTA MORPHOLOGICA
HUNGARICA
A QUARTERLY OF THE HUNGARIAN ACADEMY OF SCIENCES

Acta Morphologica publishes original papers on experimental morphology and pathology in English.

Acta Morphologica is published in yearly volumes of four issues by

AKADÉMIAI KIADÓ
Publishing House of the Hungarian Academy of Sciences
H-1054 Budapest, Alkotmány u. 21.

Manuscripts and editorial correspondence should be addressed to

Acta Morphologica
Ist Institute of Pathology and Experimental Cancer Research, Semmelweis Medical University,
1085 Budapest, Üllői út 26, Hungary

Subscription information

Orders should be addressed to

KULTURA Foreign Trading Company
H-1389 Budapest P.O. Box 149

or to its representatives abroad

Acta Morphologica Hungarica is abstracted/indexed in Biological Abstracts, Chemical Abstracts, Chemie-Information, Current Contents–Life Sciences, Excerpta Medica, database (EMBASE), Gerontological Abstracts, Index Medicus

Acta Morphologica

Hungarica

INDEX

Volume 36

Akadémiai Kiadó, Budapest
1988

ACTA MORPHOLOGICA

NUMBER 36

CONTENTS

AUTHOR INDEX

S

T

V

CONTENTS

Normal and Experimental Morphology

Pathology

Acta Morphologica Hungarica, 36 (1–2), pp. 3–6 (1988)

SEX CORD NESTS WITH ANNULAR TUBULES THE INCIDENCE OF IDENTIFYING THEM IN NORMAL OVARIES

G. S. Delides, J. Elemenoglou, G. Garas

DEPARTMENT OF PATHOLOGY, METAXA'S MEMORIAL CANCER INSTITUTE PIRAEUS, GREECE

(Received 16 May 1987)

Sections from 588 ovaries removed during various operations and reported as being within normal size limits were reviewed. In seven cases structures with the characteristic appearances of sex cord "tumours" with annular tubules (SCTAT) were found.

We called the lesions sex cord nests with annular tubules (SCNAT). Their mean diameter was 0.17 mm.

If ovaries were cut in serial sections the probabilities of identifying such lesions should increase very much.

Keywords: Sex cord tumours, sex cord nests in ovaries

Introduction

Sex cord tumour with annular tubules (SCTAT) is a rare ovarian neoplasm with distinctive appearance described by Scully in 1970 [8].

He reported 13 cases and 16 further examples have been reported since then [1–10]. Of interest (as in the case of other ovarian tumours) is the association of the above tumour to Peutz–Jeghers syndrome [9].

A small SCTAT found incidentally in an ovary removed during hysterectomy for fibroids, drew our interest to the possible excistence of "occult" SCTAT that could not have been noticed in routine work.

Materials and methods

The sections from ovaries removed during 358 operations performed for various reasons during the period 1976–1980 were reviewed.

Ovariectomy was unilateral in 128 cases and bilateral in the rest. The patient's age ranged from 32 to 67 years. Ovaries of older women were not included in the study.

In nearly all these cases the ovaries were reported as being within normal size limits. In the cases in which a lesion was found, additional sections from the paraffin blocks were also examined. The SCTAT found incidentally was included in the study (Case 1). The diameter of the lesions was measured with the use of an eyepiece with a micrometer graticule.

Send offprint requests to: G. S. Delides, Department of Pathology, Diagnostic and Therapeutic Institute of Piraeus Metaxa's Memorial Cancer Institute, 51 Botassi Str. Piraeus 30, Greece

Results

The incidentally found tumour was 1.2 cm in diameter, yellowish in colour and solid in consistency. Seven additional lesions composed of one or two structures resembling SCTAT nests were found. The mean diameter of those lesions was 1.7 $\pm$ 0.07 mm (SD).

In all cases rounded nests of epithelial cells with abundant vacuolated cytoplasm and spheric nuclei with a single nucleolus were present. There was no nuclear atypia and no mitotic figures were observed. The epithelial cells were arranged in single tubules or in complex networks that contained acidophilic hyaline bodies single or coalescent (Figs 1 and 2).

The diameter of the lesions, the reason of operation and the number of nests found, are shown in Table I. No one of the patients including Case 1 presented the Peutz–Jeghers syndrome.

Discussion

With the exception of our first case the lesions which were found in our material cannot be characterized as "tumours" and we would prefer the term "Sex cord nests with annular tubules" (SCNAT). The appearance of those single nests are not in any way different from the "nests" observed within the tumour of Case 1 or from those described in previous papers.

The incidence of SCTAT is reported to be very low. Gloor found four cases in a review of ovarian tumours among 560 000 biopsies examined during 40 years in the Institute of Pathology of the University of Lausanne [4]. In the same period in the above Institute 47 granulosa cell and 8 Sertoli and/or Leydig cell tumours were observed.

In the period 1976–1980 approx. 20 000 surgical specimens were examined in the Dept. of Pathology of "Metaxa's Memorial Cancer Institute". Among

Table I

Reason of operation, number of nests and diameter of lesions

Case	Age	Operation	Number of nests	Diameter of lesions (mm)
1 (tumour)	38	Uterine fibroids	Large number	12 (tumour diamet.)
2	45	Breast cancer-ovariectomy	1	0.26
3	36	Breast cancer-ovariectomy	1	0.24
4	49	Uterine fibroids	1	0.2
5	48	Breast cancer-ovariectomy	2	0.14–0.12
6	48	Breast cancer-ovariectomy	1	0.1
7	51	Uterine fibroids	1	0.1
8	39	Uterine fibroid-adenomyosis	1	0.26

Mean diameter of lesions $\pm$ S.D.: 0.17 $\pm$ 0.07

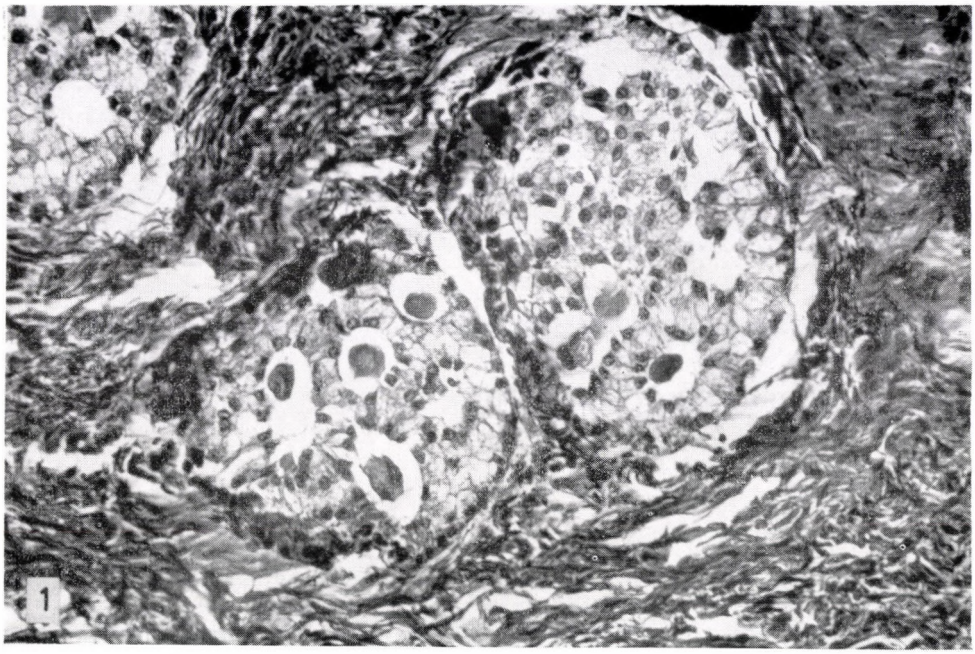

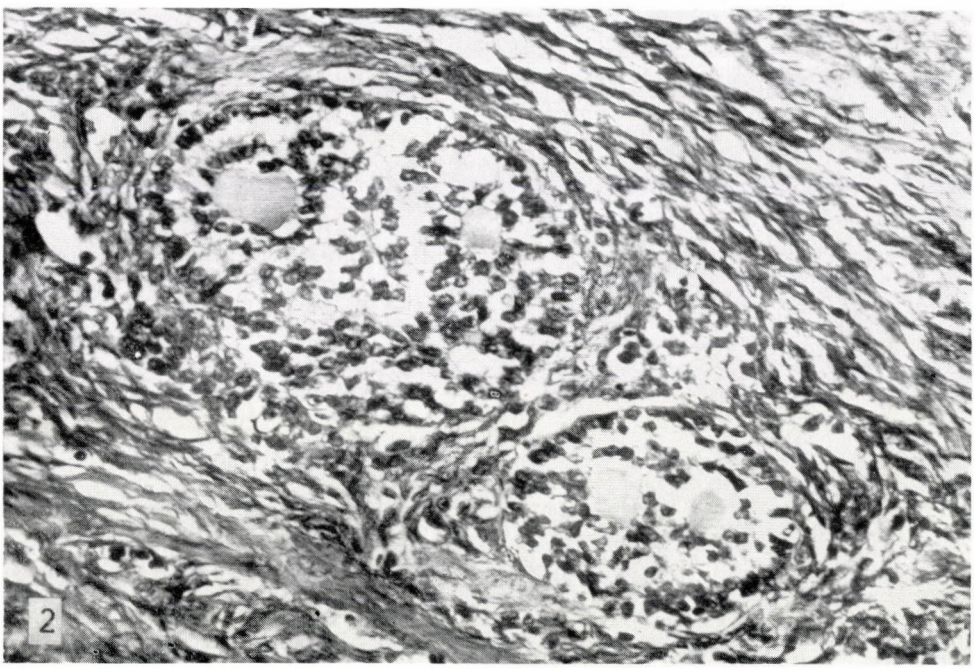

Fig. 1. Case 1. Sex cord tumour with annular tubules HE ×160
Fig. 2. Case 5. Two sex cord "nests" within the ovarian cortex HE ×100

those 8 were granulosa cell tumours, 1 Sertoli and 1 SCTAT (Case 1). The seven SCNAT found in the 588 ovaries reported as normal, give an incidence of 1.19% of this lesion.

Identification of SCNAT with a diameter of approximately 0.2 mm within a routinely sectioned ovary appears to be a matter of chance. If the ovaries were cut in serial sections the probability of identifying the lesion should increase and the incidence of the lesion should be much higher than that estimated.

The origin of SCTAT is a matter of discussion. Both a granulosa cell and a Sertoli cell origin are under consideration [1, 4].

To us it appears probable that SCTAT have their origin in SCNAT like those we described. If we accept these lesions as potential tumours then SCTAT is not so rare and a granulosa cell origin would be more probable. In our series ages ranged from 32 to 67 years but SCTAT have been described in children (1) and if SCTAT have their origin in SCNAT one should expect the nests to exist in young ages.

Differentiation of SCNAT from parts of follicles with Call Exner bodies especially if calcifications are not present is of a real difficulty. Apart of the appearances of the nest the absence of theca cells surrounding them appears to be the main criterion.

All the examined ovaries were reported as within "normal" size-limits and it seems possible that the lesion had been overlooked or characterized as part of follicles. A further research on the frequency of SCNAT in normal ovaries will be perhaps of value for the study of the histogenesis of SCTAT.

REFERENCES

1. Anderson MC, Govan ADT, Langley FA, Woodcock AS, Tyagi SP: Ovarian sex cord tumors with annular tubules. Histopath 4: 137, 1980
2. Costa J: Peutz-Jeghers syndrome. Case presentation. Obst Gynecol 50: 158, 1977
3. Gloor E: Un cas de syndrome de Peutz-Jeghers associe à un carcinome mammaire bilateral à un adenocarcinome du col uterine à des tumeurs des cordons sexuels à tubules anneles bilaterales dans le ovaries. Schweiz Med Wochenschr 108: 717, 1978
4. Gloor E: Ovarian sex cord tumor with annular tubules. Clinicopathological report of two benign and one malignant cases with long follow-ups. Virchows Arch (Path Anat) 384: 185, 1979
5. Hertel BG, Kempson RL: Ovarian sex cord tumors with annular tubules an ultrastructural study. Am J Surg Pathol I: 145, 1977
6. Netter LA, Yaneva A, Coudonel S, Netter A, Allaneaus C, Seringe P: Tumeur ovarianne et syndrome de Peutz-Jeghers. Un nouveau cas feminin de tumeur malformative des cordons sexuels. Ann Med Interne 124: 187, 1973
7. Riley E and Michael S: A family with Peutz-Jeghers syndrome and bilateral breast cancer. Cancer 15: 815, 1980
8. Scully RE: Sex cord tumor with annular tubules a distinctive ovarian tumor of the Peutz-Jeghers syndrome. Cancer 25: 1107, 1970
9. Steenstrup EK: Ovarian tumors and Peutz-Jeghers syndrome. Acta Obst Gynecol Scand 51: 237, 1972
10. Waisman J, Lischke HJ, Mwasi LM, Dignam WJ: The ultrastructure of a feminizing granulosa-theca tumor. Am J Obst Gynecol 123: 147, 1975

Acta Morphologica Hungarica, 36 (1–2), pp. 7–14 (1988)

COMPETITIVE MECHANISMS OF BASIC PEPTIDES INDUCING TRANSGANGLIONIC DEGENERATIVE ATROPHY*

J. TAJTI[1], B. PENKE[2], K. KOVÁCS[2], B. CSILLIK[1]

[1] DEPARTMENT OF ANATOMY AND [2] DEPARTMENT OF MEDICAL CHEMISTRY, SZENT-GYÖRGYI ALBERT MEDICAL UNIVERSITY, SZEGED, HUNGARY

(Received 17 March 1987)

In addition to the classical microtubule inhibitors (antimitotic agents), transganglionic degenerative atrophy of central terminals of primary sensory neurons can be induced also by means of applying to a peripheral nerve basic polypeptides (Polymyxin B and Colimycin) and two basic derivatives of glutamic acid that do not exert any microtubule inhibition. This effect is independent of other pharmacological effects (histamine liberation, Ca^{2+}-binding, etc.) of the applied compounds, and probably it is based on a competitive reaction with nerve growth factor.

Keywords: Spinal cord, degeneration nerve growth factor

Introduction

Primary nociceptive neurons are under a special transganglionic control. The most obvious sign of this transganglionic regulation is that following the transection of a peripheral sensory axon, transganglionic degenerative atrophy (TDA) ensues in the dorsal horn of the spinal cord [3]. It was shown in our earlier studies [1] that the blockade of the retrograde axoplasmic transport is responsible for TDA. It was proved by Csillik et al. [2, 5] that retrograde transport of Levi–Montalcini's nerve growth factor (NGF) plays an outstanding role in the maintenance of the structure and function of the central terminals of primary sensory neurons. In our present studies, TDA was induced by non-antimitotic polypeptide antibiotics (lacking any anti-microtubular activity) and by basic glutamic acid derivatives, which seem to interact with NGF.

Materials and methods

Investigations were performed on 51 young adult CFY rats of both sexes, 220–250 g body weight. In Nembutal anaesthesia, the left sciatic nerve was exposed and surrounded by a Gelaspon (Jenapharm) cuff (Fig. 1), soaked previously in one of the following compounds:

* Supported by Research Grants No. 527 from the Hungarian Ministry of Health and No. 05-065 from the Hungarian Academy of Sciences

[2] Send offprint requests to: Prof. Dr. B. Csillik, Department of Anatomy, 6701 Szeged, P.O. Box 512, Hungary

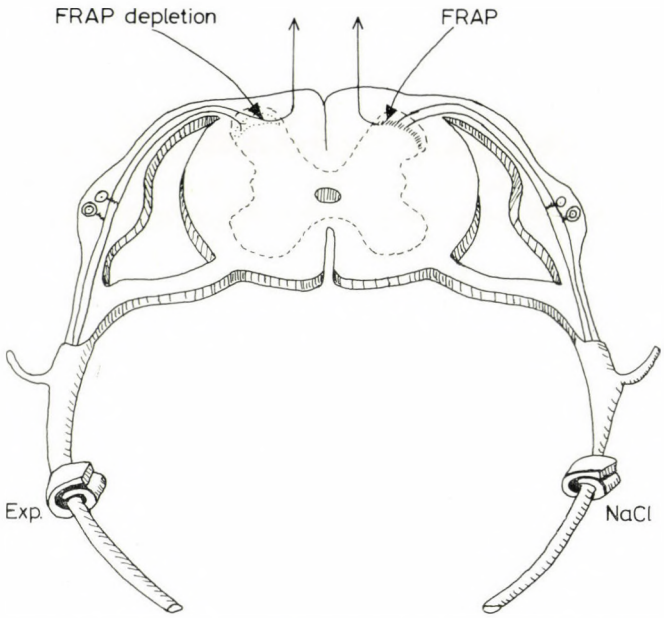

Fig. 1. Diagram of the experimental paradigm for studying the TDA-inducing effect of the investigated compounds. The sciatic nerve is surrounded by a Gelaspon cuff soaked in the experimental substance (exp) for 30 min; on the contralateral sciatic nerves a cuff soaked in physiological saline solution is applied for 30 min. After 14 days, FRAP activity of the Rolando substance is studied by histochemical methods in serial frozen sections; the sciatic nerve was studied in non-stained teased samples

Polymyxin B sulphate® (Pfizer),Colimycin sulphate® (Bellon), 48/80® (Sigma), Peremin® (Chinoin), H-Lys-OHxH_2SO_4, BOC-GLU-EDA, TFAxH-Glu-EDA-FMOC(Figs 2a, b, c and d). The contralateral sciatic nerve was surrounded by a cuff soaked in isotonic saline solution. Concentrations of the substances applied to our biological test system are summarized in Table I.

After 30 min, the cuffs were removed and the wounds closed. The animals were allowed to survive for 14 days; thereafter, in Nembutal anaesthesia, the rats were killed by the transcardial perfusion with a formaldehyde-glutaraldehyde solution [13]. After fixation, both sciatic nerves and the lumbosacral spinal cord were removed, and post-fixed for 36 h in the same fixative at +4 °C. The sciatic nerves were studied in teased samples after free-hand dissection under a Zeiss stereomicroscope, without any staining. The spinal cord was studied in serial frozen sections stained for acid phosphatase according to a modified Gömöri technique [8].

Results

Local perineural application of 1% Polymyxin B sulphate or 1% Colimycin sulphate induced TDA, which, at the light microscopic level is clearly indicated by the depletion of the extralysosomal fluoride resistant acid phosphatase (FRAP), i.e. the marker enzyme of the primary nociceptive neurons, from the central sensory axon terminals in Rexed's lamina II in the upper spinal dorsal horn (Fig. 3).

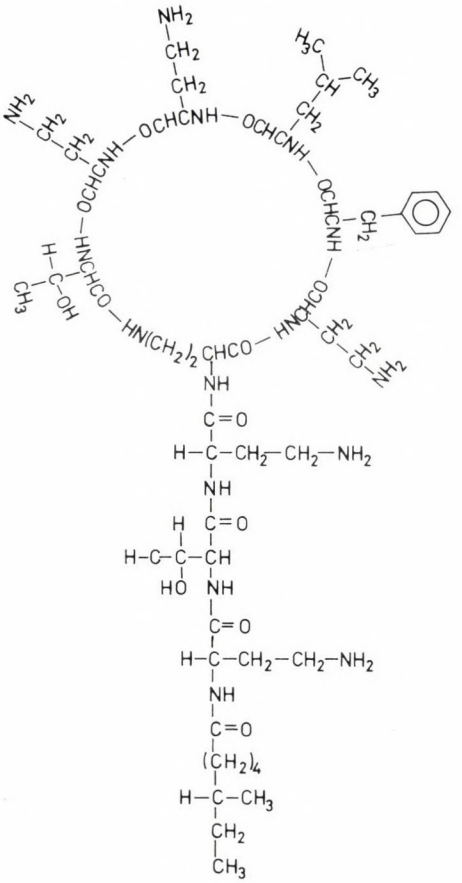

Polymyxin B_1

Fig. 2a

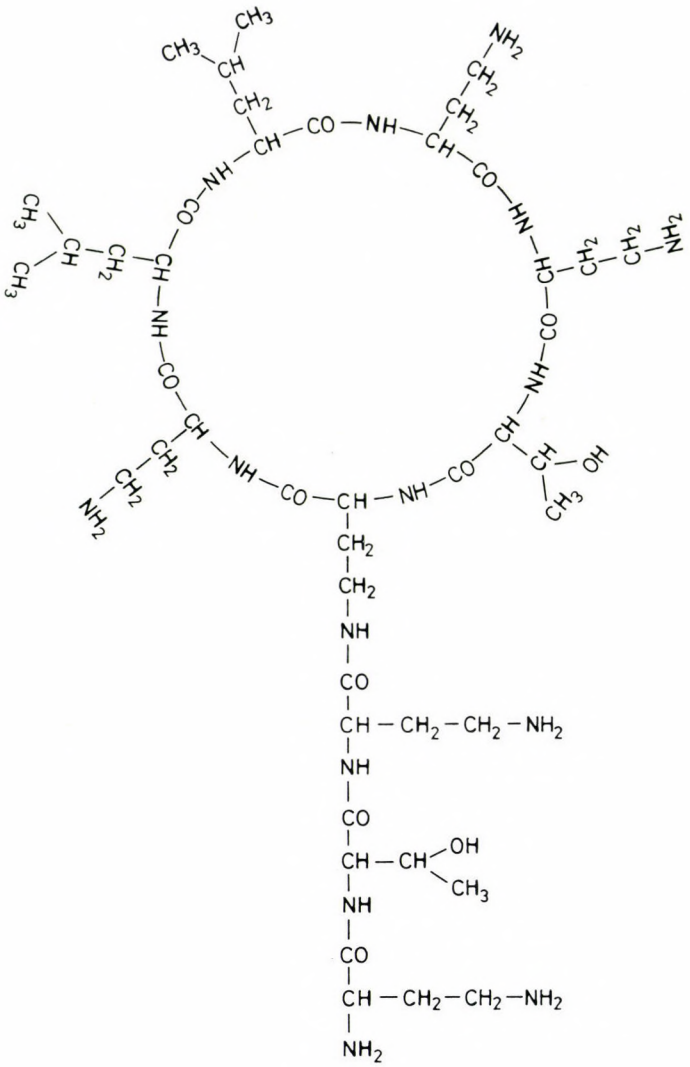

Colymycin

Fig .2b

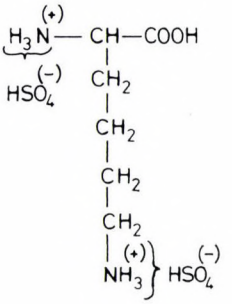

H-Lys-OH×H_2SO_4

Fig. 2c

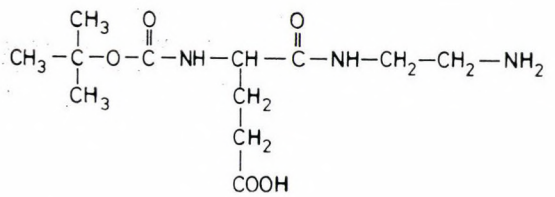

BOC-Glu-EDA
OH

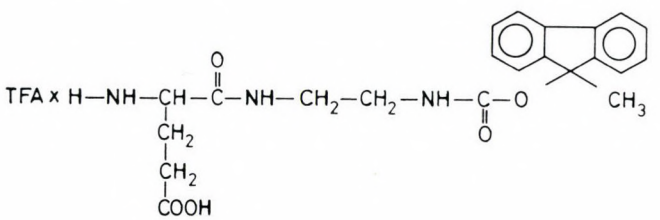

TFA×H-Glu-EDA-FMOC

Fig. 2d

Fig. 2. a—d. Chemical formulas of the substances used in perineural application

Polymyxin B is known to be a strong histamine liberator. In order to clarify the TDA-inducing effect of Polymyxin B and to exclude any eventual histamine effects, the histamine liberator poliamine 48/80 and Peremin (Histaminum bihydrochloricum) were also applied perineurally. In either case, we did not encounter any change in the FRAP reaction of substantia gelatinosa,

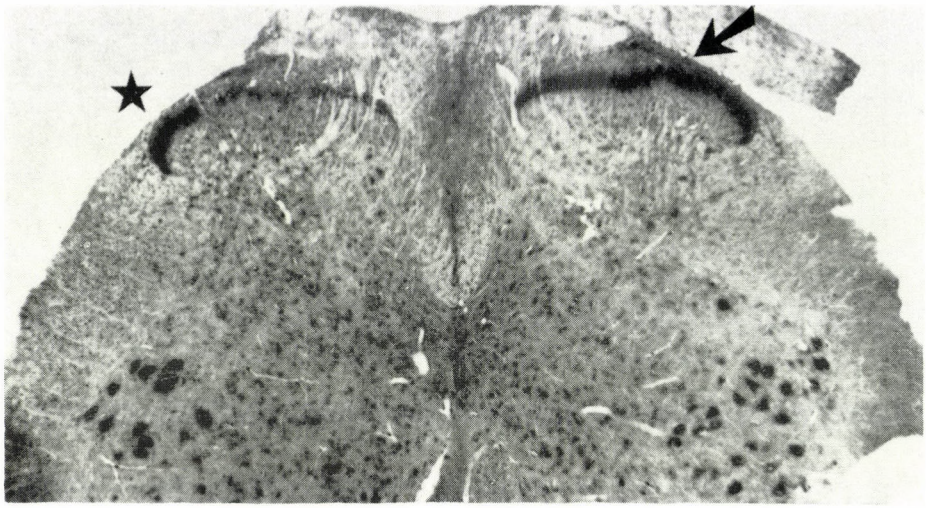

Fig. 3. The effect of the perineural application of Polymyxin B (10^{-7} M) on the FRAP activity of substantia gelatinosa Rolandi (Lamina II of Rexed). On the side of the sciatic nerve treated with Polymyxin B (apparent left) depletion of FRAP activity is nearly complete; only a minimal residual activity can be observed, mainly at the lateral edge of the substantia gelatinosa Rolandi which represents the somatotopically corresponding zone of the (intact) postaxial dermatome (asterisk). The contralateral substantia gelatinosa Rolandi (where the sciatic nerve was treated only by a physiological saline solution) shows a completely normal, intensive FRAP reaction (arrow)

indicating that TDA did not ensue; in other words, histamine liberation is not responsible for the TDA-inducing effect of Polymyxin B.

On the other hand, since both Polymyxin and Colimycin were applied in the form of sulphate salts, the TDA-inducing effect could be due to a simple binding of intraaxonal Ca^{2+} ions by the sulphate groups — it is known that Ca^{2+} plays a crucial role in axoplasmic transport mechanisms. Therefore, to exclude the role of the sulphate groups, a pH-dependent H_2-Lys-OHxH_2SO_4 was also applied perineurally. No FRAP-depletion was encountered indicating that TDA did not occur, proving that Ca^{2+} binding is not responsible for the effects of Polymyxin B and Colimycin.

Table I summarizes the biological effects of 7 different chemical compounds on the spinal cord and the sciatic nerve. Only the first four compounds induce TDA. These substances have a common chemical feature: all of them possess at least one basic centre — Polymyxin B and Colimycin even more. We assume that basic compounds like BOC-GLU-EDA and TFAxH-Glu-EDA-FMOC [4] (the monomeric units of poliantin [9]) could be active in our biological test system because they have a proper chemical structure fitting into the target molecule. Very probably, the presence of a basic (e.g. amino) group in the molecule is not satisfactory for inducing the TDA effect; the

Table I

Dose-effect correlation of perineurally applied compounds

Perineurally applied compounds	Substance concentration	Effect		n
		on FRAP in the Rolando substance	on the sciatic nerve	
Polymyxin B	10^{-7} M*	Depletion (TDA)	Ø	16
Colimycin	10^{-7} M*	Depletion (TDA)	Ø	12
TFAxH-Glu-EDA-FMOC	10^{-6} M*	Depletion (TDA)	Ø	3
BOC-Glu-EDA	10^{-6} M*	Depletion (TDA)	Ø	5
H-Lys-OHxH_2SO_4	10^{-6} and 10^{-4} M	Ø	Ø	5
48/80	10^{-9} and 10^{-6} M	Ø	Ø	5
Peremin	10^{-9} and 10^{-6} M	Ø	Ø	5

* Threshold concentration. If applied in higher amounts, Wallerian degeneration ensues. In lower than threshold concentration. FRAP depletion does not occur

presence of an amide (peptide) bond in the neighbourhood of the amino group, in proper distance seems to be necessary. This could be the reason why lysine alone proved to be inactive.

Discussion

TDA-inducing classical compounds, like Vinca alkaloids [8], Colchicin, Podophyllotoxin and Griseofulvin, exert their effect by inhibiting the microtubular function. A serendipitous observation called our attention to the peculiar TDA-inducing effect of Polymyxin B. The basic peptides applied in our investigations have no antimitotic or anti-microtubular activity; accordingly TDA induced by these compounds must be the result of some different mechanism. We assume that these compounds induce TDA as a result of interaction with NGF. Such a reaction can take place either in a competitive manner, because of the presence of the basic centers in the NGF molecule that exert similar structural properties like the basic glutamic acid derivatives, or because the basic groups fit into the stereochemical structure of the NGF; in other words, the reaction may result in modification of the conformation of NGF.

It is well known, however, that in addition to configurational similarities, the basic peptide compounds, studied by us e.g. Polymyxin, have also other pharmacological properties. Thus, for instance, in isolated mastocyte cultures Polymyxin causes marked degranulation i.e. histamine release [7, 10]. It is also well known that in the peripheral nerves, like the sciatic nerve, mastocytes are present in considerable numbers [14].

So the idea that the TDA-inducing property of Polymyxin B is based on a histamine effect, seemed to be germane. However, on the basis of our inves-

tigations carried out with the histamine liberator 48/80 and with histamine itself (Peremin), histamine liberation as a TDA-inducing factor can be excluded with certainty.

Yet there is another intriguing possibility. Both Polymyxin and Colimycin are sulphate ions. Thus it could be assumed that the sulphate groups are responsible for the TDA-inducing property of these compounds, mainly by their reaction with Ca^{2+} ions which are known to play a key role in axoplasmic transport mechanisms. According to this hypothesis, sulphate groups would form a salt with Ca^{2+} ions thus inhibiting the Ca^{2+}-activated Calmodulin effect, i.e. the activation of $Ca^{2+}-Mg^{2+}$-ATPase, resulting in a blockade of the microtubular transport [6, 12, 16].

The role of the sulphate groups has been studied in experiments where the pH-dependent H-Lys-OHxH_2SO_4 was perineurally applied. This compound behaves as an absolute cation below the pH 7.4 range; accordingly lysine is ineffective while the sulphate is active. This way, the result of the experiments performed with perineurally applied H-Lys-OH $\times$ H_2SO_4 — that is, the lack of FRAP depletion — obviously proves that SO_4 ions do not play any role in the induction of TDA.

REFERENCES

1. Csillik B, Knyihár-Csillik E, Tajti J: Blockade of retrograde axoplasmic transport induces transganglionic degenerative atrophy of central terminals of primary nociceptive neurons. Acta Biol Acad Sci Hung 33: 149, 1982
2. Csillik B: Nerve growth factor regulates central terminals of primary sensory neurons. Z mikrosk-anat Forsch 98: 1S. 11, 1984
3. Csillik B, Knyihár-Csillik E: The Protean Gate. Structure and Plasticity of the Primary Nociceptive Analyzer. Akadémiai Kiadó, Budapest, 1986
4. Csillik B, Kovács K, Penke B, Tajti J, Szilárd J, Szücs A, Knyihár-Csillik E: Transganglionic effect of basic peptides on the primary nociceptive analyzer. Proc 4th Congr Hung Pharmacol Soc Budapest Vol 2: 235, 1985
5. Csillik B, Schwab ME, Thoenen H: Transganglionic regulation of central terminals of dorsal root ganglion cells by nerve growth factor (NGF). Brain Res 331: 11, 1985
6. Iqbal Z, Ochs S: Brief communication. Calmodulin in mammalian nerve. J Neurobiol 11: 311, 1980
7. Kahlson G, Rosengren E: New approaches to the physiology of histamine. Physiol Rev 48: 155, 1968
8. Knyihár-Csillik E, Csillik B: FRAP. Histochemistry of the primary nociceptive neuron. Progr Histochem Cytochem 14: 1, 1981
9. Kovács K: Antibacterial synthetic polypeptide derivates. Nature 192: 190, 1961
10. Lagunoff D: Contributions of electron microscopy to the study of mast cells. J Invest Dermatol 58: 296, 1972
11. Levi-Montalcini R, Angeletti PO: Nerve growth factor. Physiol Rev 48: 534, 1968
12. Marcum M, Dedman JR, Brinkley BR, Means AR: Control of microtubule assembly-disassembly by calcium-dependent regulator protein. Proc Natl Acad Sci USA 75: 3771, 1978
13. Palay SL, Chan-Palay V: Cerebellar Cortex. Cytology and Organization. Springer, Berlin, Heidelberg–New York, 1974
14. Selye H: The Mast Cells. Butterworths, Washington, 1965
15. Tajti J: Effects of calmodulin inhibitors upon the structure of peripheral nerves. Z mikrosk-anat Forsch (in press)
16. Tiberi M, Lavoie PA: Inhibition of the retrograde axonal transport of acetylcholinesterase by the anticalmodulin agents Amitryptyline and Desipramine. J Neurobiol 16: 245, 1985

Acta Morphologica Hungarica, 36 (1–2), pp. 15–25 (1988)

DEVELOPMENT OF THE AUTONOMIC GROUND PLEXUS IN THE ATRIOVENTRICULAR VALVES OF THE RAT

G. KÁLMÁN

DEPARTMENT OF ANATOMY, UNIVERSITY MEDICAL SCHOOL, SZEGED, HUNGARY

(Received 23 March 1987)

The development of the adrenergic and cholinergic innervation of the rat atrioventricular valves was studied in whole mount stretch preparations. Specimens obtained from rats ageing 2–30 days were processed for the histofluorescence and enzyme histochemical demonstration of monoamines and acetylcholinesterase (AChE) activity, respectively.

Adrenergic and AChE-positive nerve fibres could be detected from the 9–10th postnatal days onwards. Fluorescence microscopy showed the presence of many brightly fluorescent mast cells in the close vicinity of the ingrowing terminals. The presence of mast cells during early stages of development of the ground plexus may be related either to the preneural state of the tissue or the structural and/or functional maturation of the autonomic nerve terminals.

Keywords: Heart valves, innervation, development, mast cells

Introduction

During an examination of the innervation in the endocardium, Smirnow [29] observed a network of thin nerve fibres in the valves of the heart and thus first drew attention to the presence of nerves in the atrioventricular valves of mammals. Michailow [22] and later Wollard [36] discovered a similar network of fibres, which revealed a close connection with the endocardial tissue. The introduction and more widespread use of the histochemical procedure have recently resulted in the demonstration of the innervation of atrioventricular valves. The AChE reaction [5, 7, 9, 12, 30, 35] and the monoamine fluorescence technique [2, 5, 7, 9–12, 20] revealed light microscopically a cholinergic and an adrenergic network of similar distribution in the valves of the heart.

Electron microscopic examination of the autonomic innervation of tissues has revealed that the sympathetic and parasympathetic nerve fibres are embedded in the cytoplasm of the same Schwann cells, producing the innervation apparatus of the tissue in this way. This means that the tissues have a double innervation. A similar arrangement of the cholinergic and adrenergic

Send offprint requests to: G. Kálmán, Department of Anatomy, University Medical School, H-6701 Szeged, Kossuth L. 40, Hungary

fibres has been observed on ultrastructural examination of the atrioventricular valves [7, 17].

Several theories have been put forward concerning the function of the nerve fibres in the valves of the heart. According to the generally accepted view, the movement of the heart valves is passive, it depends on pressure conditions regulated by the rhythmic contraction of the cardiac muscle, and the neural structures present here are not related to the function of the valves [21]. There are other theories that the movement of the atrioventricular valves is an active process and that the smooth muscle and heart muscle cells are here under neural control [5, 10, 14, 27, 31]. Lipp and Rodin [20] considered that the function of the nerves of the valves is not the innervation, but rather the "secretion" and/or uptake of noradrenaline into and from the blood stream, respectively. Most authors, however, have emphasized the sensory character of the nerve fibres of the valves [7, 12, 15, 23, 34, 35].

In the present work, light microscopic histochemical methods were used to study the development of the innervation of atrioventricular valves in rats on postnatal days 2–30, and to establish whether, in the knowledge of the ontogenesis of the ground plexus, conclusions may be drawn concerning the functional maturation of the terminals.

Materials and methods

Young 2–30-day-old white rats of both sexes were used. The animals were killed by decapitations, hearts were immersed in cold (4 °C) physiological saline solution, and the atrioventricular valves, together with the annulus fibrosus and the chordae tendineae were dissected. The development of the nerves was followed by the parallel use of the monoamine fluorescence method of Falck [13] and the AChE reaction of Koelle [18] in whole mount stretch preparations of mitral and tricuspidal valves. The leaflets were studied under a Zeiss fluorescence microscope, using a HBO 200 W high-pressure mercury lamp equipped with BG 12 exciter filter, OG 1 and GG 11 ocular filters. Non-specific cholinesterase was blocked with 2×10^{-4} M ethopropazine.

In addition to the fluorescence microscopic investigation, successive toluidine blue staining, moreover alcian blue-safranine staining of parallel preparations fixed in Carnoy's fluid according to Röhlich and Csaba [28] were used for identification and differentiation of the mast cells, respectively.

Results

The different histochemical methods gave almost identical results from the aspects of the time of ingrowth, density, enzyme activities and fluorescence intensity of the fibres in the mitral and tricuspidal valves of the rat.

Fig. 1. Fluorescence microscopic pattern in the atrioventricular valves of the rat. ×250. (a) Mitral valve on the 9th postnatal day: conspicuous mast cells along slightly fluorescent nerve fibres; (b) mitral valve on the 12th day: branching axons closely connected with mastocytes; (c) tricuspidal valve on the 14th day: axon ramification with degranulated mast cells; (d) mitral valve on the 16th day: chain-like nerve plexus

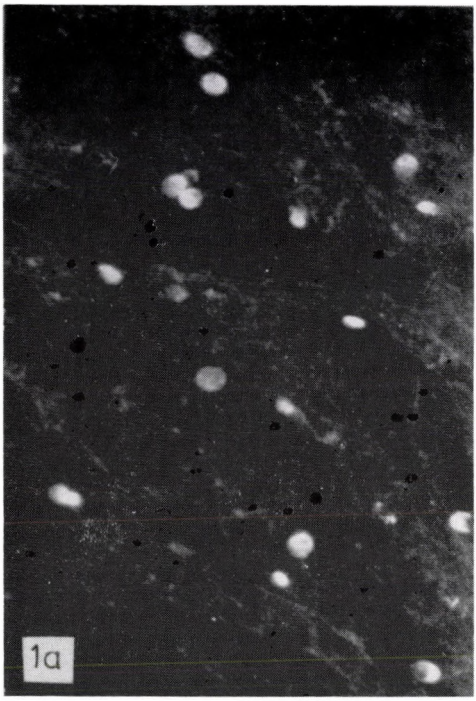
1a

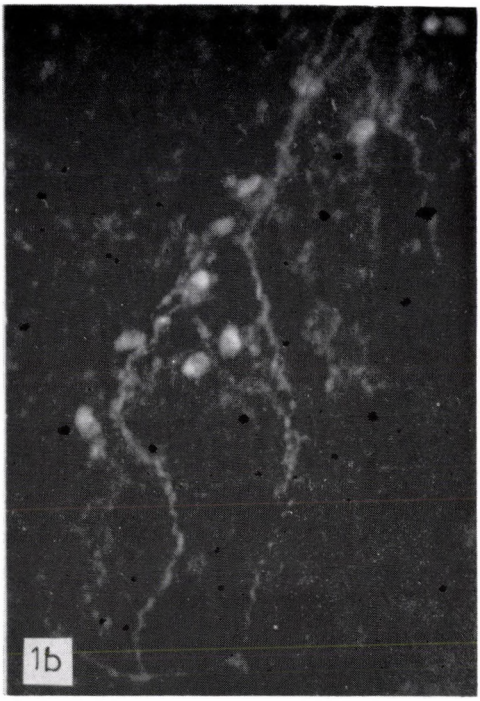
1b

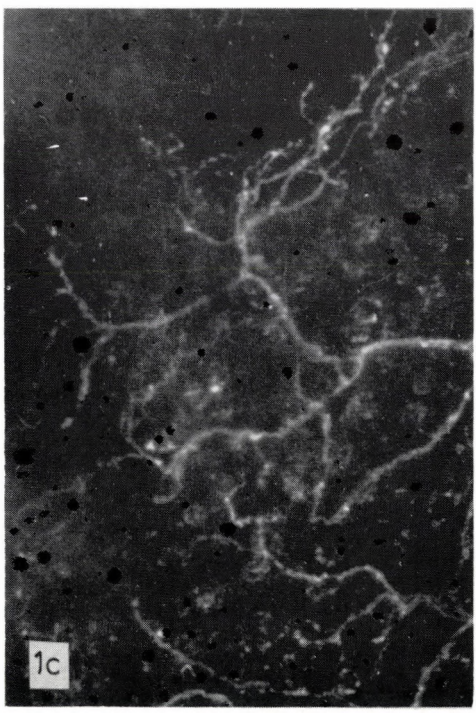
1c

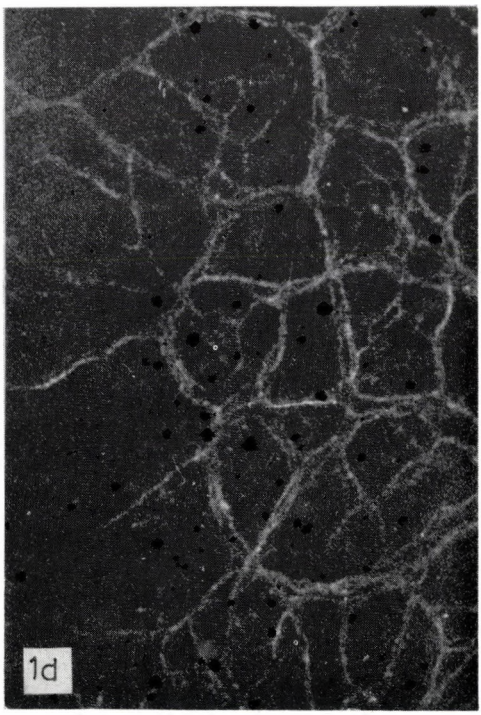
1d

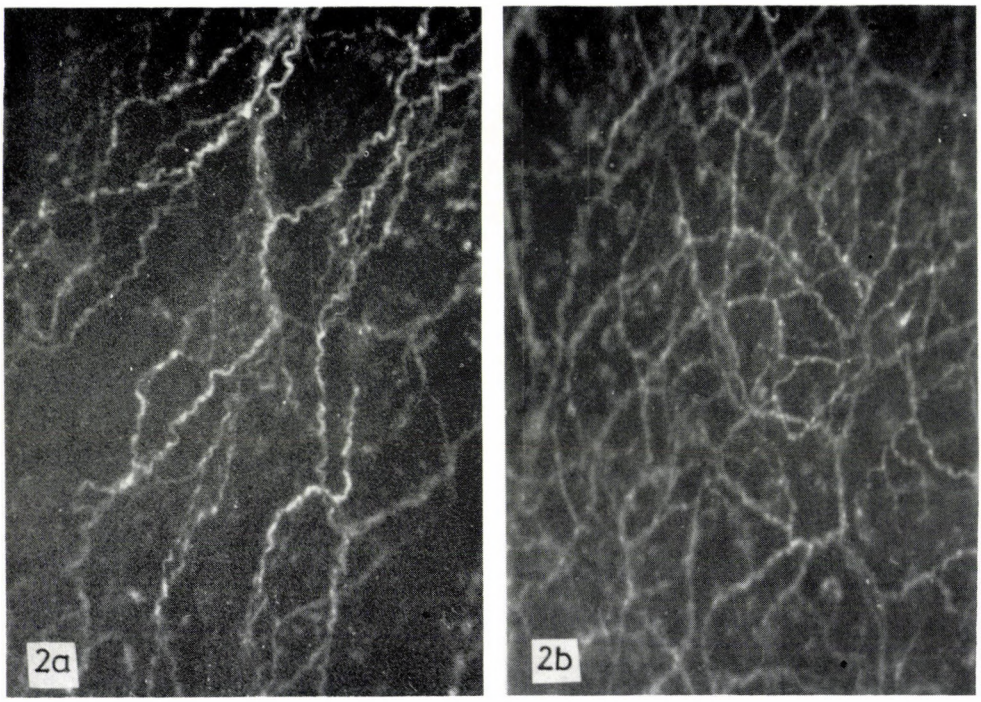

Fig. 2. Fluorescence microscopic pattern in the mitral valves of the rat. Stage of structural maturation: axon varicosities in ground plexus. ×250. (a) 20th day; (b) 30th day

With fluorescence histochemical methods, the extremely weakly fluorescent axons emerging from the annular margin were first observed in the atrioventricular valves on the postnatal day 9; only the brightly fluorescent mast cells situated along the ingrowing fibres appeared in the pictures (Fig. 1a). On day 12, intensely fluorescent primary axon-branchings could already be observed. At the same time, the perinuclear arrangement of fluorescent granules became pronounced in the mastocytes (Fig. 1b). Besides the scanty network of nerve fibres, only the outlines of the mast cells could be seen 14 days after birth (Fig. 1c). On day 16, the characteristic stage of development of the adrenergic ground plexus was conspicuous in the fluorescent pictures of the valves: due to the axon segregation and the subdivision of axon bundles, the nerve fibres showed a chain-like appearance, which later, through the widening of the chain loops, gave rise to the network of the ground plexus (Fig. 1d). On day 20, the appearance of axon varicosities and an even more abundant

Fig. 3. Distribution of AChE in the atrioventricular valves of the rat. ×250. (a) Mitral valve on the 10th postnatal day: ingrowth of enzyme-active nerve fibers from annular margin; (b) tricuspidal valve on the 12th day: primary axon branching; (c) mitral valve on the 14th day and (d) on the 16th day: development of the chain-like nerve network

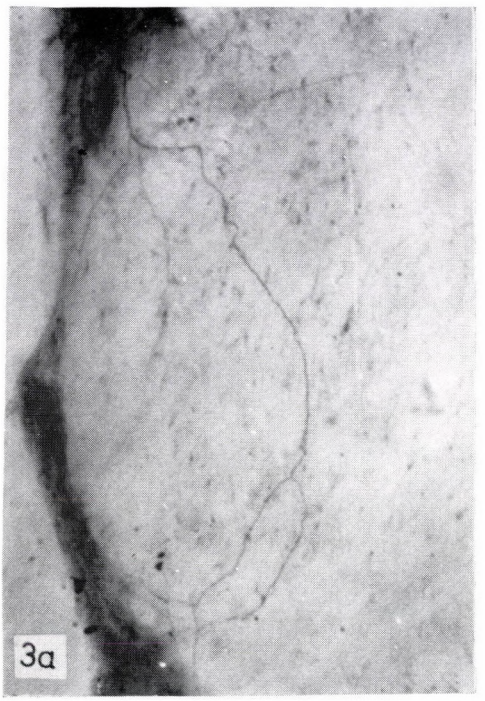
3a

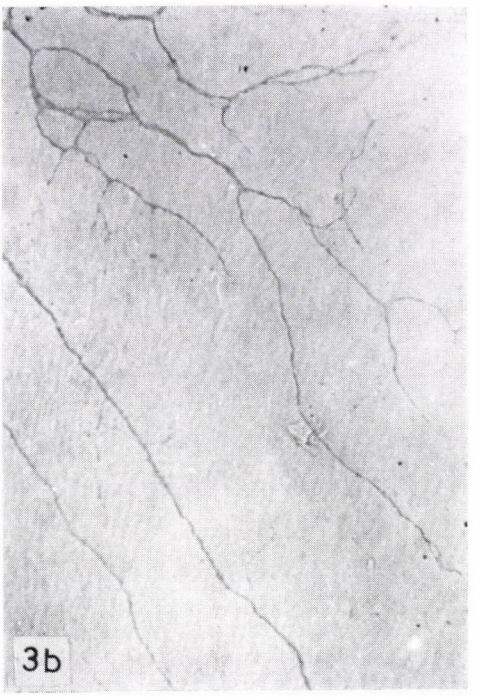
3b

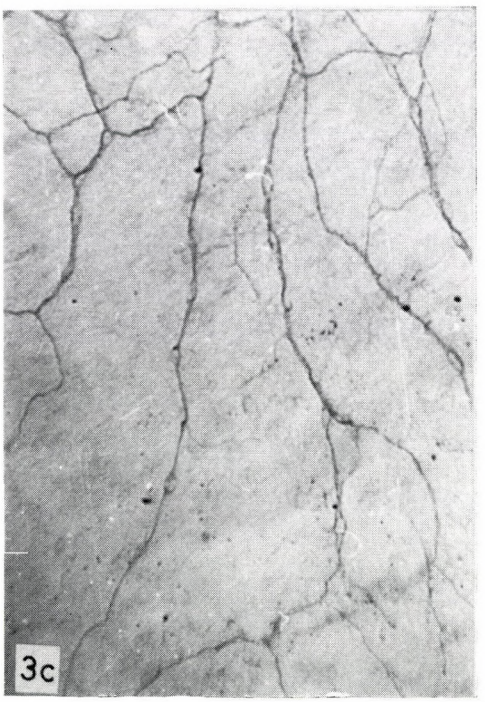
3c

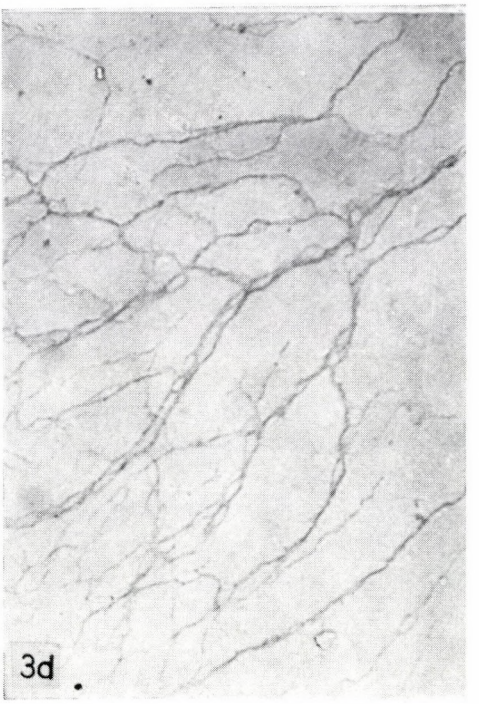
3d

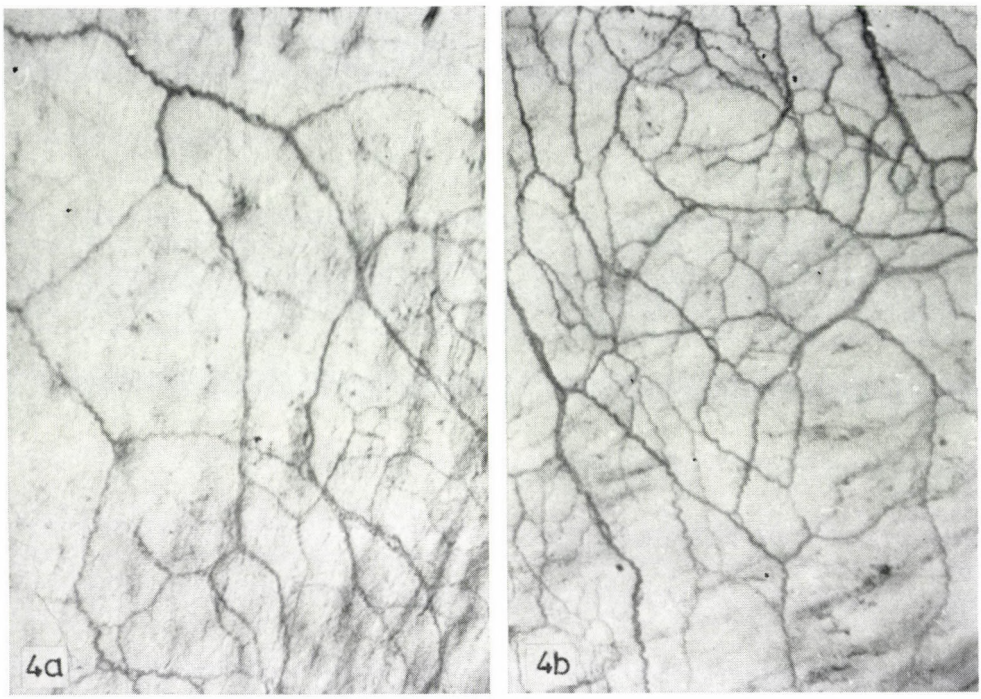

Fig. 4. Distribution of AChE in the atrioventricular valves. Structural maturation of cholinergic ground plexus. ×250. (a) Tricuspidal valve of 20-day-old rat; (b) mitral valve of 30-day-old rat

network could be observed, but it did not yet extend to the entire valve. Fluorescent mastocytes could no longer be seen. The varicose ground plexus was fully developed by postnatal day 30 (Figs 2a, b).

The earliest observation of AChE-positive nerve fibres in the leaflet was on day 10 after birth, when there was a few ingrowing nerve fibres from the annular margin (Fig. 3a). An increasing number of enzyme-active, branching nerve fibres were subsequently observed (Fig. 3b). On day 14, due to the segregation of the axons, the development of the chain-like network had started. It had become pronounced by day 16, just as in the case of the adrenergic fibres (Figs 3c, d). Besides the increasing density of the network the varicosities of fibres were noticed 20 days after birth, and by day 30, a fully mature, varicose cholinergic plexus could be seen (Figs 4a, b).

The applied non-specific cholinesterase blocking agent, 2×10^{-4} M ethopropazine did not influence either the intensity of the enzyme activity, or the density of the network.

The adrenergic and cholinergic networks developing from the ingrowing nerve fibres from the annular margin did not extend over the whole leaflets, but only to the border of the chordal third. At the same time, the ingrowth

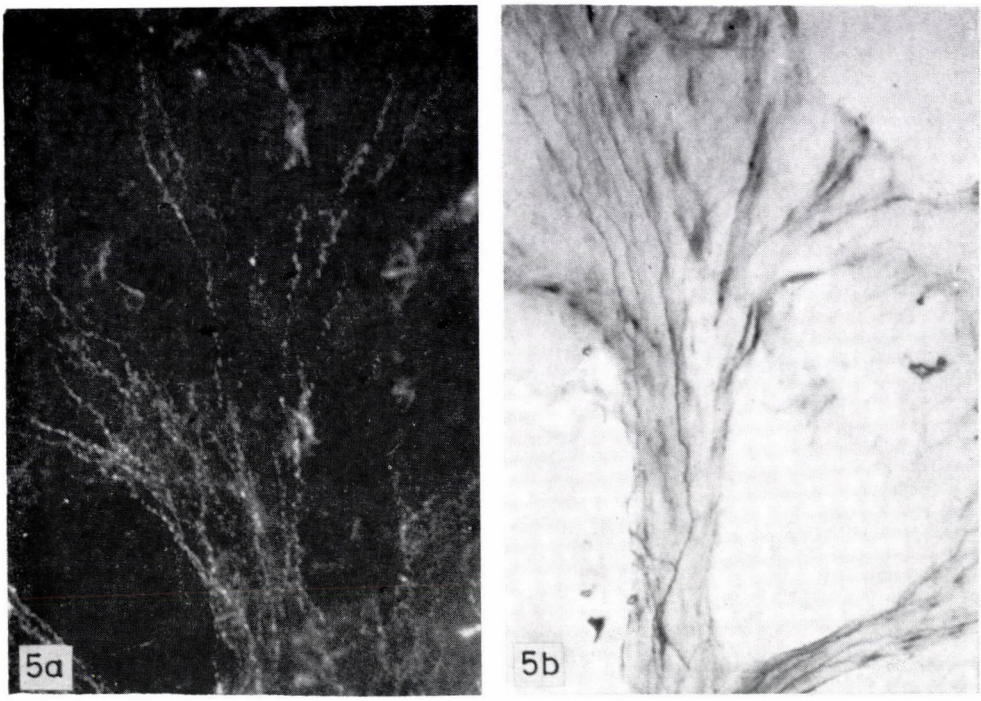

Fig. 5. Ascending nerve fibres in the atrioventricular valves of 25-day-old rat. ×160. (a) Fluorescence pattern; (b) AChE reaction

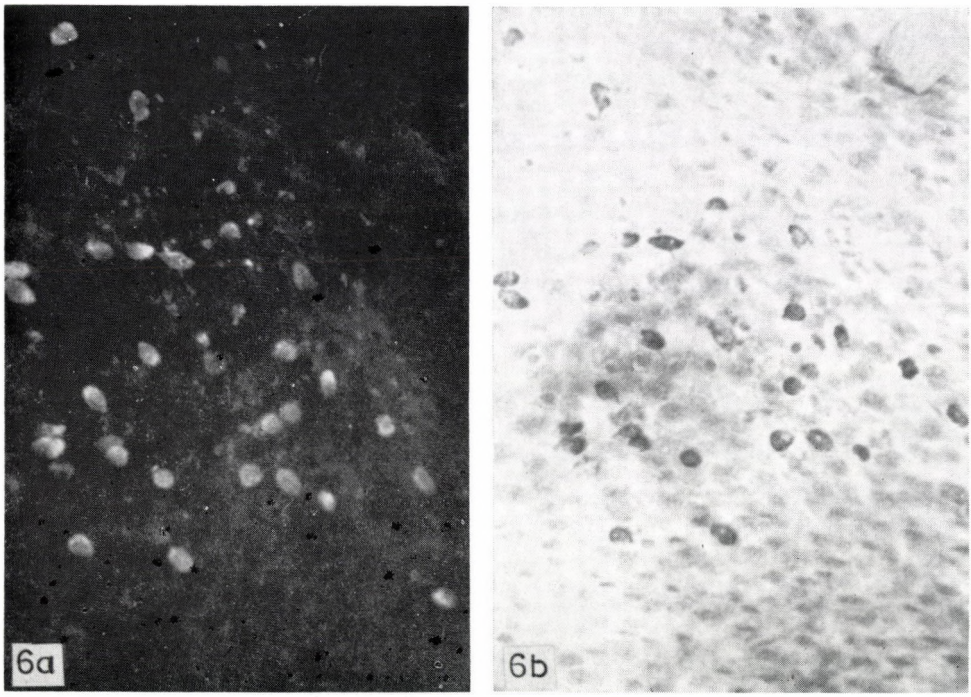

Fig. 6. Identification of mast cells in the mitral valve of 9-day-old rat. ×250. (a) Monoamine fluorescence and (b) toluidine blue staining of the same preparation

of nerve fibres to the chordae tendineae from the papillary muscles could also be observed. These fibres could be seen only from day 16 and their varicose terminals extended only into the chordal third, where they branched out in a fan-like way but did not contact the network growing from the annular margin (Figs. 5a, b).

In the early developmental stage of the ground plexus, strongly fluorescent cells revealing a close connection with the developing adrenergic terminals were present. The equivalents of these fluorescent cells stained with toluidine blue and alcian blue-safranine proved to be mast cells (Figs. 6a, b).

Discussion

In the present study of the ontogenesis of the innervation in the atrioventricular valves of the rat, the earliest appearance of both adrenergic and cholinergic nerve fibres was on postnatal days 9–10. The first fibres came from the base of the leaflets; these axons formed a network first and it is probable that they are derivates of the atrial ground plexus. At the chordal third, conspicuous axon arches can be seen, which form a peculiar borderline. Varicose axons originating from the plexus of the papillary muscles and running in the opposite direction can be observed in the chordae tendineae. After a usually straight course these fibres can also be followed up to the chordal third. This borderline probably corresponds to the systole closing area. Since there are no contractile elements in this area, we suggest that the autonomic innervation plays a role in the modulation of the reflexogenic zone.

The consistent participation of the sensory nerve fibres was supposed already by Szentágothai [32] in the structural organization of the autonomic ground plexus. Recently, electron microscopic studies have revealed that mitochondria-loaded varicosities of presumptive sensory fibres are present often close to the adrenergic terminals in the atrioventricular valves [7, 17], similar to those in the myocardium [3, 4, 19].

The presence of intensively fluorescent mast cells was observed in the early period of appearance of fluorescence in the developing adrenergic nerves, but these cells could be seen only up to days 12–14 of postnatal development. Together with the increase of the fluorescence of the axons and the progress of axon arborization, the fluorescence of the mastocytes gradually decreases and later totally disappears. It may be suggested that changes in fluorescence of mast cells reflect cytochemical changes — mainly the release of biogenic amines — after degranulation that was observed in our previous electron microscopic studies [25]. The vast majority of young mastocytes as well as the degranulated cells showed alcian blue-positivity, in accordance with earlier wide-ranging observations of Röhlich and Csaba [28].

The ontogenesis of the ground plexus in the iris of rat was first described by Csillik and Koelle [6] on the basis of parallel monoamine fluorescence and AChE histochemical reactions. They observed that at the time of development of the ground plexus, during the first two weeks of postnatal life, brightly fluorescent "sphaerical bodies" are present. Similar information was obtained about the appearance of numerous fluorescent mast cells in different tissues, particularly in the heart atrium, iris and submaxillary gland of the rat during the postnatal development of their adrenergic innervation [8, 26]. An increased number of mastocytes was also found in the liver of adult rats after partial hepatectomy, under circumstances when the adrenergic nerve regeneration probably run parallel with a considerable regenerative growth of hepatic tissues [33]. In this case the growing nerves are supposed to tend towards their newly formed target cells.

In our previous investigations, the development of the ground plexus in the rat iris was studied during normal ontogenesis and under experimental conditions [16], and we also observed intensively fluorescent mast cells during the early period of development. Our experiments on accumulation, depletion and liberation, as well as the characteristics of their fluorescence indicated that these cells contained mainly serotonin, but they could also take up the catecholamines. Our electron microscopic studies proved that the mast cells are very closely connected with the developing terminals [25]. As a general phenomenon, we observed in the newborn rats that the axon bundles containing numerous unmyelinated fibres were surrounded by the cytoplasm of a single Schwann cell, and in the vicinity of these, mastocytes showing the signs of degranulation could be seen. The bundles contained on the average 30–40 small axons running closely together. The sign of the next developmental stage is when the axon segregation starts vigorously. As a net result, the cytoplasm of the Schwann cell separates all the axons from each other. It is suggested that the axon segregation is of great importance in the development of the unmyelinated axons, and this can be regarded as the starting basis of the maturation. In the structural maturation of autonomic neurons the developmental period of terminal varicosities may be critical when the transmitter storing vesicles accumulate in enlargements which are supposed to be the sites of the functional transmitter release.

The two main stages, namely the segregation and the formation of varicosities can also be observed well on examination of the atrioventricular valves around days 16 and 20 after birth, respectively. Consequently, both essential phenomena, as well as the first appearance of the nerves occur here later than in the irides.

Lastly, the role of the mastocytes in the early period seems to be verified that, after sympathetic decentralization of the iris in newborn rats, besides the retardation of the development of adrenerg ground plexus, the involution of

the mastocytes characteristic of normal course of development does not take place. Their number are even multiplied by the locally observed mitoses, indicating an early developmental stage of innervation [16]. It seems that mast cells appear in the tissues when the growing nerves do not come in touch with their target yet. This view is supported by the studies of Aloe and Levi-Montalcini [1], who found that, after the treatment of newborn rats with nerve growth factor, there was a ten-fold increase in the number of amine-fluorescent mastocytes, suggesting a specific effect of this protein also on these cells.

Our investigation have revealed that the presence of the mastocytes during the ingrowth stage of the autonomic nerves can be observed in the atrioventricular valves as well as in the irides. The results presented here and the earlier light and electron microscopic experiments together demonstrate a close relationship between the mast cells and the developing ground plexus, and it may be suggested that the mastocytes in the tissues are somehow directly or indirectly connected with the growth of the autonomic nerves, their structural or functional maturation, and/or the preneural state of the target tissues, probably by the involvement of the transitional balance of the developing transmitter uptake systems.

REFERENCES

1. Aloe L, Levi-Montalcini R: Mast cells increase in tissues of neonatal rats injected with the nerve growth factor. Brain Res 133: 358, 1977
2. Anderson RH: Fluorescing valvular nerves in the guinea-pig heart. Experientia 27: 1063, 1971
3. Chiba T: Electron microscopic and histochemical studies on the synaptic vesicles in mouse vas deferens and atrium after 5-hydroxydopamine administration. Anat Rec 176: 35, 1973
4. Chiba T, Yamauchi A: On the fine structure of the nerve terminals in the human myocardium. Z Zellforsch 108: 324, 1970
5. Cooper T, Napolitano LM, Fitzgerald MJT, Moore KE, Daggett WM, Willman VL, Sonnenblick EH, Hanlon CR: Structural basis of cardiac valvar function. Arch Surg 93: 767, 1966
6. Csillik B, Koelle GB: Developmental histochemistry of the autonomic ground plexus. Acta Neuroveg 29: 177, 1966
7. De Biasi S, Vitellaro-Zuccarello L, Blum I: Histochemical and ultrastructural study on the innervation of human and porcine atrio-ventricular valves. Anat Embryol 169: 159, 1984
8. De Champlain J, Malmfors T, Olson L, Sachs Ch: Ontogenesis of peripheral adrenergic neurons in the rat: pre- and postnatal observations. Acta Physiol Scand 80: 276, 1970
9. Ehinger B, Falck B, Persson H, Sporrong B: Adrenergic and cholinesterase-containing neurons of the heart. Histochemie 16: 197, 1968
10. Ehinger B, Falck B, Stenevi U: Adrenergic and non-adrenergic valvular nerves of the heart. Experientia 25: 742, 1969
11. Ellison JP: The adrenergic cardiac nerves of the cat. Am J Anat 139: 209, 1974
12. Ellison JP, Hibbs RG: The atrioventricular valves of the guinea-pig. I. A light microscopic study. Am J Anat 138: 331, 1973
13. Falck B: Observations on the possibilities of the cellular localization of monoamines by a fluorescence method. Acta Physiol Scand 56: Suppl 197, 1962
14. Fenoglio JJ, Pham TD, Wit AL, Bassett AL, Wagner BM: Canine mitral complex: Ultrastructure and electromechanical properties. Circ Res 31: 417, 1972
15. Ferreira AL, Rossi MA: Innervation of human atrioventricular valves. Acta Anat 87: 57, 1974

16. Gajó M, Kálmán G: Transneuronal effects in the development of the adrenergic peripheral innervation apparatus. Acta Biol Acad Sci Hung 24: 221, 1973
17. Hibbs RG, Ellison JP: The atrioventricular valves of the guinea-pig. II. An ultrastructural study. Am J Anat 138: 347, 1973
18. Koelle GB: The histochemical localization of cholinesterases in the central nervous system of the rat. J Comp Neurol 100: 211, 1954
19. Kolb R, Pischinger A, Stockinger L: Ultrastruktur der Pulmonalisklappe des Meerschweinchens. Beitrag zum Studium der vegetativ-nervösen Peripherie. Z mikrok-anat Forsch 76: 184, 1967
20. Lipp W, Rodin M: The adrenergic nerve plexuses of cardiac valves. Acta Anat 69: 313, 1968
21. Lippe RC: Effect of atrial systole on ventricular pressure and closure of the A-V valves. Am J Physiol 166: 289, 1951
22. Michailow S: Die Nerven des Endocardiums. Anat Anz 32: 87, 1908
23. Miller MR, Kasahara M: Studies on the nerve endings in the heart. Am J Anat 115: 217, 1964
24. Nettleship WA: Experimental studies on the afferent innervation of the cat's heart. J Comp Neurol 64: 115, 1936
25. Nyiri S, Gajó M, Kálmán G: The role of mast cells in the development of adrenergic innervation in the rat iris. Z mikrosk-anat Forsch 91: 765, 1977
26. Owman Ch, Sjöberg NO, Swedin G: Histochemical and chemical studies on pre- and postnatal development of the different systems of "short" and "long" adrenergic neurons in peripheral organs of the rat. Z Zellforsch 116: 319, 1971
27. Priola DV, Fulton RL, Napolitano LM, Cooper T: Electrical activity of the canine mitral valve. Am J Physiol 216: 238, 1969
28. Röhlich P, Csaba G: Alcian blue-safranine staining and ultrastructure of rat mast cell granules during degranulation. Acta Biol Acad Sci Hung 23: 83, 1972
29. Smirnow AEV: Über die sensiblen Nervenendigungen in Herzen bei Amphibien und Säugetieren. Anat Anz 10: 737, 1895
30. Smith RB: Intrinsic innervation of the atrioventricular and semilunar valves in various mammals. J Anat 108: 115, 1971
31. Sonnenblick EH, Napolitano LM, Daggett WM, Cooper T: An intrinsic neuromuscular basis for mitral valve motion in the dog. Circ Res 21: 9, 1967
32. Szentágothai J: Einige Bemerkungen zur Struktur der peripheren Endausbreitung vegetativer Nerven. Acta Neuroveg 15: 417, 1957
33. Ungváry Gy, Donáth T, Naszály SA: Regeneration of the monoaminergic nerves in the liver after partial hepatectomy. Acta Morph Acad Sci Hung 22: 177, 1974
34. Voloschenko AA: Afferent innervation of atrioventricular valve. Fed Proc Transl (Suppl) 24: 571, 1965
35. Williams TH: Mitral and tricuspid valve innervation. Brit Heart J 26: 105, 1964
36. Wollard HH: The innervation of the heart. J Anat 60: 345, 1926

Acta Morphologica Hungarica, 36 (1–2), pp. 27–33 (1988)

THE EFFECT OF HORMONAL IMPRINTING ON ^{3}H-STEROID INCORPORATION OF *TETRAHYMENA PYRIFORMIS*

A. K. Fülöp, G. Csaba

DEPARTMENT OF BIOLOGY, SEMMELWEIS UNIVERSITY OF MEDICINE, BUDAPEST, HUNGARY

(Received 24 March 1987)

Steroid hormones are incorporated by *Tetrahymena*, and appear intracellularly in both cytoplasmic and intranuclear localizations. At primary interaction with the steroid, incorporation was the greatest at 10 min, whereas at the second interaction it tended to increase with time. The *Tetrahymena* cells preexposed to a steroid incorporated a greater amount of it at the second exposure, owing presumably to the induction of steroid receptors at the first interaction.

Keywords: Hormonal imprinting, *Tetrahymena*, steroid hormones, autoradiography

Introduction

Evidence has been accumulated that the unicellular *Tetrahymena pyriformis* is able to respond to hormones of higher organisms [3–6] and that such hormones or similar active molecules are native to the *Tetrahymena* [2, 11–14]. The primary interaction of the *Tetrahymena* with a hormone gives rise to hormonal imprinting [3, 4], which accounts for a greater intensity of response at later interactions [5, 6].

Steroid hormones also act on *Tetrahymena* [8, 10] and induce in it the formation of steroid binding sites after preexposure [9].

We examined by light and electron microscopic autoradiography the incorporation of different ^{3}H-labeled steroids into *Tetrahymena*, to obtain evidence whether or not preexposure to the given hormone influenced the intracellular accumulation of labeled steroid. The results of these studies were expected to elucidate new aspects of the phylogeny of receptor–hormone interaction.

Materials and methods

Tetrahymena pyriformis GL cells were cultured in 0.1 per cent yeast extract containing 1 per cent Bacto Tryptone (Difco, Michigan, USA) medium at 28 °C. Mass cultures were treated with the following steroids: estradiol-17 (Gedeon Richter Ltd. Budapest, Hungary);

Send offprint requests to: G. Csaba, Department of Biology, Semmelweis University Medical School, H-1445, Budapest, Nagyvárad tér 4, Hungary

dihydroepiandrosterone (DHEA, Organon-Oss, Holland); triamcinolone-acetonid (Gedeon Richter Ltd. Budapest, Hungary), dexamethasone (Serva, Heidelberg, FRG). The steroids were dissolved in ethanol and were added to the culture medium at 10^{-6} M; the ethanol concentration never increased over 0.1 per cent (and the control also got it). The steroid pretreatment lasted 72 h, after which the cells were separated by centrifugation and were returned to plain medium for 48 h before exposure to labeled steroids, such as estradiol-2,4,6,7-^{3}H (spec. act. 104 Ci/mmol), dihydro (1,2,6,7-^{3}H) epiandrosterone (spec. act. 65 Ci/mmol), dexamethasone-1,2,4-^{3}H (spec. act. 40 Ci/mmol), triamcinolone-(1,2,4-^{3}H) acetonide (spec. act. 22 Ci/mmol). All labeled molecules were products of the Amersham Ltd. (England). The pretreated and untreated mass cultures were incubated in presence of label for 10 min, 30 min, 1, 4 or 24 h. The concentration of label was 2 μCi/ml, the ethanol concentration was less than 0.2 per cent. After incubation the cells were fixed in 2 per cent glutaraldehyde (in 0.1 M, pH 7.4 phosphate buffer) for 2 h, postfixed in 1 per cent OsO_4 (in Millonig buffer) for 1 h, and were embedded in Araldite. Semithin and ultrathin sections were cut and coated with Ilford G5 and Ilford L4 emulsions, respectively. The light microscopic preparations were developed in ORWO R 9 after 8 weeks and the electron microscopic preparations in KODAK D 19B after 9 or 11 weeks of exposure. The light microscopic preparations were stained with toluidine blue and silver grains were counted over the longitudinal sections of 25 cells. Grain counts obtained were evaluated statistically by the Mann–Whitney test or Student's two-sample *t*-test; homoscedastic samples were analyzed with the F-test.

Results

Results obtained by light microscopic autoradiography are shown in Table I and Fig. 1. The cells not preexposed to dexamethasone incorporated initially little ^{3}H-dexamethasone, somewhat less after 10 min, and a slightly increasing amount after 1 h, whereas those preexposed showed an increasing tendency of incorporation at 1 h, and no change after this period. Both statistical tests indicated a significant difference between the incorporation values

Table I

Pre-treatment	Treatment	10 min	Incorporation of label after incubation for		
			30 min	1 h	4 h
—	^{3}H-dexamethasone	4.0±0.6 (25)	2.9±0.9 (15)	2.4±0.6 (20)	5.6±0.7 (16)
Dexa-methasone	^{3}H-dexamethasone	3.5±0.9 (15)	3.7±0.7 (25)	7.5±0.6 (20)^a_b	6.9±0.9 (16)
—	^{3}H-triamcinolone	4.0±0.6 (25)	4.6±1.1 (24)	7.7±0.6 (24)^a_b	
Triam-cinolone	^{3}H-triamcinolone	6.5±1.6 (25)	6.4±0.7 (25)	7.1±0.6 (24)	5.1±0.5 (25)
—	^{3}H-estradiol	15.1±0.9 (25)	10.4±0.7 (25)	10.6±0.9 (25)	12.2±0.8 (25)
Estradiol	^{3}H-estradiol	30.0±1.4 (22)^a_b	11.6±1.1 (25)	16.9±2.0 (8)^a_b	21.1±0.22^a_b
—	^{3}H-DHEA	16.5±1.1 (19)	12.0±0.7 (25)	8.1±0.5 (25)	7.6±8.8 (25)
DHEA	^{3}H-DHEA	9.2±0.6 (9)^a_b	13.8±1.1 (25)	18.8±1.3 (10)^a_b	28.3±2.1 (22)$_c$

x ± S.E. (grain count)

[a] The Mann-Whitney test showed a significant ($p < 0.01$) difference between the pretreated and untreated cells.

[b] Student's two-sample *t*-test showed a significant ($p < 0.01$) difference between the pretreated and untreated cells.

[c] The F-test showed the pretreated and untreated groups to be heteroscedastic; therefore the *t*-test was not performed

of the pretreated and not pretreated cell groups. The incorporation of ^{3}H-triamcinolone was similar to that of ^{3}H-dexamethasone, but the difference between the pretreated and not pretreated cultures was not significant statistically. ^{3}H-estradiol and ^{3}H-DHEA were incorporated more readily than labeled dexamethasone or triamcinolone, and preexposure to the same hor-

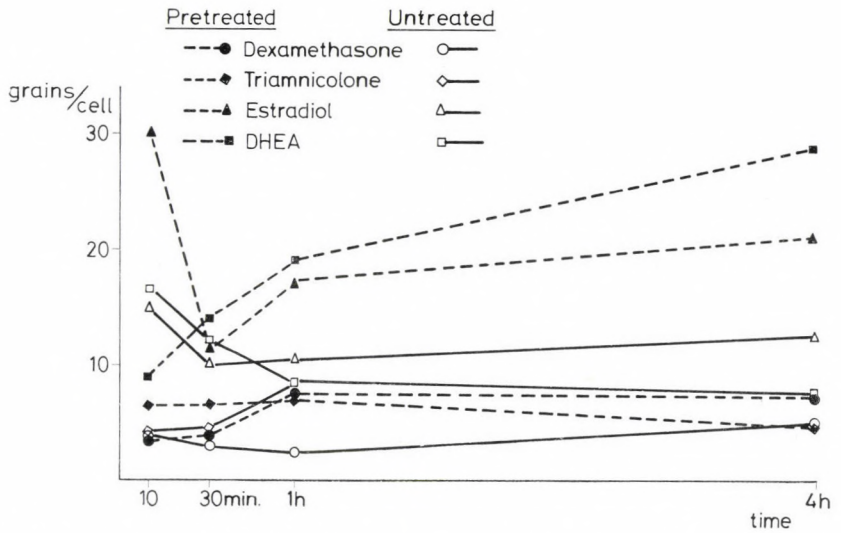

Fig. 1. Number of grains above the untreated and pretreated *Tetrahymena*

mone stimulated incorporation significantly after longer periods (1,4 h) of incubation. The shapes of the curves of incorporation of label were highly similar except in the case of the DHEA-treated cells.

Electron microscopic autoradiography complemented light microscopic findings by the detection of intracellular localization of incorporated steroids (Fig. 2). These molecules penetrate into the *Tetrahymena* cells rapidly, as judged by their appearance inside the nucleus within 10 min of exposure. It appears that the steroids can enter the cell body practically everywhere; they gain access into the nutrient vacuoles detaching from the cellular pharynx, enter the cell in sites where the external alveolar membrane is lacking, i.e. at the roots of cilia, across the membrane of the emptied mucocyst, and in all probability, across any surface site. Inside the cells labeled steroids can be detected in association with subcellular membrane structures, and also freely in the cytoplasm. The grain counts tend to increase not only above the cytoplasm, but also above the nucleus after longer incubation. In the case of ^{3}H-dexamethasone even a distinct intranuclear accumulation could be demonstrated.

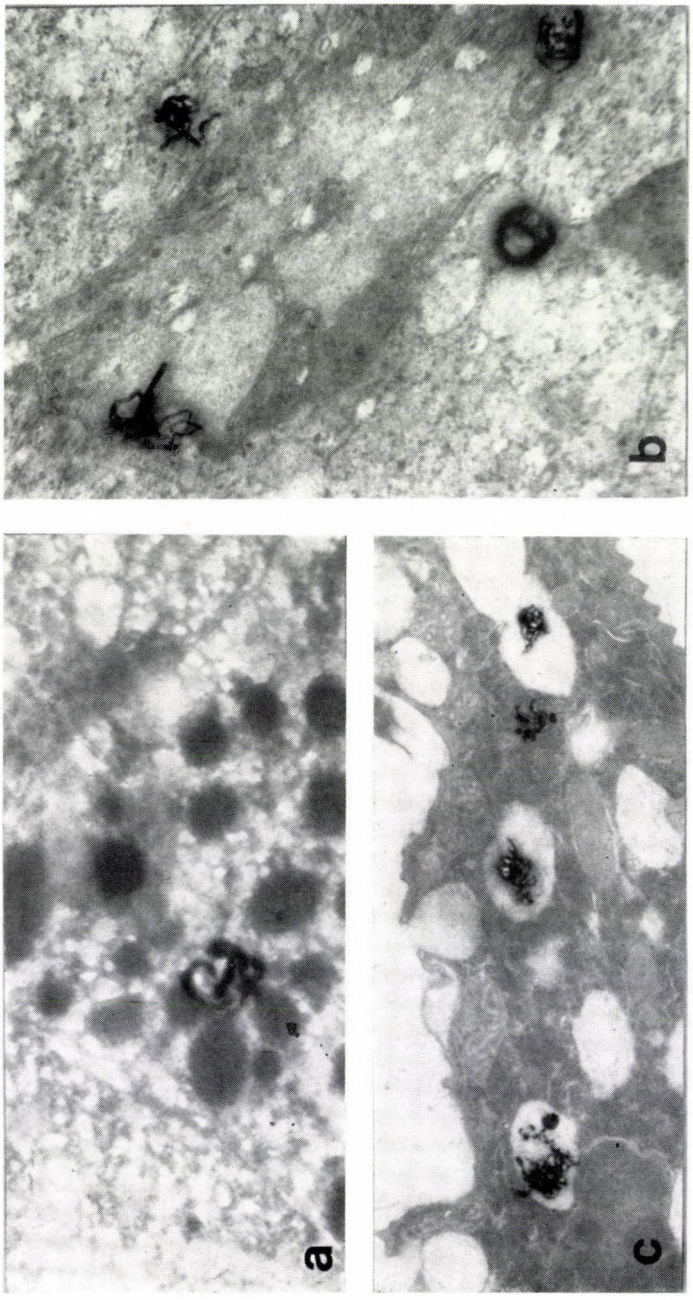
b
a
c

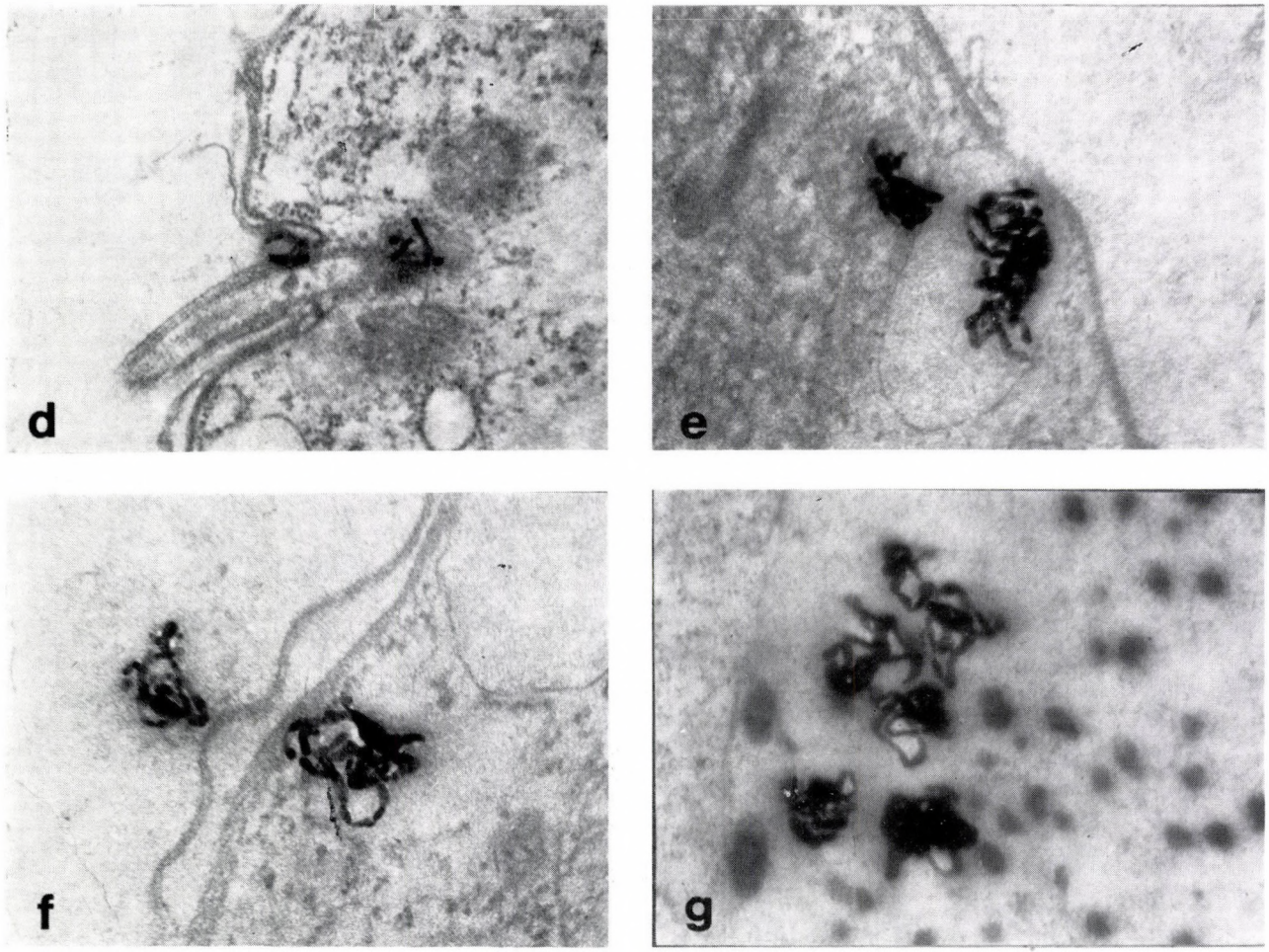

Fig. 2. Electron microscopic autoradiograms of *Tetrahymena pyriformis* incubated with different ^{3}H-steroids. Grains are above the nucleus (a: ^{3}H-dexamethasone 10 min, ×49 500 and g: ^{3}H-dexamethasone 4 h, ×28 500), around the cytopharynx (b: ^{3}H-DHEA 24 h, ×33 000), above the vacuoles (c: after 72 h estradiol pretreatment, ^{3}H-estradiol 30 min, ×22 000), around the radix of a cilium (d: ^{3}H-estradiol 4 h, ×51 500), above a mucocyst (e: after 72 h, DHEA pretreatment ^{3}H-DHEA 30 min, ×42 500), on the cell surface (f: after 72 h, DHEA pretreatment ^{3}H-DHEA 30 min, ×30 000)

Discussion

Light microscopic autoradiography indicated a low penetration rate of the examined synthetic glucocorticoids, but a considerably greater one of natural steroid hormones, such as DHEA and estradiol, into *Tetrahymena* cells. The factors responsible for variations in steroid penetration are with all probability (i) the dissimilar lipid solubility of the different steroids, and (ii) presence of steroid binding sites in *Tetrahymena*, or (iii) the joint effect of both. While an interaction between lipid solubility and binding conditions seems to be most probable, it should be taken into consideration that, with respect to penetration, the complementarity of natural steroids might be greater than that of the synthetic ones. Moreover, consideration should also be given to the fact that certain higher hormones are native to the *Tetrahymena* [2, 9, 11, 14].

The amount of the incorporated molecules changed in the function of time. The incorporation of all hormones except dexamethasone into the not preexposed cells was greatest after 10 min, and showed a relative decrease later, with occasional peaks which, however, never attained the 10 min peak again over the incubation period of 4 h. By contrast, incorporation of label into the preexposed cells tended to increase after 10 min, in the case of all hormones except estradiol. The difference between the incorporation of label into preexposed and not preexposed cells does not seem to be an accidental phenomenon, although its precise cause is not known. Probably, at primary exposure, the cell is "unprotected" against the influx of hormone until a state of equilibrium becomes established between the cell and its environment. At the second exposure, however, hormone influx seems to be controlled. This explanation does not, naturally, hold for the behaviour of dexamethasone in not pretreated cells and the behaviour of estradiol in the pretreated cells, but is should be noted that, e.g. in the case of estradiol, grain count was extremely high above the not preexposed cells whereas it tended to decrease markedly above the preexposed cells after 10 min. The different lipid solubility and longer half-life of dexamethasone, compared to the other test substances can probably explain its dissimilar behaviour [1].

Earlier investigations into the influence of dexamethasone and DHEA have shown that exposure for similar times as in this study provoked the appearance of steroid receptors, which are normally not present in *Tetrahymena*. This may explain the greater binding of labeled hormone to the hormone-pretreated cells, for the receptors, once they are present, alter the (influx- and efflux-dependent) equilibrium between the cell and its environment to the advantage of the cell.

The present experiments have subtantiated the results of earlier studies along this line [9], which indicated induction of receptor formation by pre-

exposure to the hormone, while the present findings indicated an increase in intracellular — presumably bound — hormone content of the preexposed cells.

Electron microscopic autoradiography has enabled the location of incorporated ^{3}H-steroid hormones inside the cells.

The electron microscopic findings support the hypothesis that the intracellular accumulation of a steroid depends partly on its lipid solubility, partly on the presence or absence of presumed steroid binding sites, for grains appeared not only over membrane structures, but also over the cytoplasm and nucleus, and the pretreated cells showed an increase in both cytoplasmic and nuclear grain counts. As to dexamethasone, its accumulation inside the cell nucleus indicated that the extraordinary affinity of this compound to chromatin also took effect in *Tetrahymena* [15].

REFERENCES

1. Bentley PJ: Endocrine Pharmacology. Cambridge University Press, Cambridge 1982
2. Berelowitz M, Le Roith D, von Schenk H, Newgaard C, Szabo M, Frohman LA, Shiloach J, Roth J: Somatostatin-like immunoreactivity, and bioactivity is native to *Tetrahymena pyriformis*, a unicellular eukaryote. Endocrinology 110: 1939, 1982
3. Csaba G: Phylogeny and ontogeny of hormone receptors: the selection theory of receptor formation and hormonal imprinting. Biol Rev 55: 47, 1980
4. Csaba G: Phylogeny and Ontogeny of Hormone Receptors. Karger, Basel–New York 1981
5. Csaba G: The unicellular *Tetrahymena* as a model cell for receptor research. Internat Rev Cytol 95: 327, 1985
6. Csaba G: Why do hormone receptors arise? Experientia 42: 715, 1986
7. Csaba G, Cserhalmi M: Does the *Tetrahymena* possess (amplifiable) steroid receptors? Endokrinologie 79: 431, 1982
8. Csaba G, Fülöp AK: Effect of steroid hormone (prednisolone) on the unicellular *Tetrahymena*. An electron microscopic study. Acta Protozool 26:233, 1987
9. Csaba G, Inczefi-Gonda Á, Fehér T: Induction of steroid binding sites (receptors) and presence of steroid hormones in the unicellular *Tetrahymena pyriformis*. Comp Biochem Physiol 82A: 567, 1985
10. Csaba G, Németh G, Vargha P, Kovács P: Influence of prednisolone and deoxycorticosterone (DOC) on *Tetrahymena*: explanations for receptor "memory" and surface binding. Acta Biol Hung 34: 111, 1983
11. Le Roith D, Liotta AS, Roth J, Shiloach J, Lewis AE, Pert CB, Krieger DT: ACTH and endorphin-like materials are native to unicellular organisms. Proc Natl Acad Sci USA 79: 281, 1982
12. Le Roith D, Shiloach J, Berelowitz M, Frohman LA, Liotta AS, Krieger DT, Roth J: Are messenger molecules in microbes the ancestors of the vertebrate hormones and tissue factors? Fed Proc 42: 2602, 1983
13. Le Roith D, Roberts C, Lesniak MA, Roth J: Receptors for intercellular messenger molecules in microbes: similarities to vertebrate receptors and possible implications for diseases in man. Experientia 42: 782, 1986
14. Roth J, Le Roith D, Shiloach J, Rosenzweig JL, Lesniak MA, Havrankova J: The evolutionary origins of hormones, neurotransmitters and the extracellular messengers. N Engl J Med 306: 523, 1982
15. Svec F, Harrison RW: The intracellular distribution of natural and synthetic glucocorticoids in the AtT-20 cell. Endocrinology 104: 1563, 1979

Acta Morphologica Hungarica, 36 (1—2), pp. 35—46 (1988)

TRANSGANGLIONIC REGULATION OF PRIMARY SENSORY NEURONS*

B. Csillik, Elizabeth Knyihár-Csillik

DEPARTMENT OF ANATOMY, ALBERT SZENT-GYÖRGYI MEDICAL UNIVERSITY, SZEGED, HUNGARY

(Received 2 April 1987)

Structural and functional properties of central terminals of primary sensory neurons are regulated by nerve growth factor supplied by retrograde axoplasmic transport to dorsal root ganglion cells. Two important aspects of this regulatory system: transganglionic degenerative atrophy and regenerative synaptoneogenesis are reviewed in view of electron histochemical, electrophysiological and clinical studies performed during the last decade in the authors' laboratory and abroad.

Keywords: Regulation, nerve growth factor, spinal cord, degeneration, regeneration, pain

Introduction

According to the law of neuronal trophism as it was formulated at the turn of the century, axons and axon terminals are dependent of the trophic substance(s) manufactured by the cell bodies [7]. Thus, whenever a peripheral or a central axon is transected, the distal stump undergoes a series of destructive cytological and electrophysiological changes called axonal or Wallerian degeneration.

According to this concept, also called the trophic entity of the neuron, the cytoplasm or perikaryon is essential for the synthesis of neuroproteins. These are carried distally by axoplasmic flow, so as to replace proteins in the course of the cell's metabolic activity. Therefore, the axon cannot survive long when separated from the perikaryon. Throughout its whole length, the distal stump of the axon becomes swollen and irregular during the first day after transection, crush, or ligation. In mammalian peripheral nerves, the distal stump breaks up into fragments by the 3rd to 5th day. Impulse conduction decreases gradually from the 12th h after transection; it ceases completely at 72 h.

* Supported by Research Grants No. 05-065, No. 1077 and No. Tt 175/86 from the Hungarian Academy of Sciences, and by Grant No. 527 from the Hungarian Ministry of Health

Send offprint requests to: Prof. B. Csillik, Department of Anatomy, H-6701 Szeged, P.O. Box 512, Hungary

At the same time, it has implicitly been assumed that, if the connection of the terminal with the perikaryon was intact, it had no reason to undergo degeneration. In fact, this is the basis of all the microscopic (and electron microscopic) degeneration techniques, often used in hodological research, like the Nauta or Fink-Heimer methods.

On the basis of our light- and electron cytochemical investigations started in the early 70-es [14, 57, 58, 59, 60], performed and in the course of the last decade in this laboratory and confirmed by studies done in other laboratories it became obvious that primary sensory neurons represent a remarkable exception from this general rule. It turned out that whenever the anatomical continuity of the peripheral axon of a dorsal root ganglion cell is interrupted (by a mechanical injury, like transection, crush or ligature), histochemical reactions characterizing axon terminals of primary sensory neurons in the upper dorsal horn, like FRAP (fluoride resistant acid phosphatase), TMPase (thiamine monophosphatase) [23], SP (substance P) [40], lectin-binding carbohydrate epitopes [37, 38, 85] and SSEA (stage-specific embryonic antigens) disappear or more properly, are depleted in the course of days, weeks or months; depletion is followed by fine structural alterations of primary central sensory terminals in this area that bear close resemblance to a slowly proceeding Wallerian degeneration. The term TDA (transganglionic degenerative atrophy) was coined to this process, in order to emphasize (i) its transganglionic character (ii) its similarity to, but distinct difference from, Wallerian degeneration. Also it became obvious that TDA is a transient effect; as soon as the anatomical continuity of the peripheral axon is reestablished by successful regeneration, histochemical marker substances are slowly replenished in the Rolando substance, accompanied by a restitution of the original synaptic circuitry, by means of an axonal regeneration which is unique in the central nervous system.

The objective of the present paper is to summarize the results of our team aiming to reveal the dynamic mechanism underlying TDA and synaptic restitution, and to point out the perspectives in neuroscience opened up by these investigations.

Materials and methods

Experiments were performed on albino rats (R-Amsterdam strain, of both sexes; body weight 200–250 g), and on Macacus rhesus monkeys (both sexes; body weight 8–12 kg). A buffered glutaraldehyde-paraformaldehyde solution was used for transcardial fixation for enzyme histochemical studies; Zamboni's picric acid-formalin for immunohistochemical studies; neutral 4% formalin for lectin histochemical investigation and Rakic' aldehyde fixative for electron microscopic investigations, using a nitrogen-driven pump. FRAP was demonstrated in serial frozen sections by a slightly modified Gömöri technique; TMPase was visualized by a modification of the method of Ogawa et al. (1982). For electron cytochemistry, 30–50 μm thick Vibratome slices, were used; after completing the histochemical reaction

tissue blocks measuring 1 mm^3 or less were excised with a razor blade, postfixed in S-collidine buffered 1% osmic acid, dehydrated in graded alcohols and embedded in Durcupan ACM. Silver interference sections were cut on a Reichert Ultrotome using glass or diamond (Du Pont) knives. Sections were stained with lead citrate and studied under a Tesla 500 or JEM 100 B electron microscope.

Experimental surgery was performed under Nembutal or ether anaesthesia, under semi-sterile (laboratory) conditions in rats and under aseptic conditions in monkeys.

Results

Transganglionic degenerative atrophy

Transganglionic degenerative atrophy (TDA) is a recently discovered trophic phenomenon peculiar to primary sensory neurons that apparently contradicts the neuron theory [8]. When a peripheral sensory axon is damaged (transected, crushed or ligated), dramatic alterations occur not only in the distal stump (Wallerian degeneration), but also in the central terminals of the affected primary sensory neuron. Branches and endings in the spinal cord suffer structural, cytochemical and functional impairments. Obviously related to the metabolic alterations within the perikaryon (manifested in the "axon reaction" or chromatolysis of the Nissl substance), TDA is similar in many respects to a slowly proceeding Wallerian degeneration [3, 4, 45, 46, 48, 53, 54, 80, 91, 92]. The main characteristics of TDA are as follows:

(1) Vesiculolysis which results in an electron lucent terminal axoplasm (light type of TDA), starts on the 4th postoperative day. The electron lucent terminals swell and in later stages, form intricate structures (axon labyrinths) that consist of spirally wound, onion-like, flattened axoplasmic profiles, sometimes containing flattened dendritic and glial profiles. The number of axonal labyrinths is 300/um^2 in the upper dorsal horn, 3 months after transecting the sciatic nerve in the monkey spinal cord.

(2) Shrunken electron-dense osmiophilic terminals (dark type of TDA) are occasionally engulfed by phagocytic glial elements; this is, however, far less common than in the course of Wallerian degeneration.

(3) Depletion of the marker enzymes FRAP [61] and TMPase [63] characterizing nociceptive neurons [50, 81] from a class of primary central terminals in lamina II (in rat and mouse) results in the disappearance of the enzyme positive line characterizing the Rolando substance on days 4–6 after surgery [35, 36, 41, 42, 69, 77].

(4) Depletion of putative transmitter neuropeptides from the afflicted primary afferent terminals occurs in lamina I and II [5, 28, 52, 72].

(5) Depletion of lectin-binding glycoconjugates from a class of primary central terminals occurs in lamina II in humans and in lamina I and II in rodents.

(6) There is an increased latency, decreased amplitude, and reduced duration of the dorsal root potential (DRP); the dorsal root reflex disappears [51, 78, 93].

These alterations characterize the glia-surrounded portions of the central branch and its terminals. The dorsal root proper, where axons are surrounded by Schwann cells, does not show any alterations. The changes in DRP reflect alterations in the synaptic circuitry of the upper dorsal horn rather than in the dorsal root.

TDA can be evoked not only by mechanical injury of a peripheral sensory nerve, but also by blocking retrograde axoplasmic transport by microtubule inhibitors [24, 43]. Extremely small amounts of drugs such as vinblastin, vincristin, vindesin, leurosin and formyl-leurosin, as well as podophyllotoxin and griseofulvin, that do not block anterograde transport and thus do not cause Wallerian degeneration (e.g., 10^{-8} M vinblastin or 10^{-9} M vincristin) are sufficient to induce TDA. Fine structural, histochemical, and electrophysiological consequences of TDA induced by blockers of retrograde axoplasmic transport do not differ in any respect from the TDA induced by mechanical injury of the peripheral axon.

TDA, a reversible process, should not be mistaken for transganglionic degeneration, or for a Wallerian degeneration of dorsal roots and their terminals following cell death in the dorsal root ganglion.

Circumstantial evidence suggests that blockade of the retrograde transport of nerve growth factor (NGF) is responsible for TDA [10, 32, 33, 34, 44, 86].

In sharp contrast to a Wallerian degeneration that follows dorsal rhizotomy, TDA in the upper dorsal horn is a reversible process. As soon as retrograde transport of NGF is reestablished in the peripheral sensory axon, either by axonal regeneration or by cessation of microtubule inhibition, full-scale structural, cytochemical, and functional reorganization takes place, involving reactive synaptoneogenesis.

Regenerative synaptoneogenesis

Regenerative synaptoneogenesis in the upper dorsal horn, also called regenerative proliferation, starts with the formation of axonal growth cones [64] similar to those observed in the course of embryonic development of the spinal cord [22]. Axonal growth cones contain large amounts of smooth endoplasmic (axoplasmic) reticulum which is also present in preterminal myelinated and non-myelinated portions of the reactivated dorsal root axons. Filopodia emanating from axonal growth cones establish synapses with dendritic growth cones of substantia gelatinosa cells; this process leads to a complete restoration of the original fine structure and synaptic connectivity of the upper dorsal horn which had been derailed by the effect of TDA [65, 75].

Regenerative synaptoneogenesis in the upper dorsal horn is accompanied by cytochemical replenishment of primary central afferent terminals. FRAP and TMPase, which were depleted in the course of TDA, reappear again in the regenerating terminals [12, 15, 17, 18, 20, 36, 39]. The same applies also for substance P and lectin-binding glycoconjugates. Repletion of newly formed axon terminals with marker substances takes place not only after a *sensu stricto* regeneration of the peripheral nerve following mechanical injury but also if retrograde axoplasmic transport is reestablished following microtubule inhibition in the respective peripheral nerve. Also functional properties of the formerly incapacitated upper dorsal horn are reestablished: original parameters of the dorsal root potential (latency, amplitude, and duration) gradually return to normal values in the course of regenerative synaptoneogenesis [51, 78]. Circumstantial evidence suggests that regenerative synaptoneogenesis in the upper dorsal horn is subjected to transganglionic regulation by NGF, which is taken up by peripheral receptors at the nerve endings of sensory axons and carried by means of a retrograde axoplasmic transport mechanism to their perikarya in dorsal root ganglia. Here, NGF promotes synthesis of neuroproteins by means of a second messenger.

Discussion

Transganglionic regulation, a relatively recently discovered dynamic and plastic gene expression phenomenon of primary sensory neurons, obviously calls for reassessment of the law of neuronal trophism. It offers a unique model to study neural plasticity and regeneration in the central nervous system [30].

Several characteristic features of TDA clearly indicate the regulatory role of NGF in the maintenance of central terminals, viz:

(1) *TDA is consequence of blockade of axoplasmic transport mechanisms*

This follows from the fact that application around a peripheral nerve of small amounts of microtubule inhibitors induce TDA in the segmentally related ipsilateral Rolando substance [13, 24, 29, 31]. While such small amounts of microtubule inhibitors do not induce Wallerian degeneration in the nerve, higher concentrations of microtubule inhibitors, however, may do so.

(2) *It is the (fast) retrograde component of axoplasmic transport, the blockade of which is responsible for TDA*

Application of 10^{-9} M Vincristin or 10^{-8} M Vinblastin to the dorsal roots does not induce FRAP depletion in the segmentally related upper dorsal

horn. In contrast, transection of the dorsal root, or application of 10^{-3} M Vinca alkaloid around the root, results in a rapid disappearance of the FRAP reaction [27].

(3) *TDA involves only terminal and preterminal portions of central sensory axons; the dorsal root proper is not affected*

Neither transection of the sciatic nerve, nor perineural application of any of the microtubule inhibitors, induce degeneration or atrophy in the Schwann-cell surrounded portion of the dorsal root, either at light or at electron microscope levels [1, 2, 16, 22, 25, 66].

(4) *TDA is not related to the conductivity of the peripheral nerve*

Instillation of local anaesthetics or application of tetrodotoxin around the nerve, do not induce TDA [61, 90]. On the other hand, if TDA was already induced (either by mechanical injury or by a microtubule inhibitor), replenishment of the marker enzyme cannot be obtained by electrical stimulation of the nerve [61].

(5) *TDA is the consequence of failure of nerve growth factor to reach dorsal root ganglion cells*

Applying an anti-NGF serum (raised in goat) in a Gelaspon cuff around the sciatic nerve, results in TDA in the segmentally related ipsilateral upper dorsal horn. In contrast, application of a human anti-D serum does not have any effect [32].

(6) *TDA-inducing effect of Vinca alkaloids is due to blockade of retrograde transport of NGF in the peripheral nerve*

The amount of Vinblastin, needed to block retrograde transport of experimentally injected, radio-labeled ^{125}I-NGF is identical with the threshold amount sufficient to induce TDA [34]. TDA-inducing amounts of Vinblastin and Vincristin cause accumulation of ^{125}I-labeled NGF distally from the site of application and a dramatic decrease in NGF transported to nerve cell bodies in the dorsal root ganglia.

(7) *TDA can be prevented or at least delayed by local application of NGF*

This follows from experiments when NGF was applied at the proximal stump of the transected sciatic nerve [10, 33, 44]. NGF is even more effective

if applied 40–50 h after transection, i.e. when pioneer fibres of regenerating axons have already grown out; these are known to be equipped with NGF receptors [34].

(8) *Polymyxin and Colimycin, two cyclic basic peptides with antibiotic properties, induce TDA after perineural application, via competitive inhibition of NGF*

The TDA-inducing action of these drugs is not related either to histamine release or to interaction with Ca^{2+} in a calmodulin-mediated axoplasmic transport mechanism [86].

(9) *TDA causes a derangement of synaptic transmission in the Rolando substance*

Dorsal root potentials (DRP) undergo marked alterations after blockade of retrograde axoplasmic transport in the peripheral nerve: amplitude is decreased, latency is increased [78, 88, 89]. TDA is accompanied by the increased latency of the lick reflex in the hot plate test [82].

*

An important aspect of transganglionic regulation is that small, dark nerve cells in dorsal root ganglia are more dependent on NGF than the large, pale nerve cells. Subgroups of small nerve cells are known to be involved in nociception, while large nerve cells supply other senses.

It should be noted that in contrast to FRAP and TMPase, depletion of neuropeptides like substance P, somatostatin (and probably also cholecystokinine) in the course of TDA, is never as complete as that of the marker enzymes since neuropeptides are also present in propriospinal nerve cells [72]. Obviously, these are not influenced by TDA, and even may exert compensatory effects, as shown recently by Wall's group [76].

The survival value of TDA to the animal might be that it switches off nociceptive afferentation soon after nerve injury and during the process of peripheral nerve regeneration. Thus, meaningless signals from impaired and incompletely restructured axons are prevented from kindling higher levels of sensory chains.

While the adult mammalian central nervous system is notorious for being refractory in producing new synapses in replacing degenerated ones, it is possible to induce formation of new synapses experimentally. Such reactive synaptogenesis was observed (1) in central monoaminergic neurons after electrolytic lesions [55]; (2) in the dentate gyrus and hippocampus after transection of its afferents [73, 74]; (3) in the olfactory bulb after regeneration of the olfactory nerve [49]; (4) in the ventral horn of the spinal cord,

rostral from the site of transection [6, 47], and (5) in the upper dorsal horn after TDA of central terminals of primary sensory neurons (this paper). Since this last is the only one that occurs in mammals, including primates, whenever an injured peripheral sensory nerve succeeds in regenerating, it is an important proof for the regenerative capacity of the primate (and, in general, the mammalian) central nervous system.

Since TDA can be evoked by applying microtubule inhibitors by iontophoresis to the skin of patients, it offers a non-invasive therapy for the treatment of autochtonous intractable chronic pain syndromes, like postherpetic neuralgia, intercostal neuralgia, meralgia, various polyneuropathies, irradiation-induced brachial plexus lesion, and terminal pain [9, 26, 56, 62, 65, 67, 71, 83, 84]. By disrupting the reverberating circuits in the upper dorsal horn, this treatment results in alleviation of pain for several months and, indeed, as a result of inducing formation of a proper wiring in the course of the subsequent synaptoneogenesis, in many instances it offers permanent pain relief [21, 68].

In addition to microtubule inhibitors, like the Vinca alkaloids, also substances that interfere with NGF, such as polymyxin and colimycin, are the most likely candidates for pain-relieving iontophoretic treatment [32].

Since depletion of neuropeptides, in contrast to FRAP and TMPase, is only partial in the course of TDA, it is evident that the pain-relieving action of iontophoretically administered Vinca alkaloids and basic peptides alike, is not simply due to a cytochemical depletion of central primary sensory terminals. As a working hypothesis it can be assumed that the intrinsic pain-relieving system of the organism, operating with serotoninergic and endorphinergic neurons [11], gets the upper hand after depletion by TDA of neuropeptides [19].

By extrapolation, it can be assumed that essentially similar principles may be operative in the regulation and maintenance also of other cell types of the central nervous system. In this respect, of course, the term transganglionic regulation has to be replaced by the wider concept of "transperikaryal regulation". Prestige [79] suggested long ago that the survival of ventral horn motoneurons is due to a (largely unknown) maintenance factor carried retrogradely by the motor axon to the perikaryon. Kreutzberg [70] demonstrated that the receptive field of the neuron (extension of the dendritic tree) is dependent on the structural and functional integrity of the axon. Recently, Unsicker [87] provided evidence for the existence of several trophic factors in the central nervous system, probably each factor specific for a specific cell type; and it appears that also these factors exert their action by a transperikaryal route. The idea seems germane that, by influencing transperikaryal regulatory mechanisms, embryonic developmental potencies of otherwise stagnant adult central neurons, like axonal growth and synaptogenesis can be revived. Therapeutical

application of this principle might be an important step forward in promoting regeneration of pathways and synaptic circuitries destroyed by pathological events, injuries and accidents.

REFERENCES

1. Aldskogius H, Risling M: Preferential loss of unmyelinated axons in the L7 dorsal root of kittens following sciatic neurectomy. Brain Res 289: 358, 1983
2. Aldskogius H, Cerne H, Holmberg A: The effect of sciatic nerve transection on myelinated fibers in the L5 dorsal root and lumbar dorsal column. A Marchi study in the rat. Anat Embryol 171: 181, 1985
3. Arvidsson J: An ultrastructural study of transganglionic degeneration in the main sensory trigeminal nucleus of the rat. J Neurocytol 8: 31, 1979
4. Arvidsson J, Grant G: Further observations on transganglionic degeneration in trigeminal primary sensory neurons. Brain Res 162: 1, 1979
5. Barbut D, Polak JM, Wall PD: Substance P in spinal cord dorsal horn decreases following peripheral nerve injury. Brain Res 205: 289, 1981
6. Bernstein JJ, Bernstein ME: Axonal regeneration and formation of synapses proximal to the side of lesion following hemisection of the rat spinal cord. Exp Neurol 30: 336, 1971
7. Cajal RY: Degeneration and Regeneration of the Nervous System. University Press, Oxford 1928 p. 750
8. Csillik B: Infrastructure of the neuron. In: Salánki J, Turpaev TM, (eds) Neurotransmitters. Comparative Aspects. Akadémiai Kiadó, Budapest 1980, pp 149–189
9. Csillik B: Histochemistry of pain. Bulletin et Mémoires de l'Académie Royale de Médecine de Belgique 139: 277, 1984
10. Csillik B: Nerve growth factor regulates central terminals of primary sensory neurons. Z mikrosk-anat Forsch 98: 11, 1984
11. Csillik B, Kiss J, Knyihár-Csillik E, Lajtha A: Effect of transganglionic degenerative atrophy on opiate receptors in the dorsal horn of the spinal cord. J Neurosci Res 8: 665, 1982
12. Csillik B, Knyihár E: Degenerative atrophy and regenerative proliferation in the rat spinal cord. Z mikrosk-anat Forsch 89: 1099, 1975
13. Csillik B, Knyihár E: "New" features of the trophical entity. In: Szentágothai J, Hámori J, Vizi ES, (eds) Neuron Concept Today. Symposium, Tihany. Akadémiai Kiadó Budapest 1976, pp 27–38
14. Csillik B, Knyihár E: Histochemistry of synapses. Cell Mol Biol 22: 285, 1977
15. Csillik B, Knyihár E: Biodynamic plasticity in the Rolando substance. Progr Neurobiol 10: 203, 1978
16. Csillik B, Knyihár-Csillik E: Reactions of the substantia gelatinosa Rolandi to injury of peripheral sensory axons. In: Brown AG, Réthelyi M, (eds) Spinal Cord Sensation. Scottish Academic Press, Edinburgh 1981, pp 309– 318
17. Csillik B, Knyihár-Csillik E: Regenerative synaptoneogenesis in the mammalian spinal cord: Dynamics of synaptochemical restoration in the Rolando substance after transganglionic degenerative atrophy. J Neural Transmiss 52: 303 .1981
18. Csillik B, Knyihár-Csillik E: The spinal projection area of primary nociceptive afferents: Regenerative synaptoneogenesis in the Rolando substance. In: Fehér O, Joó F, (eds) Cellular Analogues of Conditioning and Neural Plasticity. Adv Physiol Sci Vol. 36, Akadémiai Kiadó, Budapest 1981, pp 47–56
19. Csillik B, Knyihár-Csillik E: Peptidergic transmission in the Rolando substance: structural basis of the gate theory. Verh Anat Ges 76S, 507, 1982
20. Csillik B, Knyihár-Csillik E: Reversibility of microtubule inhibitor-induced transganglionic degenerative atrophy of central terminals of primary nociceptive neurons. Neurosci 7: 1149, 1982
21. Csillik B, Knyihár-Csillik E: The Pain Clinic. In: Erdmann et al. (eds) VNU Science Press 1985, pp 3–10
22. Csillik B, Knyihár-Csillik E: The Protean Gate. Plasticity of the Primary Nociceptive Analyzer. Akadémiai Kiadó, Budapest 1986
23. Csillik B, Knyihár-Csillik E, Bezzegh A: Comparative electron histochemistry of thiamine monophosphatase and substance P in the upper dorsal horn. Acta Histochem 80: 125, 1986
24. Csillik B, Knyihár-E, Elshiekh AA: Degenerative atrophy of central terminals of primary

sensory neurons induced by blockade of axoplasmic transport in peripheral nerves. Experientia (Basel) 33: 656, 1977
25. Csillik B, Knyihár E, Rakić P: Transganglionic degenerative atrophy and regenerative proliferation in the Rolando substance of the primate spinal cord: discoupling and restoration of synaptic connectivity in the central nervous system after peripheral nerve lesions. Folia Morph 30: 189, 1982
26. Csillik B, Knyihár-Csillik E, Szücs A: Treatment of chronic pain syndromes with iontophoresis of Vinca alkaloids to the skin of patients. Neurosci Lett 31: 87, 1982
27. Csillik B, Knyihár-Csillik E, Tajti J: Blockade of retrograde axoplasmic transport induces transganglionic degenerative atrophy of central terminals of primary nociceptive neurons. Acta Biol Acad Sci Hung 33: 149, 1982
28. Csillik B, Knyihár-Csillik E, Bezzegh A, Kiss J, Léránth Cs, Pór I, Záborszky Z: Transganglionic degenerative atrophy of central terminals of primary sensory neurons after perineural application of Vinblastin: Decay of dorsal root potential and depletion of neuropeptides. In: Chahl LA, Szolcsányi J, Lembeck F, (eds) Antidromic Vasodilatation and Neurogenic Inflammation. Akadémiai Kiadó, Budapest 1984, pp 141–154
29. Csillik B, Knyihár E, Jójárt I, Elshiekh AA, Pór I: Perineural microtubule inhibitors induce degenerative atrophy of central nociceptive terminals in the Rolando substance. Res Comm Chem Path Pharm 21: 467, 1978
30. Csillik B, Knyihár-Csillik E, Pór I, Szücs A, Léránth Cs, Schwab M, Thoenen H: Role of nerve growth factor (NGF) in structural and functional regulation of the primary nociceptive analyzer. Acta Physiol Hung 63: 311, 1984
31. Csillik B, Knyihár E, Szendrei K, Szücs A, Bezzegh A, Kovács A, Pór I, Tajti J, Záborszky Z, Fekete Gy: Effect of microtubule inhibitors on the transcellular regulatory mechanism of primary sensory neurons. Kísérl. Orvostud. 35: 622, 1983 (in Hungarian)
32. Csillik B, Kovács K, Penke B, Tajti J, Szilárd J, Szücs A, Knyihár-Csillik E: Transganglionic effect of basic peptides on the primary nociceptive analyzer. Proc 4th Cong Hung Pharmacol Soc, Budapest, Sect 3: Receptors and Centrally Acting Drugs. Vizi ES, Fürst S, Zsilla G, (eds) Vol 2, 1985
33. Csillik B, Schwab M, Thoenen H: Transganglionic regulation by nerve growth factor of the primary nociceptive analyzer. Neurosci Lett Suppl 14, S79, 1983
34. Csillik B, Schwab M, Thoenen H: Transganglionic regulation of central terminals of dorsal root ganglion cells by nerve growth factor (NGF). Brain Res 331: 11, 1985
35. Devor M, Claman D: Mapping and plasticity of acid phosphatase afferents in the rat dorsal horn. Brain Res 190: 17, 1980
36. Ferencsik M: Dynamism of transganglionic degenerative atrophy following crush injury to the peripheral nerve. Z mikrosk-anat Forsch 100: 3S 490, 1986
37. Fischer J, Csillik B: Lectin binding: A genuine marker for transganglionic regulation of human primary sensory neurons. Neurosci Lett 54: 263, 1985
38. Fischer J, Klein PJ, Csillik B: Ulex europaeus I lectin-binding glycoprotein in primary sensory terminals of human spinal cord. In: Bog-Hansen TC, Breborowicz J (eds) Lectins, Vol 4, Walter de Gruyter & Co, Berlin–New York 1985, pp 117–125
39. Fitzgerald M: The sprouting of saphenous nerve terminals in the spinal cord following early postnatal sciatic nerve section in the rat. J Comp Neurol 240: 407, 1985
40. Fitzgerald M, Gibson SJ: The postnatal physiological and neurochemical development of peripheral sensory C fibres. Neuroscience 13: 933, 1984
41. Fitzgerald M, Swett J: The termination pattern of sciatic nerve afferents in the substantia gelatinosa of neonatal rats. Neurosci Lett 43: 149, 1983
42. Fitzgerald M, Vrbová G: Plasticity of acid phosphatase (FRAP) Afferent terminal fields and of dorsal horn cell growth in the neonatal rat. J Comp Neurol 240: 414, 1985
43. Fitzgerald M, Woolf CJ, Gibson SJ, Mallaburn PS: Alterations in the structure, function and chemistry of C fibres following local application of vinblastine to the sciatic nerve of the rat. J Neurosci 4: 430, 1984
44. Fitzgerald M, Wall PD, Goedert M, Emson PC: Nerve growth factor counteracts the neurophysiological and neurochemical effects of chronic sciatic nerve section. Brain Res 332: 131, 1985
45. Gobel S: An electron microscopic analysis of the transsynaptic effects of peripheral nerve injury subsequent to tooth pulp extirpations on neurons in lamina I and II of the medullary dorsal horn. J Neurosci 4: 2281, 1984
46. Gobel S, Binck JM: Degenerative changes in primary trigeminal axons and in neurons in nucleus caudalis following tooth pulp extirpations in the cat. Brain Res 132: 347, 1977
47. Goldberger ME, Murray M: Restitution of function and collateral sprouting in the rat spinal cord: the deafferentated animal. J Comp Neurol 158: 37, 1974

48. Grant G, Ygge J: Somatotopical organization of the thoracic spinal nerve in the dorsal horn demonstrated with transganglionic degeneration. J Comp Neurol 202: 357, 1981
49. Graziadei PPI, Monti Graziadei GA: Continuous nerve cell renewal in the olfactory system. In: Jacobson M, (ed.) Handbook of Sensory Physiology, Vol IX, Development of Sensory Systems. Springer-Verlag, New York 1978
50. Hanzély B, Knyihár-Csillik E, Csillik B: Fluoride-resistant acid phosphatase (FRAP) activity of nociceptive nerve terminals in the dental pulp. Z mikrosk-anat Forsch 97: 43, 1983
51. Horch KW, Lisney SJW: Changes in primary afferent depolarization of sensory neurones during peripheral nerve regeneration in the cat. J Physiol (Lond) 313: 287, 1981
52. Jessell T, Tsunoo A, Kanazawa I, Otsuka M: Substance P: depletion in the dorsal horn of rat spinal cord after section of the peripheral processes of primary sensory neurons. Brain Res 168: 247, 1979
53. Johnson LR, Westrum LE: Brainstem degeneration patterns following tooth extractions: visualization of dental and periodontal afferents. Brain Res 194: 489, 1980
54. Johnson LR, Westrum LE, Canfield RC: Ultrastructural study of transganglionic degeneration following dental lesions. Exp Brain Res 52: 226, 1983
55. Katzman R, Björklund A, Owman Ch, Stenevi U, West KA: Evidence for regenerative axon sprouting of central catecholamine neurons in rat mesencephalon following electrolytic lesions. Brain Res 25: 579, 1971
56. Kiss Z, Knyihár E, Szücs A, Csillik B: Iontophoretic treatment with neurotubule inhibitors of intolerable limb pain due to diabetic neuropathy (in Hungarian). Magyar Belorvosi Archivum 37: 87, 1984
57. Knyihár E, Csillik B: Axonal labyrinths in the rat spinal cord. A consequence of degenerative atrophy. Acta Biol Acad Sci Hung 27: 299, 1976
58. Knyihár E, Csillik B: Effect of peripheral axotomy on the fine structure and histochemistry of the Rolando substance: Degenerative atrophy of central processes of pseudo-unipolar cells. Exp Brain Res 26: 73, 1976
59. Knyihár E, Csillik B: Representation of cutaneous afferents by fluoride-resistant acid phosphatase (FRAP)-active terminals in the rat substantia gelatinosa Rolandi. Acta Neurol Scand 53: 217, 1976
60. Knyihár E, Csillik B: Regional distribution of acid phosphatase-positive axonal systems in the rat spinal cord and medulla, representing central terminals of cutaneous and visceral nociceptive neurons. J Neural Transmiss 40: 227, 1977
61. Knyihár-Csillik E, Csillik B: FRAP: Histochemistry of the Primary Nociceptive Neuron. In: Progr. Histochem Cytochem Vol. 14: Gustav Fischer Verlag, Stuttgart–New York 1981,
62. Knyihár-Csillik E, Csillik B: Transcutaneously applied microtubule inhibitors induce transganglionic degenerative atrophy of primary central nociceptive terminals. New perspectives in alleviation of pain. Neurosci (Suppl) 7: S47, 1982
63. Knyihár-Csillik E, Bezzegh A, Bőti Zs, Csillik B: Thiamine monophosphatase: A genuine marker for transganglionic regulation of primary sensory neurons. J Histochem Cytochem 34: 363, 1986
64. Knyihár-Csillik E, Rakić P, Csillik B: Fine structure of growth cones in the upper dorsal horn of the adult primate spinal cord in the course of reactive synaptoneogenesis. Cell Tiss Res 239: 633, 1985
65. Knyihár-Csillik E, Rakić P, Csillik B: Reactive synaptoneogenesis in the upper dorsal horn of the adult primate: regenerative or collateral sprouting? In: Goldberger M, Gorio A, Murray M (eds), Development and Plasticity of the Mammalian Spinal Cord FIDIA Res Series Vol III, Liviana Press, Padova 1986
66. Knyihár-Csillik E, Rakić P, Csillik B: Transganglionic degenerative atrophy in the substantia gelatinosa of the spinal cord after peripheral nerve transection in rhesus monkeys. Cell Tiss Res 247: 599, 1987
67. Knyihár-Csillik E, Szücs A, Csillik B: Iontophoretically applied microtubule inhibitors induce transganglionic degenerative atrophy of primary central nociceptive terminals and abolish chronic autochtonous pain. Acta Neurol Scand 66: 401, 1982
68. Knyihár-Csillik E, Szücs A, Pór I, Csillik B: Critical evaluation of a non-invasive therapy of chronic pain syndromes. Neurosci Lett Suppl 14: S200, 1983
69. Kovács A, Ferencsik M: Mapping of spinal projection of primary nociceptive neurones in the rat. Acta Morph Hung 34: 187, 1986
70. Kreutzberg GW: The motoneuron and its microenvironment responding to axotomy. In: Das GD, Wallace RB, (eds) Neural Transplantation and Regeneration. Springer Verlag, New York 1985, pp 271–276

71. Layman PR, Argyras E, Glynn CJ: Iontophoresis of vincristine versus saline in postherpetic neuralgia. A controlled trial. Pain 25: 165, 1986
72. Léránth Cs, Csillik B, Knyihár-Csillik E: Depletion of substance P and somatostatin in the upper dorsal horn after blockade of axoplasmic transport. Histochem 81: 391, 1984
73. Lynch G, Matthews DA, Mosko S, Parks T, Cotman C: Induced acetylcholinesterase-rich layer in rat dentate gyrus following entorhinal lesions. Brain Res 42: 311, 1972
74. Lynch G, Stanfield B, Cotman CW: Developmental differences in postlesion axonal growth in the hippocampus. Brain Res 59: 155, 1973
75. Majumdar S, Mills E, Smith PG: Degenerative and regenerative changes in central projections of glossopharyngeal and vagal sensory neurons after peripheral axotomy in cats: a structural basis for central reorganization of arterial chemoreflex pathways. Neurosci 10: 841, 1983
76. McGregor GP, Gibson SJ, Sabate IM, Blank MA, Christofides ND, Wall PD, Polak JM, Bloom SR: Effect of peripheral nerve section and nerve crush on spinal cord neuropeptides in the rat; increased VIP and PHI in the dorsal horn. Neurosci 13: 207, 1984
77. Mihály A, Pór I, Bencze Gy, Csillik B: Effects of perineurally applied cytostatic, cytotoxic and chelating agents upon peripheral and central processes of primary nociceptive neurons. Z mikrosk-anat Forsch 94: 531, 1980
78. Pór I: Alterations of dorsal root potential in the course of transganglionic degenerative atrophy. Acta Physiol Hung 65: 255, 1985
79. Prestige MC: The control of cell number in the lumbar spinal ganglia during the development of Xenopus laevis tadpoles. J Embryol Exp Morph 17: 453, 1967
80. Risling M, Aldskogius H, Hildebrand C, Remahl S: Effects of sciatic nerve resection on L7 spinal root and dorsal root ganglia in adult cats. Exp Neurol 82: 568, 1983
81. Szőnyi G, Knyihár E, Csillik B: Extra-lysosomal fluorid-resistant acid phosphatase active neuronal system subserving nociception in the rat cornea. Z mikrosk-anat Forsch 93: 974, 1979
82. Szücs A, Csillik B, Knyihár-Csillik E: Functional impairment of the primary nociceptive analyzer in the course of transganglionic degenerative atrophy. Acta Biol Acad Sci Hung 34: 267, 1983
83. Szücs A, Knyihár-Csillik E, Csillik B: Treatment of terminal pain in cancer patients by means of iontophoresis of Vinca alkaloids. Recent Results in Cancer Research 89: 185, 1984
84. Szücs A, Knyihár-Csillik E, Csillik B: Treatment of chronic pain syndromes with iontophoresis of Vinca alkaloids (in Hungarian). Ideggyógyászati Szemle 36: 18, 1983
85. Tajti J, Fischer J, Knyihár-Csillik E, Csillik B: Transganglionic regulation and fine structural localization of lectin-reactive carbohydrate epitopes in primary sensory neurons of the rat. Histochemistry 88: 213, 1988
86. Tajti J, Penke B, Kovács K, Csillik B: Competitive mechanisms of transganglionic degenerative atrophy. Acta Morph Hung (in press)
87. Unsicker K, Skaper SD, Varon S: Developmental changes in the responses of rat chromaffin cells to neurotrophic and neurite-promoting factors. Develop Biol 111: 425, 1985
88. Wall PD: The effect of peripheral nerve lesions and of neonatal capsaicin in the rat on primary afferent depolarization. J Physiol (Lond) 329: 21, 1982
89. Wall PD, Devor M: The effect of peripheral nerve injury on dorsal root potentials and on transmission of afferent signals into the spinal cord. Brain Res 209: 95, 1981
90. Wall PD, Mills R, Fitzgerald M, Gibson SJ: Chronic blockade of sciatic nerve transmission by tetrodotoxin does not produce central changes in the dorsal horn of the spinal cord of the rat. Neurosci Lett 30: 315, 1982
91. Westrum LE, Canfield RC: Light and electron microscopy of degeneration in the brain stem spinal trigeminal nucleus following tooth pulp removal in adult cats. In: Anderson DJ, Matthews B, (eds) Pain in Trigeminal Region. Elsevier, Amsterdam–New York 1977, pp 171–179
92. Westrum LE, Johnson LR, Canfield RC: Ultrastructure of transganglionic degeneration in brain stem trigeminal nuclei during normal primary tooth exfoliation and permanent tooth eruption in the cat. J Comp Neurol 230: 198, 1984
93. Woolf CJ, Wall PD: Chronic peripheral nerve section diminishes the primary afferent A-fibre mediated inhibition of rat dorsal horn neurones. Brain Res 242: 77, 1982

Acta Morphologica Hungarica, 36 (1—2), pp. 47—52 (1988)

PERSONAL MICROCOMPUTER-AIDED THREE-DIMENSIONAL RECONSTRUCTIONS

J. Špaček

DEPARTMENT OF PATHOLOGY, CHARLES UNIVERSITY HOSPITAL, HRADEC KRÁLOVÉ, CZECHOSLOVAKIA

(Received 26 May 1987)

A fast, cheap and simple method is described which enables three-dimensional reconstructions to be produced from short series of sections. The reconstruction is formed and displayed either as a full line or hidden line diagram or shaded model. It may be rotated, magnified or reduced, all with the aid of a personal microcomputer, peripherals and software, the total cost of which does not exceed several hundreds of US dollars.

Introduction

It should be an effort of each microscopist to obtain three-dimensional information from two-dimensional individual or serial sections. This is particularly important for electron microscopists. To obtain such valid information, three-dimensional reconstructions have been used for more than a century in light microscopy [4, 11]. Although computer-assisted graphics has been applied for about the last ten years to make the reconstruction process easier [e.g., 3, 7, 11], only reasonably priced microcomputers made it possible for many microscopists to take advantage of this modern approach.

The total cost of an attainable hardware equipment consisting of a digitizer, microcomputer and a plotter reaches approximately from about ten thousand to several tens of thousands of US dollars [2, 5, 7]. Such a sum may, however, represent a substantial burden on the economic budget in many laboratories. Programs for small personal computers, therefore, have appeared just recently [10].

The purpose of this communication is to direct the attention of microscopists to the fact that it is possible to create satisfactory three-dimensional reconstructions from short series of sections with the aid of a personal microcomputer, peripherals and software, the total cost of which does not exceed a few hundreds of US dollars.

Send offprint requests to: Dr. Josef Špaček, Department of Pathology, Charles University Hospital, CS-500 36 Hradec Králové, Czechoslovakia

Materials and methods

The Sinclair ZX Spectrum (48 K RAM) personal computer, a cassette recorder and home TV set were used as the hardware. The "VU 3D" — a design and modelling commercial program produced specifically for this computer by Psion Ltd., 1982, was used as the software. This elegant program allows to construct objects in three dimensions from section profiles.

Outlines of structures selected from serial sections were redrawn on transparent sheets (cellophane), aligned and provided with two landmarks for mutual orientation (see 8 for the

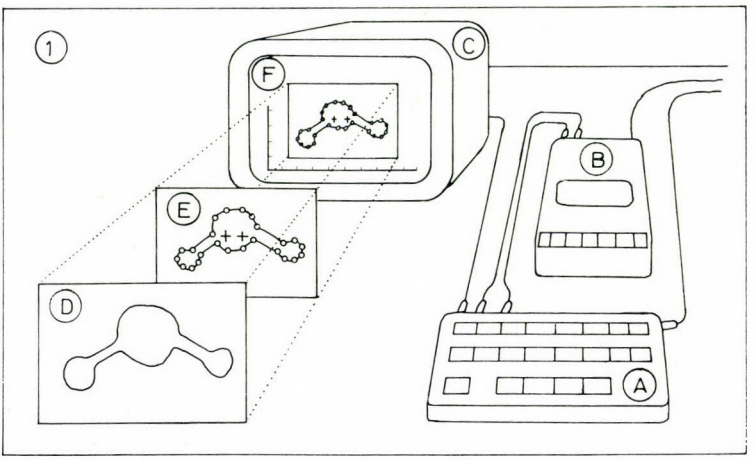

Fig. 1. Personal computer (A), casette recorder (B) and TV set (C) were used as hardware. The selected profile was traced in the form of a polygon from the electron micrograph (D) on the transparent sheet (E) and placed into the coordinate tablet projected on the TV screen (F)

details). The same landmarks were drawn on the TV screen. The sheets with the outlines were fixed in turn on the screen by an electrostatic charge or by scotch tape. Both the sheet and screen landmarks have matched to secure always the same position (Fig. 1). The outlines were traced from the sheets into an X, Y, Z coordinate system point-by-point with the aid of a cursor simply by pressing keyboard buttons. Alternatively, numerical coordinates alone were used to define the points of individual profiles.

Both the cursor and coordinate tablet are being projected on the screen as a constituent part of the VU 3D program (Fig. 2). The traced outline is defined by a set of closed lines forming a polygon. The individual outlines or produced solid objects may be viewed from any angle and any distance using commands for a rotation (Figs 6, 7, 8, 12, 15), magnification (Figs 12, 13, 15) or reduction. Stereoscopic pairs can be produced. The three-dimensional representation is displayed either as a full wire line diagram (Fig. 3), a hidden line diagram (Figs 4, 6, 8, 12, 16) or a shaded solid diagram (Figs 5, 7, 10, 11, 14, 15) each of these in full perspective. Nine directions of a light source are at disposal for the shading. The colour of the object and the background may be chosen from eight possibilities and any individual screen display or the computer data file of the reconstructed object can be stored on the tape and loaded later. When loaded into the Oxford computing art studio program (Rainbird software, 1985) the screen display can be edited in different ways (Figs 13, 17).

Both the hidden line diagram or the solid diagram can serve as a basis for a finer hand-drawn graphic reconstruction (Fig. 9).

No plotter was used in this study. Photographs from TV screen were taken for the documentation.

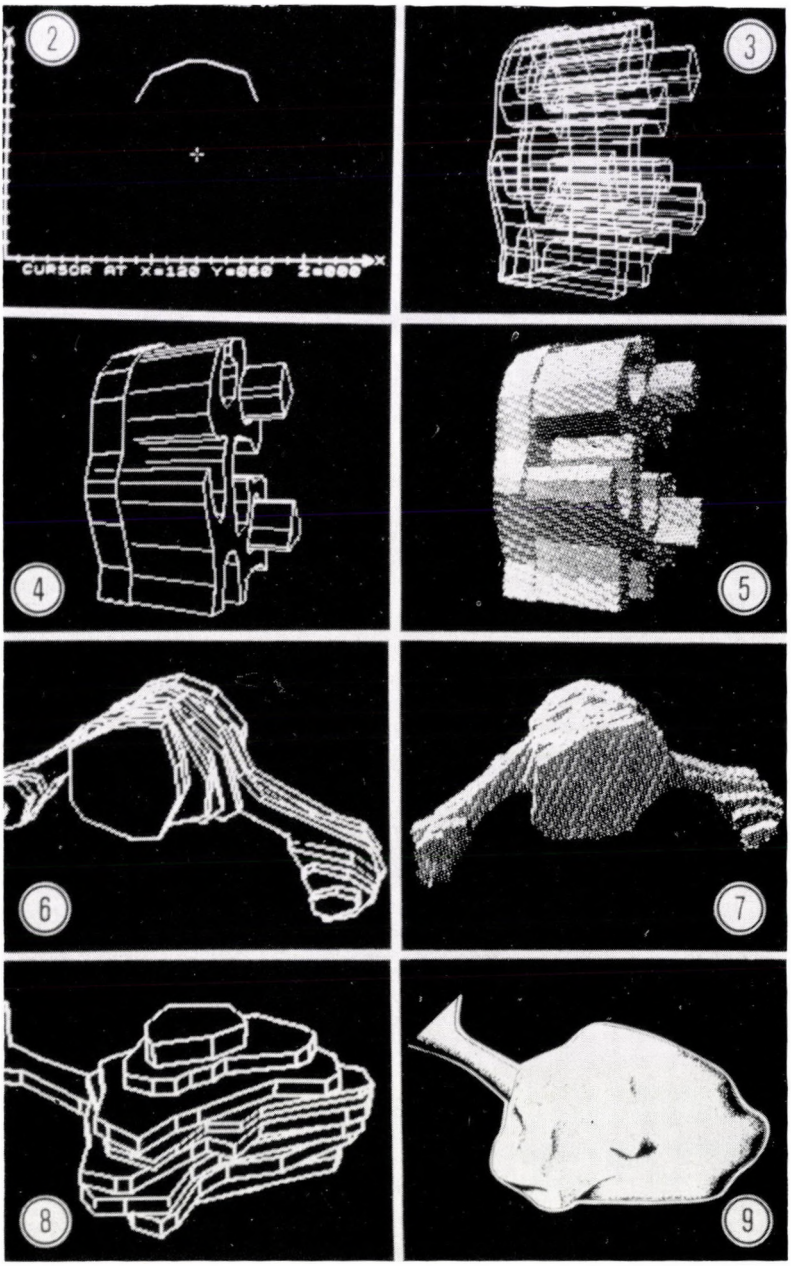

Fig. 2. The cursor and coordinate tablet projected on the TV screen. Part of section profile is also displayed

Figs 3–5. Part of Schwann cell displayed as a full wire line diagram, a hidden line diagram and shaded solid model (cardiac vegetative nerve)

Figs 6–7. Hidden line diagram and shaded solid model of a part of dendritic shaft with two drumstick-shaped dendritic spines (cerebral cortex)

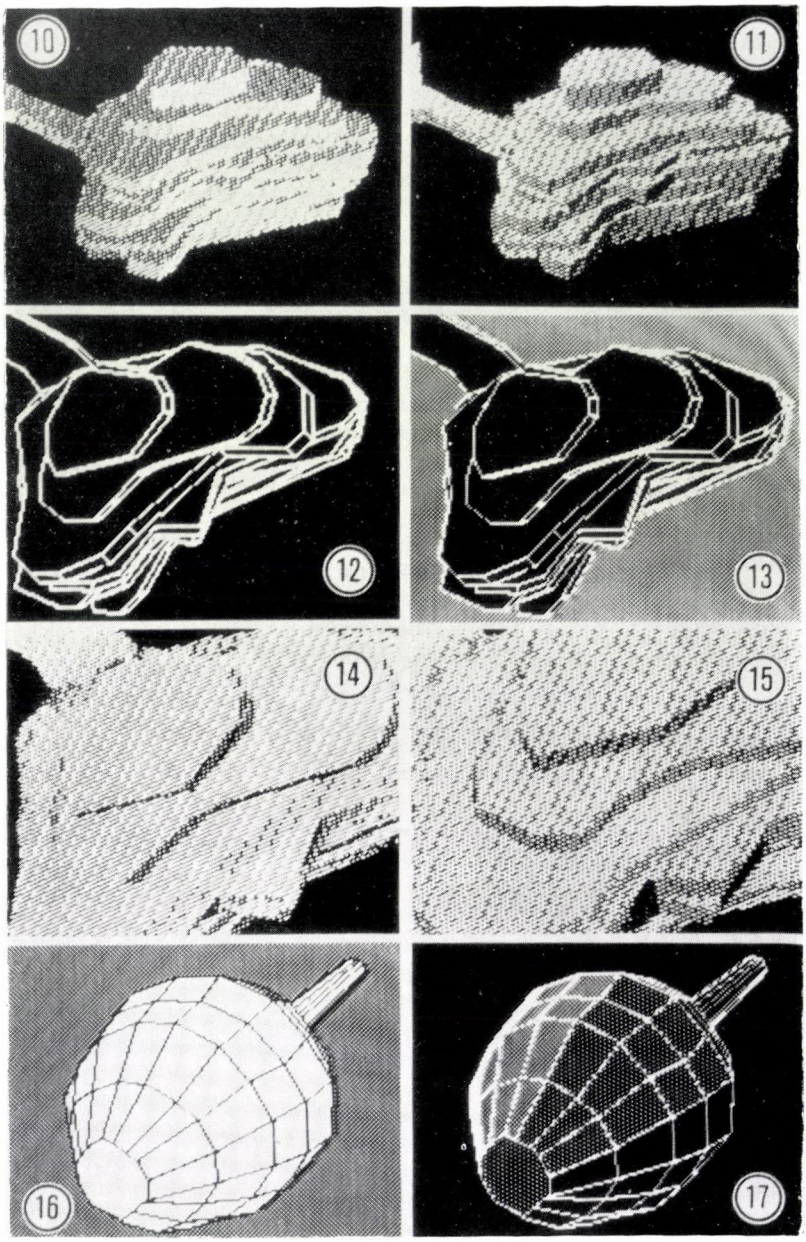

Figs 8–15. Mushroom-shaped dendritic spine displayed as hidden line diagram (8), hand-drawn graphic reconstruction (9), and shaded solid models. Direction of light source was from lower right (10) and from upper left (11). The spine was rotated (12), edited using art studio program (raster background in 13) and magnified (14, 15). The spinule is more prominent in rotated displays (12–15)

Figs 16, 17. Hidden line diagram of a drumstick-shaped dendritic spine constructed from a series of circular profiles (cerebral cortex). Shading edited by art studio program shown in Fig. 17

Results

Some of the results achieved with the method described above are shown in a variety of displays on the screen photographs (Figs 3–17) and explained in the figure legends. All of them represent small objects reconstructed from series of electron micrographs of the nervous tissue: a part of a Schwann cell from a cardiac autonomic nerve (Figs 3–5) and dendritic spines (Figs 6–17) from the cerebral cortex.

Discussion

A hand-made geometrical tilting and rotation of section profiles is a method requiring many working hours in addition to the fact that it may be a source of possible inaccuracies. Thus, if nothing more but a possibility of the rotation of individual profiles was offered by the small personal computer and VU 3D program, it would be worth of attention. It is therefore admirable that this program includes even the construction of graphic models including the enhancing effect of hidden lines removal and on the top of it — the shading.

There are, of course, many limitations resulting from the low capacity of memory of the used computer. The reconstruction program requires at least 64 kB of random access memory [5]. When the computer with only 48kB of RAM is used, as in our case, the program itself engages as much as 46 kB. The remaining free capacity is very small and, according to our calculations, it allows to receive not more than about 270 points only. Thus, either short series of small uncomplicated outlines are convenient for this program, or the series must be divided into several parts, each of them to be processed separately. Series with profiles of the same shape are especially suitable (Figs 16, 17). Another disadvantage is that the computer stacks the outlines in a plate-like form, which doubles the amount of entered points and further limits the free capacity of the memory. The number of points per profile should be, therefore, as small as possible. Neither surface and volume calculations can be done using the VU 3D program, nor more than one colour may be used in one model. The raster used for the shading is rather coarse-grained, too.

All these disadvantages cause that the created reconstructions are hardly comparable with first-class examples of computer graphics in this field [e.g. 1, 6, 9]. We suppose, however, that the reached results entitle us to conclude that the described method is, in the case of inaccessibility of more efficient equipment, highly recommendable.

Acknowledgements

The author wishes to thank Blanka Špicarová and David Špaček for their technical assistance.

REFERENCES

1. Baba N, Naka M, Muranaka I, Nakamura S, Kino I, Kanaya K: Computer-aided stereographic representation of an object reconstructed from micrographs of serial thin sections. Micron and Microscopica Acta 15: 221, 1984
2. Braverman MS, Braverman IM: Three-dimensional reconstructions of objects from serial sections using a microcomputer graphics system. J Invest Dermatol 86: 290, 1986
3. Elias H, Hyde DM: A Guide to Practical Stereology. Karger, Basel and New York 1983
4. Gaunt WA, Gaunt PN: Three-dimensional Reconstruction in Biology. University Park Press, Baltimore 1978
5. Johnson EM, Capowski JJ: Principles of reconstruction and three-dimensional display of serial sections using a computer. In: Mize RR, (ed.) The Microcomputer in Cell and Neurobiology Research. Elsevier Science Publishing Co., New York 1985, pp 249
6. Lacy ER, Reale E, Schlusselberg DS, Smith WK, Woodward DJ: A renal contercurrent system in marine elasmobranch fish: a computer-assisted reconstruction. Science 227: 1351, 1985
7. Moens PB, Moens T: Computer measurements and graphics of three-dimensional cellular ultrastructure. J Ultrastr Res 75: 131, 1981
8. Špaček J, Lieberman AR: Three-dimensional reconstruction in electron microscopy of central nervous system. Sbor Věd Prací LFUK v Hradci Králové 17: 203, 1974
9. Thompson RP, Wong YMM, Fitzharris TP: A computer graphic study of cardiac truncal septation. Anat Rec 206: 207, 1983
10. Tolivia J, Tolivia D, Alvarez-Uría M: A three-dimensional reconstruction program for personal computer. J Neurosci Meth 17: 55, 1986
11. Ware RW, Lo Presti V: Three-dimensional reconstruction from serial sections. Int Rev Cytol 40: 325, 1975

Acta Morphologica Hungarica, 36 (1—2), pp. 53—61 (1989)

PATHOGENESIS OF LIMB AND FACIAL MALFORMATIONS INDUCED BY PYRIMETHAMINE IN THE RAT*

C. HORVATH[1], A. M. TANGAPREGASSOM[1], M. J. TANGAPREGASSOM[1], M. TRECUL[1], M. BOUCHER-EHRENSPERGER[2], A. COMPAGNON[1], C. PETTER[1]

[1] LABORATORY OF PHYSIOPATHOLOGY OF DEVELOPMENT, UNIVERSITY "PIERRE ET MARIE CURIE", PARIS AND
[2] BIOLOGY OF REPRODUCTION UNIVERSITY PARIS VII., PARIS, FRANCE

(Received 28 May 1987)

The temporal sequence of morphological events resulting in limb and face malformations was studied in pyrimethamine (PY) treated female rats. 30 mg/kg of PY in a 10 ml/kg suspension of 0.9% NaCl were administered i.p. on days 12, 13 and 14 of gestation. Controls received only 0.9% NaCl solution. The females were killed at different stages of gestation (between 14 and 21 days). Early PY treated embryos showed mainly haematomas in the extremities and the mandibulo-maxillary areas. During the course of gestation, fewer haematomas and more malformations were observed. At term, malformations were observed in the same localisations where haematomas were previously seen.

Keywords: Pyrimethamine, congenital malformation, acid, antagonist rat

Introduction

In general, studies in teratology only deal with congenital malformations at term. Only little has been published on the morphological events at different stages of development in animals and in human beings [1, 13, 15, 28, 35]. The purpose of the present work was to study the teratogenesis of face and limb malformations during development in rats induced by pyrimethamine. Our previous experiment has shown that pyrimethamine (PY) induced red cell macrocytosis resulting in haemorrhages in the limb extremities [19]. PY is a well-known powerful teratogenic agent with an antifolic action. In addition, the experimental malformations were similar to those observed in clinics induced by antifolic agents [12, 26, 29, 30, 34]. Therefore, PY was used as a tool to study the morphogenesis of limb and facial malformations.

* This investigation was supported in part by C.N.R.S. (France) U.A. No. 307, and Fondation pour la Recherche Médicale

Send offprint requests to: Dr. C. Horvath, Laboratoire de Physiopathologie du Developpement, Université Pierre et Marie Curie; 4, Place Jussieu 75252 Paris Cedex 05, France

Materials and methods

Virgin female Wistar rats (Janvier, France), 80 to 100 days old weighing 180–210 g were mated with males of the same strain and age. Food (UAR, France) and water were available *ad libitum*. One male was housed overnight with three to five females. The initial time was considered to be the beginning of day 0. The females were controlled by weighing and palpation to verify for gestation on day 12. The pregnant females were randomly assigned to the control and PY groups. 30 mg of PY was dispersed in 10 ml sterile physiological saline. 30 mg/kg/day PY was administered intraperitoneally at 9 a.m. on day 12, 13, and 14 of gestation. The females were observed and weighed throughout gestation. The females were sacrificed at 8 different stages at 4 p.m. between days 14 and 21 of gestation and the uteri were examined. The number of live foetuses, the number of early and late resorptions and their location in each uterine horn were noted. All foetuses were weighed and examined for external anomalies. The 14 to 17 days old foetuses were preserved in Bouin's fixative. Half the foetuses from each litter of 18 to 21 days old were fixed in Bouin's fluid in order to allow a later dissection for visceral malformations under a low-power microscope. Some of them were histologically examined in serial sections. The other half were fixed in 96% ethanol and subsequently stained with alizarin red S and blue alcian for a later skeletal examination. Only the external malformations are discussed in the present study. The visceral and skeletal malformations will be described in forthcoming papers. The effects of PY on various days of gestation were analyzed.

Table I

Effect of pyrimethamine on litters of pregnant females examined on days 14–21 of gestation

Sacrifice day	Group	Litters No.	Implant Sites No.	Mortality; %	Total live No.	Live abnormal, %	Mean litter weight g ± S.E.
14	C	5	62	6.45	58	0	0.13 ± 0.01
	PY	4	31	3.22	30	3.33	0.15 ± 0.04
15	C	5	52	7.69	48	0	0.23 ± 0.01
	PY	6	75	6.66	70	20	0.18 ± 0.03
16	C	6	66	7.57	61	0	0.42 ± 0.01
	PY	6	55	1.80	54	83.33	0.32 ± 0.03
17	C	7	69	2.90	67	0	0.75 ± 0.03
	PY	9	85	23.53	63	100	0.42 ± 0.04
18	C	5	44	18.13	36	0	1.26 ± 0.04
	PY	6	64	10.93	57	100	0.67 ± 0.06
19	C	6	56	11.71	50	0	2.01 ± 0.08
	PY	5	55	7.27	51	100	1.17 ± 0.18
20	C	8	79	13.92	68	0	3.38 ± 0.10
	PY	5	54	9.26	49	100	1.22 ± 0.17
21	C	5	48	6.25	45	0	4.94 ± 0.09
	PY	5	57	7.02	53	100	1.92 ± 0.19

C = control groups. The mothers were treated with 0.9% NaCl (10 ml/kg/d) i.p. on days 12, 13 and 14 of gestation.

PY = pyrimethamine treated groups. The mothers were treated with PY (30 mg/kg/d) i.p. on days 12, 13 and 14 of gestation.

No significant difference in any comparison of the foetal mortality between control and PY treated groups by chi-square test.

Significant difference of the foetal weight % from control in all PY treatment group $p < 0.001$.

Results

PY was very little toxic as evidenced by virtually no weight loss and by the generally healthy appearance of the treated females. Table I summarizes the effect of PY on average foetal weight, the number of resorptions and malformed foetuses. The mean foetal weight was lower in the PY-treated groups at each gestation day excepting day 14. There was no difference in foetal mortality rates between the control and PY-treated groups. No abnormalities were found in the control groups.

Table II summarizes the frequency and types of external abnormalities observed at different days of gestation. The study was carried out on a total of 433 control and 403 treated embryos/foetuses. No malformations were observed on day 14 and 15 of gestation. Only 1 embryo had haematomas of the extremities and the mandibular area on day 14 of gestation. Haematomas were more frequent between the digital plates of the extremities, and in the maxillary region in 15-day-old foetuses. The haematomas occurred earlier and were more severe in the hindlimbs than in the forelimbs (Fig. 1B). The most serious haematomas and the highest percentage were seen on day 17 of gestation (Fig. 2). During the course of gestation, fewer haematomas and more malformations were observed. Mandibulo-maxillary malformations (micrognathia, agnathia, malposition of the external ears, open eyes, cleft palate) and limb malformations were observed. Of particular interest is the mainly

Table II

Frequency of various external abnormalities due to pyrimethamine in foetuses examined on days 14–21 of gestation

	Sacrifice day							
	14	15	16	17	18	19	20	21
No. foetuses examined	30	70	54	61	47	46	42	53
Haematomas %								
forelimbs	3.3	1.42	12.96	40.98	42.55	45.65	7.14	11.32
hindlimbs	3.3	20.00	44.44	63.93	8.51	19.56	2.38	—
mandibular part	3.3	1.42	—	—	—	—	—	—
maxillary part	4.9	4.9	12.96	21.31	10.63	8.69	4.76	—
Malformations %								
forelimbs	—	—	9.26	80.32	57.45	50.00	100.00	83.02
hindlimbs	—	—	38.89	50.32	100.00	76.09	100.00	100.00
mandibular area	—	—	—	100.00	100.00	100.00	100.00	100.00
eyes	—	—	—	—	34.04	2.17	7.14	3.77
ears	—	—	—	—	—	—	9.52	3.77
oedema	—	—	44.44	93.44	100.00	36.95	76.19	33.96
tail	—	—	18.81	100.00	38.29	58.69	97.62	100.00

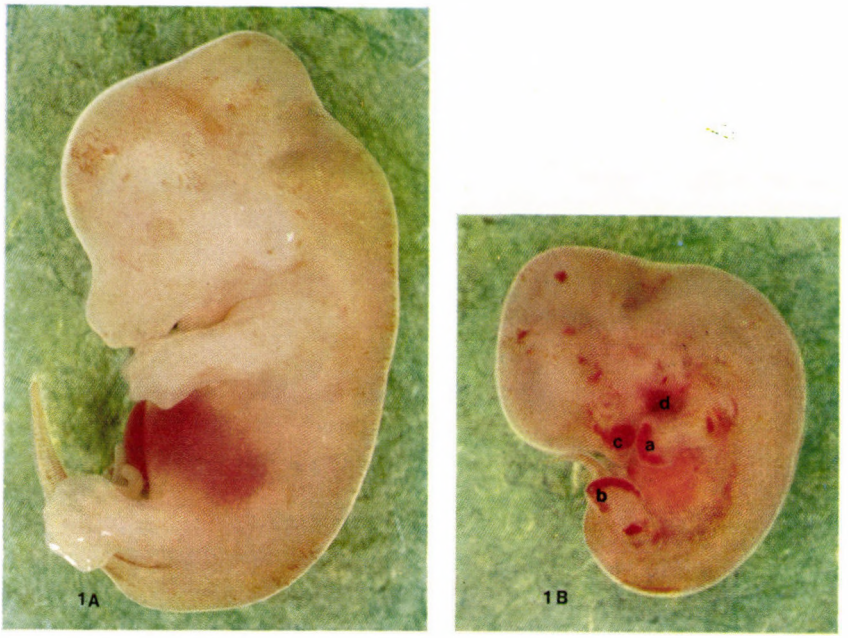

Fig. 1A. Lateral view of a 15-day-old control foetus
Fig. 1B. Lateral view of a 15-day-old abnormal foetus from a mother treated with PY showing haematomas in forelimbs (a), in hindlimbs (b) and in the mandibulo-maxillary areas (c, d)

symmetrical manifestation of the malformations. The hindlimbs were more seriously affected than the forelimbs. Syndactyly, aphalangy, ectrodactyly were mainly observed in the forelimbs and phocomelia, meromelia in the hindlimbs; short, kinky tail was generally observed at the latest stages of gestation (Fig. 3). Usually, several defects were combined in the same specimen.

Discussion

The sequence of morphological events was studied to understand the genesis of limb and facial malformations induced by PY treatment. Embryos examined at 14 and 15 days of gestation exhibited haematomas mainly in the limbs and in the mandibulo-maxillary area. After day 15, haematomas and malformations were also observed. At term, malformations were found in the above regions. This sequence suggests that the haematomas seen at earlier developmental stages led to the malformations observed at later stages of development.

Haematomas are teratogenically important since they can induce the abnormal development of contiguous structures.

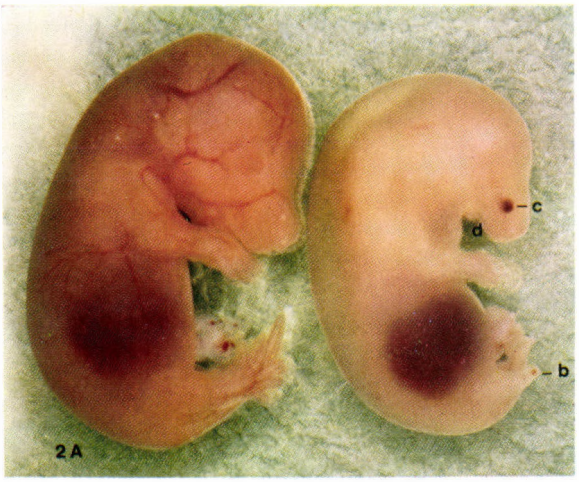

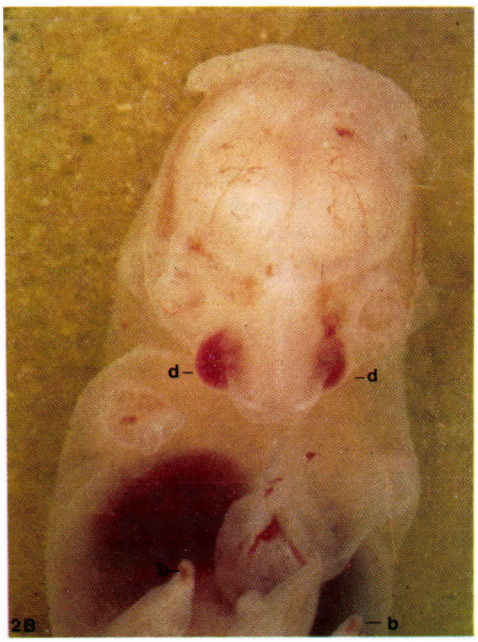

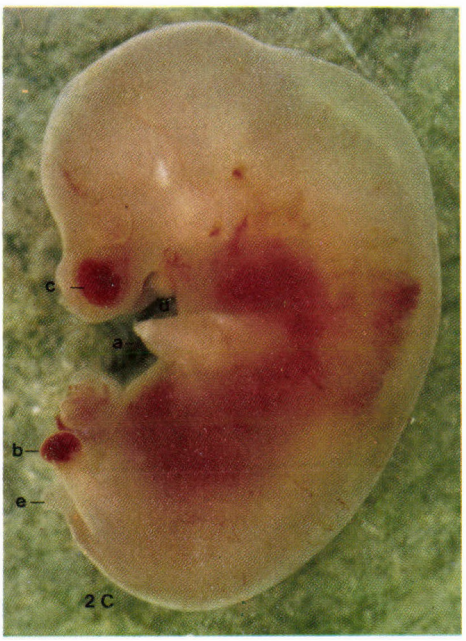

Fig. 2A. Lateral view of a 17-day-old control foetus (left) and abnormal foetus (right) showing haematomas in hindlimbs (b) and in the maxillary area (c). Note the micrognathia (d) already developed at this stage and a generalized oedema

Fig. 2B. Ventral view of a 17-day-old abnormal foetus showing symmetrically formed haematomas in the maxillary areas (d) as well as in the peromelic hindlimbs (b)

Fig. 2C. Lateral view of a 17-day-old abnormal foetus showing peromelic forelimbs (a), peromelic hindlimbs with haematomas (b). Note haematoma in the maxillary area (c), agnathia (d), short kinky tail (e) and generalized oedema

Kalter and Warkany [11] observed large haematomas on the snout of mouse foetuses subjected to riboflavin-deficient, galactoflavin-containing diets. They observed that haematomas interfered with the osteogenesis of the nasal and premaxillary areas and led to malformations. Hamburgh [9] observed caudal haematomas in mouse embryos after treatment of the mothers with trypan blue and suggested that these haematomas might have a destructive effect leading to malformations of the tail. Ferm and Carpenter [3] showed that lead salts produced caudal haematomas during early morphogenesis followed by tail and sacral malformations in the golden hamster. Haematoma is the most common consequence of hypoxia or anoxia [4, 5, 7, 8]. One of the most plausible causes of vascular rupture is high blood pressure and physiological changes in the bloodstream [5, 7, 8, 20]. Hypoxia may result from a blood disorder or the presence of abnormal haemopoietic cells. A predominance of red blood cell macrocytosis and abnormal immature megakaryoblastic cells were observed in the br/br rabbit and the hd/hd rat during the sensitive stages of limb development [2, 22, 23]. These authors concluded that abnormal haemopoietic cells induced hypoxia followed by haemorrhages in the mesenchymal tissue, leading to haematomas, necrosis, thrombosis and amputations. Treatment with hyperoxia, phenylhydrazine, folic acid + vitamine B12 partly prevented foetal blood cell macrocytosis as well as congenital malformations.

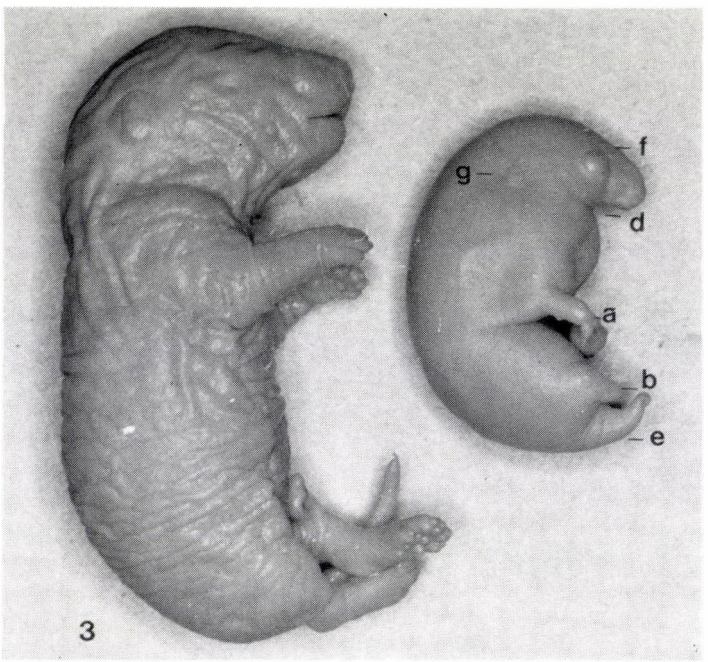

Fig. 3. Lateral view of a 21-day-old control (left) and an abnormal foetus (right) showing ectrodactyly (a), peromelia (b), agnathia (d), short kinky tail (e), open eyes (f) and malposition of external ear (g). The foetuses were fixed in Bouin's fluid. ×2.5

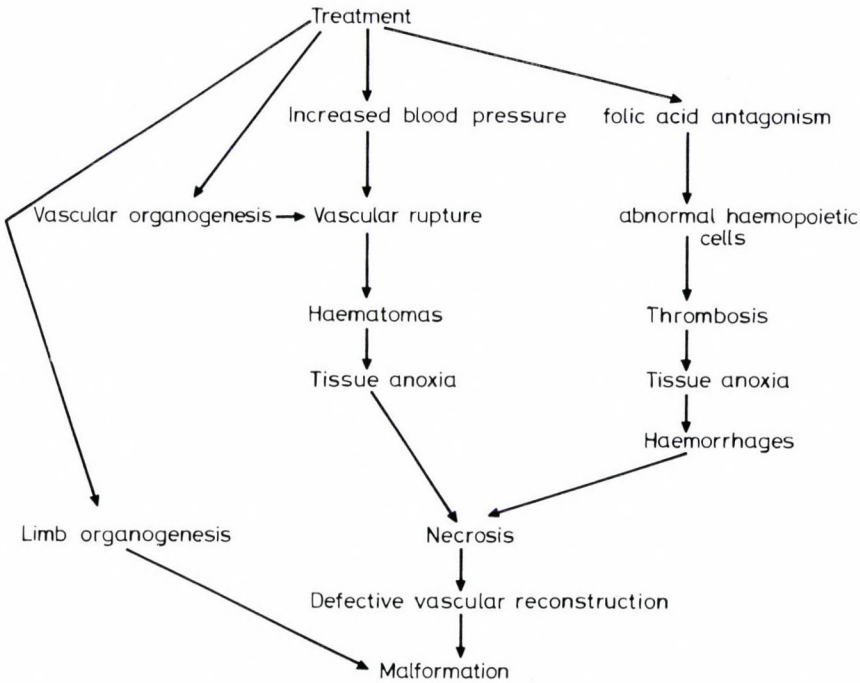

Fig. 4. Hypothesis of the pathogenesis of PY-induced limb and face malformations

According to Tangapregassom et al [27], PY induces vascular alterations resulting in haemorrhages and haematomas. At term, they observed rudimentary vessels in the affected areas. Figure 4 shows possible pathogenetic mechanisms of PY-induced malformations

The anomalies produced by folic acid antagonists in laboratory animals are strikingly similar to those observed in man [10, 29, 31, 32]. Our study concerning the sequence of morphological events beginning with a teratogenie treatment resulting in malformations at term might be helpful to clarify thc teratogenic mechanism of drugs having an antifolic action in human beings.

Acknowledgements

The authors gratefully acknowledge the expert assistance of Jean Nicolas and Jeannine Lemesle in the technical preparation of the work.

REFERENCES

1. Diewert VM: A morphometric analysis of craniofacial growth and changes in spatial relations during secondary palatal development in human embryos and fetuses. Am J Anat 167: 495, 1983
2. Ehrensperger M, Petter C, Keuky L: Foetal megakaryoblastic abnormality associated with congenital limb amputation in the br/br rabbit. Embryol Exp Morph 62: 109, 1981

3. Ferm VH, Carpenter SJ: Developmental malformations resulting from the administration of lead salts. Exp Mol Pathol 7: 208, 1967
4. Gosseye S, Golaire MC, Larroche JC: Cerebral, renal and splenic lesions due to fetal anoxia and their relationship to malformations. Dev Med Child Neurol 24: 510, 1982
5. Grabowski CT: The etiology of hypoxia-induced malformations in the chick embryo. J Exp Zool 157: 307, 1964
6. Grabowski CT: Physiological changes in the bloodstream of chick embryos exposes to teratogenic doses of hypoxia. Develop Biol 13: 199, 1966
7. Grabowski CT, Schroeder RE: A time-lapse photographic study of chick embryos exposed to teratogenic doses of hypoxia. J Embryol Exp Morph 19: 347, 1968
8. Grabowski CT, Tsai ENC, Toben HR: The effects of teratogenic doses of hypoxia on the blood pressure of chick embryos. Teratology 2: 67, 1969
9. Hamburgh M: The embryology of trypan blue induced abnormalities in mice. Anat Rec 119: 409, 1954
10. Harpey JP, Darbois Y, Lefevre G: Teratogenicity of Pyrimethamine. Lancet 2: 399, 1983
11. Kalter H, Warkany J: Congenital malformations in inbred strains of mice induced by riboflavin-deficient, galactoflavin-containing diets. J Exp Zool 136: 351, 1957
12. Meltzer HJ: Congenital anomalies due to attempted abortion with 4-aminopteroylglutamic acid. JAMA 161: 1253, 1956
13. Milaire J: Etude morphogénétique de la syndactylie postaxiale provoquée chez le rat par l'Hadacidine. I. Analyse des anomalies chez l'adulte, le foetus à terme et les embryons de 15, 16 et 17 jours. Arch Biol (Liège) 80: 167, 1966
14. Murakami U, Kameyama Y, Majima A, Sakurai T: Patterns of radiation, malformations of the mouse foetus and subjected stage of development. Ann Res Inst Environ Med 2: 71, 1961
15. Nishimura H, Takano K, Tanimura T, Yasuda M, Uchida T: High incidence of several malformations in the early human embryos as compared with infants. Biol Neonat 10: 93, 1966
16. Petter C: Foetal blood abnormality associated with hypodactyly in the hd strain of rat. Experientia 32: 1592, 1976
17. Petter C: Early foetal thrombosis induced by thalidomide in mouse: possible explanation for teratogenicity. Experientia 33: 1384, 1977
18. Petter C: DPH-induced macrocytosis in the 14 day rat foetus. Experientia 35: 1493, 1979
19. Petter C, Bourbon J: Foetal red cell macrocytosis induced by Pyrimathamine: its teratogenic role. Experientia 31: 369, 1975.
20. Petter C, Bourbon J, Maltier JP, Jost A: Production d'hémorragies des extrémités chez le foetus de rat soumis à une hypoxie in utero. CR Acad Sc Paris 272: 2488, 1971
21. Petter C, Bourbon J, Maltier JP, Jost A: Prevention des amputations congénitales héréditaires du Lapin par une hyperoxie maternelle. CR Acad Sc Paris 273: 2639, 1971
22. Petter C, Bourbon J, Maltier JP, Jost A: Hématies primordiales et amputations congénitales chez les foetus de lapin porteurs du gène br. CR Acad Sc Paris 277: 801, 1973
23. Petter C, Bourbon J, Maltier JP, Jost A: Simultaneous prevention of blood abnormalities and hereditary congenital amputations in a brachydactylous rabbit stock. Teratology 15: 149, 1977
24. Petter C, Boucher-Ehrensperger M, Trecul M, Horvath C: Is fetal necrosis responsible for multiple malformations after Pyrimethamine treatment? Teratology 29: (30A), 1984
25. Shaw EB: Fetal damage due to maternal aminopterin ingestion follow-up at age 9 years. Am J Dis Child 124: 93, 1972
26. Shaw EB, Steinbach HL: Aminopterin-induced fetal malformations: survival of infant after attempted abortion. Am J Dis Child 115: 477, 1968
27. Tangapregassom AM, Tangapregassom MJ, Horvath C, Trecul M, Boucher-Ehrensperger M, Petter C: Vascular anomalies and Pyrimethamine-induced malformations in the rat. Teratogenesis Carcinog Mutagen 5: 56, 1985
28. Tassin MT, Salzgeber B, Guenet JL: Studies on "repeated epilation" mouse mutant embryos: I. Development of facial malformations. J Craniofacial Gen Dev Biol 3: 289, 1983
29. Thiersch JB: Therapeutic abortions with folic acid antagonist 4-aminopteroylglutamic acid (4-amino P.G.A.) administered by the oral route. Am J Obstet Gynecol 63: 1298, 1952
30. Thiersch JB, Phillips FS: Effect of 4-aminopteroylglutamic acid (aminopterin) on early pregnancy. Proc Soc Exp Biol Med 74: 204, 1950
31. Van Allen MI: Fetal vascular disruptions: Mechanisms and some resulting birth defects. Ped Ann 10: 219, 1981

32. Warkany J: Aminopterin and methotrexate: folic acid deficiency. Teratology 17: 353, 1978
33. Warkany J: Teratogenicity of folic acid antagonists. Cancer Bull 33: 76, 1981
34. Warkany J, Beaudry PH, Hornstein S: Attempted abortion with aminopterin (4-aminopteroylglutamic acid). Am J Dis Child 97: 274, 1959
35. Wilson JG, Roth CBW, Warkany J: An analysis of the syndrome of malformations induced by maternal vitamin A deficiency. Effects of restoration of vitamin A at various times during gestation. Am J Anat 92: 189, 1953

Acta Morphologica Hungarica, 36 (1—2), pp. 63—77 (1988)

SOME EPIDEMIOLOGICAL CHARACTERISTICS OF DOWN'S SYNDROME IN HUNGARY

E. Czeizel

DEPARTMENT OF HUMAN GENETICS AND TERATOLOGY — WHO COLLABORATING CENTRE FOR THE COMMUNITY CONTROL OF HEREDITARY DISEASES, NATIONAL INSTITUTE OF HYGIENE, BUDAPEST, HUNGARY

(Received 21 July 1986)

Down's syndrome seems to be an adequate indicator condition of germinal numerical chromosome mutation. The true birth prevalence of Down's syndrome was 1.2 ± 0.1 per 1000 total births in Hungary 1973–1982. The rate of undernotification and misdiagnosis was 25% and 5%, resp. A significant deviation was detected in the occurrence of Down's syndrome in twenty territorial-administrative units of Hungary due to the different ascertainment. The maximum figures may represent the true birth prevalence. No significant monthly variation, i.e., seasonality was found in the birth of Down's syndrome. A Surveillance of Down's syndrome was established in 1980 based on the Hungarian Congenital Malformation Registry.

Keywords: Down's syndrome, birth prevalence, seasonality, surveillance

Introduction

Down's syndrome has been known as a clinical pattern since Langdon Down described this congenital anomaly syndrome in 1866 [12]. In 1958 Lejeune, Gauthier and Turpin detected the first human chromosome aberration type, a small extra acrocentric chromosome in group G, i.e., chromosome 21 in the cells of patients with Down's syndrome and published their paper in 1959 [27]. Later the Robertsonian translocated forms of chromosome 21 in Down's syndrome were also observed. After the introduction of chromosome banding techniques the triplication of q21.2 segment of chromosome 21 was proved as a direct cause of Down's syndrome.

Four sources of information concerning Down's syndrome are available in Hungary:

1. The Hungarian Congenital Malformation Registry (HCMR) [3] based on the obligatory notifications of malformed newborn infants diagnosed from the birth till the age of one year and the prenatally diagnosed malformed fetuses.

2. The Case-Control Surveillance System of Congenital Anomalies which incorporates the Down's syndrome as a positive control group [8].

Send offprint request to: Dr. E. Czeizel, National Institute Hygiene, 1966 Budapest, Gyáli út 2–6, Hungary

3. The Hungarian Registry of Chromosome Aberrations [2] which involves only cytogenetically verified cases of trisomy 21 without age limitation based on the data of cytogenetic laboratories.

4. Some supplementary studies connected with the material of the HCMR [22, 41] and some other Hungarian studies [24, 35].

The birth prevalence of Down's syndrome in Hungary

The recorded annual birth prevalences of Down's syndrome in the HCMR are demonstrated in Table I. On the one hand the first two years of the HCMR had a considerable undernotification. On the other hand there is a recent decrease in the birth prevalence of Down's syndrome due to the increasing trend of prenatal fetal diagnosis in women over 38. The recorded birth prevalence of Down's syndrome was 0.85 per 1000 total births between 1970 and 1984, but 0.91 per 1000 total births in the period of 1973–1982. Annual birth prevalences of Down's syndrome had a relatively narrow range (0.85–0.98)

Table I

Pregnancy outcome and sex ratio of index patients affected by notified Down's syndrome in Hungary, 1970–1984

Year	Livebirth			Stillbirth		Total		Male	Female	Sex ratio
	No.	(No.	%)**	No.	%	No.	%			
1970*	95	20	21.1	0	—	95	0.62	52	43	0.547
1971	111	16	14.4	0	—	111	0.73	50	61	0.450
1972	128	12	9.4	0	—	128	0.83	71	57	0.555
1973*	137	18	13.1	1	0.7	138	0.88	70	68	0.507
1974	173	18	10.4	2	1.1	175	0.93	100	75	0.571
1975	160	28	17.5	8	4.8	168	0.86	78	90	0.464
1976	165	10	6.1	4	2.4	169	0.90	89	80	0.527
1977	165	14	8.5	3	1.8	168	0.94	87	81	0.518
1978*	154	12	7.8	0	—	154	0.91	89	65	0.577
1979	136	37	27.2	2	1.4	138	0.85	64	74	0.464
1980*	146	29	19.9	1	0.7	147	0.98	72	75	0.489
1981*	125	19	15.2	3	2.3	128	0.89	63	65	0.492
1982	124	21	16.9	1	0.8	125	0.93	70	55	0.560
1983	96	16	16.7	1	1.0	97	0.76	54	43	0.557
1984	82	25	30.5	1	1.2	83	0.70	44	39	0.530
Total										
1970–1984	1997	295	14.8	27	1.3	2024	0.85	1053	971	0.520
1973–1982	1485	206	13.9	23	1.5	1510	0.91	782	728	0.518

* Completed by some later notified cases
** Notification with karyotype

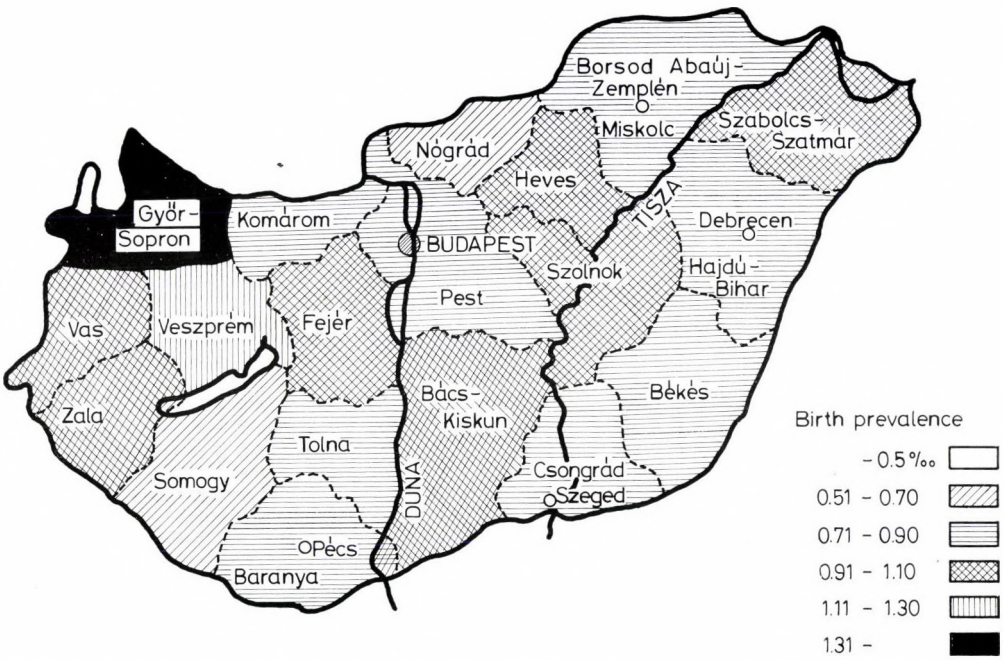

Fig. 1. The territorial distribution of births with Down's syndrome in Hungary, 1973–1982

within the above ten year period. It is worthwhile mentioning that the minimum and maximum occurred in two successive years.

Only 1.3–1.5% of Down's syndromes was diagnosed in *stillborns*. It is nearly the double of the population stillbirth figure (about 0.8), but there must be a considerable underascertainment. The clinical diagnosis of Down's syndrome is a difficult and unreliable task in the late fetal death. At the same time the chromosome analysis is used only in exceptional cases of stillborns.

It is not worthwhile separating live- and total birth prevalences because they represent nearly the same rates due to the low proportion of stillbirths (less than 1% in total births).

Only 15% of liveborn with Down's syndrome was notified with *karyotype confirmation*. Later on chromosome analysis was made in several other cases too but without a new notification.

The *sex ratio* does not differ significantly from the sex ratio of Hungarian birth (0.515) in the study period but the well-known male preponderance is existing [17].

As in general, there are *two* important *criteria* of the Down's syndrome surveillance.

a) *Completeness of ascertainment.* There are two possibilities to estimate the rate of notifications.

Table II

Territorial distribution of cases with Down's syndrome and the proportion of index patients' mothers over 35

Territorial unit	Birth prevalence of Down's syndrome per 1000 total births	Proportion of index patients' mother over 35 (%)
Budapest	0.90	5.2
Baranya	0.86	3.2
Bács-Kiskun	0.97	4.4
Békés	0.79	4.2
Borsod-Abaúj-Zemplén	0.76	4.5
Csongrád	0.87	4.3
Fejér	1.02	4.0
Győr-Sopron	1.39	4.0
Hajdú-Bihar	0.77	4.3
Heves	1.01	3.3
Komárom	0.88	3.5
Nógrád	0.69	3.1
Pest	0.75	4.2
Somogy	0.59	3.3
Szabolcs	1.01	4.7
Szolnok	0.97	4.5
Tolna	0.81	3.2
Vas	0.99	3.9
Veszprém	1.25	4.0
Zala	1.01	4.0
Total	0.91	4.2

First, the *territorial distribution* of index patients affected by Downs' syndrome. Hungary of 93,000 km^2 has twenty administrative-geographic entities (19 counties and the capital, Budapest). As Fig. 1 shows there is a significant deviation in the birth prevalence of cases with Down's syndrome among 20 units. The explanation may be found in three factors: (1) technical biases, mainly differences in diagnostic skill and notification discipline, (2) differences in confounding variables, e.g., maternal age distribution and (3) in true environmental and/or genetic differences. The mathematical analysis indicated some differences in the distribution of maternal age groups (Table II). However, the proportion of mothers over 40 was very low: 1–2%. The age-group of 35–39 also represented a small fraction of mothers (about 3%). Thus only a weak, no significant correlations was found ($r = 0.2153$) between the birth prevalence of Down's syndromes and the proportion of mothers over 35 in 20 territorial units, 1973–1982 (Table II). It is not reasonable to postulate any significant differences in environmental and genetic factors within such a small country. Thus the main explanation of observed territorial differences may be the different ascertainment. The county or counties with highest birth prevalences may be near to the true birth prevalence of Down's syndromes in

Hungary. The County Győr-Sopron has the maximum figure: 1.39 per 1000 total births. The second is the County Veszprém with a figure of 1.25. However, these two counties are near to each other and the cytogenetic service is supplied by the same lab in the town of Győr. The head of paediatric and genetic services in the County Győr-Sopron (Dr. K. Méhes) has had a special interest concerning autosomal numerical chromosome aberrations for a long time [32]. Furthermore the proportion of mosaicism was significantly higher (11.4%) in his cytogenetic lab due to the much higher number of cells analyzed [1]. Four other counties have figures over 1 per 1000 total births. Two of them are in the western part of Hungary (the so-called Transdanubia = Dunántúl).

Second, co-workers of our department [41] organized a cytogenetic epidemiological study of 248 index patients born in Budapest, 1970–1979 and recorded in the HCMR (Table III). Two supplementary sources of ascertainment were used. On the one hand the so-called Record of Infant Death Evaluation Committee was scrutinized. It was a satisfactory finding that this source did not give new cases. On the other hand all paediatricians working in outpatient paediatric clinics in Budapest were asked to send from their catchment area a list of babies with Down's syndrome independently of their age. This approach resulted in 92 new Down's syndromes. All notified cases were over the age of one year. According to the results of this study the birth prevalence of cytogenetically verified Down's syndromes was 1.17 ± 0.11 per 1000 total births in Budapest. In Budapest the completeness of notification was 72.9% in the cases of Down's syndromes between 1970 and 1979. However, two points

Table III

Data of a cytogenetic-epidemiological study of Down's syndromes born in Budapest, 1970–1979

Years	HCMR		Complementary ascertainment by paediatricians		Total of confirmed cases	
	Notified cases	Confirmed cases	Notified cases	Confirmed cases	No.	‰
1970	24	21	8	8	29	1.21
1971	19	17	12	11	28	1.24
1972	15	12	11	11	23	0.96
1973	23	21	9	9	30	1.23
1974	28	26	8	7	33	1.08
1975	31	30	10	10	40	1.21
1976	28	28	6	6	34	1.08
1977	25	24	11	11	35	1.16
1978	31	30	7	7	37	1.32
1979	24	23	10	9	32	1.24
Total No.	248	232	92	89	321	1.17
%	—	93.6	—	96.7	—	—

have to be considered. After the first two years of the HCMR, the completeness of notification increased significantly (Table I). Furthermore Budapest was a somewhat more undernotified area than the whole country in the study period (Fig. 1).

On the basis of the above available data, the estimated underascertainment rate is 25% in Hungary, 1973–1982. Higher underascertainment rates: 44% were found in New York State [17] and 38% in British Columbia [29].

b) *Validity of diagnosis.* The material of Down's syndromes within the HCMR was checked-up cytogenetically twice.

A clinical and cytogenetic study was performed in 1480 cases with multiple congenital abnormality (MCA) of the HCMR, 1970–1974 [22]. Of the 997 identified MCAs, so-called congenital anomaly syndromes, 581 were Down's syndromes. We planned to carry out chromosome studies in 100 randomly chosen cases of Down's syndrome, but it was possible only in 81 children. Trisomy 21 was found in 77 cases. Thus the clinical diagnosis was confirmed cytogenetically in 95.1 per cent of notified Down's syndromes. (Other chromosome aberrations were found in two, hypohydrotic ectodermal dysplasia in one and an unidentified MCA-entity in one case.) The above-mentioned Budapest study (Table III) showed a similar validity rate of diagnosis (93.6%). Only two misdiagnoses were found among Down's syndromes lately notified by paediatricians. Thus, the rate of misdiagnosis was about 5% in the study period.

The purpose of two other Hungarian studies was to determine the distribution of different subtypes of trisomy 21 (Table IV). Papp et al [35] summarized the data of eight cytogenetic laboratories including our own, in the period of 1965 and 1974 while Kosztolányi [24] collected chromosome aberra-

Table IV

Distribution of different types of trisomy 21 in two Hungarian samples compared with a combined international material

Karyotype	Papp et al. [25]			Kosztolányi [24]		Combined international material*		
	Number		%	Number	%	Number		%
47,21 +**	332		91.7	656	93.2	8845		93.1
46/47,21 +	16		4.4	15	2.1	229		2.4
46,D-, t(DqGq)	9	14	2.5	33***	4.7	242	426	2.5
46,G-, t(Gq, Gq)	5		1.4			184		2.0
			3.9					4.5
Total	362		100.0	704	100.0	9500		100.0

* Materials of Giroud and Matter [14], Matsunaga and Fujita [30], Lindsten [28] and Hock [17].

** Including cases with double trisomy and any other combined chromosomal aberrations.

*** Including two special structural aberrations

Table V

The distribution of maternal age groups in Hungary

Year	–19	20–24	25–29	30–34	35–39	40–49	Total	$\bar{X}$
1930	8.0	31.2	27.1	19.0	10.8	3.9	100.0	27.25
1960	13.1	39.9	26.5	13.3	6.3	0.9	100.0	25.10
1970	15.0	41.0	26.6	11.8	4.4	1.2	100.0	24.65
1980	14.5	41.1	29.9	10.5	3.3	0.7	100.0	24.90
1984	14.1	37.2	31.1	13.4	3.6	0.7	100.0	25.33

Table VI

Expected (E) and observed (O) cases in maternal age-groups of index patients with Down's syndrome in the Hungarian Case-Control Surveillance System of Congenital Anomalies

Maternal age-groups	Expected No.	Observed No.	O/E
–19	3.1	4	1.29
20–24	48.8	25	0.51
25–29	75.4	57	0.76
30–34	41.9	45	1.07
35–39	13.2	22	1.67
40–44	2.4	21	8.75
45–	0.3	11	36.67
Total	185.1	185	1.00

tions from the material of three cytogenetic laboratories. The Hungarian distribution of different types of trisomy 21 fits in well with the well-known international data.

The true birth prevalence of Down's syndrome is estimated about 1.2 ± 0.1 per 1000 total births in Hungary during the main study period, i.e., in 1973–1982. There were about 25% undernotification and about 5% misdiagnosis in the Down's syndrome material of the HCMR. The estimated 1.2 per 1000 birth prevalence of Down's syndrome is, of course, the consequence of a considerable shift in the maternal age (Table V). According to our previous calculation the birth prevalence of Down's syndrome might be reduced by about 33% due to the decreasing mean maternal age between 1930 and 1960 [9]. However, only a moderate further decrease was found in the advanced maternal age groups (over 35) in the last 25 years (Table V). The material of the Case-Control Surveillance System of Congenital Anomalies System confirms the well-known maternal age effect, i.e., an increase in the maternal age-specific birth prevalence of Down's syndrome (Table VI).

Some random fluctuations [15, 26] and significant clusterings in space and time [e.g., 32, 34] in the birth prevalence of Down's syndrome have been

reported several times. However, in general the significant changes in the birth prevalence of Down's syndrome can be explained by the different ascertainment and confounding factors. For example the previously mentioned cluster in the County Győr-Sopron, Hungary (Fig. 1) was caused by the better ascertainment and different laboratory method. Recently an unusual cluster of babies with Down's syndrome born to former pupils of an Irish boarding school has been published [38]. The more widespread use of prenatal fetal chromosomal examination (by amniocentesis or CVS) in pregnant women over 38 resulted in the recent general decline in time. Furthermore the higher prenatal loss [7] and the lack of any restriction in the legal termination of pregnancy in women over 35 have also led to a considerable decline in the proportion of birth from with advanced age.

Seasonal changes in the birth prevalence of Down's syndrome

Significant monthly variation in the birth prevalence of a congenital anomaly may indicate the role of environmental factors in its pathogenesis. However, there are at least three explanations for this phenomenon. First, the occurrence of conception in which the specific congenital anomaly will be manifested differs in different months. Thus the different time-distribution of abnormal meiotic divisions may result in a monthly variation. It might be caused by both extrinsic (e.g., mutagens) and intrinsic (e.g., pre- or post-ovulatory overripeness of ova) factors. Second, teratogens, e.g., virus epidemics may be bound to certain seasons. However, this supposition cannot be harmonized with the preconceptional origin of Down's syndrome. Third, prenatal selection varying from month to month may lead to a monthly variation of birth prevalence. A seasonality in spontaneous abortion rate [7] exists but it seems less likely that a time-determined specific prenatal selection can modify the birth prevalence of Down's syndrome. However, the recent hypothesis of Stein et. al. [40] concerning the attrition of trisomies as a maternal screening device may prefer this possibility.

The seasonality of births with Down's syndrome has been published [10, 15, 19, 20, 21, 25, 26, 37] though the majority of previous papers did not find any significant seasonality [4, 31, 33, 39, 43]. Recently Jongbloet and Vrieze [21] have divided 287 patients with Down's syndrome into four categories: those resulting from (1) a non-disjunctional event in paternal meiosis I (13%), (2) in paternal meiosis II (7%), (3) in maternal meiosis I (63%) and (4) in maternal meiosis II (17%). The non-disjunctions during maternal meiosis I, by far the most common category, occurred more frequently during the seasonal "restoration" and "inhibition" phase of the "ovulatory seasons" and less frequently when the ovulation rate is stabilized. The hypothesis of the Seasonal Preovulatory Overripeness Ovopathy coined by Jongbloet [19]

is based on the existence in humans of an ovulatory vestige of "ovulatory seasons" alternating with "anovulatory seasons" as occurs in non-human primates. In his opinion the seasonal periodicity of the prolactin concentration in women and "transient hyperprolactinaemia" with an antigonadotrophic activity may be related to these seasonal clusters of Down's syndrome's conceptions due to the delayed ovulation. Later, by testing the above data of Jongbloet et al. [19], Videbach and Nielson [42] did not find a statistically significant seasonality ($\chi^2_{11} = 8.2$; $0.6 < p < 0.7$). Another study of seasonality has been made in birth of individuals with verified chromosome aberrations of Down's syndrome registered in the Danish Cytogenetic Central Register before January 1, 1981 [42]. No significant seasonal variation was found in conceptions of index patients with Down's syndrome. However, during the first 4 months of the year, using a chi square with 2 degrees of freedom a significant increase was observed in the frequency of conceptions for Down's syndrome. This corresponds with what was found by Lander et al. [25] in a study of 1192 patients with Down's syndrome born in Sweden. Leck [26] observed a significantly higher frequency of conceptions from April to September in 482 patients with Down's syndrome in the U. K. Rothman and Fabia [37] studied 2469 patients with Down's syndrome born in the USA and found a slight, but significant peak of monthly distribution of births in summer.

All these suggest that the seasonality of births with Down's syndrome is a debated question worth of further studies.

Three methods are worthwhile using for the evaluation of monthly variation in the birth prevalence of Down's syndrome. First, it is necessary to determine whether or not there is a significant difference in the monthly distribution of births with Down's syndrome. In the case of a significant heterogeneity, i.e., monthly variation after the correction concerning the total number of births in different months, the next step is to distinguish between harmonic, e.g., seasonal and periodic, i.e., non-harmonic variations. The so-called Edwards [13] method is good to fit a sinus curve to the recorded differences between observed and expected numbers of cases in each calendar month. According to Wehrung and Hay [43] "$0 \leq \Phi \leq 2n$" is the angle corresponding to the data of maximum incidence on the "fitted curve" this estimation is very rough, therefore the least squares' method have been used. Maximum probability is not suitable for this purpose. If χ^2_9 is large and p is under 0.05, it is against the sinus curve, i.e., a harmonic-seasonal monthly distribution. There is a supplementary approach and it is a comparison between the figures of above χ^2_{11} and χ^2_9 tests. If $\chi^2_2 = \chi^2_{11} - \chi^2_9$ is significant, it confirms a significant seasonality. The third approach is a non-parametric one [16, 36] when the monthly birth prevalences are ranked from the highest 12 down to the lowest 1. Because the random probability is to obtain the largest possible sum for six successive months is smallest for $r = n/2$, the rank-sum for six successive

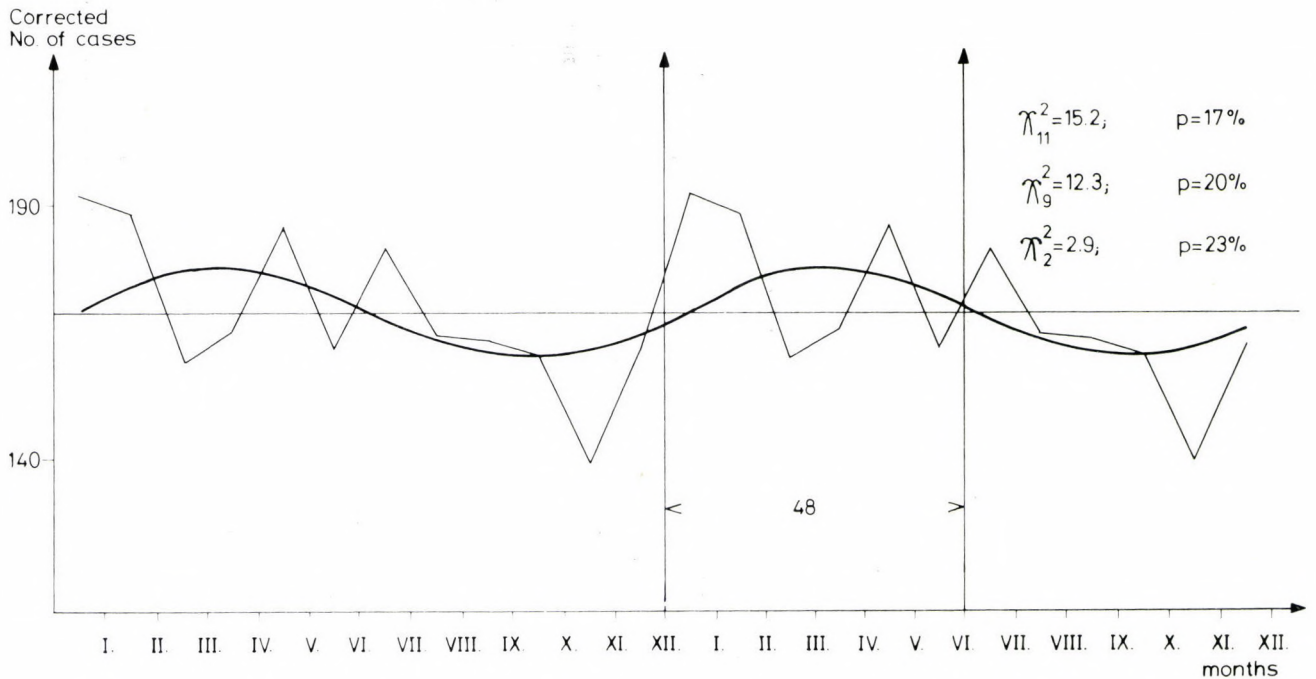
Corrected
No. of cases
190
140
χ^2_{11}=15.2; p=17%
χ^2_9=12.3; p=20%
χ^2_2=2.9; p=23%
48
I. II. III. IV. V. VI. VII. VIII. IX. X. XI. XII. I. II. III. IV. V. VI. VII. VIII. IX. X. XI. XII.
months

Fig. 2a

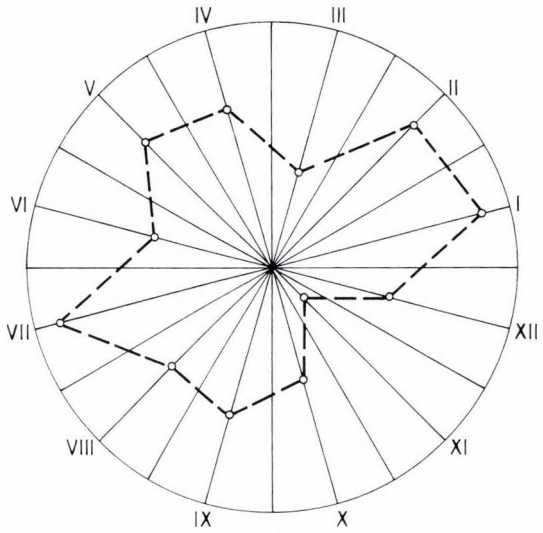

Fig. 2b

Fig. 2.a—b. The monthly distribution of births with Down's syndrome in Hungary, 1973–1982 (a) and according to the Edwards' method (b)

months was chosen for study. A figure of the test criterion equal to or smaller than 26 is significant at the conventional 5% level.

The monthly distribution of 1997 recorded cases affected by Down's syndrome born in Hungary, 1970–1984 was analyzed. No significant variation was found among months of years studied (Fig. 2). The homogeneity of births with Down's syndrome is explained by chance. According to the Edwards' method it is not a harmonic-seasonal, and the periodic variation is probably explained by the different ascertainments (Fig. 2b). The modified Hewitt's method did not show a significant seasonality of births with Down's syndrome either (Fig. 2a). The period of December and July had a higher level of births with Down's syndrome while its occurrence was lower in the period of June and January. However, these differences did not reach the level of significance, i.e., these were the manifestations of random fluctuations except in 1970 and 1981.

Summing up the results of these studies environmental factors exerting their effects seasonally do not seem to play an important role in the etiology of Down's syndrome.

Surveillance of Down's syndrome

Owing to an obvious increase by exposures to ionizing radiations and chemicals, the extent of germinal mutations is a matter of public concern in developed societies [44]. The surveillance of Down's syndrome seems to be a

useful system for the recurrent measurement of one genetic endpoint in the population at large to detect changes in the occurrence of *de novo* germinal numerical chromosome mutations as soon as possible in order to take some course of counter-measures [18]. Within the Hungarian Centre for Congenital Anomaly Control [5] we have attempted to use the Down's syndrome for this purpose.

There are five arguments for the *surveillance* of Down's syndrome as an endpoint related to mutation:

(1) Down's syndrome is a common congenital anomaly, its birth prevalence exceeds the level 1 per 1000 total births. The registration of prenatally diagnosed and electively terminated fetuses affected by Down's syndrome is a useful complementary approach in a population-based system with high ascertainment.

(2) Only a few kinds of numerical autosomal chromosome aberrations commonly survive to birth. Down's syndrome seems to be the exception, because two thirds of recognized cases are born and it represents 87% of al. autosomal numerical chromosome aberrations in livebirths [18]. After the perinatal period only Down's syndrome cases have a chance to survive.

(3) Among germinal chromosome aberrations the numerical ones represent a much higher proportion than structural aberrations. The ratio of structural to numerical aberrations is about 1 : 4 to 1 : 5 at livebirths [44]. No less than 0.3% of all newborns are aneuploid and the incidence of aneuploidy is higher in the human than any other organisms investigated. The trisomy 21 seems to be an adequate model for the study of the origin of aneuploidy in humans [11].

(4) Down's syndrome almost always (98%) occurs as a *de novo* event, i.e., the consequence of a new mutation. Thus, it is an adequate indicator of germinal numerical chromosome mutations.

(5) Down's syndrome is reliably recognizable on its clinical symptoms. Additionally karyotyping is an easy means to confirm or to exclude the clinical diagnosis and to separate the different subtypes of Down's syndrome.

Nevertheless, there are some methodological problems unsolved in the surveillance of Down's syndrome. First, the clinically diagnosed Down's syndrome represents a heterogeneous group from the nosological point of view. "Pure" trisomy 21 is caused by non-disjunction, Robertsonian translocation is caused by chromosome mutations and mosaicism are caused by somatic mutations. However, the cytogenetic analysis can identify these subgroups Second, within the subgroup of pure trisomy 21 the first and second meiotic non-disjunction may take place at quite different times before or after fertilization both in mother and father. However, the recent DNA and other method offer a possibility for their separation. Third, a number of fetuses with trisomy 21 die in the pre- and postrecognition periods of fetal life but before birth.

Thus, one of the most important purposes of the surveillance of Down's syndrome is to record all prenatally diagnosed cases, too.

The completeness and validity of the Hungarian recorded annual birth prevalences of Down's syndrome seemed to be good for the population surveillance of germinal numerical chromosome mutations, thus the Surveillance

Table VII

Estimated numbers of births needed to detect an increase in the birth prevalence of cases affected by Down's syndrome

Magnitude of increase	Number of births
1.5×	51 042
2×	15 026
3×	4 811
4×	2 578
5×	1 687

of Down's syndrome was established in 1980. It is part of the Hungarian Surveillance of Indicator Conditions caused by Germinal Mutations which involves also the Mutation Surveillance of Sentinel Anomalies as indicators of germinal gene mutations [6] and the program entitled Pairwise Analysis of Unidentified Multiple Congenital Abnormalities as indicators of germinal gene and chromosome mutations [23]. The mean number of *new germinal chromosome mutations* detected by this approach was about 114 in a 10.6 million population per year between 1980 and 1984.

Assuming a *Poisson* distribution of events with a background rate of 1.2 Down's syndrome per 1000 births and a 98 per cent proportion of sporadicity, a sample size of 15 000 would be needed to detect a doubling of mutation rate with probabilities of type I and II errors of 0.05 level (Table VII). Knowing the average number of yearly births (135 548) in Hungary in the early eighties, the detection of a significant increase in germinal numerica chromosomal mutations through this surveillance system seems to be feasible. Additionally this updating record system provides an opportunity to give some medical, educational and social help to these patients and their parents (e.g., there is a course for parents teaching them the most effective methods how to bring up these babies).

REFERENCES

1. Bajnoczky K: Unusual cases of Down's syndrome in the material of Budapest and Transdanubia (Hungarian). Magyar Pediater 16: 479, 1982
2. Béres J: Registry of cases with Down's syndrome. (In press)
3. Bod M, Czeizel A: Congenital malformation surveillance. Teratology 24: 277, 1981

4. Collmann B, Stoller A: A survey of mongoloid births in Victoria, Australia, 1942–1957. Am J Publ Health 52: 813, 1962
5. Czeizel A: Hungarian Center for Congenital Anomaly Control. (In press)
6. Czeizel A, Kis-Varga A: Mutation Surveillance of Sentinel Anomalies in Hungary, 1980–1984. Mut Res 186: 73, 1987
7. Czeizel A, Bognár Z, Rockenbauer M: Some epidemiological data on spontaneous abortion in Hungary, 1971–1980. J Epid Com Hlth 38: 143, 1984
8. Czeizel A, Pázsy A, Pusztai J, Nagy M: Aetiological monitoring of congenital abnormalities: A Case-Control Surveillance System. Acta Pediat Acad Sci Hung 24: 91, 1983
9. Czeizel A, Tusnády G: Some biological aspects of differential family planning. Adv Biol Human Population 13: 193, 1972
10. Dalén P: Season of Birth. North Holland, Amsterdam 1975, p. 15
11. Dellarco VL, Voytek PE, Hollaender A: Aneuploidy. Etiology and Mechanism. Plenum Press, New York, London 1985
12. Down JLH: Observation on an ethnic classification of idiots. Lond Hosp Rep 3: 259, 1866
13. Edwards JH: Seasonal incidence of congenital diseases in Birmingham 1945–1956. Ann Hum Genet 25: 89, 1961
14. Giraud F, Mattei JF: Aspects epidemiologiques de la trisomie 21. J Genet Hum (Suppl.) 23: 1, 1975
15. Harlap S: A time series analysis of the incidence of Down's syndrome in West Jerusalem. Am J Epid 99: 210, 1974
16. Hewitt D, Milner J, Csima A, Pakula O: On Edward's criterion of seasonality and a non-parametric alternative. Br J Prev Soc Med 25: 174, 1971
17. Hook EB: Down syndrome. Frequency in human population and factors pertinent to variation in rates. In: de la Cruz FF, Gerald PS, (eds) Trisomy 21 (Down syndrome) Research Perspectives. University Park Press, Baltimore 1981, p. 3
18. Hook EB, Cross PK: Surveillance of human populations for germinal cytogenetic mutations. In: Sugimura T, Kondo S, Takebe H, (eds) Environmental Mutagens and Carcinogens. Univ. Tokyo Press, Tokyo — Alan R. Liss. New York 1982, p. 613
19. Jongbloet PH: Month of birth and gametopathy. An investigation into patients with Down's, Klinefelter's and Turner's syndrome. Clin Genet 2: 313, 1971
20. Jongbloet PH, Mulder AM, Hamers AJ: Seasonality of preovulatory non-disjunction and the aetiology of Down syndrome. A European Collaborative Study. Hum Genet 62: 134, 1982
21. Jongbloet PH, Vrieze OJ: Down syndrome: increased frequency of maternal meiosis I non-disjunction during the transitional stages of the ovulatory seasons. Hum Genet 71: 241, 1985
22. Kiss P, Osztovics M, Pazonyi I, Czeizel A: Clinical and cytogenetical study of congenital multiple malformations registered in Hungary 1920–1974. In: Szabó G, Papp Z, (eds) Medical Genetics. Excerpta Medica, Amsterdam, Oxford 1977, p. 487
23. Kis-Varga A, Czeizel A: A pair-wise evaluation of component congenital abnormalities in unidentified multiple congenital abnormalities. Mut Res 1988 (In press)
24. Kosztolányi G: Recurrence risk of Down's syndrome (in Hungarian). Magyar Paediater 16: 475, 1982
25. Lander E, Forssman H, Akesson HO: Season of birth and mental deficiency. Acta Genet (Basel) 14: 265, 1964
26. Leck I: Incidence and epidemicity of Down's syndrome .Lancet ii. 457, 1966
27. Lejeune J, Gautier M, Turpin R: Etudes des chromosomes somatiques de neuf enfants mongoliens. CR Acad Sci (Paris) 248: 1721, 1959
28. Lindsten J: Incidence of Down's syndrome in Sweden during the years 1968–1977. In: Burgio GR, Fraccaro M, Tiepolo L, Wolf U. (eds) Trisomy 21. Springer Verl Berlin 1981, p. 195
29. Lowry RB, Jones DC, Renwick DHC, Trimble BK: Down syndrome in British Columbia. 1952–1973: Incidence and mean maternal age. Teratology 14: 29, 1976
30. Matsunaga E, Fujita H: A survey on maternal age and karyotype in Down's syndrome in Japan, 1947–1975. Hum Genet 37: 221, 1977
31. McDonald AD: Yearly and seasonal incidence of mongolism in Quebec. Teratology 6: 1, 1972
32. Méhes K: Clinically recognizable autosomal anomalies in neonates. Lancet i. 1262, 1973
33. Nielson J, Peterson GB, Therkelsen AJ: Seasonal variation in the birth of children with aneuploid chromosome abnormalities. Report from Danish Cytogenetic Central Register. Hum Genet 19: 67, 1973
34. Paneth N, Lansky M, Hialt IM, Hegyi T: Congenital malformation clusters in Eastern United States. Lancet ii. 808, 1980

35. Papp Z, Osztovics M, Schuler D, Méhes K, Czeizel A, Horváth L, Szemere G, László J: Down's syndrome: chromosome analysis of 362 cases in Hungary. Hum Hered 27: 305, 1976
36. Rockenbauer M, Czeizel A: Investigation of the monthly incidence, the so-called seasonality of the births of persons with common congenital malformations. Demográfia 2–3: 315, 1978
37. Rothman KJ, Fabia JJ: Place and time aspects of the occurrence of Down's syndrome. Am J Epid 103: 560, 1976
38. Sheehan PME, Hillary IB: An unusual cluster of babies with Down's syndrome born to former pupils of an Irish boarding school. Brit Med J 287: 1428, 1983
39. Stark CR, Mantel N: Lack of seasonal or temporal-spatial clustering of Down's syndrome births in Michigan. Am J Epid 86: 199, 1967
40. Stein Z, Stein W, Susser M: Attrition of trisomies as a maternal screening device. An explanation of the association of trisomy 21 with maternal age. Lancet i. 944, 1986
41. Szollár J, Osztovics M, Pazonyi I, Balogh L: Data of Down syndrome cases born in Budapest, 1970–1979 (in Hungarian). Magyar Paediater 16: 483, 1982
42. Videbach P, Nielson J: Chromosome abnormalities and season of birth. Hum Genet 65: 221, 1984
43. Wehrung DA, Hay S: A study of seasonal incidence of congenital malformations in the United States. Br J Prev Soc Med 24: 24, 1970
44. WHO: Guidelines for the Study of Genetic Effects in Human Population. IPCS International Programme on Chemical Safety. Environmental Health Criteria. 46. WHO, Geneva 1985

Acta Morphologica Hungarica, 36 (1—2), pp. 79—93 (1988)

THE EFFECT OF IPRIFLAVONE TREATMENT ON OSTEOPOROSIS INDUCED BY IMMOBILIZATION

I. Földes[1], Marianna Rapcsák[2], Á. Szöőr[3], J. Gyarmati[4], T. Szilágyi[2]

[1] INSTITUTE OF ANATOMY, [2] INSTITUTE OF PATHOPHYSIOLOGY, [3] INSTITUTE OF PHYSIOLOGY, [4]DEPARTMENT OF RADIOLOGY, DEBRECEN UNIVERSITY MEDICAL SCHOOL, DEBRECEN, HUNGARY

(Received 2 April 1987)

The purpose of these experiments was to study the effect of Ipriflavone (7 isopropoxy-isoflavone) on the osteoporosis induced by immobilization. The immobilization was produced by plaster cast of the right hind limb in young and old rats. Ipriflavone was administered via a gastric tube in a daily dose of 40 mg/kg body weight for 8 weeks. On the basis of histological and histomorphometric examinations of the tibia, results of Ipriflavone treatment are the following:

1) The decrease in the density and volume of spongy trabecules was less apparent in both meta- and diaphysis;

2) The amount of persisting cartilage core and structural rarefication of trabecules were diminished;

3) In the metaphysis osteoblastic activity was considerably enhanced;

4) Bone resorption and cortical thinning were decreased;

5) Bone remodeling was increased subperiosteally and to small extent also endosteally;

6) The treatment did not prevent the development of osteoporosis but significantly diminished it.

Keywords: Immobilization, osteoporosis, Ipriflavone, rat, histology, histomorphometry

Introduction

It is known that the state of weightlessness of astronauts results in osteoporosis [15, 26]. Experimental inactive osteoporosis can be produced by different immobilizations (denervation, plaster cast, etc.). Many authors [3, 4, 5, 11] have shown that the rat is a suitable model of immobilization. In our recent studies we have confirmed that the plaster cast immobilization method is also capable of inducing marked osteoporosis in rats [7, 10, 24].

According to the different personal communications Ipriflavone increased the retention of Ca and P, and the Ca contents of tibia in experimental strontium rachitic chicken. During the preparation of our article many papers were published by Japanese authors on the effect of Ipriflavone on the bone or osteoporotic bone produced by different experimental methods [18, 25,

Send offprint requests to: Dr. I. Földes Institute of Anatomy, Debrecen University Medical School, H-4012 Debrecen, Hungary

30, 31], or on the calcitonin secretion by means of estrogen [28, 29]. The earlier data prompted us to investigate the effect of Ipriflavone on the experimental osteoporosis produced by plaster cast.

Materials and methods

For the experiments 35 male Wistar rats were used. Out of 20 young rats (initial body weight 100 g) 15 were immobilized whereas out of adult rats (initial weight 250 g) 10 were subjected to plaster cast immobilization. The right hind limb was fixed in a slightly flexed position using bandage applied in the area between the ankle and the middle of thigh under anaesthesia of pentobarbital Na (5 mg/100 g body weight). The plaster cast was continuously checked and strengthened or replaced when it was necessary. In the group of young rats 8, whereas in the old rats group 4 animals received daily Ipriflavone (7 isopropoxy-isoflavone, a product of Chinoin Pharmaceutical and Chemical Works LTD, Budapest). Ipriflavone suspension was prepared in the following manner: 500 mg Ipriflavone was suspended in 100 ml 0.9% NaCl solution containing 1 ml Tween 80. This suspension was administered to rats via a gastric tube at a daily dose of 40 mg/kg body weight for 8 weeks. Five-five rats in both young and old groups served as untreated controls. The animals were fed LATI rat chow. At the end of experiment the tibia was removed and haved in the midsagittal plane, fixed and decalcified in Susa-solution, 8–10 μ thick sections were stained with haematoxylin-chromotrop, Goldner and Azan's methods. The stained histological sections were first assessed qualitatively and then quantitative histomorphometric measurements were carried out by a pointcounting method as described by Schenk and Oláh [22].

Bone formation was estimated by determining the surface density of osteoid seams (OS), of osteoblast-osteoid interface (OB), the trabecular surface (Sv) and trabecular volume (Vv) and osteoblast index (OBI). The surface density of total Howship's lacunae (HL), of osteoclast-bone interface (HO) and osteoclast index (OCI) served as parameters of bone resorption. From each bone to the pointcounting investigations 2–2 sections, and from these 5–5 visual fields were examined. By contrast to general practice, values for Sv, Vv, OS, OB, and OBI were separately evaluated in the meta- and diaphysis. Standard deviation and significance were calculated for the parameters studied.

Results

Young group (Table I)

Control group. The spongy trabecules were of normal density and thickness in both the meta- and diaphysis. Mostly in the metaphysis the trabecules were covered by thin osteoid seams and osteoblastic activities were present in several places. The medullary cavity was of normal size. The cortical bone was of normal width, its periosteal surface was slightly eroded. In some areas Howship's lacunae appeared with a few osteoclasts. At the endosteal surface slight osteoblastic activity was observed. Inside the bone signs of regenerative osteogenesis (vascularization, osteoblasts) also appeared occasionally.

Plaster cast immobilized group. In the metaphysis the spongy trabecules were more scattered and thinner. In the trabecules cartilage-cores were seen. The structure of trabecules was also looser, the osteocytic capsule was

Table I

	Young animals			Old animals		
	C	P	P + T	C	P	P + T
1. Number of spongy trabeculae in the metaphysis	0	−−	−	0	−	−
2. Thickness of spongy trabeculae in the metaphysis	0	−−	±	0	−−	−
3. Number of spongy trabeculae in the diaphysis	0	−−−	−−	0	−−−	−
4. Thickness of spongy trabeculae in the diaphysis	0	−−−	−−	0	−−−	−
5. Persisting cartilage in the spongy trabeculae	±	+	±	0	++	+
6. Structural rarefication of trabeculae	0	++	±	0	+++	+
7. Osteoblastic activity in juxtaposition to the trabeculae	+++	+	++	0	±	+
8. Enlargement of osteocytic capsule	0	+	+	0	++	+
9. Goldner's osteoid	0	++	+	0	+	±
10. Enlargement of medullary cavity	0	+++	++	0	+++	++
11. Thinning of the cortex	0	−−	−	0	−−−	−−
12. Howship's lacunae	±	+++	+	+	++	+
13. Osteoclastic activity	0	+++	±	±	+++	+
14. Endosteal oesteoblastic activity	0	+	+	0	+	±
15. Osteocytic osteolysis	0	++	++	0	++	+
16. Cortical osteolysis	0	++	±	0	++	+
17. Goldner's positivity in the cortex	0	++	±	0	+	±
18. Subperiosteal osteogenesis						+
19. Endosteal osteogenesis						+
20. Bone regeneration (remodeling)	0		+	0	±	++

P = plaster cast
P + T = plaster cast + treatment
C = control
0 = normal
\+ = moderately increased
++ = markedly increased
+++ = very markedly increased
− = moderately decreased
−− = markedly decreased
−−− = very markedly decreased

enlarged, the osteoid seams were more apparent; after all, instead of active osteoblasts, quiescent osteoblasts and progenitor cells could be seen (Fig. 1).

In the diaphysis the trabecules were even more scattered, their structure was much looser and these areas stained red with Goldner's stain indicating demineralization. The medullary cavity was extremely enlarged. The cortical bone was considerably thinned, the periosteal surface strongly eroded, many Howship's lacunae occupied by osteoclasts were observable (Fig. 2). The structure of the bone was also altered, several areas showed Goldner's positivity. Osteocytic osteolysis was also prominent. On the basis of these findings an apparent osteoporosis was diagnosed.

Plaster cast immobilized group with drug treatment. The spongy trabecules of the metaphysis were more rare and thinner as compared to control or contralateral bone. Occasionally inside the trabecules there was a minimal amount of cartilage cores. At the surface of the trabecules there was a thin osteoid seam. Beside the trabecules osteoblastic activity was enhanced (Fig. 3). The osteocytic capsule inside the trabecules was also slightly enlarged. The

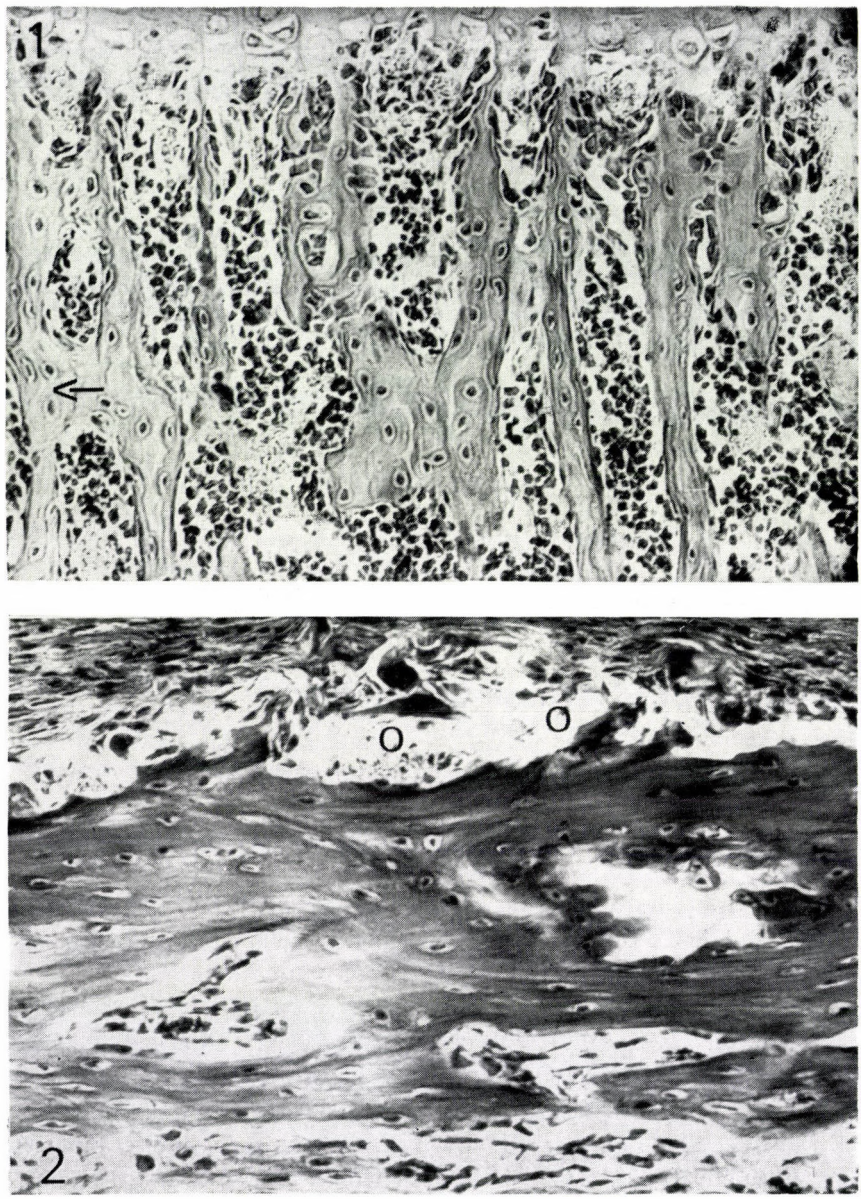

Fig. 1. Plaster cast. Metaphysis trabecules. Enlargement of osteocytic capsule (←), structural rarefication of the trabecules, few osteoblasts. Haematoxylin-eosin staining, ×130

Fig. 2. Plaster cast. Cortical bone. Howship's lacunae, osteoclasts (o), structural rarefication. Goldner's staining, ×130

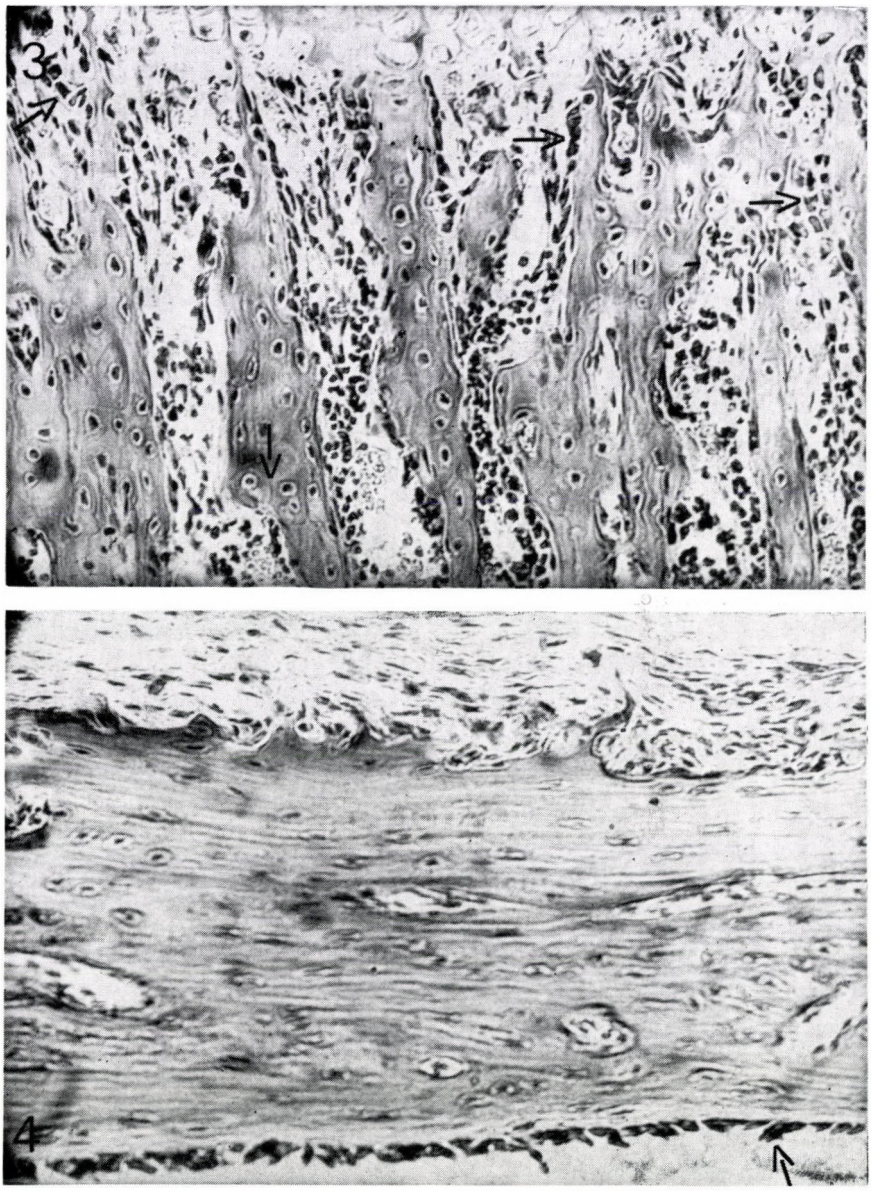

Fig. 3. Plaster cast + drug treatment. The structures of the metaphyseal trabecules are better preserved. Osteocytic capsules are enlarged (↓). In the proximity of the epiphyseal cartilage many active osteoblasts (→). HE staining, ×130

Fig. 4. Plaster cast + drug treatment. Cortical bone. Howship's lacunae without appearance of osteoclasts, osteocytic capsules are enlarged. Vascularization, endosteally osteoblasts (↑). HE staining, ×130

decrease in the number of spongy trabecules in the diaphysis was more apparent than in the metaphysis or in the control bone. The trabecular structure was also altered, Goldner's red positive areas also appeared inside the trabecules. The medullary cavity was also enlarged.

The cortical bone was slightly thinned. At the periosteal surface Howship's lacunae (Fig. 4) and a few osteoclasts appeared. The osteocytic osteolysis was also apparent here, the structural rarefication of the bone and Goldner's positivity were of moderate degree. Inside the cortical bone regenerative osteogenesis of moderate degree was seen. Thus alterations indicated the development of a slight-degree of osteoporosis.

Old group (Table I)

Control. The spongy trabecules of the metaphysis were dense and of normal thickness. At the surface of the trabecules a very thin osteoid seam appeared populated moderately with osteoblasts. The trabecules did not show signs of structural anomaly. The trabecules in the diaphysis were more rare than in the metaphysis. The extension of the osteoid was small, osteoblastic activity was hardly seen. The thickness of the cortical bone was normal, it showed periosteally some pits and Howship's lacunae sparsely populated with osteoclasts. Regenerative osteogenesis appeared more enhanced (Fig. 5).

Plaster cast immobilized group. In the metaphysis the density of trabecules was moderately diminished as compared to the control. Alterations in

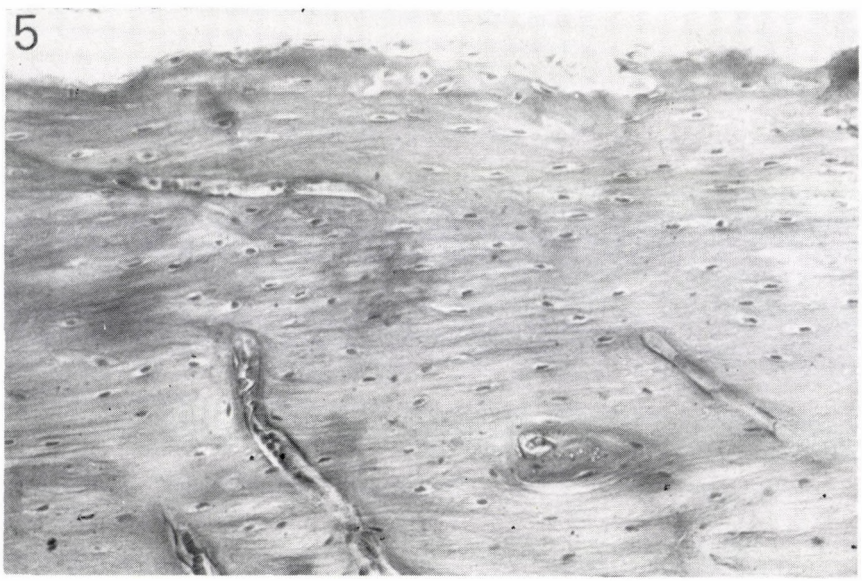

Fig. 5. Control. Cortical bone. Goldner's staining, ×130

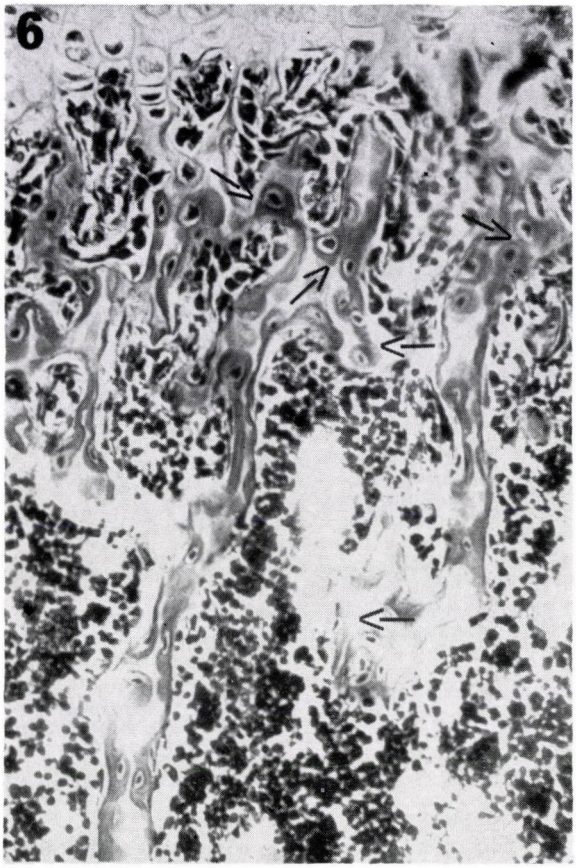

Fig. 6. Plaster cast (old rat). Structure of metaphyseal trabecules are looser, enlarged osteocytic capsules (↘), osteon disintegration (←). Goldner's staining, ×130

trabecular thickness and structure were more apparent (Fig. 6). Thus accumulation of cartilage cores, enlargement of osteocytic capsule and rarefication of trabecular structure were prominent. The osteoid seam was thin, osteoblastic activity appeared rarely. In the diaphysis the diminution of spongy trabecules was even more conspicuous. The structure of the remaining trabecules was also looser. The medullary cavity was considerably enlarged. The thinning of the cortical bone was also more expressed with occasional fractures. A great number of Howship's lacunae filled with osteoclasts was present (Fig. 7). The osteocytic osteolysis was more enhanced, disintegration of osteons could also be observed. These findings indicated the development of a severe-grade of osteoporosis.

Plaster cast immobilized group with drug treatment. In both the metaphysis and diaphysis the number of cancellous trabecules diminished moderately as compared to the control. Reductions in trabecular density and

Fig. 7. Plaster cast (old rat). Cortical bone. Howship's lacunae with osteoclasts (0). Osteon disintegration (→). Goldner's staining, ×130

thickness were more apparent in the diaphysis than in the metaphysis. Alterations in trabecular structure were manifested in a moderate enlargement of osteocytic capsule and rarefication of bone (Fig. 8). The osteoblastic activity and the osteoid seams were very mild. The medullary cavity was markedly enlarged. The cortical bone was thinner than in the control. At the periosteal surface of bone a fairly high number of Howship's lacunae was present containing only few osteoclasts. Osteocytic osteolysis was also seen. A striking finding was the appearance of the subperiosteal (Fig. 9) and partly endosteal osteogenesis. On the basis of the above findings the alterations were considered as manifestations of a moderate-grade osteoporosis associated with apparent signs of bone regeneration. It is to be noted that the contralateral limb essentially corresponded to limbs of control animals. The difference was manifested in signs of a moderate increase of osteogenesis.

Histomorphometric results

Group of young animals (Table II)

The quantitative data substantiated the qualitative histological findings. Namely, the treatment in the metaphysis significantly increased the trabecular

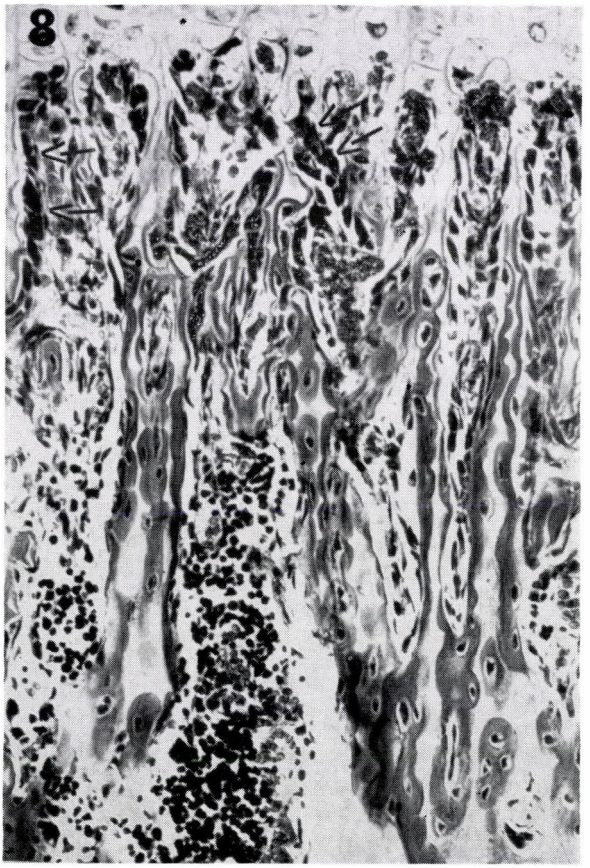

Fig. 8. Plaster cast + drug treatment (old animal). The structures of metaphyseal trabecules are moderately disintegrated, osteoblastic activities (←↙) appear at several sites along the trabeculas. Goldner's staining, ×130

surface (Sv) and osteoblastic activity (OB and OBI). In rats with plaster cast immobilization the extension of the osteoid (OS) was significantly greater indicating that calcification did not occur and/or demineralization took place from the trabecules. The trabecular volume in both experimental groups diminished considerably as compared to the control, the surface density of osteoblast-osteoid interface (OB) did not attain the control level. In the diaphysis there was no significant difference in the trabecular surface between the experimental groups but it was much less than in the controls. The extension of osteoid (OS) was significantly higher than in the control in both experimental groups. Signs for bone resorption such as surface density of osteoclast-bone interface (HO), osteoclastic activity (OCI) indicated that the drug treatment significantly suppressed osteoclastic activity.

Table I

Young

	Parameters	Control	Immobilized
Metaphysis	Sv mm^2/cm^3	2915.1 ± 198.0	1822.0 ± 211.8
	Vv%	22.0 ± 1.7	15.6 ± 2.1
	OS%	14.7 ± 6.4	36.2 ± 3.5
	OB%	52.3 ± 8.1	19.0 ± 4.0
	OB index	95.0 ± 6.4	51.7 ± 3.7
Diaphysis	Sv mm^2/cm^3	1616.7 ± 48.8	966.6 ± 73.6
	Vv%	12.0 ± 1.0	8.7 ± 1.4
	OS%	5.3 ± 1.5	25.6 ± 5.4
	OB%	8.4 ± 3.3	8.5 ± 6.6
	OB index	21.7 ± 3.5	11.8 ± 5.4
	HL%	3.4 ± 0.4	6.4 ± 1.4
	HO%	0.5 ± 0.2	1.4 ± 0.25
	OC index	5.5 ± 1.3	22.8 ± 2.1

1 symbol $p < 0.10$; 2 symbols $p < 0.05$; 3 symbols $p < 0.025$; 4 symbols $p < 0.02$; 5 symbols $p < 0.01$; 6 symbols $p < 0.005$; 7 symbols $p < 0.001$.

Symbols: ● Immobilized vs. control; ○ Immobilized + drug treatment vs. control; + Immobilized + drug treatment vs. contralateral side; × Immobilized + drug treatment vs. immobilized; N.S. not significant

Group of old animals (Table III)

In both the metaphysis and diaphysis the extension of trabecular surface (Sv) was significantly higher in the drug-treated group than in the plaster

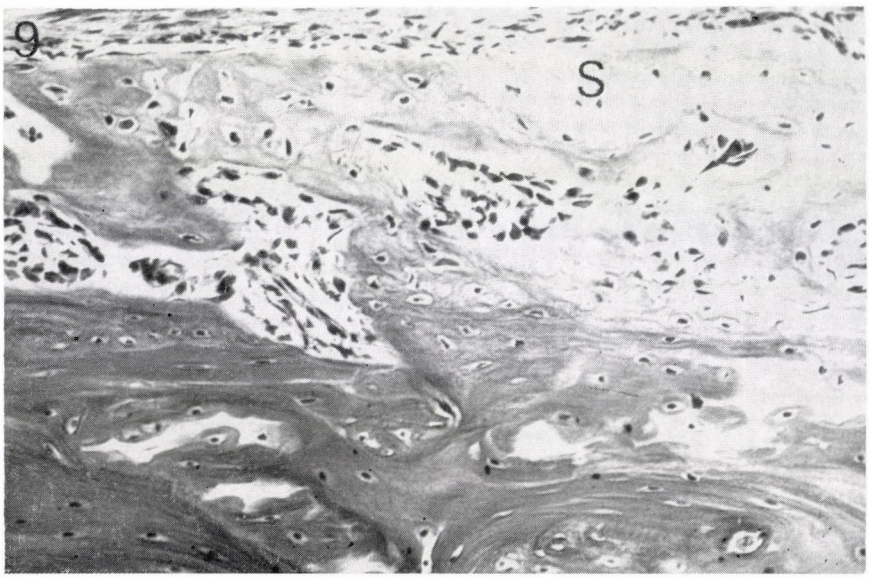

Fig. 9. Cortical bone. Area of subperiosteal osteogenesis (S). Goldner's staining, ×130

animals

Contralateral (control) side	Immobilized + drug treatment	Results (differences)
2711.4 ± 103.0	2377.8 ± 45.7	●●, ○○, +++++++, ×××××××
24.2 ± 2.0	15.1 ± 1.0	●●●●, ○○○○○○○, ++
33.3 ± 2.3	20.3 ± 3.3	●●●●●●●, +++++++, ×××××××
37.0 ± 5.2	31.8 ± 2.2	●●●●, ○○, ×××××××
61.1 ± 15.1	133.8 ± 10.7	●●●●●●●, ++++, ○○○○○○, ×××××××
1744.0 ± 162.1	1161.0 ± 93.4	●●●●●●●, ○○○○○○, +++++++
14.2 ± 2.6	8.6 ± 2.7	●●, ○, +
35.1 ± 2.3	49.1 ± 4.9	●●●●●, ○○○○○○○, ++++, ×××××××
17.5 ± 10.1	14.7 ± 5.5	N.S.
18.8 ± 4.9	19.7 ± 3.5	N.S.
4.6 ± 1.4	6.8 ± 2.1	●●●
0.66 ± 0.4	0.8 ± 0.2	●●●●●●●, ××
5.0 ± 0.5	8.5 ± 1.7	●●●●●●●, ++, ×××××××

Sv = Surface density of trabecular bone; $V_v\%$ = Trabecular bone volume % of total cancellous bone; OS% = Surface density of osteoid seams % of total trabecular surface; OB% = Surface density of osteoblast-osteoid interface; HL% = Howship's lacunae % of total trabecular surface; HO% = Surface density of osteoclast-bone interface

cast group. The extension of osteoid (OS) was increased in comparison to the control in both experimental groups: osteoblastic activity (OBI) was reduced. In the treated group, however, the values of osteoblastic activity (OBI) was significantly increased compared to the plaster cast-group. Signs of bone resorption osteoclastic activity were significantly enhanced in rats with plaster cast immobilization as compared to the respective values of control or drug-treated rats.

Discussion

The present histological and histomorphometric data showed unequivocally that osteopenic osteoporosis produced by immobilization can mainly be accounted for the accelerated resorptive activity both in osteoclasts and in osteocytes. Johnston [12] raises the question: is the loss of trabecular bone due to a decrease in the number (density) of trabecules, or to a decrease in the thickness of individual trabecules? His studies indicate that both mechanisms are in part responsible. The pathogenesis of trabecular bone loss in osteoporosis is still the subject of numerous controversies. Although it is now recognized that the bone remodeling activity is heterogeneous [19, 27] the mechanism leading to bone loss have been successively attributed to an increased bone resorption [13] or to a decreased formation. Parfitt et al. [19] suggest that during the accelerated phase of bone loss, osteoclasts perforate

Table III

Old animals

	Parameters	Control	Immobilized	Contralateral (control) side	Immobilized + drug treatment	Results (differences)
Meta-physis	Sv mm²/cm³	2915.1 ± 198.0	2195.0 ± 138.0	2240.5 ± 156.0	2741.2 ± 194.4	●, ×××
	V_V%	22.0; ± 1.7	15.3 ± 1.1	22.6 ± 2.4	18.4 ± 2.2	●●●●●●, ×
	OS%	14.1 ± 7.0	31.6 ± 11.3	26.6 ± 4.4	33.3 ± 9.5	●, ○○
	OB%	52.3 ± 8.1	27.5 ± 3.6	28.3 ± 3.0	35.4 ± 2.2	●●●●, ○○○○, ×××
	OB index	95.0 ± 6.4	68.5 ± 4.4	90.6 ± 7.2	75.4 ± 4.5	●●, ×
Dia-physis	Sv mm²/cm³	1616.7 ± 48.8	1126.7 ± 66.3	2005.0 ± 111.4	1662.2 ± 91.3	●●●, ×××××
	V_V%	12.0 ± 1.0	7.4 ± 0.4	19.2 ± 5.3	13.9 ± 1.3	×××××
	OS%	5.3 ± 1.5	35.7 ± 3.4	6.7 ± 2.2	42.5 ± 4.7	●●●●●●, +++++++, ○○○○○○○, ×
	OB%	8.4 ± 3.3	15.2 ± 1.7	10.6 ± 3.1	12.8 ± 1.0	N.S.
	OB index	21.7 ± 3.5	17.4 ± 4.7	31.8 ± 8.3	13.3 ± 6.5	++
	HL%	4.4 ± 0.4	7.0 ± 2.0	6.0 ± 2.5	7.3 ± 2.7	N.S.
	HO%	0.5 ± 0.2	2.2 ± 0.8	0.8 ± 0.4	1.2 ± 0.2	●●●●, ○○, ×××
	OC index	5.5 ± 1.3	31.2 ± 1.4	6.7 ± 1.1	6.1 ± 2.1	●●●●●●, ×××××

1 symbol $p < 0.10$; 2 symbols $p < 0.05$; 3 symbols $p < 0.025$; 4 symbols $p < 0.02$; 5 symbols $p < 0.01$; 6 symbols $p < 0.005$; 7 symbols $p < 0.001$.

Symbols: ● Immobilized vs. control; ○ Immobilized + drug treatment vs. control; + Immobilized + drug treatment vs. contralateral side; × Immobilized + drug treatment vs. immobilized; N.S. not significant.

Sv = Surface density of trabecular bone; V_V = Trabecular bone volume % of total cancellous bone; OS% = Surface density of osteoid seams % of total trabecular surface; OB% = Surface density of osteoblast-osteoid interface; HL% = Howship's lacunae of total trabecular surface; HO% = Surface density of osteoclast-bone interface

trabecules, thus there is no remaining structure upon which new bone can be rebuilt. It is important to make a distinction between two pathways that would both lead to bone loss [1, 8]: (i) uncoupling, a situation in which the coupling message is not functioning and where osteoblasts do not appear in the remodeling focus, therefore leading to an accumulation of Howship's lacunae without osteoclasts; (ii) imbalance, a situation in which the coupling occurs but where the osteoblasts do not synthetize as much matrix as was previously resorbed by the osteoclasts. Among the many causes of diminished skeletal mass, parathyroid hormone (PTH) mediated bone resorption has been the most widely studied experimentally. PTH has been shown to stimulate bone resorption and inhibit bone formation in organ culture. The effect on bone formation appears to be direct and due in part to decreased transcription of procollagen in RNA, but direct effect on preosteoclasts or osteoclasts have not been ruled out [20].

Mechanical loading perhaps acting through a direct or an indirect stimulation of osteoblasts thereby producing a positive remodeling balance may be important in attainment of adult bone mass, and in subsequent rates of loss. It is known that mechanical stimuli leads such as the pressure of active muscles are needed for the normal remodeling, metabolism and blood supply of bones.

All these factors may participate in the development of osteogenic osteoporosis induced by immobilization. According to our present investigations the treatment of Ipriflavone decreased the bone alterations of immobilization. The treatment decreased the loss of trabecular mass (density and volume) both in the proximal metaphysis and the diaphysis, and resorption of cortical bone as compared to the immobilized tibia. The interruption or the decrease of resorption process was determined by the moderate number of Howship's lacunae and by osteoclasts index. These data are in agreement with the results obtained in the different experiments with Ipriflavone. Results indicate that in osteoporosis produced by steptozotocin and glucocorticoid treatment or ovariectomy Ipriflavone markedly suppresses bone resorption [23, 30, 31]. In fetal long bone culture system Ipriflavone inhibited basal ^{45}Ca release from bones, and this inhibitory effect was demonstrated in the presence of submaximal concentration of parathyroid hormone.

According to Ohata et al [18] Ipriflavone inhibits the bone resorption provoked by calcitriol, but it does not influence bone formation. The question arises, how can Ipriflavone inhibit bone resorption, or how can the treatment influence osteopenic osteoporosis.

Recently it has been suggested that calcitonin release from the thyroid gland is stimuled by estrogen [6, 28, 29] and it has been demonstrated that Ipriflavone enhanced the action of estrogen stimulated calcitonin secretion. Endogenous estrogen promotes formation of 1.25 $(OH)_2D$ from 25-OHD and

it may reciprocally inhibit synthesis of 24, 25 $(OH)_2D$ [2]. According to Kuntz et al. [14] and Gruber et al. [9] the calcitonin treatment in post-menopausal women may induce a reduction of bone resorption. It was demonstrated by Nakamura et al. [17] that a transient inhibition of osteoclastic bone resorption occurred in the bones of calcitonin treated rats.

According to our investigations Ipriflavone treatment of immobilized rats resulted in a mild increase of osteoblastic activity and thereby in an increased subcortical osteogenesis. This may indicate that Ipriflavone may change the uncoupling pathway, or may reduce the imbalance situation. This effect of Ipriflavone may be connected with the other effect of calcitonin. Immunocytochemical evidence was found by Morel et al. [16] for the internalization of calcitonin in osteoblasts, a direct participation of calcitonin in the regulation of osteoblasts, while the absence of estradiol receptors in osteoblasts. Salmon et al. [21] described that chronic calcitonin treatment stimulated the bone alkaline phosphatase in growing rats. It was found, on the other hand, that Ipriflavone behaves as an electron acceptor in the terminal part of the respiratory chain. Ipriflavone increased the cytochrome-oxidase enzyme-activity in the liver and the blood O_2 level. However, the details of these actions are still obscure.

Finally, we have to mention that our experiments started in 1984 differ from the investigations of Yamazaki et al. [30, 31] in the doses used, the experimental test, the investigational method and the mode of administration. However, the main results are similar and these yield a hopeful possibility in the treatment of osteoporosis.

REFERENCES

1. Baron R, Magee S, Silverglate A, Broadus A, Lang R: Estimation of trabecular bone resorption by histomorphometry: evidence for a prolonged reversal phase with normal resorption in postmenopausal osteoporosis and coupled increased resorption in primary hyperparathyroidism. In: Frame B, Potts JT jr, (eds) Clinical Disorders of Bone and Mineral Metabolism. Excerpta Medica Amsterdam, Oxford, Princeton 1983, p. 191
2. Buchanan JB, Santen R, Cauffman S, Cavaliere A, Greer RB, Demers LM: The effect of endogenous estrogen fluctuation on metabolism of 25-Hydroxyvitamin D, Calcif Tissue Int 39: 139, 1986
3. Cann CE, Adachi RR, Holton EM: Bone and calcium absorption in rats during space-flight. In: Hideg, J, Gazenko. O (eds) Adv. in Physiological Sciences Vol. 8. Gravitational Physiology. Pergamon Press, Amsterdam 1980, p. 121
4. Conoway HH, Waite LC, Kenny AD: Immobilization and bone mass in rats. Effects of parathyreoidectomy and acetazolamide. Calcif Tissue Res 11: 323, 1973
5. Donaldson CL, Hulley SB, Vogel JM, Hattner RS, Bayers JH, McMillan DE: Effect of prolonged bed rest on bone mineral. Metabolism 19: 1071, 1970
6. First BP, Miller M, Deftos LJ: Effects of oophorectomy (OOPHX) and estrogen replacement on calcitonin levels in sexually mature female rats. Calcif Tissue Int 33: S 304, 1981
7. Földes I, Gyarmati J jr, Rapcsák M, Szöőr Á, Szilágyi T: Effect of plaster cast immobilization on the bone. Acta Physiol Hung 67: 413, 1986
8. Frost HM, Osteopenia: The ADFR Treatment. In: Frame B, Potts JT jr, (eds) Clinical Disorders of Bone and Mineral Metabolism. Excerpta Medica, Amsterdam, Oxford, Princeton 1983, p. 368

9. Gruber HE, Ivey JL, Baylink DJ, Matthews M, Nelp WB, Sisom K, Chesnut CH: Long-term calcitonin therapy in post-menopausal osteoporosis. Metabolism 33: 295, 1984
10. Gyarmati J jr, Földes I, Rapcsák M, Szöőr Á, Szilágyi T: Tartós immobilizáció okozta elváltozások patkányok végtagcsontjaiban (radiológiai és szövettani vizsgálatok). Kísérl Orvostud 36: 16, 1984
11. Izawa J, Makita T, Hino S, Hashimoto Y, Kushida K, Inove T, Orimo H: Immobilization osteoporosis and active vitamin D: Effect of active vitamin D analogs on the development of immobilization osteoporosis in rats. Calcif Tissue Int 33: 623, 1981
12. Johnston CC: Osteoporosis. An overview. In: Frame B, Potts JT jr. (eds) Clinical Disorders of Bone and Mineral Metabolism. Excerpta Medica Amsterdam, Oxford, Princeton 1983, p. 317
13. Jowsey J, Kelly PJ, Riggs BL, Bianco AJ, Scholz DA, Gershon-Cohen J: Quantitative microradiographic studies of normal and osteoporotic bone. J Bone Jt Surg 47A: 785, 1965
14. Kuntz D, Marie D, Berthel M, Caulin F: Treatment of post-menopausal osteoporosis with phosphate and intermittent calcitonin. J Clin Pharmacol Res 6: 157, 1986
15. Lutwak L, Singer FR, Urist MR: Current concepts of bone metabolism. Ann Intern Med 80: 630, 1974
16. Morel G, Boivin L, Dubois PM, Meunier PJ: Immunocytochemical evidence for endogenous calcitonin and parathyroid hormone in osteoblasts from the calvaria of neonatal mice. Absence of endogenous estradiol and estradiol receptors. Cell Tissue Res 240: 89, 1985
17. Nakamura T, Toyofuku F, Kanda S: Wholebody irradiation inhibits the escape phenomenon of osteoclasts in bones of calcitonin — treated rats. Calcif Tissue Int 37: 42, 1985
18. Ohata M, Nakamachi H, Sakagami Y, Funasako M: Ipriflavone effects on calcitriol induced changes of mineral phases in calvarial bone of neonatal rat. In: Cohn DV, Fuyita T, Potts JT, Talmage RV, (eds) Endocrine Control of Bone and Calcium Metabolism. Elsevier Science Publ, Amsterdam 1984, p. 380
19. Parfitt AM, Matthews C, Rao D, Frame B, Kleerekoper M, Villanueva AR: Osteoporosis. In: DeLuca HF, Frost HM, Jee WSS, Johnston CC, Parfitt AM, (eds) Recent Advances in Pathogenensis and Treatment. Park Press, Baltimore 1981, p. 321
20. Raisz LG: Mechanism of parathyroid hormone mediated bone loss. In: Frame B, Potts JH jr, (eds) Clinical Disorders of Bone and Mineral Metabolism. Excerpta Medica, Amsterdam, Oxford, Princeton 1983, p. 196
21. Salmon DM, Azria M, Zanelli JM: Decreased responsiveness to chronic salmon calcitonin treatment in rat kidney and calvaria studied using quantitative enzyme cytochemistry. Acta Endocrinol 108: 570, 1985
22. Schenk RK, Oláh AJ: Histomorphometrie. In: Handbuch der inneren Medizin VI/1 A. Knochen, Gelenke, Muskeln. Springer-Verlag, Berlin, Heidelberg 1980, p. 437
23. Shino A, Matsuo T, Tsuda M, Yamazaki I, Tsukuda R, Kitazaki T, Shiota K, Odaka H, Yoshida K: Effects of Ipriflavone on bone and mineral metabolism in the streptozotocin diabetic rat. JBMM 3: 27, 1986
24. Szilágyi T, Rapcsák M, Szöőr Á, Földes I, Gyarmati J jr: The effect of immobilization on the rat's bone. Physiologist 26: S 94, 1983
25. Tsuda M, Kitazaki T, Ito T, Fujita T: The effect of Ipriflavone (TC-80) on bone resorption in tissue culture. J Bone Mineral Res 1: 207, 1986
26. Whedon GD, Lutwak L, Rambaut PC, Whittle MW, Smith MC, Reid J, Leach C, Stadler CR, Sanford DD: Mineral and nitrogen metabolic studies experiment MO71. Biomed Result Skylab NASA SP 377: 164, 1977
27. Whyte MP, Bergfeld MA, Murphy WA, Avioli LV, Teitelbaum SL: Postmenopausal osteoporosis. A heterogeneous disorder as assessed by histomorphometric analysis of iliac crest bone from untreated patients. Am J Med 72: 193, 1982
28. Yamazaki I: Effect of Ipriflavone on the response of uterus and thyroid to estrogen. Life Sci 38: 757, 1986
29. Yamazaki I, Kinoshita M: Calcitonin secreting property of Ipriflavone in the presence of estrogen. Life Sci 38: 1535, 1986
30. Yamazaki I, Shino A, Tsukuda R: Effect of Ipriflavone on osteoporosis induced by ovarectomy in rats. JBMM 3: 55, 1986
31. Yamazaki I, Shino A, Shimizu Y, Tsukuda R, Shirakawa Y, Kinoshita M: Effect of Ipriflavone on glucocorticoid induced osteoporosis in rats. Lief Sci 38: 951, 1986

Acta Morphologica Hungarica, 36 (1—2), pp. 95—99 (1988)

CUPRIC IONS AND DOPA OXIDASE ACTIVITY IN MELANOCYTES

BHANU IYENGAR, P. C. MENDIRATTA

INSTITUTE OF PATHOLOGY-ICMR, SAFDARJANG HOSPITAL, NEW DELHI, INDIA

(Received 15 May 1987)

The inhibition of DOPA oxidase activity by cupric ions has been quantitated in cases of vitiligo showing dendritic and non-dendritic melanocytes at the margins. Cupric sulphate was added to the substrate solution, containing a reacting quantity of 12.12 μg of DOPA, to give 42.8 μg, 85.6 μg, 128.4 μg and 171.2 μg of cupric ions. Control slides were incubated with DOPA alone as substrate.

On cytospectrophotometric analysis, it was seen that the initial level of enzyme activity determines the type of inhibition curve. Thus, there is a gradual fall in activity with dendritic melanocytes which have a very high enzyme content, whereas the non-dendritic melanocytes show complete inhibition with one dose. It was observed that 15.75 μg of cupric ions were reduced by 12.12 μg of DOPA. The enzyme activation by cupreous ions is countered by the enzyme inhibition by cupric ions, the rate of inhibition being determinated by the level of cupric ions.

Keywords: DOPA oxidase, melanocyte, cupric, cupreous, enzyme inhibition

Introduction

It was observed in earlier studies [1, 2] that addition of cupric ions in the substrate inhibits the tyrosinase/DOPA oxidase activity in the dendritic melanocytes of vitiligo. In the present work this inhibition has been quantitated, to study the inhibition patterns in dendritic and non-dendritic melanocytes in vitiligo.

Materials and methods

Skin from 20 cases suffering from vitiligo were fixed in cold buffered formol glutaraldehyde Tor 24 h at 4 °C. Frozen sections were cut at 5 μ thickness on a Lipshaw cryotome at −25 °C. Ten of these were from cases with dendritic melanocytes at the margin and 10 from non-dendritic melanocytes.

Copper sulphate was added to the DOPA substrate [3, 4] in the following concentrations: 350 mg, 700 mg, 1050 mg, 1400 mg in the stock solution giving a final reacting quantity of cupric ions as 42.8 μg, 85.6 μg, 128.4 μg and 171.2 μg. The amount of DOPA in this solution is 12.12 μg contained in 0.016 ml of solution overlying the tissue. Control slides were incubated with DOPA as substrate without the addition of $CuSO_4$ [4]. Staining was done on serial cryosections so that the same set of cells was followed. The enzyme levels in 20 melanocytes were measured at the margins of the vitiliginous zone in each case on a Reichert Zetopan, Binolux cytospectrophotometer.

Send offprint request to: Dr. Bhanu Iyengar, Institute of Pathology-ICMR, Safdarjang Hospital, P.O. Box 4909, New Delhi 110029, India

Results

1. *Controls:* The enzyme levels in dendritic melanocytes were very high, the average absorption value being 1.134, in non-dendritic melanocytes the average values were 0.628 (Table I).

2. *Treatment with cupric sulphate:* (Table I, Fig. 1).

Table I

Copper levels (μg)	K(o)	42.8	85.6	128.4	171.2
DOPA level (μg)	12.12	12.12	12.12	12.12	12.12
Dendritic melanocytes	1.134	0.594	0.437	0.280	0.301
Non-dendritic melanocytes	0.628	0.316	0.359	0.275	0.282

Absorption values of DOPA oxidase activity in dendritic and non-dendritic melanocyte on treatment with different levels of cupric ions

a) *Dendritic melanocytes:* A gradual loss of DOPA oxidase activity occurred with an increasing level of cupric ions. Thus after 42.8 μg, the absorption is 0.594, after 85.6 μg it is 0.437, after 128.4 μg it is 0.280 and 0.301 after 171.2 μg (Table I). There was a complete inhibition of activity seen in Fig. 1.

b) *Non-dendritic melanocytes:* In non-dendritic melanocytes a nearly complete inhibition took place even after the 1st dose. The curve had a plateau inspective of increasing doses i.e. 0.316 after 42.8 μg, 0.359 after 85.6 μg, 0.275 after 128.4 μg and 0.282 after 171.2 μg of copper (Table I, Fig. 1).

Tyrosinase/DOPA-oxidase is a copper dependant enzyme. There are reports suggesting that the first part of the reaction i.e. conversion of tyrosine to DOPA is due to a peroxidase and the second part converting DOPA to DOPA-quinone is catalyzed by DOPA-oxidase, a copper dependent enzyme originally considered to be tyrosinase [5, 6, 7, 8].

DOPA oxidase functions in the presence of cupreous ions, the cupric ions being reduced to cupreous ions in the presence of trace amounts of DOPA [9, 10]. In the present work the effect of a high level of cupric ion on the enzyme function has been studied.

It was observed that there is an inhibition of DOPA oxidase and tyrosinase on increasing the cupric ion concentration [1]. In this work different doses have been used to quantitate the inhibition by cupric sulphate and to study the pattern of inhibition in the highly dendritic melanocytes and non-dendritic melanocytes seen at the margins of the vitiliginous zone.

It was noted that the basic levels of DOPA oxidase activity differ markedly in the cell types. Thus the enzyme levels are very high in the dendritic melanocytes, slightly increased in the non-dendritic melanocytes.

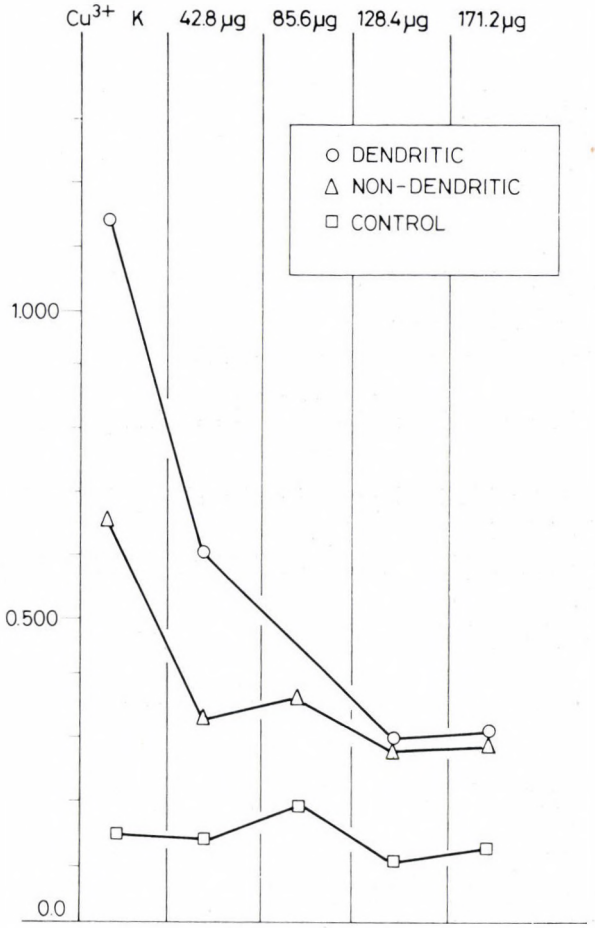

Fig. 1. Inhibition of DOPA oxidase activity, in dendritic and non-dendritic melanocytes on increasing the cupric ion levels in the substrate

In dendritic melanocytes, increasing levels of copper sulphate give rise to an early phase of a gradual fall in enzyme activity complete inhibition occurring on addition of 128.4 μgms indicating a stoichiometric reaction to cupric ions (Fig. 1).

In comparison, non-dendritic melanocytes show complete inhibition even after addition of 42.8 μg of cupric sulphate showing an all or none type of a reaction. This feature is possibly due to the difference in enzyme levels in the two cell types (Fig. 1).

From the above measurements the amount of cupric ions reduced to cupreous ions by the presence of 12.12 μg DOPA can be calculated from the effect on the dendritic melanocytes which have a high level of enzyme.

Thus the control (K) activity of the dendritic melanocytes i.e. 1.134 is taken as 100% activity and 0.280 on treatment with 128.4 μg of cupric ions is taken as 0% activity as this is the baseline absorption in the section on counterstaining (Table I).

The 0.016 ml substrate solution contains 12.12 μg DOPA which reacts with the cupric ions. DOPA reduces cupric to cupreous ions. Thus on addition of 42.8 μg copper the absorption is 0.594 i.e. 36.8% activity remains and 63.2% is inhibited.

Thus 36.8% activation is due to the conversion of Cu^{3+} to Cu^{2+} in 42.8 μg Cu by 12.12 μg DOPA.

If 100% cupric ions are taken as 42.8 μg,

$$36.8\% \text{ cupric ions equal to: } \frac{42.8 \times 36.8}{100} = 15.77 \ \mu g \text{ of cupric ions.}$$

On treatment with 85.6 μg Cu^{3+} the absorption value falls to 0.437 which is 18.4% of the initial activity.

Thus, there is 18.4% activation of Cu^{3+} to Cu^{2+} in 85.6 μg of copper by 12.12 μg DOPA.

Thus if 100% cupric ions are taken as 85.6 μg

$$18.4\% \text{ cupric ions equal to: } \frac{85.6 \times 18.4}{100} = 15.75 \ \mu g$$

Thus 12.12 μg DOPA reduces 15.75 μg of copper till complete inhibition takes place.

Non-dendritic melanocytes, in comparison with the dendritic melanocytes show almost complete inhibition already with the first dose.

The initial level of activity within the non-dendritic melanocytes is 70.25% of the control levels of dendritic activity (0.876). On addition of 42.8 μg only 4.8% activity remains. Thus the inhibition is 65.45% which is close to that seen with dendritic melanocytes i.e. 63.2%. As the level of DOPA is the same, the level of cupreous ions is also maintained. This indicates that the rate of inhibition of DOPA oxidase is determined by the level of cupric ions and not by that of cupreous ions in the medium.

In conclusion, 15.75 μg of cupric ions is reduced by 12.12 μg of DOPA. The non-dendritic melanocytes with an initial 70.25% enzyme activity, compared to that of dendritic melanocytes show 65.45 inhibition after 42.8 μg of Cu^{3+}. Thus enzyme activation by Cu^{2+} is countered by the enzyme inhibition by Cu^{3+}, the rate of inhibition being determined by the level of Cu^{3+} ions in the medium and not by the level of Cu^{2+} ions.

From the above observations it is evident that the level of enzyme activity determines the type of inhibition curve seen. Thus, there is a gradual

fall in activity with the dendritic melanocytes which show a high enzyme activity. In comparison, the non-dendritic melanocytes show almost complete inhibition with the first dose itself.

REFERENCES

1. Iyengar B, Misra RS: The reaction of dendritic melanocytes in vitiligo to the substrates of tyrosine metabolism. Acta Anat 129: 203, 1987
2. Iyengar B, Timar J, Szende B: Chemical milieu and the biphasic differentiation of the amelanotic melanoma, HT-18. (Sent for publication)
3. Manual of Histologic Staining Methods. AFIP. Luna LG (ed.) 3rd Edition. McGraw Hill Book Co., New York 1968
4. Pearse AGE: Histochemistry. 4th Edition Churchill, Livingstone, Edinburgh, London, New York 1980,
5. Okun MR, Edelstein L, Or N, Hamada G, Donnellan B: The role of peroxidase vs the role of tyrosinase in enzymatic conversion of tyrosine to melanin in melanocytes mast cells and eosinophils. J Invest Derm 1: 55, 1970
6. Okun MR, Edelstein L, Or N, Hamada G, Donnellan B: Histochemical studies of conversion of tyrosine and DOPA to melanin mediated by mammalian peroxidase. Life Science, Part, II 19: 491, 1970
7. Okun MR, Edelstein L, Or N, Hamada G, Donnellan B, Lever W: Histochemical differentiation of peroxidase mediated from tyrosinase mediated oxidation of tyrosine to melanin. Histochemie 23: 295, 1970
8. Okun MR, Edelstein L, Patel RP, Donnellan B: Revised concept of mammalian melanogenesis. The possible synergistic function of aerobic DOPA oxidase and peroxidase. A review. Yale J Biol Med 46: 535, 1973
9. Kertesz D: Tyrosinase and polyphenoloxidase. The role of metallic ions in melanogenesis. Biochim et Biophys Acta 9: 170, 1952
10. Kertesz D: The phenol-oxidizing enzyme system of human melanomas; substrate specificity and relationship to copper. JNCI 14: 1081, 1954

Acta Morphologica Hungarica, 36 (1—2), pp. 101—120 (1988)

HISTOGENESIS OF METASTATIC TUMOURS: LECTIN REACTIVE SUBSTANCES AND INTERMEDIATE FILAMENT PROTEINS

L. Pajor, J. Fischer, G. Kelényi

DEPARTMENT OF PATHOLOGY, UNIVERSITY MEDICAL SCHOOL OF PÉCS, HUNGARY

(Received 7 May 1987)

The reactivity of 38 anaplastic tumours for cytokeratin, vimentin, desmin, milk fat globule membrane antigen, Ia antigen as well as peanut agglutinin and Ulex europaeus I lectins were investigated immunohistologically in paraffin embedded tissue samples. By this typing of tumours establishment of the histogenesis of 34 out of 38 neoplasms was possible. Among the epithelial markers milk fat globule membrane antigen proved to be superior to cytokeratin. Vacuolar or intraluminal binding of peanut lectin was found to be more sensitive than PAS reaction for detecting early secretory activity. Our study substantiates the previous data that binding of Ulex europaeus I lectin is indicative of nasopharyngeal carcinoma. In this study we also provide evidence for vimentinization in solid metastases as well as for shift in the cytokeratin profile upon malignant transformation.

Keywords: Anaplasia, intermediate filament proteins, lectins

Introduction

Surgical pathologist frequently face the problem of establishing the histogenesis of primary or metastatic tumours of unknown origin. The differentiation of malignant lymphomas from metastases of the lymph nodes is of great practical importance. In the case of metastases knowledge of the location of the primary tumour might also have clinical consequences.

Electron microscopy can be of help with these diagnostic problems; however, it needs special processing of the biopsy tissues and is relatively time consuming. A reliable and rapid characterization of the tumour cells can be obtained by immunohistology. The typing of intermediate filament proteins (IFPs) proved to be suitable for distinguishing tumours of epithelial, mesenchymal, myogenic or neuronal origin [2, 3, 26]. In addition, lectins specific for terminal sugar components of glycoproteins are also helpful in establishing the origin and degree of differentiation of a given tumour [5, 8, 10, 20, 27].

In the present study cytokeratin (CK), vimentin, desmin, human milk fat globule membrane antigen (MFGMA) and Ia antigen were studied immunohistologically in 38 anaplastic tumours. In addition, peanut agglutinin (PNA,

Send offprint requests to: L. Pajor M.D., Department of Pathology, University Medical School of Pécs, H-7643 Pécs, P.O. Box 99, Hungary

demonstration of early secretory activity [10] and Ulex europaeus I (UEA I, identification of endothelial cells and nasopharyngeal carcinomas) were used [24]. In certain cases prostate specific acid phosphatase (PSAP) and neurofilaments (NF) were demonstrated immunohistologically. The pre-B-cell selective monoclonal antibody VIB-C5 cross-reacting with cells of neuroectodermal origin were also used.

On the basis of our studies establishment of the histogenesis of 34 out of 38 tumours (90%) was possible. In 26 out of 38 cases (68%) it was also possible to indicate special differentiation and/or location of the primary tumours.

Materials and methods

Light microscopy

For light microscopical investigations materials were fixed in 10% formalin, then embedded in paraplast. 5 μm thick sections were stained with haematoxylin-eosin, PAS, Giemsa and reticulin.

Immunohistology

Cytokeratin, vimentin, desmin and neurofilament immunoreactivity were studied on 5 μm thick formol-paraffin sections using the peroxidase-antiperoxidase (PAP) method. For these investigations polyclonal anti-cytokeratin and desmin as well as monoclonal anti-vimentin and anti-neurofilament protein antibodies were employed (Histogen^c PAP kits, BioGenex Laboratories). For demonstrating the Ia antigen and the neuroepithelial nature OKIa (Ortho Diagnostic System Inc.) and VIB-C5 [19] monoclonal antibodies (dilution 1 : 40) were used (PAP method; Histogen^c PAP basic kit; BioGenex Laboratories). Prostate specific acid phosphatase (PSAP) was detected by means of polyclonal anti-PSAP (Immunoloc Inc.).

In a limited number of cases cryostat sections obtained from samples frozen in isopentan by liquid nitrogen were also used. Frozen sections were cut at -20 °C, then air-dried and fixed in acetone for 10 min at 4 °C. The sections were stored at -20 °C and used for immunohistology within a week.

Human milk fat globule membrane antigen (MFGMA) was isolated by PNA affinity chromatography and a polyclonal, monospecific antibody was generated against the protein moiety of the antigen in rabbit as described elsewhere [9]. The indirect immunoperoxidase method was used for immunostaining.

The reaction products were visualized by either 3,3'-diaminobenzidine-HCL (DAB, Serva) or 3-amino-9-ethylcarbazol (Sigma).

Lectin histochemistry

Lectins from peanut (PNA) and Ulex europaeus (UEA I) labelled with horseradish peroxidase were purchased from Sigma. Deparaffinized and rehydrated sections were treated with labelled lectins (10 μg/ml, 30 min, room temperature). After incubation the slides were washed three times in PBS. Lectin binding sites were visualized by means of 3-amino-9-ethylcarbazol. To uncover the masked binding sites for PNA, tissue sections were pretreated with neuraminidase (N-PNA reaction; 0.1 U neuraminidase/ml, Vibrio Cholerae, Boehring).

Cytokeratin, vimentin, desmin, N-PNA, UEA-I and MFGMA were tested on skin, tonsil, nasopharyngeal epithelium, bronchial epithelium, mammary gland, stomach, small and large intestines, urinary bladder, prostate and striated muscle as positive and negative controls. All the test materials were routinely processed using 10% formalin as fixative.

Electron microscopy

In selected cases, where electron microscopy was done, small blocks of the tissues were fixed in 2.5% glutaraldehyde, postfixed with 1% OsO_4 and dehydrated in graded acetone. Ultrathin sections were stained with lead citrate and uranyl acetate, then examined in a JEOL 100 C electron microscope.

Results

(1) *Reactivity pattern of antisera with normal tissues*

The reactivity of the antibodies to cytokeratin (CK), vimentin and desmin was consistent with reports on immunohistological and biochemical studies [22, 26, 37]. Two exceptions were, however, found: (i) a rather slight and equivocal positivity for CK was seen in the epithelium throughout the gastrointestinal tract; (ii) the antibody directed against vimentin exhibited consistent negativity in lymphoid cells, the negativity being independent of the normal or malignant nature of the cells and of whether formol-paraffin sections, frozen sections or cytopreps were used.

After neuraminidase treatment PNA (N-PNA) reacted distinctly with the epithelial cells of mammary glands, particularly with their apical membrane and with the secreted material. Slight to strong positivity was seen in stratified squamous epithelium, urothelium, in the membranes of podocytes and in the tubular epithelium of the kidney, in bronchial epithelium and pneumocytes I as well as in the columnar epithelium of prostatic glands. N-PNA was practically negative in normal gastrointestinal epithelium and mucus with the exception of the supranuclear dot-like staining of the Golgi regions in the glandular epithelium of the stomach. The epithelium of the tonsillar crypts and of the nasopharynx were positive with UEA-I; however, they failed to show binding for N-PNA.

The reactivity of the antibody directed against the protein moiety of the PNA receptor in the human milk fat globule membranes followed the reaction pattern of N-PNA except for the strong positivity of tonsil crypt epithelium and columnar epithelium of the gastrointestinal tract as well as the negativity for MFGMA of the membranes of podocytes.

(2) *Immuno- and lectin histochemical findings in tumours*

The age and sex of the patients, the sites of the biopsies, the reaction patterns of the tumours with the antibodies and lectins, the histopathologic diagnoses and the locations of the primary tumours are summarized in Table I. The combination of the routine histologic methods with immuno- and lectin histochemistry enabled the histogenesis in 34 out of 38 tumours (90%) to be established. Moreover, in 26 out of 38 cases (68%) an assessment of their differentiation or some indication of the location of the primary tumours could be given. In four cases (No 14, 17, 20, 22) the tumour cells failed to show any positivity with the antibodies and lectins used. Thus, only 4 out of 38 tumours (approx. 10%) remained unclassified.

Table I

The clinical data and the results of immunohistological finding in 38 tumours

No.	Age/sex (yrs)	Location	N-PNA	UEA-I	MFGMA	CK	V	D	Ia	Diagnosis[a]	Primary tumour[b]
1	60 ♂	urinary bladder	+	n.d.	+	−	−	−	n.d.	prostatic carcinoma[c]	prostatic gland
2	82 ♂	l.n., inguinal	−	−	+	+	−	−	n.d.	prostatic carcinoma[c]	prostatic gland
3	55 ♂	urinary bladder	+	−	+	+	−	−	n.d.	prostatic carcinoma[c]	prostatic gland
4	49 ♀	l.n., axillar	+	−	+	+	−	−	n.d.	adenocarcinoma	breast
5	14 ♂	l.n., cervical	−	+	+	+	−	−	−	NPC	nasopharynx
6	67 ♂	l.n., cervical	−	−	+	−	−	−	−	epithelial tumour	lung
7	78 ♀	colon	−	−	+	−	−	−	n.d.	epithelial tumour	colon
8	63 ♀	l.n., cervical	−	−	+	+	−	−	n.d.	epithelial tumour	unknown
9	80 ♀	l.n., cervical	+	−	+	−	−	−	n.d.	adenocarcinoma	thyroid gland
10	76 ♀	l.n., cervical	−	−	−	−	−	−	+	malignant lymphoma	l.n.
11	3 ♀	l.n., axillar	−	−	−	−	−	−	−	neuroblastoma[d]	adrenal gland
12	35 ♀	l.n., cervical	−	−	+	+	−	−	n.d.	epithelial tumour	unknown
13	57 ♂	l.n., cervical	+	−	+	+	−	−	−	adenocarcinoma	unknown
14	73 ♀	l.n., inguinal	−	−	−	−	−	−	n.d.	anaplastic tumour	unknown
15	31 ♂	bone marrow	+	−	+	n.d.	n.d.	n.d.	+	adenocarcinoma	stomach
16	70 ♂	l.n., cervical	−	−	+	−	−	−	n.d.	epithelial tumour	unknown
17	38 ♂	l.n., cervical	−	−	−	−	−	−	n.d.	anaplastic tumour	lung
18	57 ♀	l.n., cervical	−	+	+	−	−	−	n.d.	NPC	nasopharynx
19	54 ♂	l.n., cervical	−	+	+	+	−	−	−	NPC	nasopharynx
20	66 ♀	l.n., axillar	−	−	−	−	−	−	n.d.	anaplastic tumour	unknown
21	72 ♂	l.n., inguinal	−	−	+	+	−	−	n.d.	epithelial tumour	unknown
22	55 ♀	l.n., axillar	−	−	−	−	−	−	n.d.	anaplastic tumour	unknown
23	56 ♀	l.n., cervical	−	−	+	+	−	−	−	epithelial tumour	ovary
24	70 ♂	epipharynx	−	+	−	+	−	−	n.d.	NPC	epipharynx
25	74 ♂	l.n., axillar	+	−	+	+	+	−	−	adenocarcinoma	stomach
26	75 ♂	l.n., cervical	−	+	+	+	−	−	n.d.	NPC	nasopharynx
27	63 ♀	l.n., abdominal	+	−	+	+	−	−	n.d.	adenocarcinoma	unknown
28	74 ♂	l.n., cervical	+	−	−	−	−	−	n.d.	adenocarcinoma	stomach

29	69 ♀	l.n., inguinal	+	−	−	−	−	−	n.d.	adenocarcinoma	colon
30	34 ♀	parotid gland	−	+	+	+	−	−	n.d.	NPC	parotid gland
31	67 ♂	l.n., cervical	−	−	+	+	−	−	−	oat-cell carcinoma[d]	lung
32	36 ♂	retroperitoneum	−	+	+	+	−	−	n.d.	mesothelioma	retroperitoneum
33	13 ♂	retroperitoneum	−	−	−	−	+	−	n.d.	liposarcoma	retroperitoneum
34	54 ♀	l.n., inguinal	n.d.	−	−	+	+	−	−	adenocarcinoma	thyroid gland
35	60 ♂	l.n., axillar	−	−	−	−	−	−	+	malignant lymphoma	l.n.
36	32 ♀	l.n., cervical	−	−	+	+	−	−	n.d.	hypernephroma	kidney
37	52 ♂	l.n., cervical	+	−	+	−	+	−	−	adenocarcinoma	colon
38	50 ♂	skin	+[f]	−	+	+	−	−	n.d.	Merkel cell tumour[e]	skin

NPC = nasopharyngeal carcinoma
l.n. = lymph node
N-PNA = peanut agglutinin after neuraminidase treatment
UEA-I = Ulex europaeus agglutinin I
MFGMA = human milk fat globule membrane antigen
CK = cytokeratin; V = vimentin; D = desmin, Ia = Ia antigen
\+ = positive
− = negative
n.d. = not done
[a] = diagnosis made by routine pathologic study supplemented with immunohistology, lectin histochemistry as well as electron microscopy
[b] = primary tumour unknown means that either the clinical-radiological examination gave negative results or the patient dropped out the follow-up
[c] = prostate specific acid phosphatase positive
[d] = VIB-C5 positive
[e] = neurofilament positive
[f] = intra- or intercellular luminal membrane staining was absent

Table II

Histogenetic subtyping of tumours (n = 38)

Epithelial	28/38	74%
Neuroectodermal	3/38	8%
Malignant lymphoma	2/38	5%
Non-muscle sarcoma	1/38	3%
Myogenic	0/38	0%
Unclassified	4/38	10%
Total	38	100%

Table III

The distribution of MFGMA, CK and N-PNA reactivity among the epithelial tumours (n = 28)

MFGMA$^+$	24/28	86%
CK$^+$	18/28	64%
N-PNA$^+$	11/28	39%
MFGMA$^+$ + CK$^+$	16/28	57%
MFGMA$^+$ + CK$^+$ + N-PNA$^+$	5/28	18%
MFGMA$^+$ + N-PNA$^+$	9/28	32%
MFGMA$^+$ + N-PNA$^-$	15/28	54%
MFGMA$^-$ + N-PNA$^+$	2/28	7%

Among the classifiable tumours the epithelial ones (28 out of 38) represented the overwhelming majority (74%). In addition, there were 3 (8%) tumours of neuroectodermal origin, 2 (5%) malignant lymphomas, 1 (3%) non-muscle sarcoma, whereas myogenic tumours were absent in this series (Table II).

(a) *Epithelial markers.* The diagnosis of epithelial tumour was established when either MFGMA or CK, or both were shown to be present or early secretory activity could be demonstrated by means of N-PNA (Table III). MFGMA positivity proved to be the most consistent feature of epithelial tumours (in 24 out of 28 neoplasias, 86%). It was followed by CK being present in 18 out of 28 cases (64%), whereas secretory activity was detected in 11 out of 28 malignancies (39%). Glandular epithelial origin was established only in those cases when besides the intracellular dot-like staining of the Golgi regions intracellular vacuolar or luminal membrane stainings were seen with N-PNA. A shift from the luminal membrane to dot-like cytoplasmic staining was observed with increasing anaplasia. It is remarkable that among the 11 tumours with N-PNA positivity there were only 5 (No 3, 4, 13, 25, 17) showing also MFGMA and CK reactivity (Fig. 1). Three of them proved to be of glandular epithelial origin, whereas in 2 cases the primary tumours were unknown at the time of this study.

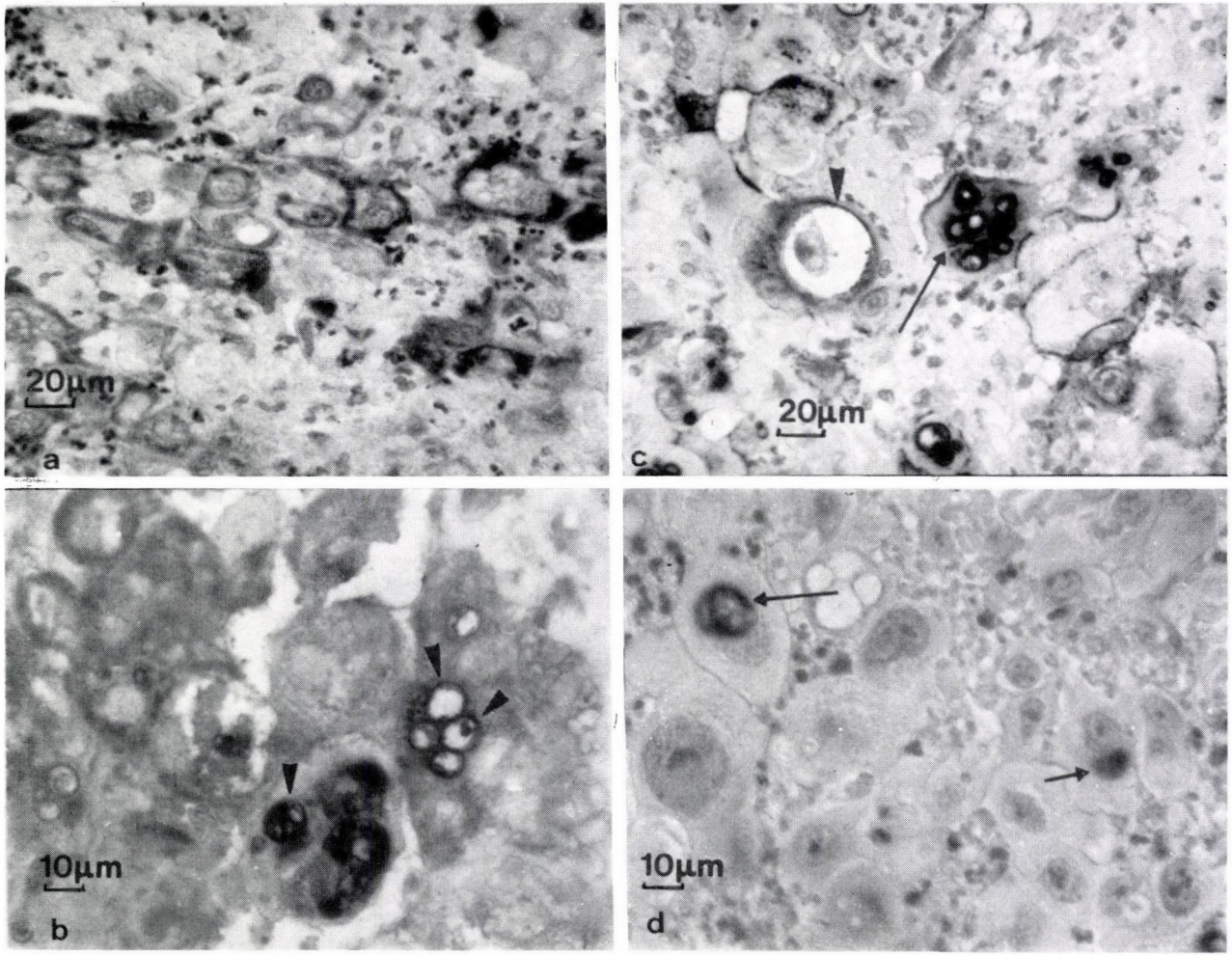

Fig. 1. Metastatic adenocarcinoma (No 25). *a.* CK (×250); *b.* and *c.* MFGMA and N-PNA, positively stained intra (arrow)-, and intercellular (arrowhead) lumen-like structures (×400 and ×250); *d.* vimentin positive paranuclear whirl-like structures (arrows, ×400)

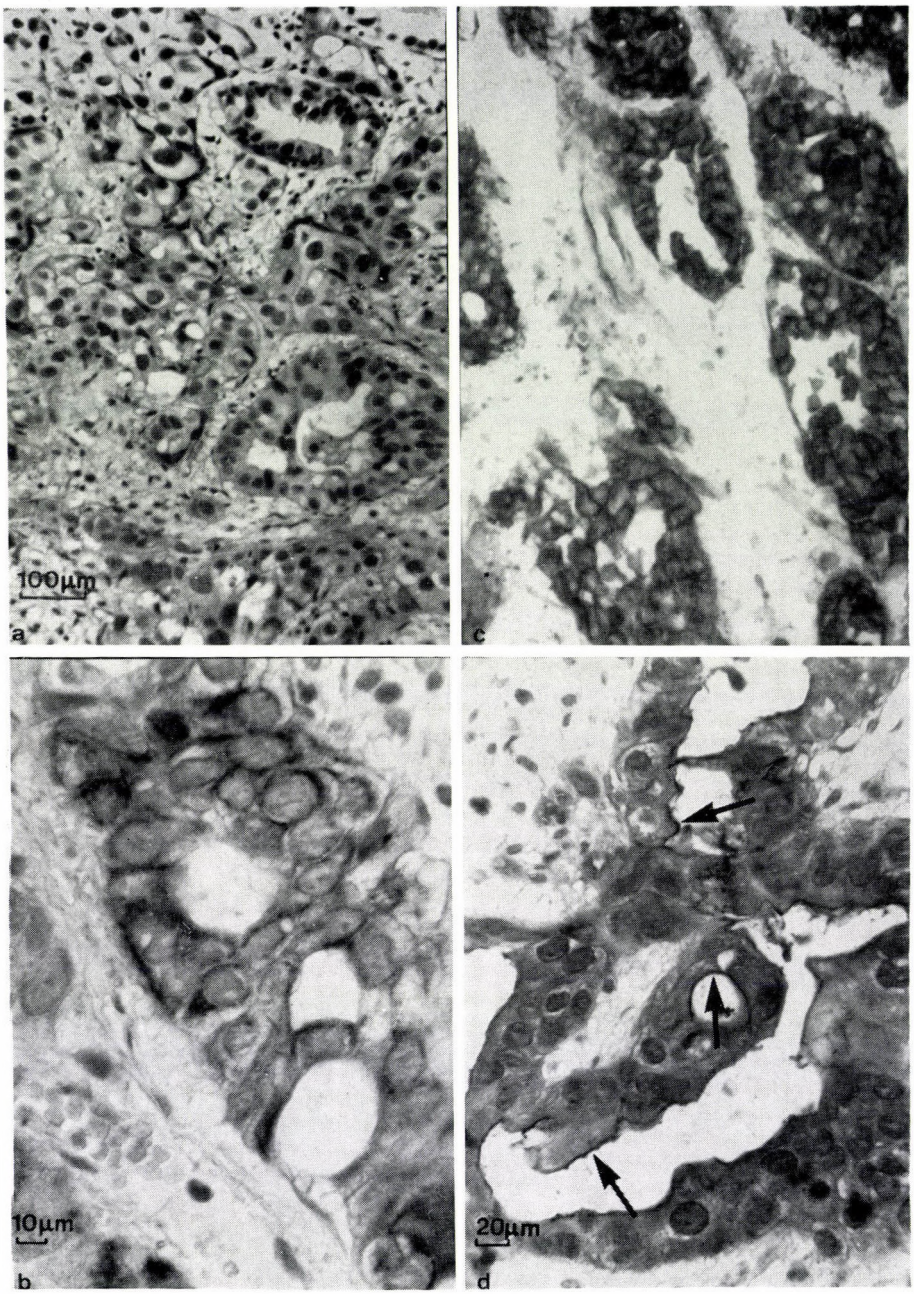

Fig. 2. Metastatic prostatic carcinoma (No 2). *a.* Haematoxylin-eosin (×100); *b.* CK (×400); *c.* PSAP (×100); *d.* MFGMA staining at luminal membranes (arrows) of the neoplastic cells (×250)

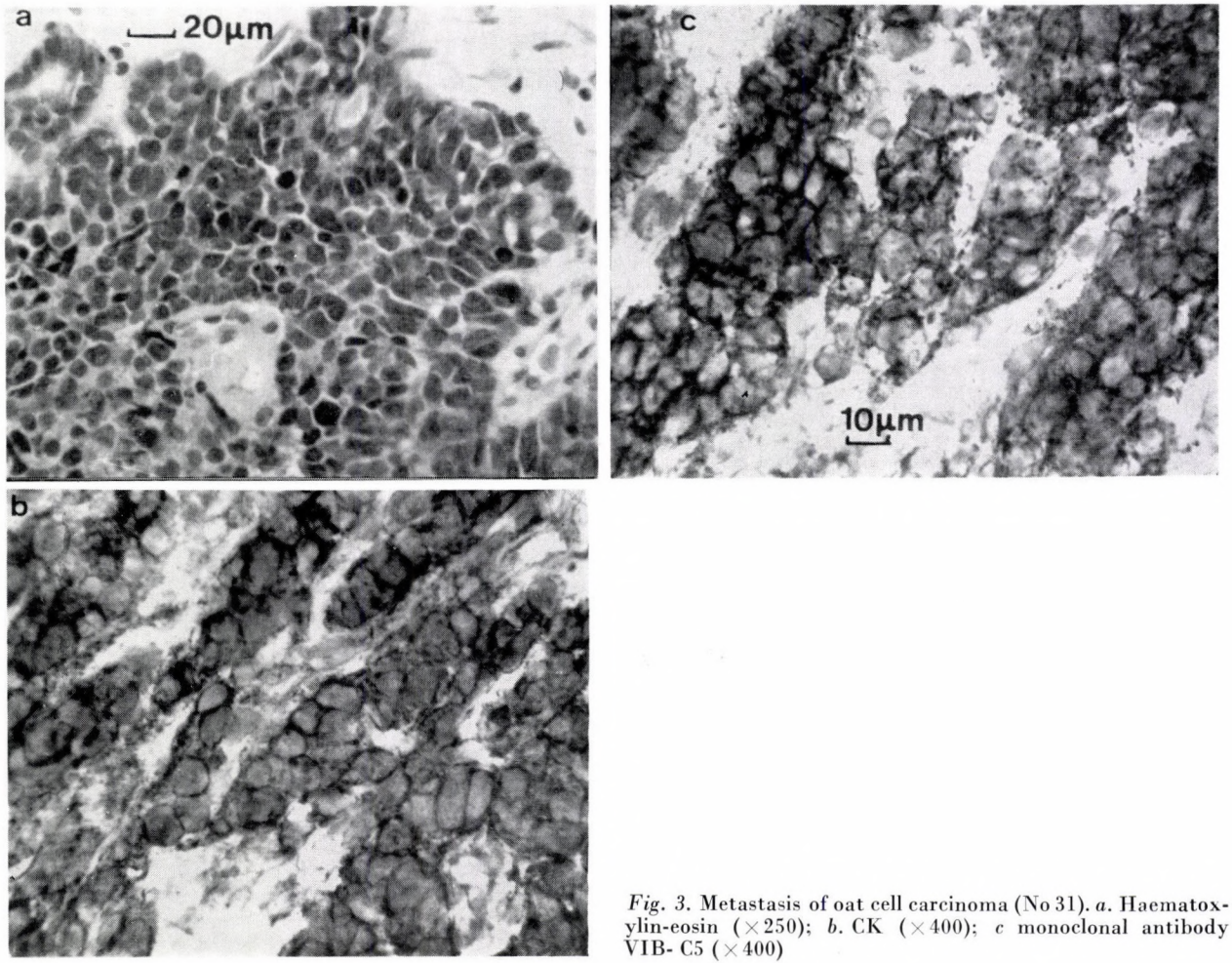

Fig. 3. Metastasis of oat cell carcinoma (No 31). *a.* Haematoxylin-eosin (×250); *b.* CK (×400); *c* monoclonal antibody VIB- C5 (×400)

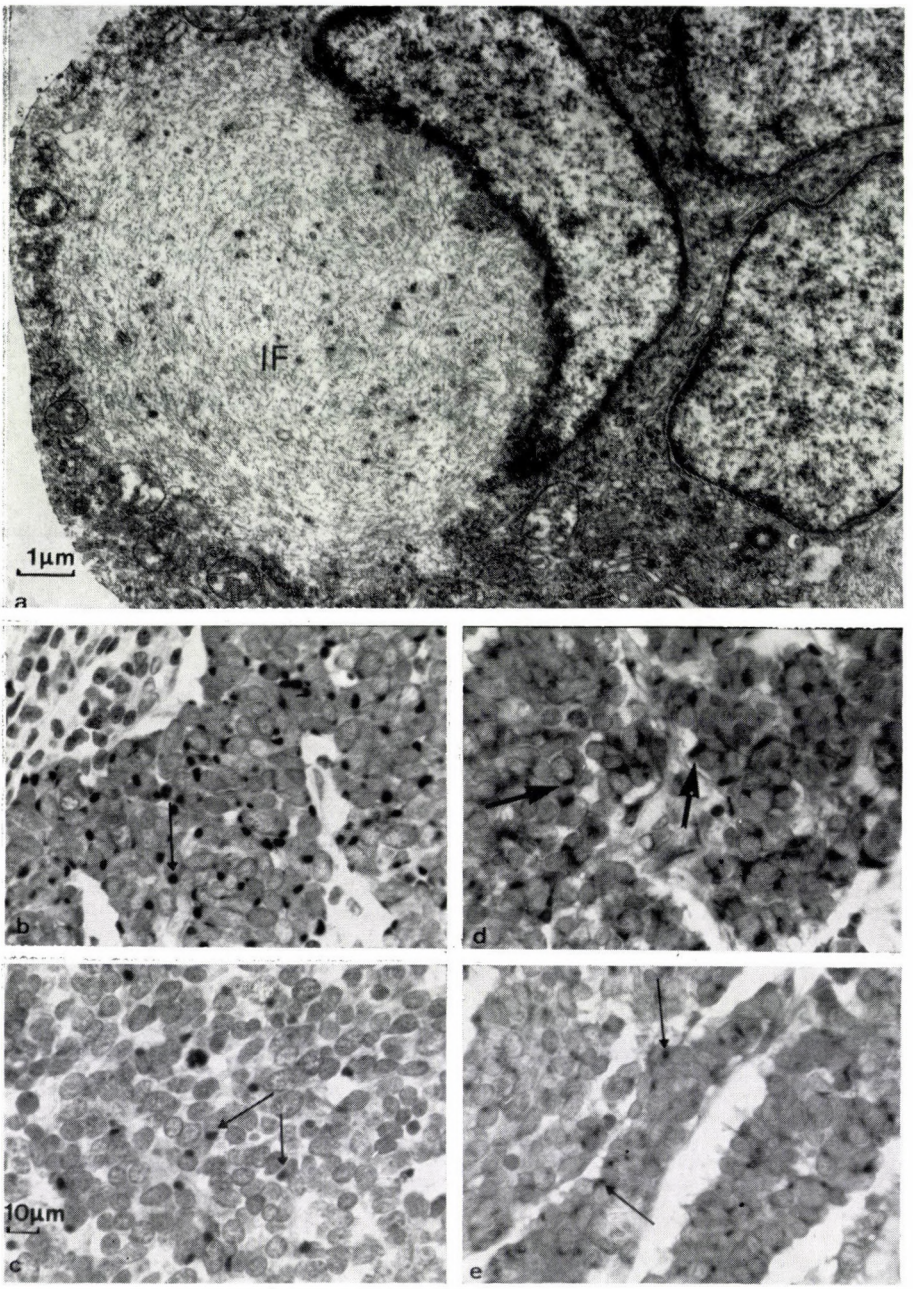

Fig. 4. Metastasis of Merkel tumour (No 38). *a*. EM whirl-like arrangement of intermediate filaments (IF, ×8300); *b*, *c*, *d* and *e* dot-like cytoplasmic positivity (arrows) for cytokeratin, neurofilament, MFGMA and with N-PNA (×400)

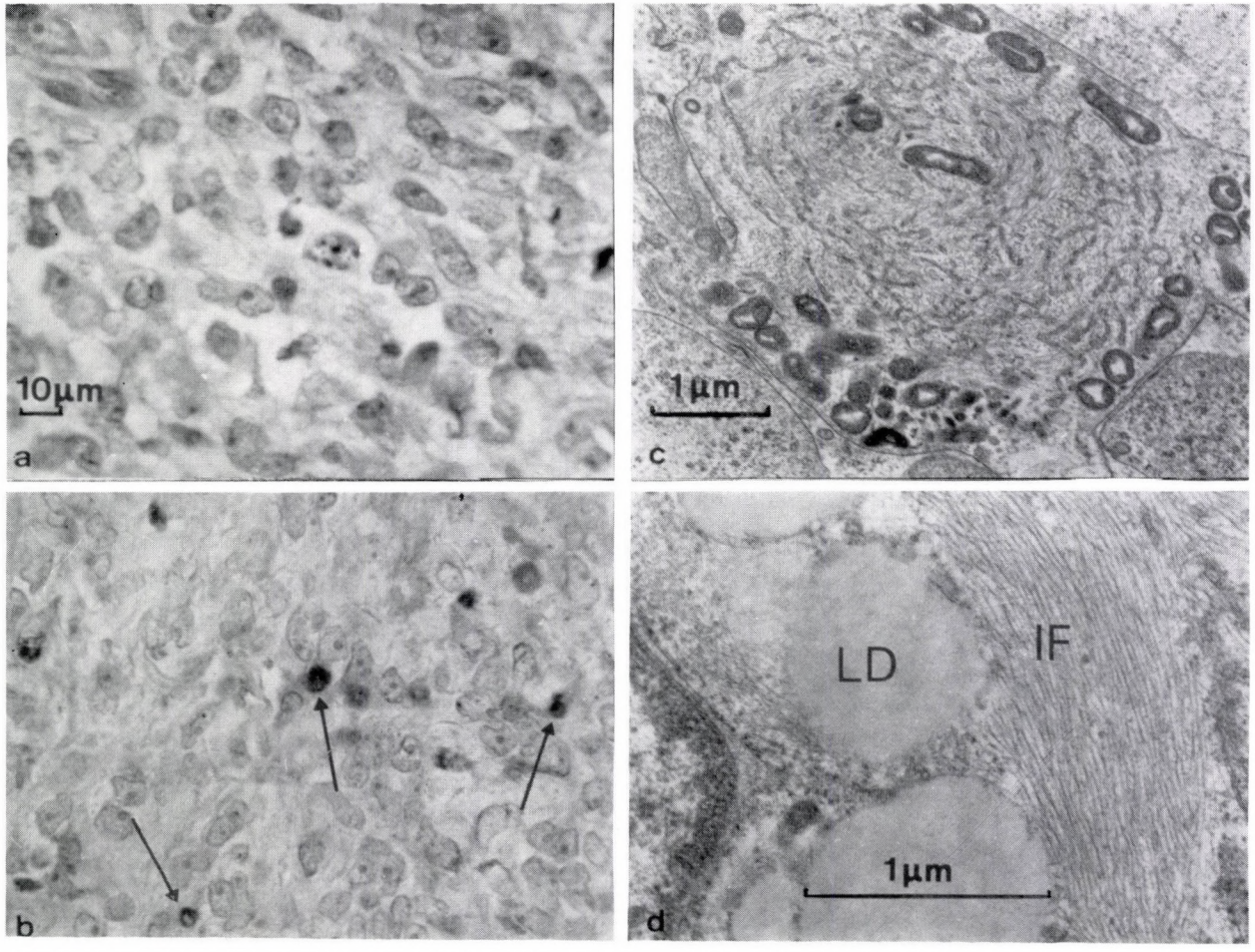

Fig. 5. Mesenchymal tumour (liposarcoma) (No 33). *a.* Giemsa staining (×400); *b.* dot-like cytoplasmic positivity for vimentin (arrows, ×400); *c.* EM whirl-like arrangement of intermediate filaments studded with mitochondria (×13 000); *d.* EM lipid droplets (LD) and bundle of intermediate filaments (IF, ×26 000)

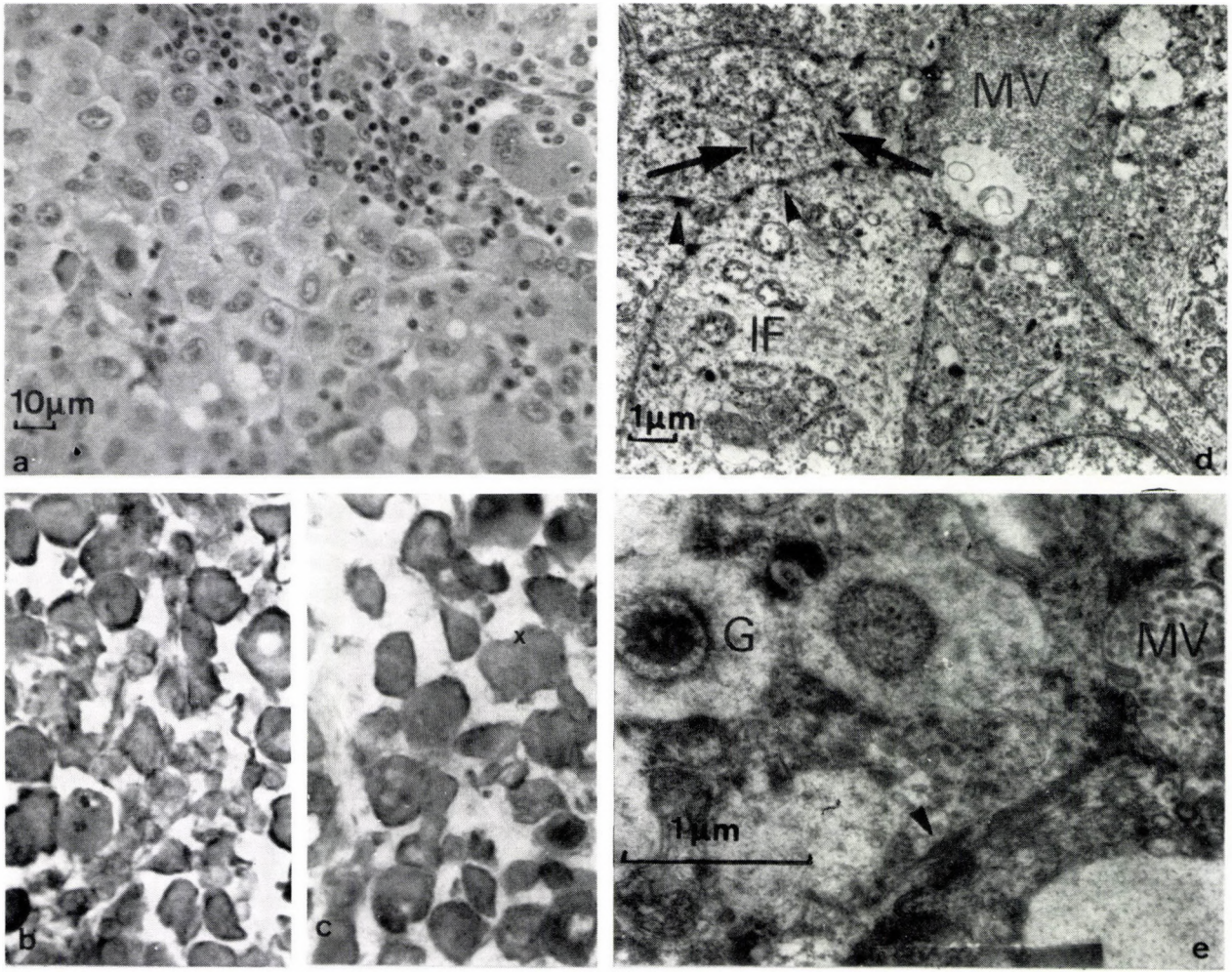

Fig. 6. Metastatic adenocarcinoma (No 34). *a.* Haematoxylineosin (×400); *b.* and *c.* strong positivity for CK and vimentin (×400); *d* and *e.* EM glandular structure with microvilli (MV) in the lumen, the surrounding cells contain secretory granules (G), intermediate filaments (IF), tonofilaments (arrows) and desmosome-like junctional complexes (arrowheads) (×5000 and ×20 000)

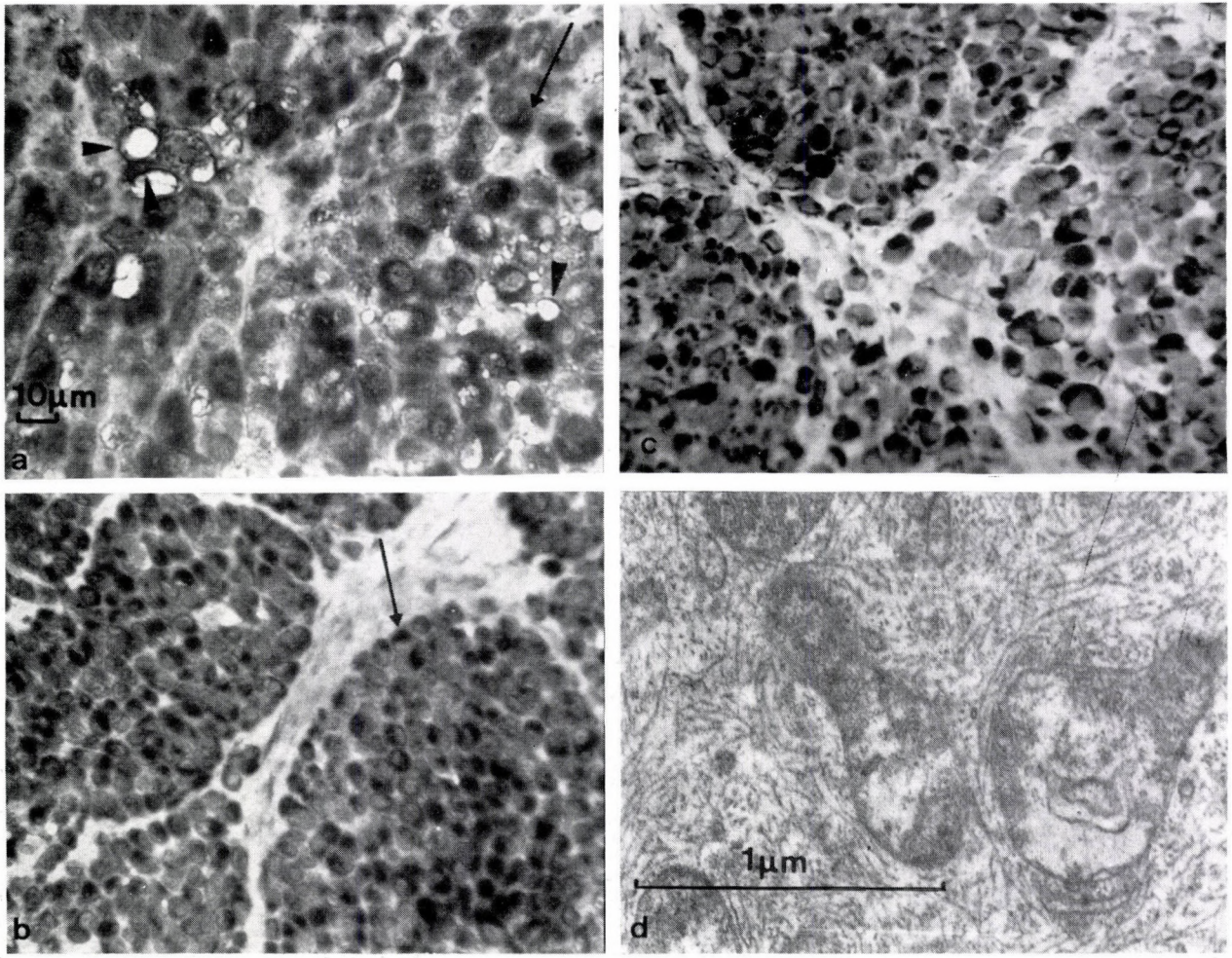

Fig. 7. Metastatic adenocarcinoma (No 37). *a* and *b*. Dot-like cytoplasmic (arrow) and luminal membrane staining (arrowhead) with N-PNA and for MFGMA (×400); *c*. intensive positivity for vimentin (×400); *d*. EM mitochondria and intermediate filaments in the poorly differentiated cytoplasm (×33 000)

It is also worth mentioning that of the 24 MFGMA positive tumours only 9 (32%) showed simultaneous reactivity to N-PNA and MFGMA whereas 15 tumours failed to exhibit a N-PNA binding property (Fig. 2). Moreover, there were two cases of neoplasia in which luminal membrane staining by N-PNA was not accompanied with anti-MFGMA binding.

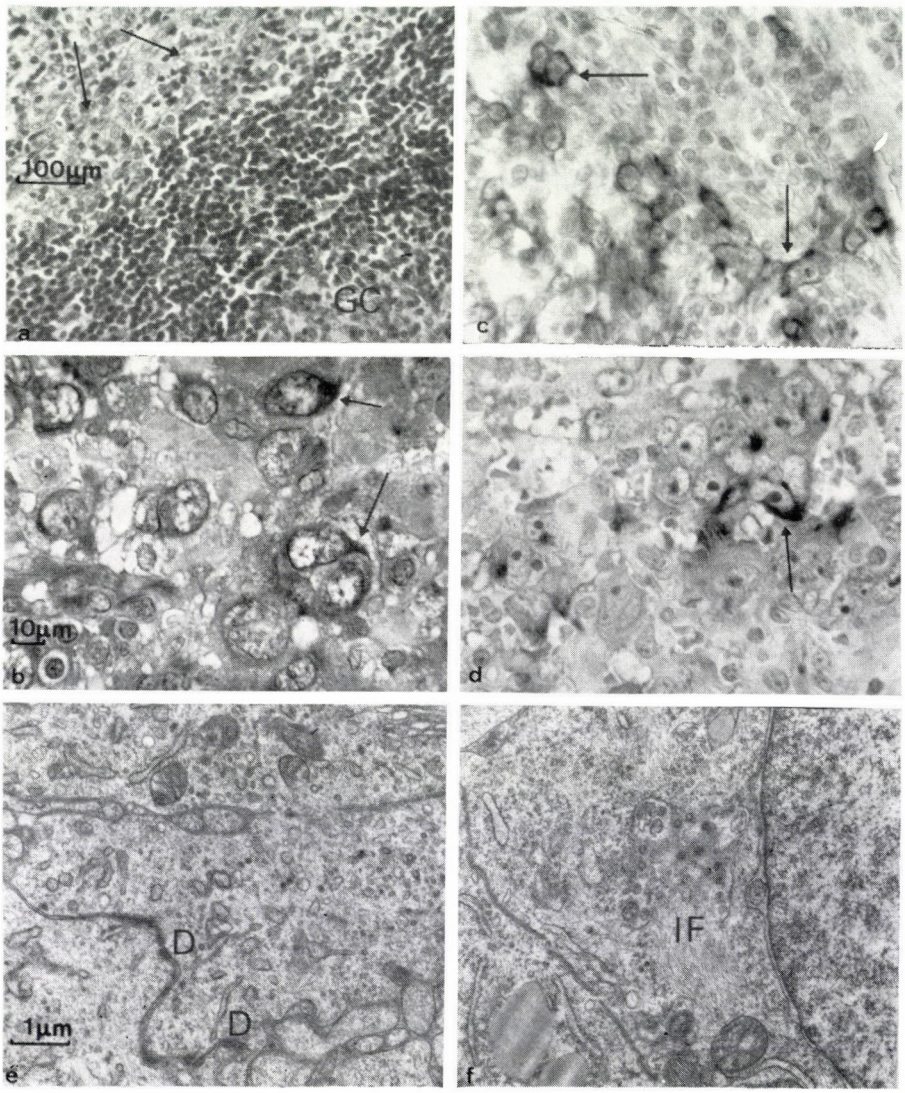

Fig. 8. Metastasis of nasopharyngeal carcinoma (No 19). *a.* Haematoxylin-eosin, infiltrating cells (arrows) in the parafollicular space, GC germinal centre (×100); *b, c* and *d* anaplastic cells positive for MFGMA, CK and with UEA-I (arrows) (×400); *e, f.* EM desmosomes (D) and intermediate filaments (IF) (×8300)

(b) *Tumours of neuroectodermal origin.* Out of the tumours with a definite diagnosis of neuroectodermal origin two proved to be positive for MFGMA and CK (No 31, 38) and to (No 11, 31) with antibody (VIB-C5) indicating their neuroepithelial nature (Fig. 3). In addition to the MFGMA and CK reactivity the tumour cells in case No 38 showed dot-like cytoplasmic positivity with N-PNA and for neurofilament protein (Fig. 4).

(c) *Vimentin reactivity.* Four (No 25, 33, 34, 37) out of the 38 investigated tumours were positive for vimentin but none for desmin. One of the vimentin positive tumours (No 33) proved to be only vimentin reactive indicating its mesenchymal origin (Fig. 5), the other three exhibited simultaneous reactivity for epithelial markers (Figs 1, 6 and 7).

(d) *UEA-I reactivity.* Seven tumours (No 5, 18, 19, 24, 26, 30 and 32) showed UEA-I staining, and all of them were also positive for at least one of the epithelial markers (Fig. 8). In five out of 7 the subsequent clinico-radiological investigations revealed the primary tumours to be situated in the nasopharynx whereas in the remaining two in the parotid gland and in the retroperitoneum.

(e) *Ia antigen.* Three (No 10, 15, 35) out of 13 tumours were positive for Ia antigen in cryostat sections, two of the three failed to react with any of the antibodies or lectins used. However, the third (No 15) was reactive with MFGMA and exhibited secretory activity as well.

(f) *Electron microscopic findings.* In the few cases where electron microscopy was made findings confirmed the histogenetic assumption based on immuno- and lectin histochemistry. In cases No 6 and 19, bundles of intermediate filaments and desmosome-like junctional complexes were observed (Fig. 8). In case No 34, in addition to the desmosomes and tonofilaments, early signs of glandular differentiation with lumen-like formations, lined with microvilli, surrounded with epithelial cells containing secretory granules were seen (Fig. 6). In case No 37 a large number of intermediate filaments were observed whereas secretory granules could not be revealed (Fig. 7). In case No 33, tumour cells were heavily packed with intermediate filaments and a large number of lipid droplets were seen (Fig. 5). The tumour cells in No 38 contained a large number of intermediate filaments forming whirl-like structures as well as neurosecretory granules (Fig. 4).

Discussion

The aim of the present study was to estimate the efficacy of immunohistology and lectin histochemistry in establishing the histogenesis of anaplastic tumours. Among the markers studied the IFPs have recently been taken for reliable and highly specific indicators of the known embryonic pathways of

differentiation [2, 3]. It is also known that tumour cells, even in metastases, retain the specific IFP pattern of the corresponding normal cells [21].

Fixation significantly influences the immunohistological demonstration of IFPs. The use of frozen sections was undoubtedly the most reliable method; nevertheless, a number of authors reporting on IFP typing used formol-paraffin sections [17, 34, 35]. The results can be improved by alcohol fixation [2].

When the antibodies used in the present study were tested on formol-paraffin sections, a strong, distinct and specific reaction was seen in all the cells and tissues where it was to be expected. Nevertheless, two points need some consideration. First, the reactivity of gastrointestinal epithelium with the polyclonal antibody directed against cytokeratin was not unequivocal. Because this antibody was prepared predominently against 56 kD and 64 kD cytokeratin filaments, the poor reactivity of the gastrointestinal tract epithelium is likely to be due to the failure of this antibody to react with cytokeratin proteins of lower molecular weight which are more characteristic of columnar epithelium [38]. Second, we were not able to demonstrate vimentin in lymphoid cells of different origins. This is surprising because vimentin has recently been demonstrated at least in the lymphoid elements of the T-zone as well as in malignant lymphomas [13, 14].

By means of combined application of immunohistology and lectin histochemistry about 90% of tumours was classified. These results are in good agreement with that was reported by Poston and Sidhu [28] in their recent study.

Tumours of epithelial origin

(1) *MFGMA reactivity*. MFGMA positivity proved to be the most constant feature of the epithelial origin: 86% of epithelial tumours expressed this antigen. Similarly, Zotter et al. [42] reported 90% reactivity in non-mammary epithelial tumours using a monoclonal antibody (MAM-6) against human MFGMA on paraffin sections. It should be mentioned that on the basis of biochemical and immunological analysis MFGMA isolated by PNA affinity chromatography seems to be very similar if not identical with the epithelial membrane antigen [9]. Thus the wide tissue specificity, including simple, squamous and stratified epithelia, of the antibody against MFGMA used in this study may explain the superiority of MFGMA as an epithelial marker.

(2) *Cytokeratin reactivity*. Epithelial tumours were positive for CK in 64%. This result is similar to the 57% reactivity found by Schlegel et al. [35] using formol-paraffin sections.

Studies on CK biochemistry led to the recognition that stratification and keratinization result in a shift of CK polypeptide expression to higher

apparent molecular weight [41]. Consequently, the specificity range of the antibody used by us makes the demonstration of CK of columnar epithelial type somewhat uncertain. This may be one of the factors responsible for the lower value of anti-CK in epithelial tumours. Nonetheless, only 5 out of 11 tumours with sign of an early secretory activity were reactive to CK. Although Moll et al. [22] did not report any significant changes in the CK pattern due to malignant transformation, this observation suggests that in the above-mentioned cases the malignant transformation may have been accompanied with a shift of CK profile. This assumption was further supported by the finding of strong CK reactivity in one of the tumours (No 34) in which electron microscopy revealed intercellular lumina lined with microvilli. Besides fine and scanty IFs there were, however, also rough bundles corresponding to tonofilaments, which are present all but exclusively in squamous epithelial cells [12].

(3) *N-PNA reactivity: secretory potential.* N-PNA specific to the terminal D-galactosyl-(1-3)-N-acetyl-D-galactosamine moiety has recently been shown to be an excellent marker of early secretory activity [8, 18]. In addition, PNA reactivity seems to closely parallel the estrogen receptor status in mammary carcinomas [16]. Our results confirm that N-PNA is superior to the PAS reaction in demonstrating early secretory activity (11 N-PNA positive and PAS negative tumours vs. one tumour with combined reactivity, data not shown). Three types of N-PNA staining were observed: dot-like cytoplasmic cytoplasmic vacuolar and intraluminal staining. Depending on the maturity of the tumour the latter two were more or less pronounced probably indicating secretory malfunction with complete or incomplete inhibition of secretion. Dot-like cytoplasmic staining in itself is not indicative of an anaplastic adenocarcinoma because a number of neoplasias including melanoma, malignant histiocytosis and Merkel tumour were found to show this feature [10, 27].

Neuroectodermal tumours

Two out of three tumours considered to be of neuroectodermal origin proved to be positive for MFGMA and CK indicating that these markers are reliable and overall indicators of the ectodermal origin. The CK reactivity of oat cell carcinoma substantiates the recent finding of Blobel et al. [6], however, it contradicts that of Lehto et al. [21], who found negativity for CK in oat cell carcinomas. The tumour diagnosed as neuroblastoma metastasis failed to show positivity for any of the markers supporting the finding of Osborn et al. [25]. Although there are contradictory reports regarding the IFP content of Merkel cell tumours [15, 33, 39], the combined reactivity to CK, neurofilament, N-PNA and to MFGMA in case of tumour No 38 spoke unequivocally for a neuroectodermal malignancy [27].

Coexpression of vimentin and CK

As a rule a single cell type is characterized by a single IFP [39]. There are, however, exceptions among both normal and transformed cells [3, 4, 7, 26]. Although tumour cells do retain their original IFP pattern in the course of dissemination, sometimes they additionally acquire vimentin, a phenomenon referred to as vimentinization [29]. Generally, vimentinization is considered to occur when tumour cells spread in body fluids resulting in pleural effusion or ascites [30]. In three of our cases we demonstrated the presence of vimentin in solid metastases of epithelial tumours which might be due to the vimentinization.

Ulex europaeus agglutinin I reactivity

The histogenesis of nasopharyngeal carcinoma (NPC) is somewhat controversial, but, in the light of recent investigations, the balance is just leaning towards the respiratory epithelial origin [36]. Besides the characteristic CK protein pattern, NPC cells have recently been found to bind preferentially to the fucose specific UEA-I lectin. The differential diagnostic value of this feature was emphasized [23]. In our hands the combined reactivity to UEA-I and MFGMA/CK proved to be a very reliable diagnostic tool in differentiating NPC from other epithelial tumours or from malignant lymphomas.

Ia antigen reactivity

On the basis of Ia antigen reactivity, two tumours (No 10, 35) were diagnosed as malignant lymphoma [32]. However, in contrast to the observation of Osborn et al. [26] and Gabbiani et al. [11] as well as in agreement with that of Giorno [13] and Giorno and Sciotto [14] we were unable to demonstrate vimentin in lymphoma cells. Ia antigen has also been detected in a series of non-haematologic cells and tumours [1, 40]. In case of tumour No 15, positive for Ia antigen, the simultaneous reactivity to N-PNA and MFGMA helped us in establishing the glandular origin.

Acknowledgement

The authors thank Prof. Dr. W. Knapp (Department of Immunology, University of Vienna) for providing the monoclonal antibody VIB-C5, as well as Heintel GmbH (Vienna) for the anti-cytokeratin, anti-desmin and anti-vimentin antibodies.

REFERENCES

1. Aichinger G, Fill H, Wick G: In situ immune complexes, lymphocyte subpopulations, and HLA-DR-positive epithelial cells in Hashimoto thyroiditis. Lab Invest 52: 132, 1985
2. Altmannsberger M, Osborn M, Schauer A, Weber K: Antibodies to different intermediate filament proteins. Cell type-specific markers on paraffin-embedded human tissues. Lab Invest 45: 427, 1981
3. Altmannsberger M, Weber K, Hölscher A, Schauer A, Osborn M: Antibodies to intermediate filaments as diagnostic tools. Lab Invest 46: 520, 1982
4. Altmannsberger M, Weber K, Droste R, Osborn M: Desmin is a specific marker for rhabdomyosarcomas of human and rat origin. Am J Pathol 118: 85, 1985
5. Aub JC, Tieslan C, Lankester A: Reactions of normal and tumour cell surface enzymes I. Wheat germ lipase and associated mucopolysaccharides. Proc Natl Acad Sci USA 50: 613, 1963
6. Blobel GA, Gould VE, Moll R, Lee I, Huszár M, Geiger B, Franke WW: Coexpression of neuroendocrine markers and epithelial cytoskeletal proteins in bronchopulmonary neuroendocrine neoplasms. Lab Invest 52: 39, 1985
7. Caselitz J, Jänner M, Breitbart E, Weber K, Osborn M: Malignant melanomas contain only the vimentin type of intermediate filaments. Virchows Arch (Pathol Anat) 400: 43, 1983
8. Fischer J, Klein PJ, Vierbuchen M, Skutta B, Uhlenbruck G, Fischer R: Characterization of glycoconjugates of human gastrointestinal mucosa by lectins. I. Histochemical distribution of lectin binding sites in normal alimentary tract as well as in benign and malignant gastric neoplasms. J Histochem Cytochem 32: 681, 1984a
9. Fischer J, Klein PJ, Farrar GH, Hanisch FG, Uhlenbruck G: Isolation and chemical and immunochemical characterization of the peanut-lectin-binding glycoprotein from human milk-fat-globule membranes. Biochem J 224: 581, 1984b
10. Fischer J, Klein PJ: Differential diagnosis of anaplastic gastric cancers by lectins. Lectins 4: 101, 1985
11. Gabbiani G, Kapanci Y, Barazzone Ph, Franke WW: Immunochemical identification of intermediate-sized filaments in human neoplastic cells. Am J Pathol 104: 106, 1981
12. Ghadially FN: Is it a squamous cell carcinoma or an adenocarcinoma? In: Ghadially FN, (ed.) Diagnostic Electron Microscopy of Tumours. Butterworth, London, Boston 1980, pp 68–78
13. Giorno R: Immunohistochemical analysis of the distribution of vimentin in human peripheral lymphoid tissues. Anat Rec 211: 43, 1985
14. Giorno R, Sciotto CG: Use of monoclonal antibodies for analyzing the distribution of the intermediate filament protein vimentin in human non-Hodgkin's lymphomas. Am J Pathol 120: 351, 1985
15. Gray C: Merkel cell carcinomas. Histopathology 7: 803, 1983
16. Helle M, Krohn K: Reactivity of a monoclonal antibody recognising an estrogen receptor regulated glycoprotein in relation to lectin histochemistry in breast cancer. Virchows Arch (Pathol Anat) 410: 23, 1986
17. Jasani B, Edwards RE, Thomas ND, Gibbs AR: The use of vimentin antibodies in the diagnosis of malignant mesothelioma. Virchows Arch (Pathol Anat) 406: 441, 1985
18. Klein PJ, Citoler P, Newman RA, Uhlenbruck G: Die Bedeutung von Lektin-Rezeptoren für das Carcinoma lobulare in situ (CLIS) der Mamma. Verh Dtsch Ges Path 63: 591, 1979
19. Knapp W: Monoclonale antikörper in der Leukämiediagnose. Diagnose und Labor 35: 12, 1985
20. Lehman TP, Cooper HS, Mulholland SG: Peanut lectin binding sites in transitional cell carcinoma of the urinary bladder. Cancer 53: 272, 1984
21. Lehto VP, Stenman S, Miettinen M, Dahl D, Virtanen I: Expression of a neural type of intermediate filament as a distinguishing feature between oat cell carcinoma and other lung cancers. Am J Pathol 10: 113, 1983
22. Moll R, Franke WW, Schiller DL: The catalog of human cytokeratins: patterns of expression in normal epithelia, tumours and cultured cells. Cell 31: 11, 1982
23. Möller P, Lennert K: On the angiostructure of lymph node in Hodgkin's disease. An immunohistochemical study using the lectin I of Ulex europaeus as endothelial marker. Virchows Arch (Pathol Anat) 403: 257, 1984
24. Möller P, Wirbel R, Hofmann W, Schwechheimer K: Lymphoepithelial carcinoma (Schmincke type) as a derivate of the tonsillar crypt epithelium. Virchows Arch (Pathol Anat) 405: 85, 1984

25. Osborn M, Altmannsberger M, Shaw G, Schauer A, Weber K: Various sympathetic derived human tumors differ in neurofilament expression. Virchows Arch (Pathol Anat) 40: 141, 1982
26. Osborn M, Weber K: Tumour diagnosis by intermediate filament typing: a novel tool for surgical pathologist. Lab Invest 48: 372, 1983
27. Pajor L, Balázs M, Balogh J, Brittig F, Joós L, Linse R, Scholz M, Suba Zs, Tóth P Ultrastructural, lectin histochemical and immunohistological observations on Merkel cell tumours. Path Res Pract 181: 45, 1986
28. Poston RN, Sidhu YS: Diagnosing tumours on routine surgical sections by immunohistochemistry: use of cytokeratin, common leukocyte and other markers. J Clin Pathol 39: 514, 1986
29. Ramaekers F, Puts J, Moesker O, Kant A, Jap PHK Vooijs GP, Demonstration of keratin in human adenocarcinomas. Am J Pathol 111: 213, 1983a
30. Ramaekers FCS, Haag D, Kant A, Moesker O, Jap PHK, Vooijs GP: Coexpression of keratin- and vimentin-type intermediate filaments in human metastatic carcinoma cells. Proc Natl Acad Sci USA 80: 2618, 1983b
31. Ramaekers FCS, Moesker O, Huysmans A, Schaart G, Westerhof G, Wagenaar SS, Herman CJ, Vooijs GP: Intermediate filament proteins in the study of tumor heterogeneity: an in-depth study of tumors of the urinary and respiratory tract. Ann NY Acad Sci 455: 614, 1985
32. Ritz J, Griffin JD: Cell-surface antigens in acute leukemia. Ia antigen. In: Minich, E (ed.) Biological responses in cancer, Vol. 1: Progress toward potential applications. Plenum Publishing Corporation, New York 1982, pp 4–5
33. Ruiter DJ, van Muyen GNP, Warnaar SO: Intermediate filaments in Merkel cell tumours. J Pathol 145: 120A, 1985
34. Said JW, Nash G, Banks-Schlegel S, Sassoon AF, Murakami S, Shintaku IP: Keratin in human lung tumors. Patterns of localization of different-molecular-weight keratin proteins. Am J Pathol 113: 27, 1983
35. Schlegel R, Banks-Schlegel S, McLeod JA, Pinkus GS: Immunoperoxidase localization of keratin in human neoplasms. Am J Pathol 101: 41, 1980
36. Shi S-R, Goodman ML, Bhan AK, Pilch BZ, Chen LB, Sun T-T: Immunohistochemical study of nasopharyngeal carcinoma using monoclonal keratin antibodies. Am J Pathol 117: 53, 1984
37. Sun T-T, Shih C, Green H: Keratin cytoskeletons in epithelial cells of internal organs. Proc Natl Acad Sci USA 76: 2813, 1979
38. Tseng SchCG, Jarvinen MJ, Neison WG, Huang J-W, Woodcock-Mitchell J, Sun T-T: Correlation of specific keratins with different types of epithelial differentiation: monoclonal antibody studies. Cell 30: 361, 1982
39. Virtanen I, Miettinen M, Lehto V-P, Kariniemi A-L, Paasivuo R: Diagnostic application of monoclonal antibodies to intermediate filaments. Ann NY Acad Sci 455: 635, 1985
40. Wilson BS, Herzig MA, Lloyd RV: Immunoperoxidase staining for Ia-like antigen in paraffin embedded tissues from human melanoma and lung carcinoma. Am J Pathol 115: 102, 1984
41. Woodcock-Mitchell J, Eichner R, Nelson WG, Sun T-T: Immunolocalization of keratin polypeptides in human epidermis using monoclonal antibodies. J Cell Biol 95: 580, 1982
42. Zotter S, Lossnitzer A, Kunze K-D, Müller M, Hilkens J, Hilgers J, Hageman PH: Epithelial markers for paraffin-embedded human tissues. Immunohistochemistry with monoclonal antibodies against milk fat globule antigens. Virchows Arch (Pathol Anat) 406: 237, 1985

Acta Morphologica Hungarica, 36 (1–2), pp. 121–132 (1988)

EFFECT OF CADMIUM ON THE RAT INTESTINE

D. Hulínská, M. Vojtíšek, D. Bittnerová, M. Cikrt, V. Hulínský

INSTITUTE OF HYGIENE AND EPIDEMIOLOGY, PRAGUE VŠCHT, LABORATORY OF ELECTRON MICROSCOPY, PRAGUE, CZECHOSLOVAKIA

(Received 30 May 1987)

The effect of cadmium on rat jejunal mucosa was observed after application of $CdCl_2$ doses: acute single (32.5 mg · kg^{-1}) or combined (32.5 + after 24 h 162.5 mg · kg^{-1}) and chronic (250 mg · l^{-1}, daily consumption 10 ml for 3 months). Inhibition of mucosal respiration, measured by a Clark electrode was 44, 50.4 and 38.4% respectively, as related to 100% of controls. Metallothionein was determined in the mucosa for combined and chronic doses.

Electron X-ray microanalysis has shown Cd^{2+} distribution in dependence on pathological changes: greater regressive changes caused smaller Cd^{2+} retention. In acute experiments Cd^{2+} penetrate by passive diffusion through foci of damaged villi into the lamina propria. In crypt absorptive cells with preserved alcalic phosphatase and succinate dehydrogenase activity and in Paneth cells Cd^{2+} retention was determined. Combined dose of Cd^{2+} damaged homeostasis and prevented Cd^{2+} retention. In chronic experiments occurred a diffuse distribution of Cd^{2+} in the mucosa.

Keywords: Mucosal respiration, metallothionein, Paneth cells

Introduction

Little is known about the mechanism of absorption and transport of cadmium through the wall of small intestine into the organism [8, 14]. Pathological changes in small intestine after oral application of low Cd^{2+} doses were observed by Richardson and Spivey-Fox [13]. Taguchi and Suzuki [17] ascertained very fast uptake of Cd^{2+} by absorptive cells and its binding to metallothionein in the intestinal mucosa. Also the presence of cellular organelles in cadmium storage has not been fully explained. Even the opinion of Steibert et al. [15] about the importance of mitochondria in storage and transport of cadmium is of a relative value only, as well as binding of cadmium to cellular nuclei, as supposed by Goyer and Wilson [5].

The aim of this study is to contribute to the understanding of transport mechanism of cadmium in gastrointestinal tract after its oral entry.

Send offprint request to: D. Hulínská, Institute of Hygiene and Epidemiology, Electron Microscopy, Prague, Šrobárova 48, 100 42, Czechoslovakia

Materials and methods

Experiments were performed on female Wistar rats, average weight 200–250 g. In an acute test with a single dose (a) rats were given in ether narcosis 32.5 mg · kg^{-1} $CdCl_2$ on the first day by gavage. This dose was effective for 24 h. In acute test with combined doses (b) rats were premedicated with an oral dose of 32.5 mg · kg^{-1} $CdCl_2$ for 24 h before the application of second oral dose of 162.5 mg · kg^{-1} $CdCl_2$ by gavage. Second dose was effective for 1 h, in respiration tests also for 3 h. In chronic tests (c) rats were drinking daily 10 ml on average a solution with 250 mg · l^{-1} $CdCl_2$ for 3 months. Control rats drank distilled water only. After 3 months rats were killed by decapitation and after laparotomy the jejunum was isolated.

For biochemical study the jejunum was soaked with a cold saline and mucosa was scraped by means of microscopic glass. Oxygen consumption was measured on jejunal mucosal scraping in a Krebs–Ringer phosphate buffer (pH = 7.4) by means of Clark electrode in a glass vessel at 37 °C, provided with magnetic stirring. For range calibration air oxygen at the start and nitrogen at the end of measurement were used.

Determination of metallothionein in the jejunal mucosa cytosol was performed according to Squibb et al. [14]. After previous mucosa homogenisation and centrifugation in cold mucosal cytosol was separated on a chromatographic column with Sephadex G-75. Individual fractions were measured spectrophotometrically on Unicam SP-1800 and atomic absorption spectrophotometer Varian Techtron AA 175 was used for cadmium determination.

For histochemical study the jejunum was frozen in liquid nitrogen and cut on cryocut (Reichert). Succinate dehydrogenase (SDH) activity, Mg^{2+} adenosine triphosphatase (ATPase) activity as well as acid (AcP) and alcalic (AlP) phosphatase activities were determined according to Lojda and Papoušek [9].

Another part of the jejunum was fixed in Baker's neutral formaldehyde, dehydrated and embedded in paraffin. Energy dispersive spectrometer (EDS) together with Jeol JCX II microscope was used for the study of ultrathin jejunal sections in transmission (TEM), scanning (SEM) and scanning transmission (STEM) mode. Samples for X-ray microanalysis were fixed either with 2,5 glutaraldehyde in 0.1 mol · l^{-1} cacodylate buffer or were snap frozen in liquid nitrogen and freeze substituted with 1% osmium tetroxide. After dehydration with acetone samples were embedded in Epon 812.

For ultrastructural study tissue was fixed with Karnovsky's glutaraldehyde-paraformaldehyde fixative in Thyroid buffer, postfixed with 1% OsO_4, dehydrated and embedded in Epon. Thin sections were mounted on Cu or Al grids, carbonized for STEM and SEM study or stained with uranyl acetate (UA) or lead citrate (LC) for TEM study. For determination of selected area composition with EPMA following conditions were chosen: 80–100 kV, 80 μA emission current, slope angle 45°, detector distance 21 mm, sampling time 200 s.

Results

Biochemically, the effect of Cd^{2+} on the respiration of jejunal mucosa and induction of metallothionein (MT) were observed. The results of the effects of cadmium on oxygen consumption of mucosa are depicted in Table I. Both acute (a, b) and chronic (c) tests cadmium caused significant inhibition of respiration. In acute tests with combined doses (b) degree of inhibition was increasing with duration of $CdCl_2$ exposure.

The presence of metallothionein induction in mucosa was not determined in acute (a) tests but in acute (b) tests MT was demonstrated even if microanalysis has not proved cadmium. The presence of MT was confirmed also in chronic experiments (Table I).

Table I

Inhibition of respiration by cadmium in jejunal mucosa scraping

Application	$CdCl_2$ dose	Exposure period	Inhibition
Acute single (a)			
Controls	0		0
Experiment	32.5 mg · kg^{-1}	24 h	44%
Acute combined (b)			
Controls	0		0
Experiment	32.5 + 162.5 mg · kg^{-1}	24 + 1 h	50.4%
Experiment	32.5 + 162.5	24 + 3	56.3%
Chronic (c)			
Controls	0		0
Experiment	250 mg · l^{-1} 10 ml/day/rat	3 months	38.4%

All inhibition values are related to 100% value of controls. All inhibitions are statistically significant, *t*-test: $P < 0.01$

Histochemical changes

In all experiments there were histologically proved focal lesions in the jejunal mucosa. Morphological changes corresponded to histochemical alterations which in turn depended on the extent of lesions:

In acute (a) tests foci of regressively changed villi with vacuolar dystrophic cells were seen. At the base of the crypts no damaged goblet and Paneth cells occurred. From the brush border of the group of villi in lesion area, AIP activity has disappeared (Fig. 1). In the surrounding villi and crypts outside lesions AIP activity was detected, though smaller than in controls. No Mg^{2+} ATPase was shown in absorptive cells of villi in lesion area. Crypts were slightly positive. In absorptive dystrophic cells of villi no SDH activity could be demonstrated while it was present in the crypts. AcP activity was increased in lamina propria at the base.

In acute (b) tests there were extensive regressive villous changes, their cells were necrotic. Brush border was absent or greatly reduced. Hypertrophic goblet cells covered mucosal surface. Pathological product formed granules in the mucus of goblet cells, but also in enterocytes and plasm of mucosa histiocytes. AIP and Mg^{2+} ATPase activities disappeared entirely from the regressively changed mucosa. SDH-active sites were rare.

In chronic (c) tests microscopic lesions appeared in the mucosa, focally affecting isolated villi. Bases of absorptive cells formed vacuoles. Goblet cells were unchanged. AIP activity was decreased in isolated absorptive cells at the top of villi and negative in the focus of regressively changed crypts (Fig. 2). Outside lesion foci there was a marked SDH activity.

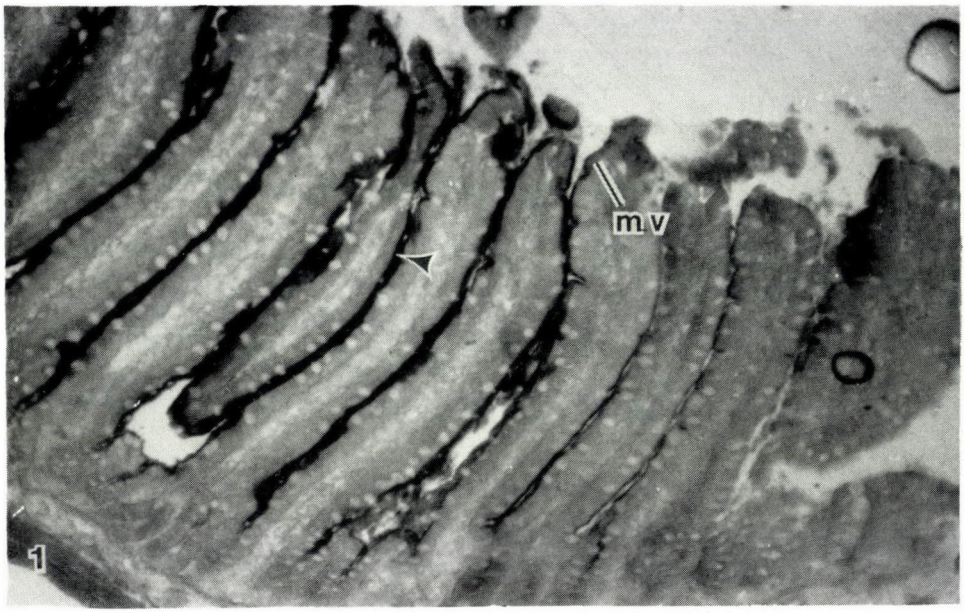

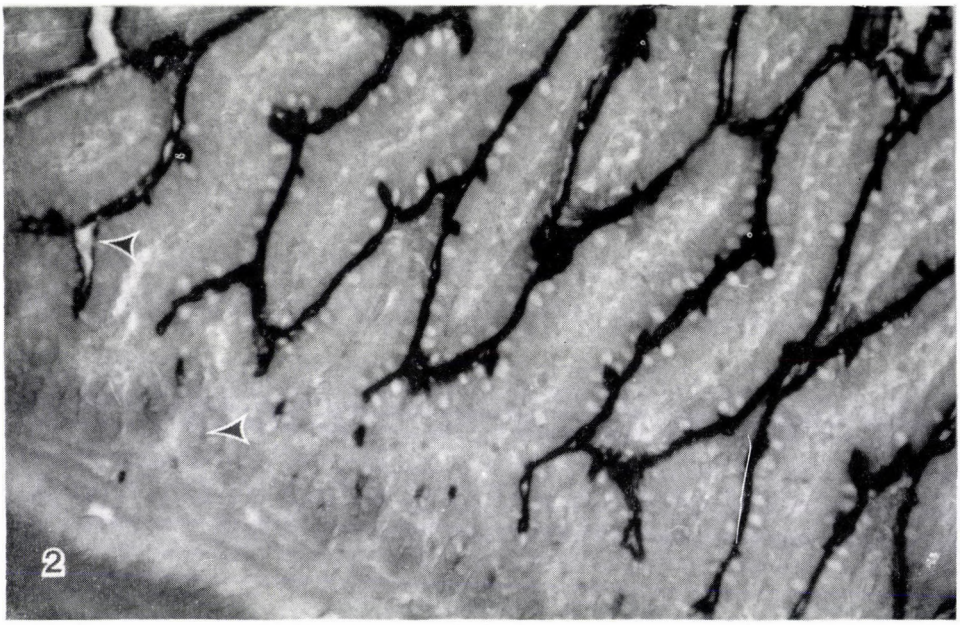

Fig. 1. Rat jejunum. Acute Cd^{2+} dose (a). Microvillar border (mv) of damaged villi has no AlP activity contrary to undamaged villi. (Arrow). ×250

Fig. 2. Rat jejunum. Chronic Cd^{2+} dose (c). Local AlP activity decrease in the base of villi and crypts. (Arrow). ×250

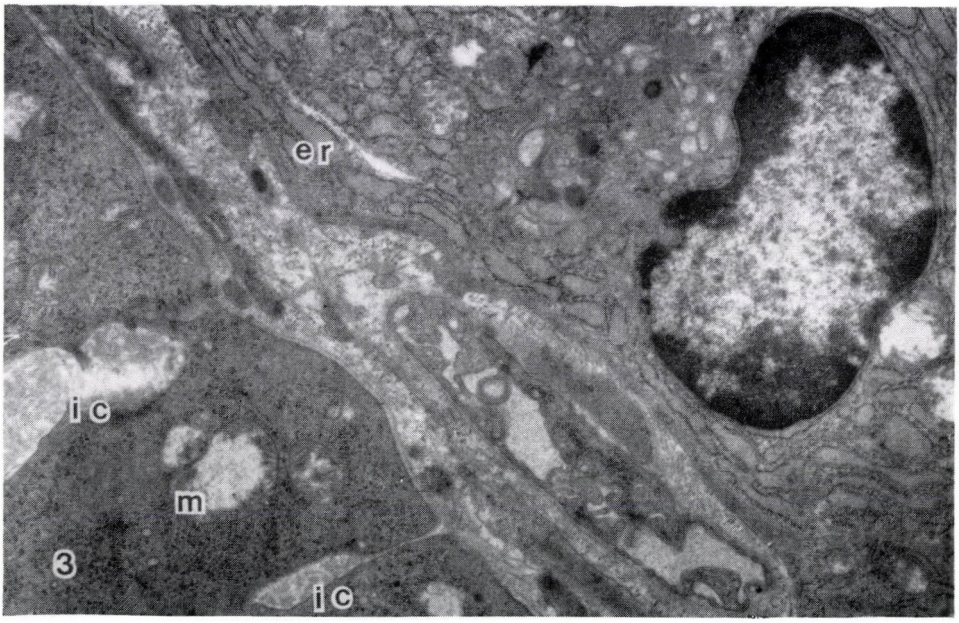

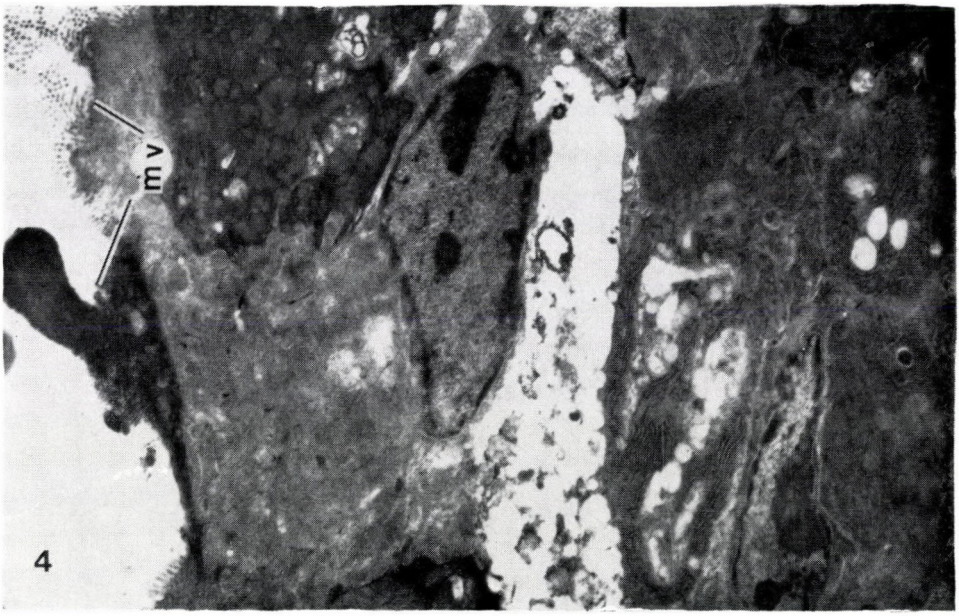

Fig. 3. Rat jejunum. Acute Cd^{2+} dose (a). Dilatation of intercellular connections (ic) of absorptive cells, swelling of mitochondria (m) and dilatation of endoplasmatic reticulum (er). ×14 800

Fig. 4. Rat jejunum. Acute Cd^{2+} dose (b). Necrosis in the microvillar border (mv) and in the cytoplasm after fusion of lateral connections. ×7600

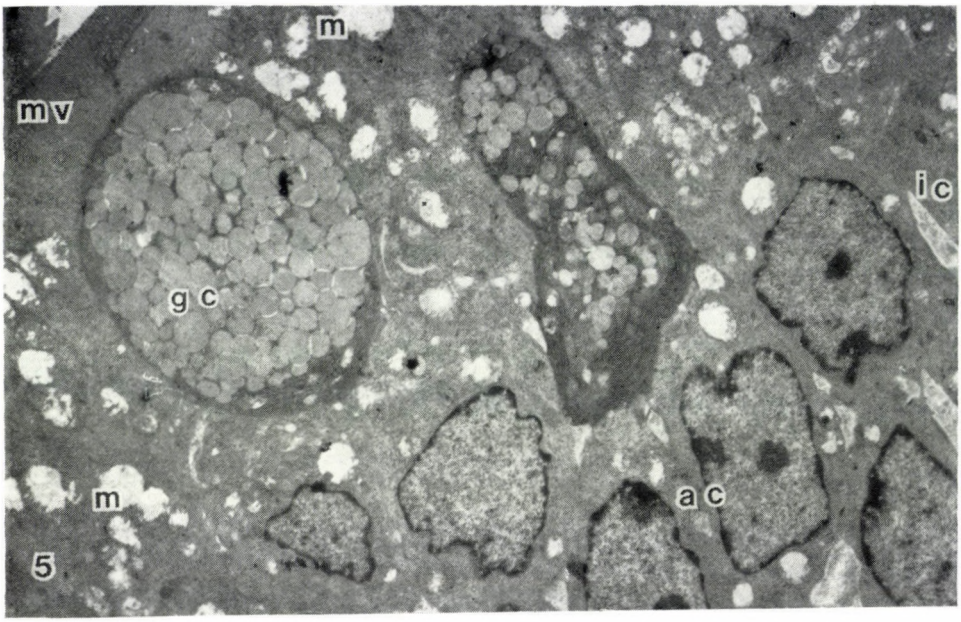

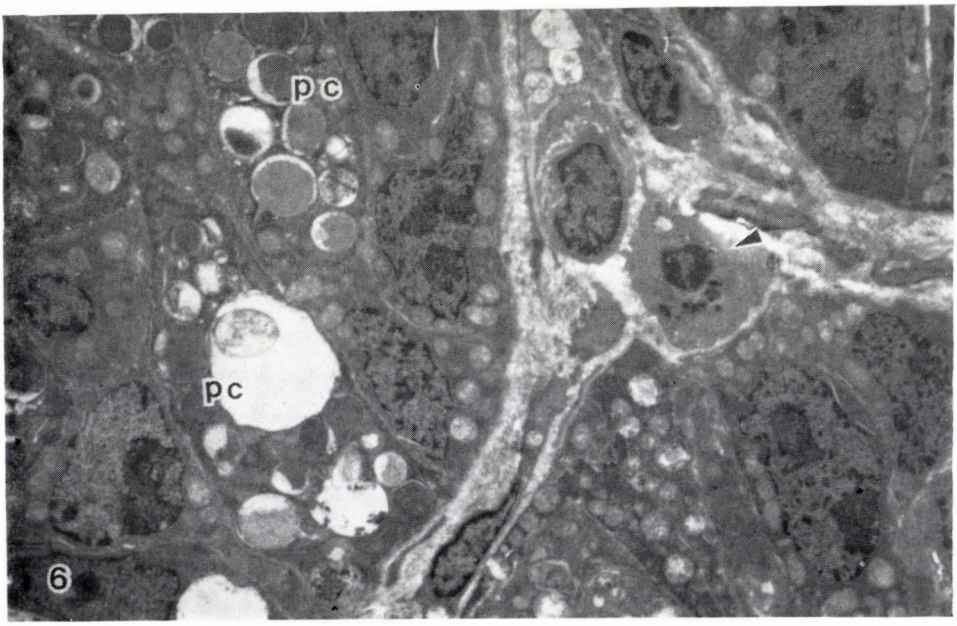

Fig. 5. Rat jejunum. Chronic Cd^{2+} dose (c). Normal goblet cells (gc) and microvillar border (mv) but vacuolizing mitochondria (m) of absorptive cells (ac). ×4900

Fig. 6. Rat jejunum. Chronic Cd^{2+} dose (c). Vacuolization of Paneth cells (PC) and infiltration of lamina propria. (Arrow). ×4900

Ultrastructural changes

In acute (a) tests ultrastructural changes occurred in the absorptive cells of villi. Numerous vacuoles in cells originated from swollen mitochondria, some of which were surrounded by a double membrane and contained isolated cristae, while others were covered by a single membrane only. Absorptive cells in crypts were not vacuolized and in the mitochondria had an electron-dense matrix. Paneth cells of crypts contained granules. Plasma cells in lamina propria had dilated endoplasmatic reticulum (Fig. 3).

In acute (b) tests extensive changes were affecting both the absorptive and goblet cells. Necrotic cells protruded into the lumen (Fig. 4). Microvilli in the necrotic focus were reduced, shortened and without filaments. Goblet cells also suffered from necrosis, their nuclei being pycnotic or vacuolized. In the secreted mucus electron dense granules were seen. Crypt Paneth cells were also vacuolized.

In chronic (c) test vacuolized absorptive cells showed focal alterations. Goblet cells were unchanged (Fig. 5). Tight junctions of absorptive cells were dilated and filled with vesicles in some places. Paneth cells were vacuolized, nuclei of crypt absorptive cells were active. In the lamina propria macrophages with greatly vacuolized cytoplasm (Fig. 6) were encountered.

Electron probe microanalysis

X-ray spectrum of jejunal mucosa has shown in acute and chronic tests the presence of cadmium K_α and K_β lines. Microvillar border, absorptive and goblet cells, lateral membranes and nuclei of Paneth cells and lamina propria in the mucosal base were investigated. Point microanalysis did not prove the presence of Cd^{2+} in mitochondria.

X-ray spectrum in acute (a) tests: dotted line depicts previous liver analysis from the same experiment and below there is an analysis of proper absorptive cells of villi base (Fig. 7). Diffuse Cd^{2+} distribution in the cytoplasm of absorptive cells as shown by surface analysis in STEM (Fig. 8). Higher Cd^{2+} distribution appeared in crypts. In SEM mode, the distribution of Cd^{2+} in lateral membranes of cells surface analysis was ascertained (Fig. 9).

In acute (b) tests EDS analysis did not detect Cd^{2+} either in the mucosal epithelium or in the lamina propria. In the pathologically changed crypts there was no Cd^{2+} retention. Cadmium applied probably entered the blood system through the changed mucosa.

In chronic (c) tests there appeared to be an elevated Cd^{2+} content in crypt base and lamina propria. EDS system did not prove the presence of Cd^{2+} either in the microvillar border or in absorptive cells. Retention of Cd^{2+}

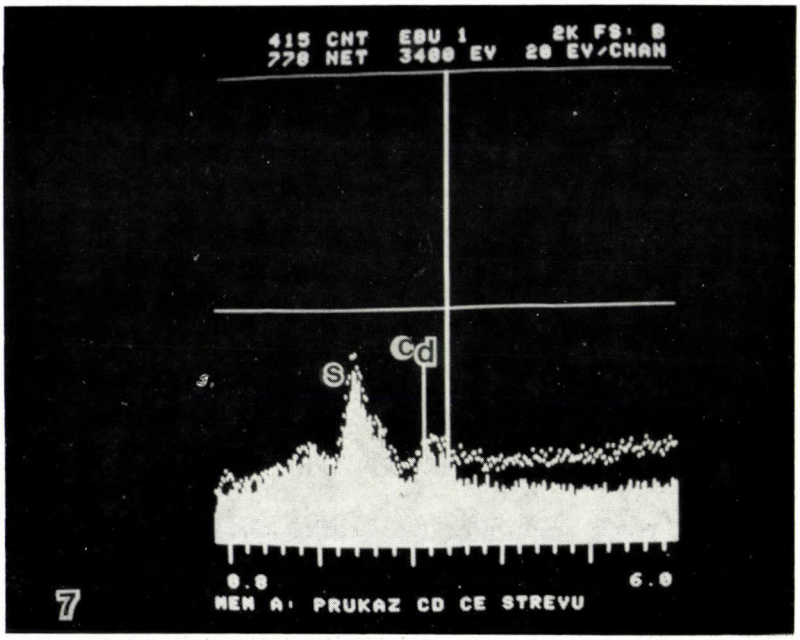

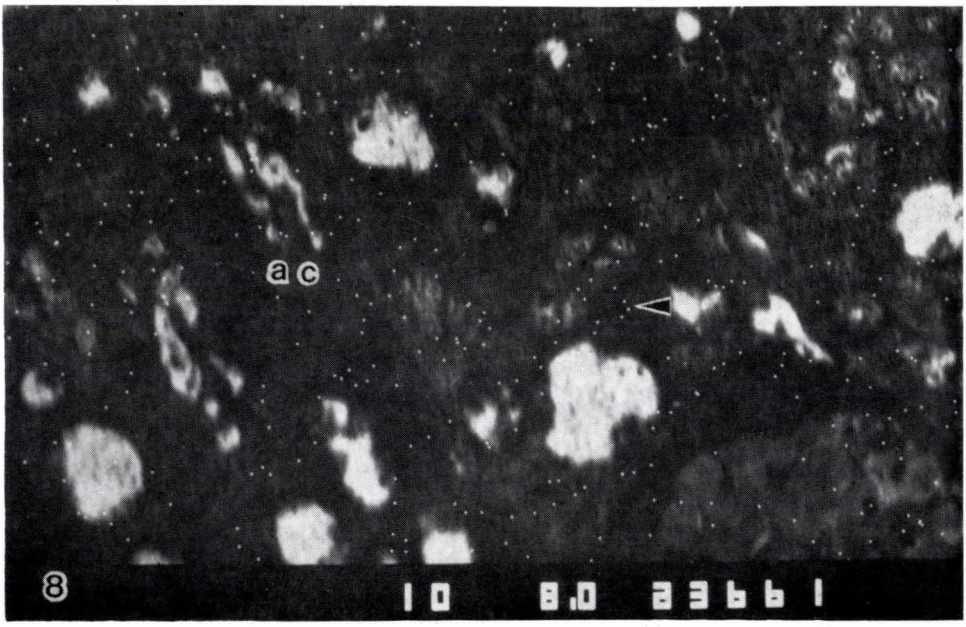

Fig. 7. Rat jejunum. Acute Cd^{2+} dose (a). X-ray spectrum of jejunal mucosa base. Dotted line: liver analysis. ×10 000

Fig. 8. Rat jejunum. Acute Cd^{2+} dose (a). Surface Cd^{2+} analysis in the absorption cells (ac), demonstrating diffused distribution of cadmium ions. (Arrow). ×10 000

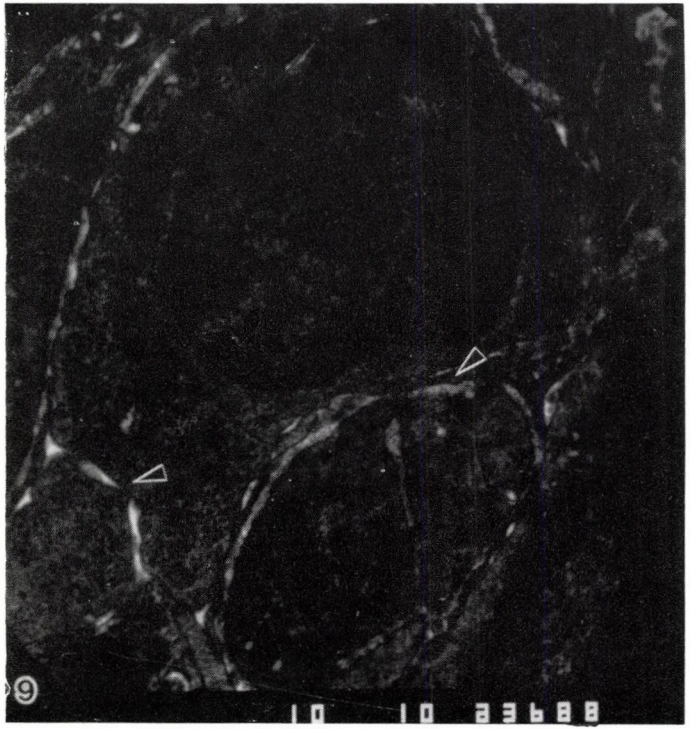

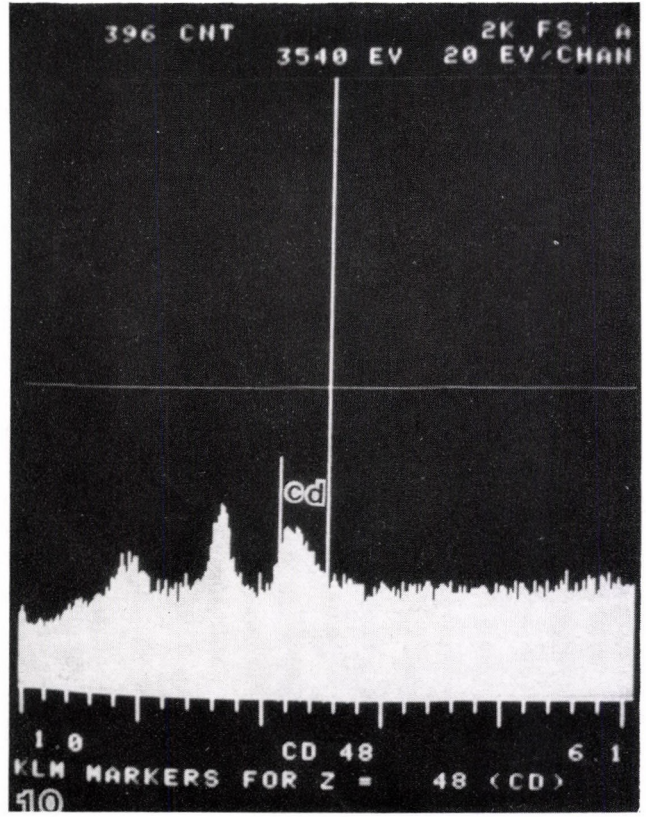

Fig. 9. Rat jejunum. Acute Cd^{2+} dose (a). Surface Cd^{2+} analysis depicts Cd^{2+} distribution inside of cellular membranes in the crypt base. (Arrow). ×10 000

Fig. 10. Rat jejunum. Chronic Cd^{2+} dose (c). X-ray spectrum demonstrates higher peak of K_α, K_β lines in cadmium position. ×10 000

in crypt base was proved by X-ray peaks, which were higher than those in acute tests (Fig. 10). Surface analysis has shown a diffuse distribution of cadmium.

Discussion

Findings suggest that cadmium influences the respiration of jejunal mucosa depending on dose and length of exposure. Degree of respiration inhibition in these experiments is lower than that from in vitro tests [22, 23]. It is interesting, that inhibition of respiration by a single acute dose is comparable to decrease shown for oxygen consumption in chronic tests. An explanation of this may be that the total retained quantity of cadmium in chronic tests is near to the amount used in acute single dose (a) tests. Long-term application of Cd^{2+} in lower concentrations simultaneously causes in the intestine a binding of toxic Cd^{2+} into MT, while the remaining cadmium produces structural focal changes. These changes may lead to decreased respiration levels.

Functional changes are in agreement with ultrastructural and histochemical findings. The results from our acute chronic tests indicate various degrees of permeability changes of cellular membranes in the jejunal mucosa, which operates as a sieve. Cumulation of Cd^{2+} in undamaged cells was demonstrated by X-ray microanalysis. In tests with combined doses (b) cadmium was not proved in pathologically changed mucosa or in chronic tests cadmium was found diffusedly in the crypt epithelium and lamina propria. In pathologically changed spots the retention of Cd^{2+} either did not occur and cadmium was rapidly transported by the blood into the liver [24] or was lower than the detection limit.

Truchet [19] detected Li^{+} by using a microanalyzer in the liver in concentrations higher than 10 mg l^{-1}. Hart et al [6] pointed out MT by immunocytochemistry in the lung but using the LAMMA method they found no cadmium. Binding of cadmium to MT in intestinal or liver cytosol has been proved by Squibb et al [14].

In agreement with Aungst and Fung [1] we presume, that with increased damage to the mucosal epithelium a higher degree of passive diffusion in metal transport can be supposed.

In chronic experiments the problem of defense of organism against cadmium toxicity by MT is discussed [3, 18, 20, 25].

According to our results the magnitude of premedication dose is significant. In our tests with combined doses (b) the first dose was higher than that, used by Yoshikawa [25] and Cherian [3]. Similarly to Yoshikawa [25], we found regressive changes leading to jejunal mucosa necrosis.

In our acute (b) tests rats were surviving and in chronic tests there were

no pathological findings in the liver even if the intestine had focal lesions in mucosal epithelium. According to Morita [11] a defensive mechanism against Cd^{2+} toxicity develops already in the intestine.

Cells of absorptive villi are more sensitive to the toxic Cd^{2+} influence than goblet and Paneth cells [4, 21]. Richardson and Spivey-Fox [13] observed dense deposits of Cd^{2+} in endothelial and in absorptive cells of the quail. Similarly to Holt and Webb [7] we presume, that the speed and degree of Cd^{2+} transport into the intestine depend on dose. According to Nordberg [12] intestinal uptake of cadmium is much greater than its transport into the body.

The origin of binding places for Cd^{2+} at the subcellular level is not quite clear yet. Taguchi [16] observed binding of Cd^{2+} to membranes of epithelial cells. In our tests the presence of cadmium could not be proven in intestinal mitochondria by point microanalysis. This is consistent with ultrastructural finding of mitochondrial vacuolization. Also Makashew and Verbolovich [10] described mitochondrial changes under the effect of lead. Brunner and Bucher [2] supposed the passage of cadmium through the mitochondrial membrane.

In all experiments the correlation between mucosal respiration and mitochondrial structural changes was apparent.

REFERENCES

1. Aungst BJ, Fung HL: Kinetic characterization of in vitro lead transport across the rat small intestine. Toxicol Appl Pharmacol 61: 39, 1981
2. Brunner G, Bucher Th: Determination of the quantitative relationship of outer and inner membrane proteins in rat liver mitochondria by means of enzymology and electron microscopy. FEBS Letters 6: 105, 1970
3. Cherian MG, Goyer RA, Valberg LS: Gastrointestinal absorption and organ distribution of oral cadmium chloride and cadmium metallothionein in mice. J Toxicol Environ Health 4: 861, 1978
4. Foulkes EC: Some determinants of intestinal cadmium transport in the rat. J Environ Pathol Toxicol 3: 471, 1980
5. Goyer RA, Wilson MH: Lead-induced inclusion bodies. Lab Invest 32: 149, 1975
6. Hart BA, Cherian MG, Angel A: Cellular localization of metallothionein in the lung following repeated cadmium inhalation. Toxicology 37: 171, 1985
7. Holt D, Webb M: Intestinal and hepatic binding of cadmium in neonatal rat. Arch Toxicol 52: 291, 1983
8. Kello D, Sugawara N, Voner C, Foulkes EC: On the role of metallothionein in cadmium absorption by rat jejunum in situ. Toxicology 14: 199, 1979
9. Lojda Z, Papoušek F: Základy histochemického průkazu enzymů. Skripta, Brno 1970
10. Makashew KK, Verbolovich VP: Succinatedehydrogenase and cytochromeoxidase of duodenum in lead intoxication. Izv Akad Nauk Kaz SSR Ser Biol Nauk 5: 59, 1967
11. Morita S: Defense mechanisms against cadmium toxicity. I. A biochemical and histological study of the effects of pretreatment with cadmium on the acute oral toxicity of cadmium in mice. Jpn J Pharmacol 35: 129, 1984
12. Nordberg GF: Effects and Dose Response Relationship of Toxic Metals. Elsevier, Amsterdam 1976
13. Richardson ME, Spivey-Fox MR: Dietary cadmium and enteropathy in the Japanese quail. Lab Invest 31: 722, 1975
14. Squibb KS, Cousins RJ, Silbon BL, Levin S: Liver and intestinal metallothionein: Function in acute cadmium toxicity. Exp Mol Pathol 25: 163, 1976

15. Steibert E, Krol B, Sowa B, Gralewska K, Kaminski M, Kusz E: Cadmium induced changes in the histoenzymatic activity in liver, kidney and duodenum of pregnant rats. Toxicol Lett 20: 127, 1984
16. Taguchi T: Observations on the distribution and movement of cadmium in epithelial cells of rat small intestine by light and electron radioautography. J Toxicol Environ Health 15: 509, 1985
17. Taguchi T, Suzuki S: Cadmium binding components in the supernatant fraction of the small intestinal mucosa of rats administered cadmium. Nippon Eiseigaku Zasshi 33: 467, 1978
18. Terhaar CJ, Vis E, Roudabush RL, Fassett DW: Protective effects of low doses of cadmium chloride against subsequent high oral doses in the rats. Toxicol Appl Pharmacol 7: 500, 1965
19. Truchet M: Ion microanalysis in metal toxicology. In: Echlin P, Kaufman R, S. (eds) Microscopica Acta, (Suppl.) 2, Microprobe Analysis in Biology and Medicine. Hirzel Verlag, Stuttgart 1978, p. 355
20. Valberg LS, Haist J, Cherian MG, Delaquerriere-Richardson L, Goyer RA: Cadmium induced enteropathy: Comparative toxicity of cadmium chloride and cadmium thionein. J Toxicol Environ Health 2: 963, 1977
21. Victery W, Miller CR, Fowler BA: Lead accumulation by rat renal brush border membrane vesicles. J Pharmacol Exp Ther 231: 589, 1984
22. Vojtíšek M: Influence du cadmium sur le transport du D-glucose par la paroi chez le rat. J Physiol Paris 78: 51A, 1982
23. Vojtíšek M: The effect of $CdCl_2$ on the respiration of rat small intestine mucosa. J Hyg Epidemiol Microbiol Immunol 27: 381, 1983
24. Vojtíšek M, Hulínská D: Unpublished observations
25. Yoshikawa H: Preventive effects of pretreatment with low dose of metals on the acute toxicity of metals in mice. Ind Health 8: 194, 1970

Acta Morphologica Hungarica, 36 (1–2), pp. 133–140 (1988)

THE STUDY OF STEROID HORMONES IN EPITHELIAL OVARIAN TUMOURS

ILONA PÉTER, ÉVA GÁTI, J. SUGÁR

RESEARCH INSTITUTE OF ONCOPATHOLOGY, NATIONAL OF ONCOLOGY, BUDAPEST, HUNGARY

(Received 3 June 1987)

We examined the estradiol and testosterone content of 13 benign, 5 border-line and 26 malignant epithelial ovarian tumours with the aid of an indirect immunoperoxidase method. While the two hormones were rarely detected in the epithelium of benign tumours, they were frequently present in border-line or malignant tumours. In cases where the intersitial substance of the tumours was coupled to a glandular hyperplasia of the endometrium, estradiol predominance could be demonstrated.

In the epithelial cells of malignant tumours of cytological grade 2 of the Broders grading system, which are of the highly differentiated and border-line types, the simultaneous presence of estradiol and testosterone is more frequent (4/5 and 6/9) than in poorly differentiated tumours of grades 3 and 4 (4/17).

In the group of grade 2 with better prognosis, the tumour cells also contain estradiol. Similar tendency can be observed in patients with poorly differentiated tumours.

Our observations refer to the possible prognostic value of the estradiol content of tumour cells.

Keywords: Ovarian tumours, steroid hormones

Introduction

The indirect immunperoxidase method proved to be suitable for the immediate detection of steroid hormone-content in tissues embedded in paraffin and fixed in formalin. This method has been used by several researchers to investigate steroid-content and localization of sex cord tumours in the ovary and the testis as well as in case of breast cancer and endometrium cancer [5, 8, 9, 15, 17, 19]. However, there are no similar data available for ovarian tumours of epithelial origin. In the stroma of endocrinologically active epithelial ovarian tumours enzymes having direct contact with steroid genesis have been found [7, 14].

In our previous investigations we examined the prognostic value of histological grading systems in cases of ovarian tumours of epithelial origin [4]. The present study was aimed at the demonstration of the estradiol and testosterone content of tumours mentioned above, searching for possible correlation between the hormone content and the grade of differentiation.

Send offprint request to: Ilona Péter, Research Inst. of Oncopathol., National Inst. of Oncology, Budapest, Ráth Gy. 7–9, H-1112 Hungary

Materials and methods

Paraffin sections of 10% formalin-fixed tissue derived from border-line and benign tumour cases [4] were prepared, selected according to different histological types of ovarian carcinomas, previously grouped as to their grade of differentiation. We also performed the histological examination of the uterus sent together with the tumours. For detecting endogenous estradiol and testosterone, indirect immunperoxidase (PAP) reaction has been carried out according to Sternberger et al [18] using Immunostaining Systems kits (Ortho Diagn. Syst. Inc. Raritan, N.Y. USA). As a positive control for endogenous estradiol display, normal ovary, for endogenous testosterone normal testis was used. For negative control examinations we incubated the sections with normal rabbit-serum instead of using a primary antibody.

Results

The intercellular substance of the examined benign cystic tumours was positive to estradiol (12/13) and to testosterone (10/13) in immunperoxidase reactions in most cases (Table I). According to the relative intensity of the reactions, estradiol predominance or the mere presence of estradiol could be observed in cases where the benign ovarian tumour occurred together with glandular hyperplasia of the endometrium, endometriosis or Brenner-tumour (Table I, cases 1, 2, 4, 6, 9, 12, 13, and 7). The hormone content of the tumour cells could be demonstrated only in two cases (Table I, cases 1, 5).

Table I

Benign tumours — Steroid hormone content in the tumour cells and the stroma

Case No.	Age years	Histol. type	Uterus assoc. lesions	Hormone content			
				epithelial		stromal	
				estr.	test.	estr.	test.
1	39	serous	gl. hypl. end.	+	+	++	+
2	48	serous	gl. hypl. end.	—	—	++	—
3	51	serous	—	—	—	—	+
4	64	serous	gl. hypl. end.	—	—	++	+
5	21	mucinous	—	+	+	++	++
6	49	mucinous + serous	endometriosis	—	—	+	—
7	53	mucinous + Brenner	—	—	—	++	+
8	53	mucinous	—	—	—	+	+
9	58	mucinous	fibromy.	—	—	+	—
10	65	mucinous	fibromy.	—	—	+	+
11	67	mucinous	—	—	—	++	++
12	78	mucinous	gl. hypl. end.	—	—	++	+
13	83	mucinous	gl. hypl. end. fibromy.	—	—	++	+

estr. = estradiol
test. = testosterone
gl. hypl. end. = glandular hyperplasia of endometruim
fibromy. = fibromyomatosis

Intensity of immunperoxidase reaction
++ = strongly positive
+ = moderately, slightly positive
— = negative

Table II

Border-line tumours — Steroid hormone content in the tumour cells and stroma

Case No.	Age years	Histol. type	Uterus assoc. lesions	Hormone content			
				epithelial		stromal	
				estr.	test.	estr.	test.
1	48	serous	gl. hypl. end. fibromy.	+	+	++	+
2	55	serous	gl. hypl. end.	+	+	++	+
3	56	serous	gl. hypl. end.	−	+	++	+
4	63	serous	gl. hypl. end. fibromy.	+	++	++	+
5	65	mucinous	fibromy.	+	++	+	++

Table III

Malignant tumours — Steroid hormone content in the tumour cells and the stroma

Case No.	Age years	Histol. type	Uterus assoc. lesions	Hormon content			
				epithelial		stromal	
				estr.	test.	estr.	test.
1	35	serous	−	++	++	++	++
2	36	serous	−	+	+	+	++
3	41	serous	fibromy.	+	++	+	++
4	47	serous	−	+	++	+	+
5	48	serous	−	+	+	++	++
6	48	serous	−	−	+	+	+
7	54	serous	−	++	+	+	+
8	60	serous	−	−	+	++	++
9	62	serous	fibromy.	−	++	+	++
10	64	serous	−	−	+	+	+
11	64	serous	fibromy.	+	++	+	+
12	69	serous	−	−	++	−	++
13	73	serous	fibromy.	+	−	+	+
14	28	mucinous	gl. hypl. end.	−	+	−	+
15	47	mucinous	fibromy.	+	+	++	++
16	50	mucinous	fibromy.	−	++	−	+
17	60	mucinous	gl. hypl. end.	++	+	++	+
18	60	mucinous	−	+	−	+	++
19	71	mucinous	gl. hypl. end.	++	−	++	−
20	36	endometr.	−	−	+	−	+
21	43	endometr.	adenocc. end.	−	−	+	−
22	44	endometr.	adenoacanth. end.	+	−	+	−
23	48	endometr. + mucinous	adenocc. end.	−	+	+	++
24	48	endometr.	adenocc. end.	+	−	++	+
25	50	endometr.	−	+	+	+	+
26	50	endometr.	adenocc. end.	−	+	+	++

endometr. = endometrioid
adenocc. end. = adenocarcinoma of endometrium
adenoacanth. end. = adenoacanthoma of endometrium

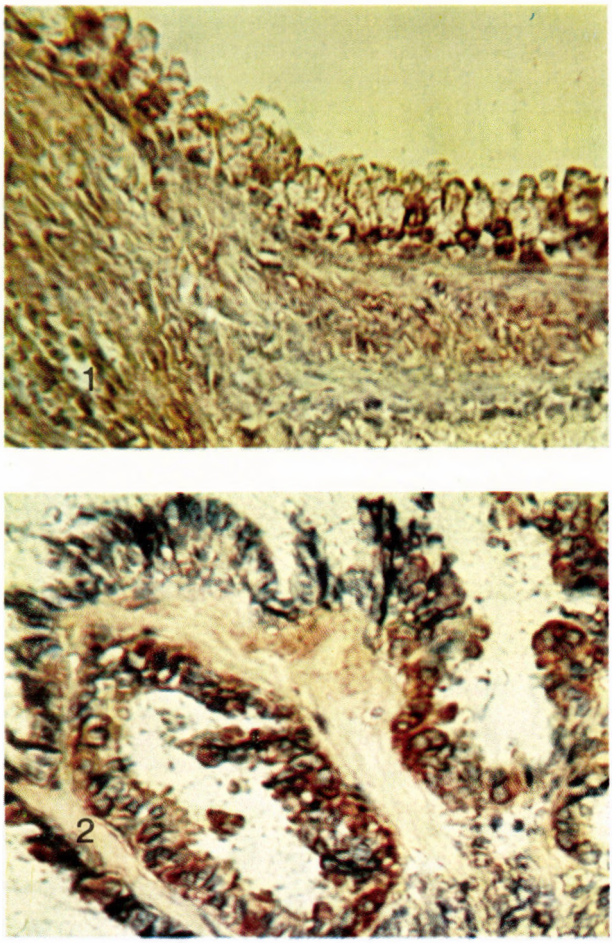

Fig. 1. Mucinous tumour of border-line type. Moderately intense estradiol reaction in the epithelial cells and the stroma (Table II, case 5)

Fig. 2. Intensive epithelial and stromatic testosterone positivity on other parts of the same tumour

The epithelial cells in the tumours of border-line type (low malignancy) contained estradiol (4/5) and testosterone (5/5) (Table II). In the tumours accompanied by glandular hyperplasia of the endometrium, reaction of the connective tissue was more intensive for estradiol then for testosterone (Table II, cases 1, 2, 3, 4).

Similarly to the border-line type, the presence of these two steroid hormones could be observed more often in the epithelium of malignant tumours (Table III) than in benign ones. Positive estradiol reaction was recorded in more than half of the cases (15/26) and it was even higher in the case of testo-

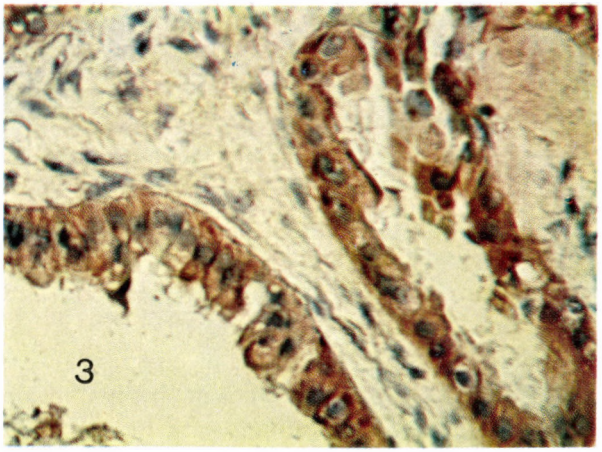

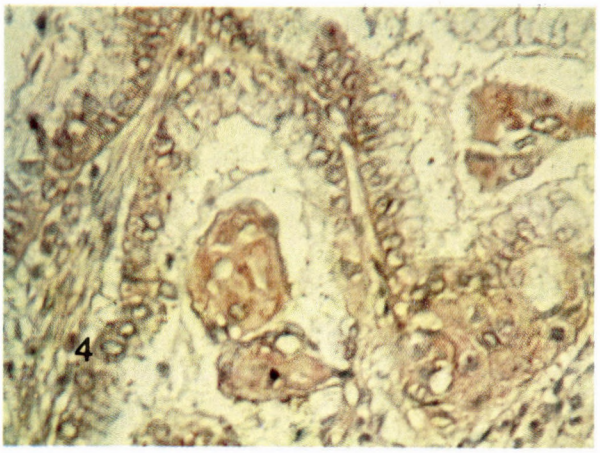

Fig. 3. Mucinous carcinoma of cytological grade 3. Strong testosterone immunperoxidase reaction in the tumour cells, the stroma is slightly positive (Table III, case 16)

Fig. 4. An endometrioid malignant tumour of cytological grade 2 (adenoacanthoma). Estradiol positive, moderate reaction in the cells of the pavement epithelium, the glandular epithelium and in the interstitial cells (Table III, case 25)

sterone positivity (19/26). In one case the tumour cells contained no hormone at all (Table III, case 21).

The variation of hormone-content in tumour cells could be observed in all three histological types, in some cases both hormones simultaneously, in others they contained either testosterone or estradiol (Figs 1—4). There was no correlation between the hormone-content of the tumours and the age of the patients.

The estradiol predominance of the connective tissue could be shown in two of three cases occurring together with glandular hyperplasia of the endo-

metrium (Table III, cases 17, 19) and in three of five cases with endometrium carcinoma (Table III, cases 21, 22, 24).

Examining the steroid hormone-content of malignant tumours in correlation with their grade of differentiation (Table IV), we can note the simultaneous presence of estradiol and testosterone more often in the group of highly differentiated tumours (6/9), cytological grade 2 in Broders grading system, than among tumours belonging to grade 3 (3/10) or grade 4 (1/7).

The course of disease shows significant individual differences within the same clinical stage having the same cytological grade. In the group of grade 2, in case of better prognosis (Table IV, cases 25, 17, 2, 3, 11 and 4) estradiol in the tumour cells could also be pointed out in contrast to cases of poor prognosis (Table IV, cases 10, 20, 12). The chance of survival of a patient in clinical stage 1 with a tumour grade 3 containing both hormones (Table IV, case 7) proved to be better than that of the patients in the same group with tumours

Table IV

Malignant tumours — Steroid hormone content and cytological granding

Case No. (accord. to Table III)	Histol. type	Clinical stage	Epithelial hormone content		Clin. follow-up (months)	
			estr.	test.		
Cytological grade: 2						
25	endometr.	I/c	+	+	alive,	134
17	mucinous	II/a	++	+	died,	44
2	serous	II/b	+	+	alive,	61
3	serous	II/b	+	+	died,	101
11	serous	II/b	+	+	alive,	95
4	serous	II/b	+	++	alive,	155
10	serous	II/b	—	+	died,	12
20	endometr.	II/b	—	+	died,	1
12	serous	III	—	++	died,	1
Cytological grade: 3						
7	serous	I/c	++	+	alive,	70
14	mucinous	I/c	—	+	died,	19
19	mucinous	II/b	++	—	died,	14
18	mucinous	II/b	+	—	died,	9
16	mucinous	II/b	—	++	died,	23
13	serous	II/b	+	—	died,	30
21	endometr.	II/b	—	—	died,	8
15	mucinous	III	+	+	died,	2
6	serous	III	—	+	died,	12
5	serous	IV	+	+	died,	10
Cytological grade: 4						
24	endometr.	II/a	+	—	died,	63
23	endometr.	II/b	—	+	died,	3
1	serous	III	++	++	died,	11
8	serous	IV	—	+	died,	16
9	serous	IV	—	++	died,	12
22	endometr.	IV	+	—	died,	16
26	endometr.	IV	—	+	died,	7

containing no estradiol (Table IV, case 14). Patients with tumours of grade 4, but estradiol positive and endometrioid type have a better survival than those of the same group but with estradiol negative tumours (Table IV, cases 24, 23, 22, 26).

Discussion

The indirect immunperoxidase reaction used in our examinations gives information about steroid hormones obtained either from the serum or secreted by the cells [9, 19]. The role of enzymatically active stroma cells of epithelial ovarian tumours in steroid synthesis is well known and can be correlated with the estrogenic or androgenic functions of these tumours [10, 11]. The interstitial estradiol predominance found in tumours occurring with glandular hyperplasia of the endometrium, post-menopausal bleedings and endometrium carcinoma corresponds to the above data of the literature. Enzymes of estrogenic metabolism have also been isolated in the epithelial components of breast cancer [13].

We cannot exclude that the demonstrated hormone-content partly corresponds to hormones bound by receptors. The biochemical detection of estrogenic and testosterone receptors in epithelial ovarian tumours had a diversified result. In malignant tumours the occurrence of estrogenic receptor was 50–100% while that of testosterone receptors was 41–72% [2, 6]. Receptors were found in approximately half of the highly differentiated endometrial carcinomas, while in the case of poorly differentiated ones, receptors were only sporadically detected [3]. The prognostical value of receptor status is still argued.

In our previous examinations based on Broders system the prognosis of tumours of grade 2 was significantly better than that of tumours of grade 3 or 4, while there was no difference regarding survival according to histological type [4]. Although in larger examination series significant differences can be demonstrated in the prognosis of the patients according to clinical stages or the grade of differentiation [1, 12, 16], nevertheless great individual differencies occur within each group concerning the course of disease, which is due to tumour heterogeneity. Estradiol and testosterone were simultaneously present more often in cases of highly differentiated tumours of grade 2 with low malignancy (border-line) than in tumours of grade 3 or 4.

The prognosis of patients with highly differentiated tumours containing estradiol was better than the prognosis of patients in the same group with estradiol negative tumours. A similar tendency could be observed in our patients with poorly differentiated tumours in clinical stage 1 as well as in patients with poorly differentiated tumours of endometrioid type.

The possible prognostic value of estradiol-content of tumour cells requires confirmation in a larger population of patients.

REFERENCES

1. Anderson T, Young R: Recent advances in the staging and treatment of ovarian cancer. Med Clin N Amer 61: 1001, 1977
2. Bojar H, Petzinna D: Hormone receptors in ovarian cancer. In: Bender HG, Beck L, (eds) Carcinoma of the Ovary. Vol 7, Gustav Fischer Verlag, Stuttgart, New York 1983, p. 39
3. Friberg LG, Kullander S, Persyn JP, Karsten CB: On receptors for estrogens (E82) and androgens (DHT) in human endometrial carcinoma and ovarian tumours. Acta Obstet Gynec Scand 57: 261, 1978
4. Gáti É, Sugár J, Szentirmay Z, Töttössy B: Significance of histologic grading in the prognosis of ovarian tumors. Tumori 72: 427, 1986
5. Ghosh L, Ghosh BC, Das Gupta TK: Immunocytological localization of estrogen in human mammary carcinoma cells by horseradish-antihorseradish peroxidase complex. J Surg Oncol 10: 221, 1978
6. Kaiser R: Receptors in ovarian cancer. In: Bender HG, Beck L. (eds) Carcinoma of the Ovary. Vol 7, Gustav Fischer Verlag, Stuttgart, New York 1983, p. 47
7. Koudstall JB, Bossenbrock MJ, Hardouk MJ: Ovarian tumors investigated by histochemical and enzyme histochemical methods. Amer J Obstet Gynec 102: 1004, 1968
8. Kurman RJ, Andrade D, Goebelsmann U, Taylor CR: An immunohistological study of steroid localization in Sertoly-Leydig tumors of the ovary and testis. Cancer 42: 1772, 1978
9. Kurman RJ, Goebelsmann U, Taylor CR: Steroid localization in granulosa-theca tumors of the ovary. Cancer 43: 2377, 1979
10. MacDonald PC, Grodin FJ, Edman FC, Vellios FF, Sooteri PK: Origin of estrogen in a postmenopausal woman with a non-endocrine tumor of the ovary and endometrial hyperplasia. Obstet and Gynec 47: 644, 1976
11. Morris JM, Scully RE: Endocrine Pathology of the Ovary. Mosby CV, St. Louis 1958, p. 87
12. Ozols RF, Garvin AJ, Costa J, Simon RM, Young R: Advanced ovarian cancer: Correlation of histologic grade with response to therapy and survival. Cancer 45: 572, 1980
13. Partanen S: Histochemistry of estrogen sulfatases in human breast diseases. Virchows Arch Path Anat (Cell Path) 49: 53, 1985
14. Pfleiderer A, Teufel G: Incidence and histochemical investigation of enzymatically active cells in stroma of ovarian tumors. Amer J Obstet Gynec 102: 997, 1968
15. Shimizu M, Wajima O, Miura M, Katayama I: PAP immunoperoxidase method demonstrating endogenous estrogen in breast carcinomas. Cancer 52: 486, 1983
16. Sorbe B, Frankeldal B, Veress H: Importance of histologic grading in the prognosis of epithelial cancer. Obstet and Gynec 59: 576, 1982
17. Sugár J, Tóth J, Péter I, Számel I, Besznyák I: A hormonreceptorok, a patohisztológiai típus és prognózis kapcsolata az emlőrákban. Magy Onkol 29: 211, 1985
18. Sternberger LA, Hardy PH Jr, Cuculis JJ, Meyer HG: The unlabelled antibody-enzyme method of immunohistochemistry. Preparation and properties of soluble antigen-antibody complex (horseradish peroxidase-antiperoxidase) and its use in identification of spirochetes. J Histochem Cytochem 18: 315, 1970
19. Taylor CR, Cooper CL, Kurman RJ, Goebelsmann U, Markland FS: Detection of estrogen receptors in breast and endometrioid carcinoma by immunoperoxidase technique. Cancer 47: 2634, 1981

Acta Morphologica Hungarica, 36 (1—2), pp. 141 (1988)

BOOK REVIEW

W. F. NEISS: *Ultracytochemistry of intracellular membrane glycoconjugates.* Vol. 99.
Advances in anatomy, Embryology and Cell Biology. Eds: F. BECK, W. HILD, W. KRIZ, R. ORTMANN, J. E. PAULY, T. H. SCHIEBLER.
Springer V. Berlin, Heidelberg, New York, London, Paris, Tokyo, 1986. 92 pp, 113 Figs. Price: DM 65, soft cover

The book has appeared in the series of Advances in Anatomy, Embryology and Cell Biology as Volume 99 published by Springer Verlag Publishing Company (Berlin, Heidelberg, New York, London, Paris and Tokyo) in 1986. The editors are: F. Beck, W. Hild, W. Kriz, R. Ortmann, J. E. Pauly and F. H. Schiebler.

This book consists of 92 pages text and 113 excellent quality EM figures. The topic is comprehensive and joins the main stream of recent membrane research. The author's aim was to study the topology of intracellular glycoconjugates of the post-Golgi membranes: lysosomes, peroxisomes, secretory granules and mitochondria. At the time, it is the first attempt to fill the gap between biochemical and morphological data by the use of selected ultracytochemical methods. The techniques used were as follows: neutral- and sialo-glycoconjugate-specific phosphotungstic acid or periodic acid oxidation-thiocarbohydrazide-silver proteinate reactions and sialyl group-specific mild periodate oxidation, thiocarbohydrazide-silver proteinate reaction at the ultrastructural level. These reactions demonstrated the protein-bound glycoconjugates but not the glycolipids. The study revealed a coat of glycoconjugates on the inner surface of post-Golgi membranes, such as the lysosomal and secretory granular membranes. Based on these observations, the author proposed a general model of the inner membranes of lysosomes and secretory granules, which represents an intracellular glycocalyx — similar in structure to the coat present on the cell membrane. This intracellular glycocalyx appears only on intracellular membranes originating from the Golgi-apparatus or which are fusion-compatible with each other and the cell membrane. These membranes are joined by the membrane recycling of exo- and endocytosis and crinophagy. The function of their inner coat could be the separation of the organelle-membrane from the matrix of lysosomes and secretory granules and could perform a mechanical/chemical barrier to protect the membrane against the action of lytic enzymes from within. The book may attract the attention of membrane biologists, morphologists and pathologists, but can be highly recommended to general biologists as well.

J. TIMÁR

PRINTED IN HUNGARY

Akadémiai Kiadó és Nyomda Vállalat, Budapest

INSTRUCTIONS TO AUTHORS

Form of manuscript

Contributors are requested to supply two complete copies of the manuscript including all tables and illustrations. Manuscripts should be typed double-spaced with margins of at least 4 cm. Pages should be numbered consecutively.

The *headline* should include the title of the paper, authors' names, and name and short postal address of the institute where the work was done.

An *abstract* of not more than 200 words should be supplied typed before the text. It should briefly describe the purpose of the investigations, the methods utilized, the results obtained, and the authors' principal conclusions.

Abbreviations and symbols

Abbreviations should be spelled out when first used in the text or, alternatively, a list of abbreviations might be given. The *International System of Units (SI)* should be used for all measurements. Symbols for physical quantities are to be printed in italics and should, therefore, be underlined in the manuscript. Unusual symbols should be identified on the margin.

References

References should be numbered in alphabetical order, and these numbers only should be inserted in the text (in parentheses). In the reference list each item should include the names and initials of all authors; the title of the article; the title of the journal abbreviates according to the style used in *Index Medicus* (a list of the journals indexed is printed annually in the January issue); the volume number; the first page number; and the year of publication.

Kaplan AP, Kay AB, Austen KF: A pre-albumin activator of prekallikrein. J Exp Med 135:81, 1972

Titles of books should be followed by the publisher; place of publication; and the year.

Oláh I, Röhlich P, Törő I: Ultrastructure of Lymphoid Organs. Akadémiai Kiadó, Budapest 1975

Halász B: The endocrine effects of isolation of the hypothalamus from the rest of the brain. In: Frontiers in Neuroendocrinology, eds Ganong WF, Martini L, Oxford University Press, Oxford 1969, p. 307

Tables and illustrations

Tables should be comprehensible to the reader without reference to the text. The headings should be typed above the table. Tables should be numbered with Roman and illustrations with Arabic numerals.

Figures should be identified by number and authors' name written lightly in pencil on the back. The top should be indicated on the back of prints. The letters a, b etc. should be placed in the lower left-hand corner of prints. Staining techniques and the original magnification of photomicrographs should be stated. Figure captions should be typed on a separate sheet. The approximate place of figures and tables in the text should be indicated in the manuscript on the left-hand margin.

Proofs and reprints

Reprints and proofs will be sent to the first author unless otherwise indicated. A hundred reprints of each paper will be supplied free of charge.

Periodicals of the Hungarian Academy of Sciences are obtainable at the following addresses:

AUSTRALIA
C.B.D. LIBRARY AND SUBSCRIPTION SERVICE
Box 4886, G.P.O., *Sydney N.S.W. 2001*
COSMOS BOOKSHOP, 145 Ackland Street
St. Kilda (Melbourne), Victoria 3182

AUSTRIA
GLOBUS, Höchstädtplatz 3, *1206 Wien XX*

BELGIUM
OFFICE INTERNATIONAL DES PERIODIQUES
Avenue Louise, 485, *1050 Bruxelles*
E. STORY-SCIENTIA P.V.B.A.
P. van Duyseplein 8, *9000 Gent*

BULGARIA
HEMUS, Bulvar Ruszki 6, *Sofia*

CANADA
PANNONIA BOOKS, P.O. Box 1017
Postal Station "B", *Toronto, Ont. M5T 2T8*

CHINA
CNPICOR, Periodical Department, P.O. Box 50
Peking

CZECHOSLOVAKIA
MAD'ARSKA KULTURA, Národní třida 22
115 66 Praha
PNS DOVOZ TISKU, Vinohradská 46, *Praha 2*
PNS DOVOZ TLAČE, *Bratislava 2*

DENMARK
EJNAR MUNKSGAARD, 35, Nørre Søgade
1370 Copenhagen K

FEDERAL REPUBLIC OF GERMANY
KUNST UND WISSEN ERICH BIEBER
Postfach 46, *7000 Stuttgart 1*

FINLAND
AKATEEMINEN KIRJAKAUPPA, P.O. Box 128
00101 Helsinki 10

FRANCE
DAWSON-FRANCE S.A., B.P. 40, *91121 Palaiseau*
OFFICE INTERNATIONAL DE DOCUMENTATION ET LIBRAIRIE, 48 rue Gay-Lussac
75240 Paris, Cedex 05

GERMAN DEMOCRATIC REPUBLIC
HAUS DER UNGARISCHEN KULTUR
Karl Liebknecht-Straße 9, *DDR-102 Berlin*

GREAT BRITAIN
BLACKWELL'S PERIODICALS DIVISION
Hythe Bridge Street, *Oxford OX1 2ET*
BUMPUS, HALDANE AND MAXWELL LTD.
Cowper Works, *Olney, Bucks MK46 4BN*
COLLET'S HOLDINGS LTD., Denington Estate,
Wellingborough, Northants NN8 2QT
WM DAWSON AND SONS LTD., Cannon House
Folkstone, Kent CT19 5EE
H. K. LEWIS AND CO., 136 Gower Street
London WC1E 6BS

GREECE
KOSTARAKIS BROTHERS INTERNATIONAL BOOKSELLERS, 2 Hippokratous Street, *Athens-143*

HOLLAND
FAXON EUROPE, P.O. Box 167
1000 AD Amsterdam
MARTINUS NIJHOFF B. V.
Lange Voorhout 9-11, *Den Haag*
SWETS SUBSCRIPTION SERVICE
P.O. Box 830, 2160 Sz Lisse

INDIA
ALLIED PUBLISHING PVT. LTD.
750 Mount Road, *Madras 600002*
CENTRAL NEWS AGENCY PVT. LTD.
Connaught Circus, *New Delhi 110001*
INTERNATIONAL BOOK HOUSE PVT. LTD.
Madame Cama Road, *Bombay 400039*

ITALY
D. E. A., Via Lima 28, *00198 Roma*
INTERSCIENTIA, Via Mazzé 28, *10149 Torino*
LIBRERIA COMMISSIONARIA SANSONI
Via Lamarmora 45, *50121 Firenze*
SANTO VANASIA, Via M. Macchi 58
20124 Milano

JAPAN
KINOKUNIYA COMPANY LTD.
Journal Department, P.O. Box 55
Chitose, *Tokyo 156*
MARUZEN COMPANY LTD., Book Department
P.O. Box 5050 Tokyo International, *Tokyo 100-31*
NAUKA LTD., Import Department
2-30-19 Minami Ikebukuro, Toshima-ku, *Tokyo 171*

KOREA
CHULPANMUL, *Phenjan*

NORWAY
TANUM-TIDSKRIFT-SENTRALEN A.S.
Karl Johansgata 43, *1000 Oslo*

POLAND
WĘGIERSKI INSTYTUT KULTURY
Marszalkowska 80, *00-517 Warszawa*
CKP I W, ul. Towarowa 28, *00-958 Warszawa*

ROUMANIA
D. E. P., *Bucuresti*
ILEXIM, Calea Grivitei 64-66, *Bucuresti*

SOVIET UNION
SOYUZPECHAT — IMPORT, *Moscow*
and the post offices in each town
MEZHDUNARODNAYA KNIGA, *Moscow G-200*

SPAIN
DIAZ DE SANTOS Lagasca 95, *Madrid 6*

SWEDEN
ESSELTE TIDSKRIFTSCENTRALEN
Box 62, *101 20 Stockholm*

SWITZERLAND
KARGER LIBRI AG, Petersgraben 31, *4011 Basel*

USA
EBSCO SUBSCRIPTION SERVICES
P.O. Box 1943, *Birmingham, Alabama 35201*
F. W. FAXON COMPANY, INC.
15 Southwest Park, *Westwood Mass. 02090*
MAJOR SCIENTIFIC SUBSCRIPTIONS
1851 Diplomat, P.O. Box 819074,
Pallas, Tx. 75381-9074
READ-MORE PUBLICATIONS, INC.
140 Cedar Street, *New York, N. Y. 10006*

YUGOSLAVIA
JUGOSLOVENSKA KNJIGA, Terazije 27, *Beograd*
FORUM, Vojvode Mišiča 1, *21000 Novi Sad*

Index: 26.017

Acta Morphologica Hungarica

VOLUME 36, NUMBERS 3–4, 1988

Akadémiai Kiadó, Budapest
ACTA MORPH. HUNG. HU ISSN 0236–5391

ACTA MORPHOLOGICA
HUNGARICA
A QUARTERLY OF THE HUNGARIAN ACADEMY OF SCIENCES

Acta Morphologica publishes original papers on experimental morphology and pathology in English.

Acta Morphologica is published in yearly volumes of four issues by

AKADÉMIAI KIADÓ
Publishing House of the Hungarian Academy of Sciences
H-1054 Budapest, Alkotmány u. 21.

Manuscripts and editorial correspondence should be addressed to

Acta Morphologica
Ist Institute of Pathology and Experimental Cancer Research, Semmelweis Medical University,
1085 Budapest, Üllői út 26, Hungary

Subscription information

Orders should be addressed to

KULTURA Foreign Trading Company
H-1389 Budapest P.O. Box 149

or to its representatives abroad

Acta Morphologica Hungarica is abstracted/indexed in Biological Abstracts, Chemical Abstracts, Chemie-Information, Current Contents–Life Sciences, Excerpta Medica, database (EMBASE), Gerontological Abstracts, Index Medicus

CONTENTS

Normal and experimental morphology

Pathology

Acta Morphologica Hungraica, 36 (3—4), pp. 143—146 (1988)

PERMANENT METACHROMATIC EFFECT OF 1,9-DIMETHYL-METHYLENE BLUE ON ACIDIC MUCOPOLYSACCHARIDES OF MASTOCYTES

E. Pokorny, T. Kremmer, L. Holczinger

NATIONAL INSTITUTE OF ONCOLOGY, RESEARCH INSTITUTE OF ONCOPATHOLOGY, BUDAPEST, HUNGARY

(Received 29 July 1987)

The 1,9-dimethyl-methylene blue (SERVA) has a very strong metachromatic reaction with sulphated mucopolysaccharides of mastocytes at pH=1 (Tris-HCl buffer). This metachromasia is retained also at increasing pH (2.5—5), and is not affected either by the quality or by the concentration of the ions present (1/240 M Tris-HCl, and 0.2 M phosphate buffer).

The smears do not need any special mounting medium, only Canada balsam. The metachromasia is preserved for a considerable length of time.

Keywords: Mastocytes, sulphated mucopolysaccharides, 1,9-dimethyl-methylene blue (DMMB), metachromasia

Introduction

Reactions based on the phenomenon of metachromasia play an important role in the histochemical detection of sulphated mucopolysaccharides [2, 5, 10, 11, 13, 17].

Disadvantage of these staining techniques lies, however, in the fact that results are considerably influenced by the pH and ion concentration of the staining medium and the preparations, in the majority of cases, lose their metachromasia within a short time and fade out [3, 6, 13].

Present investigations have been performed with the dye 1,9-dimethyl-methylene blue chloride (SERVA) on mouse mast cells. Attention to this dye has been called upon by Taylor and Jaffree [14] and Toepfer [16] because of its strong metachromatic properties. Mast cells contain, beside histamine and serotonin, mainly heparin [1, 9]. Consequently, these cells seem to be most suitable to test the staining reaction.

Materials and methods

Mast cells were separated by the technique of Thon and Uvnäs [15] from the abdominal cavity of Swiss mice. From the cells obtained smears were prepared. After having air-dried the smears were fixed in Carnoy's solution for 15 min then washed in distilled water for 4 × 1 min and dried at room temperature.

Send offprint requests to: Dr. E. Pokorny, National Institute of Oncology, Research Institute of Oncopathology, Budapest, Ráth Gy. u. 7—9, H-1122, Hungary

After drying the preparations were stained with 0.05% 1,9-dimethyl-methylene blue (DMMB) dye solution at pH = 1, pH = 2.5 and pH = 5. It is well known that at pH = 1 only sulphate groups, at pH = 2.5 phosphate groups and at pH = 4 carboxyl groups are dissociated and able to enter in reactions within biological objects [4, 8]. pH values were adjusted with 0.001 M Tris buffer (Tris-/hydroxy-methyl/-amino-metan/ — 0.1N HCl, or with 0.2 M phosphate buffer.

After staining and drying at room temperature the smears were covered with Canada balsam.

Results and discussion

In preparations stained at pH : 1 only the granules of mast cells were stained metachromatically, while other cellular elements remained unstained. Absorption maximum of granules stained purple, was shifting to 570 nm instead

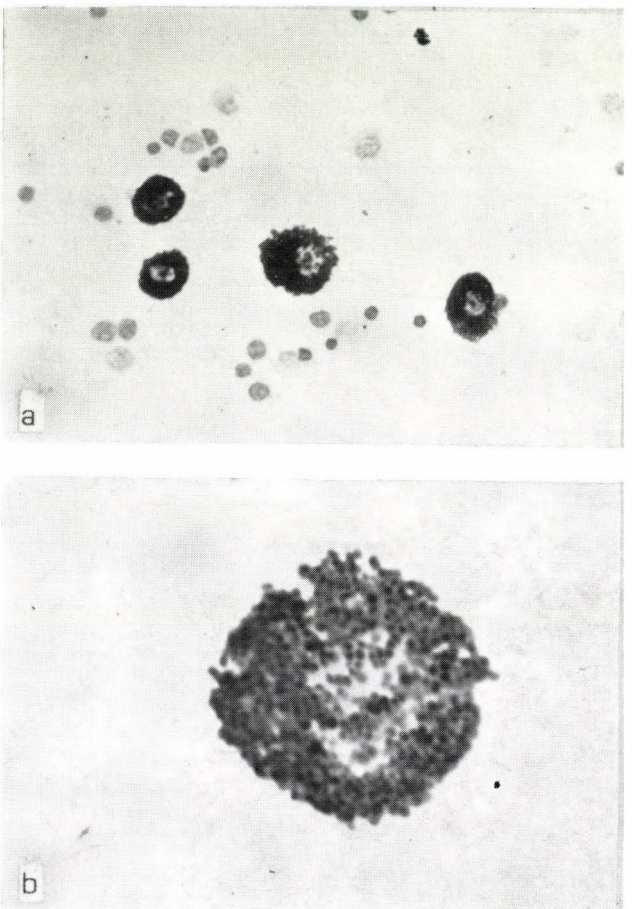

Fig. 1a Mast cell preparation stained with DMMB solution at pH = 1. Mast cells are intensively stained while other cells are hardly visible in the background. (× 320)

Fig. 1b Mast cells stained with DMMB solution at pH = 1. Within the cells only the granules get stained no other cellular components are visible. (×1820)

of the 660 nm original maximum of the dye in cells. Absorption maxima were recorded by scanning and integrating cytophotometer (Barr and Stround, Glasgow). Some other cells present in the preparations displayed a faint blue colour. Background staining was hardly discernible. Consequently, no or minimal adsorptive staining took place (Fig 1a, b). With increasing pH (2.5—5), other cellular components become also visible, but while the mast cell granules retain their metachromatic staining properties, they stain orthochromatically.

It can be stated that the DMMB staining at pH : 1 is highly selective for sulphated mucopolysaccharides. Strong metachromasia granules (shifting the absorption maximum from 660 to 570 nm) remains at pH : 2.5 and pH : 5 as well. The phenomenon is not affected, even within very wide limits, either by the quality or by the concentration of the ions present.

It is of additional significance that no special mounting medium is needed and under a layer of Canada balsam metachromasia is preserved for a considerable length of time.

Further characterization of DMMB staining and the study of its applicability are in progress.

REFERENCES

1. Hahn von Dorsche H, Fehrmann P, and Sulzmann R: Die Mastzelle als einzellige endokrine Drüse. Acta Anat 77 : 560, 1970
2. Klein MD, Drongowski RA, Linhardt RJ, Langer RS: A colorimetric assay for chemical heparin in plasma. Anal Biochem 124 : 59, 1982
3. Landsmeer JMF: Some colloid chemical aspects of metachromasia. Influence of pH and salts on metachromatic phenomena evoked by toluidine blue in animal tissue. Acta Physiol Pharmacol Nederl 2 : 112, 1951
4. Lev R, Spicer SS: Specific staining of sulphate groups with alcian blue at low pH. J Histochem Cytochem 12 : 309, 1964
5. Módis L, Batschwarowa M: Fluorescence histochemical investigations of connective tissue. III. Fluorescence histochemistry of the heparin content of mast cells. Acta Morph 17 : 235, 1969
6. Radden BG: An investigation of the factors influencing the metachromatic staining of mast cell granules. J Histochem Cytochem 9 : 165, 1961
7. Scott JE: Ion binding in solutions containing acid mucopolysaccharides. In: Quintarelli G (ed.) The Chemical Physiology of Mucopolysaccharides. (By 17 authors) Boston Little Brow and Company, 1968
8. Scott JE: Critical electrolyte concentration (CEC) effects in interactions between acid glycosaminoglycans and organic cations and polycations. In: Chemistry and Molecular Biology of the Intercellular Matrix. Vol 2 Academic Press, New York, 1970, 1105
9. Selye H: The Mast Cells. Butterworths, Washington, 1965
10. Stone ALL, Childers LG, Bradley DF: Investigations of structural aspects and classification of plant sulphated polysaccharides on the basis of the optical properties of their complexes in metachromatic dyes. Biopolymers 1 : 111, 1963
11. Stone ALL, Bradley DF: Aggregation of cationic dyes on acid polysaccharides. Biochim Biophys Acta 148 : 172, 1967
12. Tas J, Geenen LHM: Microspectrophotometric detection of heparin in mast cells and basophilic granulocytes stained metachromatically with toluidine blue O. Histochem J 7 : 231, 1975
13. Tas J: Histochemical conditions influencing metachromatic staining. A comparative study by means of a model system of polyacrylamide films. Histochem J 7 : 1, 1975

14. Taylor KB, Jaffree GM: A new basic metachromatic dye, 1,9-dimethyl methylene blue. Histochem J 1 : 199, 1969
15. Thon IL, Uvnäs B: Degranulation and histamine release, two consecutive steps in the response of rat mast cells to compound 48/80. Acta Physiol Scand 71 : 303 1967
16. Toepfer K: Spektralphotometrische und histochemische Eigenschaften von 1 : 9 Dimethyl-Methylenblau als metachromatischem Farbstoff. Histochemie 21 : 64, 1970
17. Villanueva GB, Danishefsky I: Differential effect of high affinity heparin and low affinity heparin on methylene blue titration. Thromb Res 21 : 191, 1981

Acta Morphologica Hungarica, 36 (3—4), pp. 147—154 (1988)

RE-INNERVATION OF PANCREATIC TISSUE IMPLANTS IN NORMAL AND IN SYMPATHETICALLY DENERVATED EYES OF RATS

T. Donáth, E. Adeghate

1st DEPARTMENT OF ANATOMY, HISTOLOGY AND EMBRYOLOGY, SEMMELWEIS UNIVERSITY MEDICAL SCHOOL, BUDAPEST, HUNGARY

(Received 12 October 1987)

Embryonic, newborn and adult pancreatic tissue fragments were implanted into the anterior eye-chamber of rats of the same offspring to determine whether there is any difference in the pattern of their re-innervation. In another experiment the embryonic pancreatic tissue fragments were implanted into sympathetically denervated eyes of homologous rats. Newborn, adult and embryonic pancreatic tissue implants were removed under a stereo-microscope after 17, 45 and 53 days, respectively. The embryonic pancreatic tissue implants in denervated eyes were removed after 46 days. The implants were processed for electron microscopy.

The embryonic, newborn and adult pancreatic tissue implants were equally well re-innervated by agranular and granular vesicle-containing nerve terminals and varicosities from the host iris. The embryonic pancreatic tissue implants were also re-innervated in sympathetically denervated eyes, most likely by parasympathetic nerves of the iris. Except for the few intrinsic nerve profiles, the re-innervating nerve fibres seemed to reach the implant stroma through the blood vessels revascularizing the implants. The re-innervation of the endocrine pancreas is more pronounced than that of the whole tissue.

Keywords: Re-innervation, pancreatic implants, eye-chamber

Introduction

In spite of the fact that pancreas has been extensively transplanted experimentally to treat induced diabetes mellitus, less attention has been paid to the ultrastructural morphology of the transplants [3], and even much less to its re-innervation. Since intact innervation is probably vital to the endocrine secretion of pancreas, the importance of a detailed knowledge of the pattern of re-innervation of pancreatic tissue implants cannot be overemphasized.

In the present study, newborn and adult pancreatic tissue fragments were implanted into the anterior eye-chamber of rats of the same offspring to determine if there is any difference in their pattern of re-innervation from the host iris. In another experiment, embryonic pancreatic tissue fragments were implanted into sympathetically denervated eyes of homologous rats to study the phenomenon of re-innervation from the pool of parasympathetic nerves in the iris.

Send offprint requests to: Dr. T. Donáth Ist Dept. of Anatomy, Semmelweis University Medical School, Budapest, Tűzoltó u. 58, H-1450 Hungary

Materials and methods

18-day-old embryonic, newborn and adult rats were anaesthetized with aether and chloral hydrate. Median laparatomy was performed and the tail of or the whole (embryonic and newborn) pancreas were removed and cut into small pieces in physiological solution. The pieces were immediately implanted with fine watchmaker's forceps into the anterior eye-chamber of anaesthetized, homologous rats through a small incision (3—4 mm) made on the cornea. Prior to implantation, the host rats received 0.5 ml of 0.05% atropine to enhance pupil dilatation and to minimise the by-effects of the anaesthetics. Plastubol spray (EGIS, Hungary) producing a sterile methylmetacrylate film was used to cover the incision on the cornea. 8000 i. u. of penicillin was given intramuscularly against any procured infection.

In another experiment, 18-day-old pancreata were implanted as described above into sympathetically denervated eyes of homologous rats. Sympathetic denervation of the iris was performed by the extirpation of the superior cervical ganglion. After 17 days, animals having received newborn pancreatic tissue fragments were anaethestized as described above, perfused transcardially with Karnovsky's solution, the eyes dissected out and the implants removed under a stereo-microscope, while those with adult and embryonic pancreatic tissue implants were treated in the same way after 45 and 53 days, respectively. The embryonic pancreatic tissue fragments implanted into sympathetically denervated eyes were removed after 46 days as described above.

The implants were refixed and postfixed in Karnovsky's and in 1% osmium tetroxide solutions, respectively. They were dehydrated in graded ethanol and propylene oxide. Ulthrathin sections stained with lead citrate and uranyl acetate were investigated under a Tesla BS 500 electron microscope.

Results

Adult pancreatic tissue implants

After 45 postimplantation days, a nerve plexus with different types of varicosities were found around the acinar cells. Empty round vesicles were seen in one type of axon, medium dense-cored vesicles in another while a third type contained flattened or oval-shaped vesicles. The axons were enclosed in Schwann cell processes which opened towards the acinar cell (Fig. 1). Parallel with acinar degenration, proliferation of pancreatic tubules and existence of endocrine cells were also observed.

Newborn pancreatic tissue implants

At 17 days after implantation, newly formed neuro-insular complex was found around fenestrated capillaries in the substrate of the implants. (Fig. 2). Nerve fibre terminals containing agranular vesicles were observed on the cell membrane of the beta cells. (Fig. 3). The nerve fibres were enclosed in Schwann cell processes and open towards the endocrine cells except when they lied on the plasma membrane of the endocrine cells.

In the beta cell, light and dark secretory granules were discernible. Some granular vesicle-containing nerve fibre terminals were also found on the plasma membrane of delta cells. Around them many axons with neurotubular structures and varicosities containing medium dense-cored vesicles were seen. (Figs 4, 5).

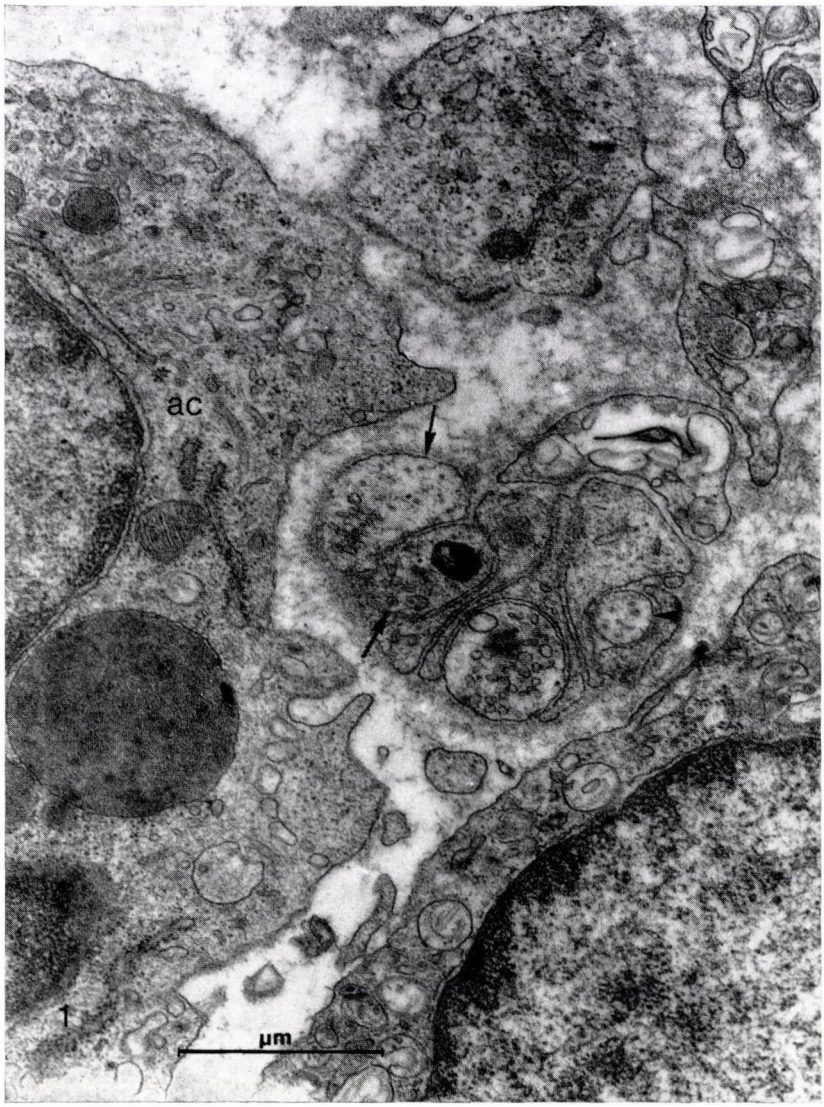

Fig. 1. 45-day-old adult pancreatic tissue implant: Nerve plexus with different types of varicosities around degenerating acinar cell (ac). Empty round vesicles are found in one axon (arrow head), medium dense-cored vesicles in another (thin arrow), while a third contains flattened or oval-shaped vesicles (thick arrow). × 40600

In addition to the above observations, there was a marked re-vascularization of the implanted tissue to be seen. In harmony with gradual acinar degeneration there occurred a proliferation of pancreatic tubules resulting in duct-islet and duct-acinar transformation. The ratio and organization of the endocrine cells to each other did not change except for a slight increase in the number of beta cells.

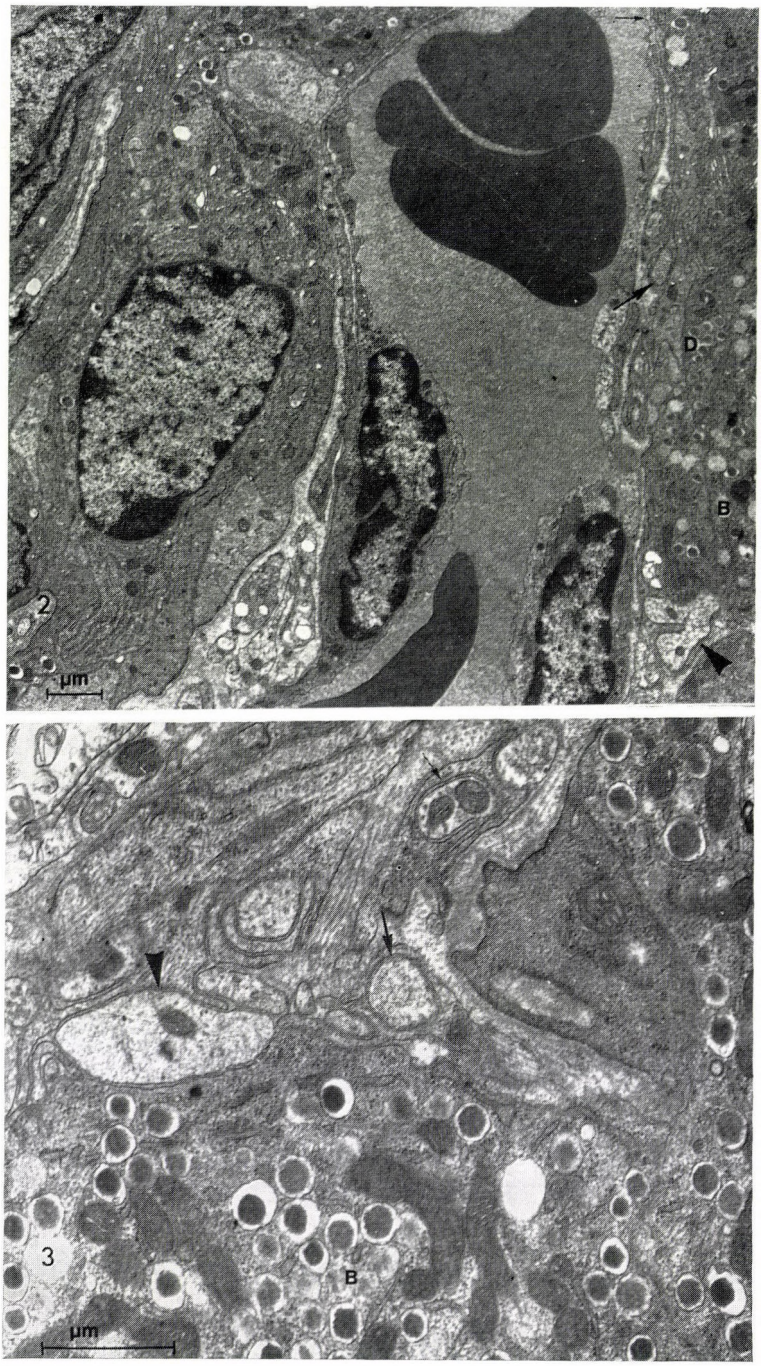

Fig. 2 17-day-old pancreatic tissue implant: Neuro-insular complex consisting of beta (B) and delta (D) cells, nerve fibre terminals (arrow head) and axons (thick arrow) around fenestrated capillaries (thin arrow). × 11600

Fig. 3 17-day-old pancreatic tissue implant: Nerve fibre terminals (arrow head) and axons (thick arrow) containing agranular vesicles on the plasma membranes of beta (B) cells. Nerve fibre varicosities (thin arrow) are also found on the periphery of the cells. × 29000

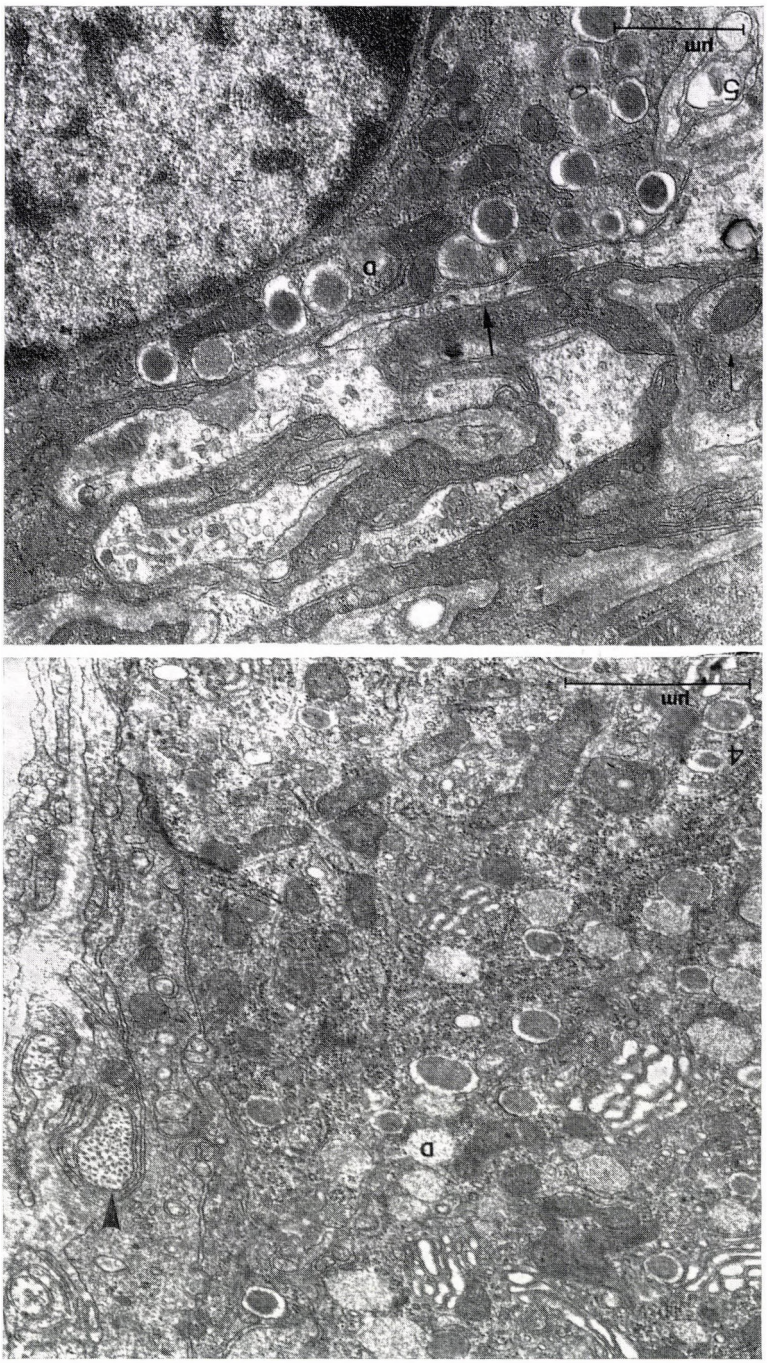

Fig. 4 17-day-old pancratic tissue implant: Axon (arrow head) with medium dense-cored vesicles around delta (D) cells. × 40600

Fig. 5 17-day-old pancreatic tissue implant: Medium dense-cored vesicles containing nerve fibre terminals (thick arrow) on plasma membrane of delta (D) cells. A nerve fibre varicosity (thin arrow) containing many agranular vesicles in the periphery of delta (D) cells. × 29000

Embryonic pancreatic tissue implants

After implantation of 18 embryonic days old pancreatic tissue fragments for 56 days, nerve plexus with varicosities and axons enclosed in Schwann cell processes were observed around beta cells. The varicosities contained agranular vesicles and mitochondria. Some nerve fibres were myelinated. (Fig. 6). The differentiation of the implants which were composed mostly of pancreatic tubules seemed to be delayed because relatively undifferentiated pancreatic tubular and islet cells could still be recognized at this stage.

Embryonic pancreatic tissue implants in sympathetically denervated eyes

46 days after implantation of 18 embryonic days old pancreatic tissue fragments, axon profiles with neurotubular structures were discernible around beta cells. The axons were enclosed in Schwann cell processes which opened up as they came closer to the endocrine cells (Fig. 7). Nerve fibre varicosities were also observed among the Schwann cell enclosed nerve fibres.

Discussion

Results of the present study corroborate that embryonic, newborn and adult pancreatic tissue implants are equally well re-innervated in the anterior eye-chamber [1]. Simard [7] and Coupland [2] have also reported the existence of nervous elements in pancreatic implants. They attributed this to the survival of the nervous elements which are observed only in fully differentiated adult pancreatic tissue implants and not in embryonic pancreas. The discrepancy might be due to the fact that Simard [7] and Coupland [2] used only light microscope to examine the structure of the implants. The light microscope is not capable of demonstrating smaller and fine nervous elements.

The pronounced re-innervation of the endocrine pancreas might probably explain the stronger intimacy of the endocrine pancreas to the nervous system. Since it is well established that the secretion of endocrine pancreas is finely regulated by the autonomic system [5], intact innervation is therefore essential for the normal regulation of endo- and exocrine secretion of the pancreas. Most of the re-innervating nerve profiles contain agranular vesicles, probably denoting a predominance of parasympathetic over sympathetic nerves in re-innervating the rat pancreatic tissue implants. Embryonic pancreatic tissue implanted into sympathetically denervated eyes are re-innervated. The re-innervating nerve fibres are likely to be parasympathetic, because superior cervical ganglionectomy causes complete degeneration of sympathetic nerve fibres in the iris. [6].

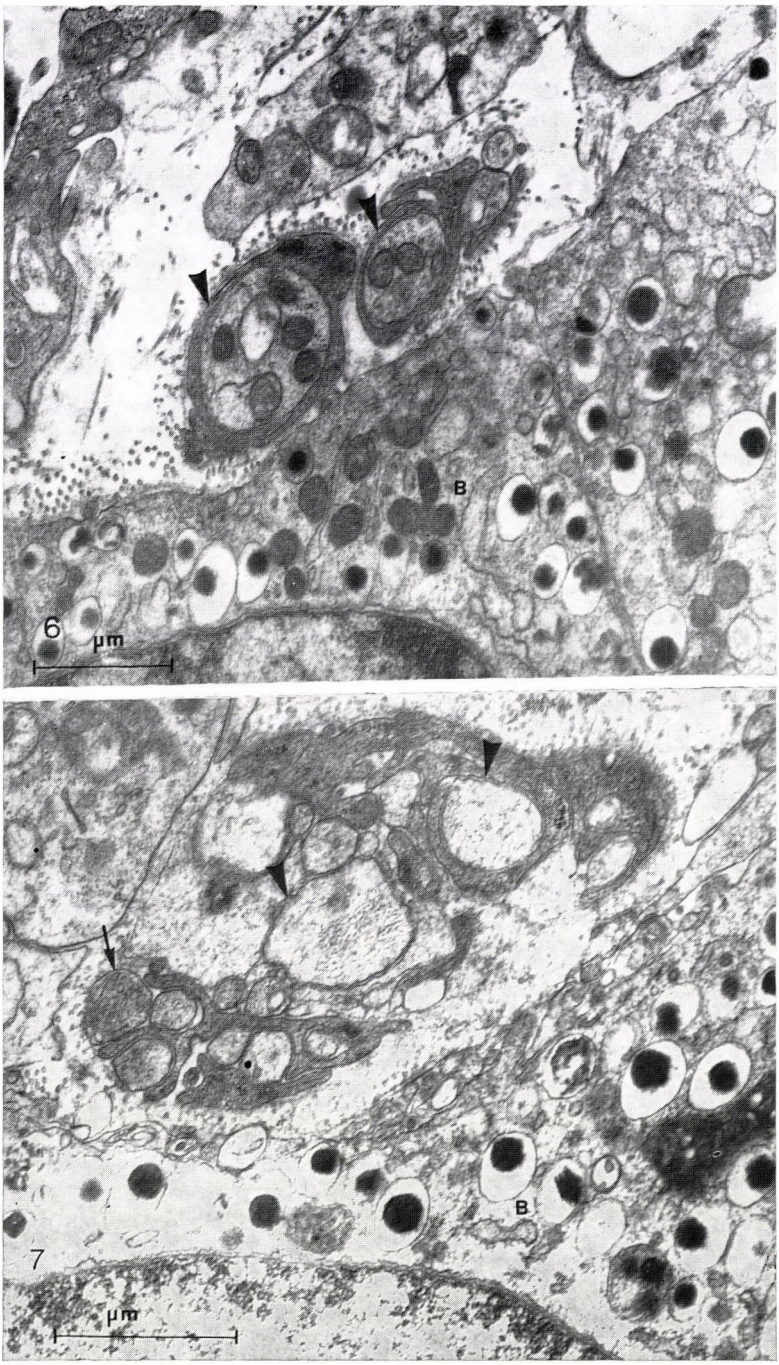

Fig. 6 18 embryonic days old pancreatic tissue implant: Nerve fibre varicosities (arrow heads around beta (B) cells. × 29000

Fig. 7 18 embryonic days old pancreatic tissue implant in sympathetically denervated eyes: Nerve plexus with axons containing empty vesicles (arrow) around beta (B) cells. × 40600

Though nerve fibre terminals are found on the plasma membranes of the endocrine cells suggesting a possibly parenchymatic origin, it appears that the re-innervating nerve fibres reach the implants through the re-vascularizing blood vessels also from the iris. The axons without vesicles might represent regenerating and/or developing nerve fibres.

REFERENCES

1. Adeghate E and Donáth T: Re-innervation of pancreatic tissue implants in the anterior eye-chamber of CRF rats. Neuroscience 22 (Suppl): S259, 1987
2. Coupland RE: The survival and growth of pancreatic tissue in the anterior chamber of the eye of the albino rat. J Endocrinol 20 : 69, 1960
3. Donáth T and Adeghate E: Light- and electron microscopy of postnatal pancreatic tissue implants in the anterior eye-chamber of rats. Z mikr anat Forsch 102 : 512, 1988
4. Karnovsky MJ: A formaldehyde-glutaraldehyde fixative of high osmolality for use in electron microscopy. J Cell Biol 27 : 137A, 1965
5. Luiten PGM, ter Horst GJ and Steffens AB: The hypothalamus, intrinsic connections and outflow pathways to the endocrine system in relation to the control of feeding and metabolism. Prog Neurobiol 28 : 1, 1987
6. Roth CD and Richardson KC: Electron microscopical studies of axonal degeneration in the rat iris following ganglionectomy. Am J Anat 124 : 341, 1969
7. Simard LC: Étude histologique de pancréas, greffes dans la paroi abdominal, chez le chien (complexes neuroinsulaires, ganglion nerveux, cellules insulaires). Rev Canad Biol 4 : 264, 1945

Acta Morphologica Hungarica, 36 (3—4), pp. 155—166 (1988)

INTERCONNECTION OF DEMYELINATION PROCESSES AND INFLAMMATION IN THE DYNAMICS OF EXPERIMENTAL ALLERGIC ENCEPHALOMYELITIS

M. G. KHIZHNYAK, Y. L. ZHITNUKHIN, G. V. KONOVALOV, S. P. SEMENOV

INSTITUTE FOR EXPERIMENTAL MEDICINE, USSR ACADEMY OF MEDICAL SCIENCES, LENINGRAD, USSR

(Received 20 October 1987)

Using a new method for the simultaneous demonstration of myelin breakdown products and cell elements in the demyelinated nervous tissue, a number of previously unknown regularities were revealed concerning interconnection between demyelination processes and inflammation in the dynamics of experimental allergic encephalomyelitis (EAE). Alterations in osmophilia and in size of myelin breakdown products in the demyelination foci are demonstrated to be the most essential in the EAE pathomorphology, a certain type of cellular reaction corresponding to each stage of periaxonal changes. A close relationship was found between demyelination processes and inflammation which determines the structure of the demyelination foci at various stages of the disease.

Introduction

Despite prolonged efforts to investigate the pathogenesis of demyelinating disease, their underlying mechanisms are still not clarified. Up to the present time, the problem of pathogenic effect of cellular and humoral factors of the immune response to myelinated structures of the brain is argued. There cannot be any progress in this field without a fundamental study of all the factors of nervous tissue lesions in their interaction to determine the sequence of their appearance and their significance in development of demyelination.

A suitable model to study the demyelinating process is the experimental allergic encephalomyelitis (EAE). In the literature one can come across conflicting views on the interconnection of the demyelinating processes and inflammation in EAE — beginning with their topographic discrepancy [2, 3, 13] up to the idea about possible development of EAE without demyelination [1, 7, 9, 10]. The cause of similar conclusions is the fact that some inadequate methods are used to demonstrate demyelination and its connection with other alterations in the nervous tissue (for example, Weigert's, Kultschitzky's, Spielmeyer's methods, staining after Klüver-Barrera). Luxol Fast Blue, MBS

Send offprint requests to: M. G. Khizhnyak M. D. Institute for Experimental Medicine, USSR Academy of Medical Sciences, Pavlov's Str. 12, 197022 Leningrad, USSR

and some other stainings are capable to reveal only advanced stages of demyelination, and Marchi's highly sensitive method cannot identify safely neurological and inflammatory cells. Electron microscopy is known to be suitable to investigate both aspects of the pathological process — inflammation and demyelination. Since, however, the pathological alterations in the CNS at EAE appear in small areas and in large space-time ranges, the volume of the material necessary for the investigation is often beyond the methodical possibilities of electron microscopy.

The aim of the present investigation was to study the relationship between the processes of demyelination and inflammation in the EAE dynamics using the method developed at our institute for simultaneous demonstration of myelin breakdown products and cell elements in demyelinated nervous tissue.

Materials and methods

EAE was induced in non-inbred mature guinea pigs (body weight 350—400 g) with a single subcutaneous injection in a forefoot pad of 0.001 mg myelin basic protein fraction (BPF) or 20 mg (wet weight) of brain tissue homogenate (BHT) in mixture with 0.05 ml complete Freund adjuvant (CFA). BPF was isolated from bovine spinal cord by means of column chromatography [14]. Histological signs of EAE were detected and examined in 113 animals sensitized with BPF and in 49 sensitized with BTH. The animals investigated were killed at various stages of the EAE development: at 8—10 days (latent period), at 14—17 days (neurological signs of EAE) and 48—365 days (clinical recovery). According to our modification of Marchi's method [4], CNS materials were fixed in 10 per cent formaldehyde, kept in 3 per cent potassium bichromate solution followed by 1 per cent osmic acid solution for 2 days in each. Samples were then washed in tap water for 12 h, dehydrated successively in 70, 96, 100 per cent eathanol and embedded in celloidine. Histological sections of 2.5—5 thickness were stained with toluidin blue and mounted with balsam. A part of the material was fixed in 70% ethanol and stained with the Nissl method. Rapid preparations were obtained by means of a freezing microtome after specimen impregnation in osmic acid.

Results

Neurological symptoms of EAE-pareses and paralyses of hind limbs, pelvic disorders, haemipareses and hyperkineses were observed in the animals for the first time in 10—14 days after the injection of encephalitogenic mixture. Lethality at EAE, induced with BPF, was 85%, while among the animals, inoculated with BTH, 100% death was registered (usually on the 3rd—4th days from the onset of the disease). In 3 animals, inoculated with BTH, a hyperacute course of EAE was observed with a shortened latent period up to 8 days and a rapid (during several hours) mortal outcome.

The main pathological changes, revealed during the latent period of EAE, beginning from the 10th day after inoculation of the encephalitogenic mixture, were demyelination and cellular inflammatory infiltration. The inflammatory

reaction, found mainly in the lumbosacral segments of the spinal cord and in the zone of the pons Variolii, produced two types of cellular infiltrations: either lymphocytes and haematogenic macrophages, or macrophages and neutrophilic granulocytes. Already at this stage of the disease, the peculiarity of the inflammatory process was its close connection with demyelination. In the areas, free of haematogenic elements, the myelin breakdown products were absent and certain stages of periaxonal changes corresponded to definite types of cellular reactions. For example, in areas where the white substance was infiltrated with lymphocytes and haematogenic macrophages, single myelin breakdown products were detected (Fig. 1a), while in the zones where macrophages and neutrophilic granulocytes occurred, focal accumulations of osmiophilic granules were ob-

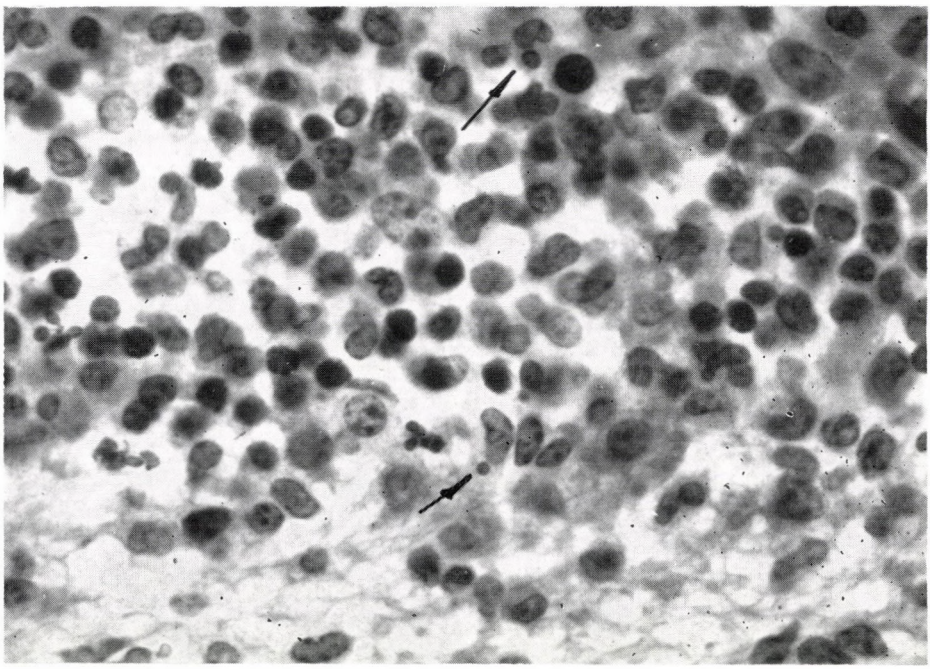

a

Fig. 1. White matter of the spinal cord lumbar segment. Marchi's modified method with toluidine blue staining. *a* — lympho-monocytic, infiltration in the zone of single small slightly osmiophilic myelin breakdown products (arrows). EAE. The 11th day after inoculation with BPF. ×460, *b* — infiltration with macrophages and neutrophilic granulocytes in the zone of focal accumulation of small slightly osmiophilic myelin breakdown products (arrows). EAE. The 11th day after inoculation with BPE. ×280 *c* — haematogenic macrophages with an admixture of astrocytes and a neutrophilic granulocyte among focal accumulation of the myelin breakdown products possessing various degree of osmiophilia (arrows). EAE. The 17th day after inoculation with BPF. ×460 *d* — large intensively osmiophilic myelin breakdown products among glial cells. EAE, induced with BPF. The 5th day of the clinical recovery. ×580 *e* — desintegrated fragments of myelin sheaths of small size and weak degree of osmiophilia. The cerebellar white matter. Modified Marchi's method. EAE, induced by BPF. Twelve months after clinical recovery. ×140

served (Fig. 1b). Usually, in the foci of initial demyelination lymphoid cells were absent. These foci were often revealed rather far from the lymphoid infiltrates. Small size (0.5—2.5 mcm) and extremely low osmiophilia in fragments of destroyed myelin sheaths in the areas of the initial demyelination attracted our attention.

An essential manifestation, dissemination and polymorphism were specific for the pathomorphology of EAE during the period of neurological signs. Besides the changes described above, the inflammatory infiltration of the CNS white matter was produced by haematogenic macrophages and astrocytes, among which the myelin breakdown products were situated; their osmiophilia was of higher degree and they were larger in size (Fig. 1c).

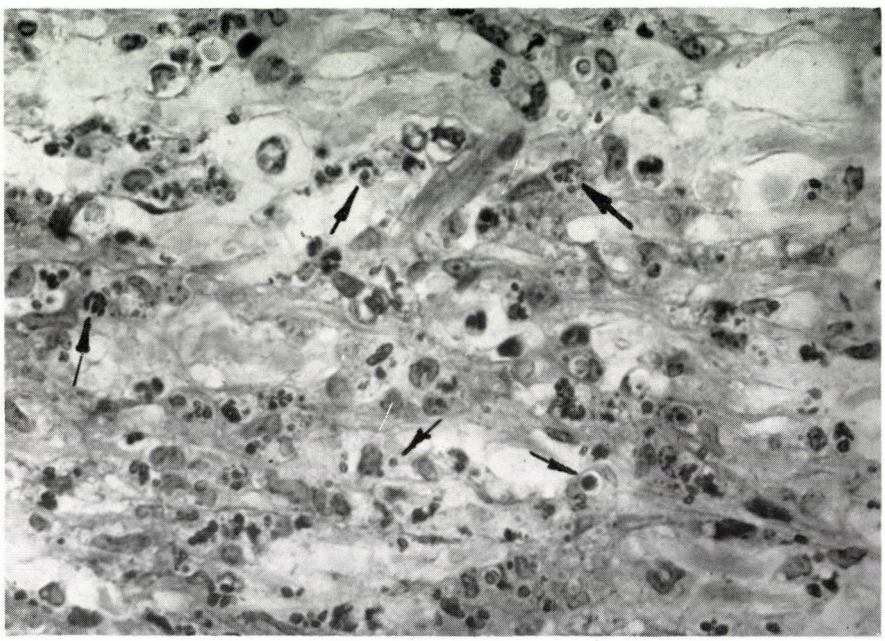

b

Various zones of the inflammatory infiltrates could noticeably differ by their ratio of cellular elements. Near large vessels and in the pia mater encephali, as a rule, lymphocytes predominated, in the deeper zones — haematogenic macrophages, and at the border of the inflammatory infiltrates with the white matter — haematogenic macrophages and neutrophiliac granulocytes. If near the large vessels and the pia mater the macrophages usually had a peculiar round form, in the depth of the white matter and especially in the demyelination foci these cells acquired an elongated form.

On the first days after the disappearance of visible neurological disturbances, certain lesions of the spinal cord white matter of various intensity were

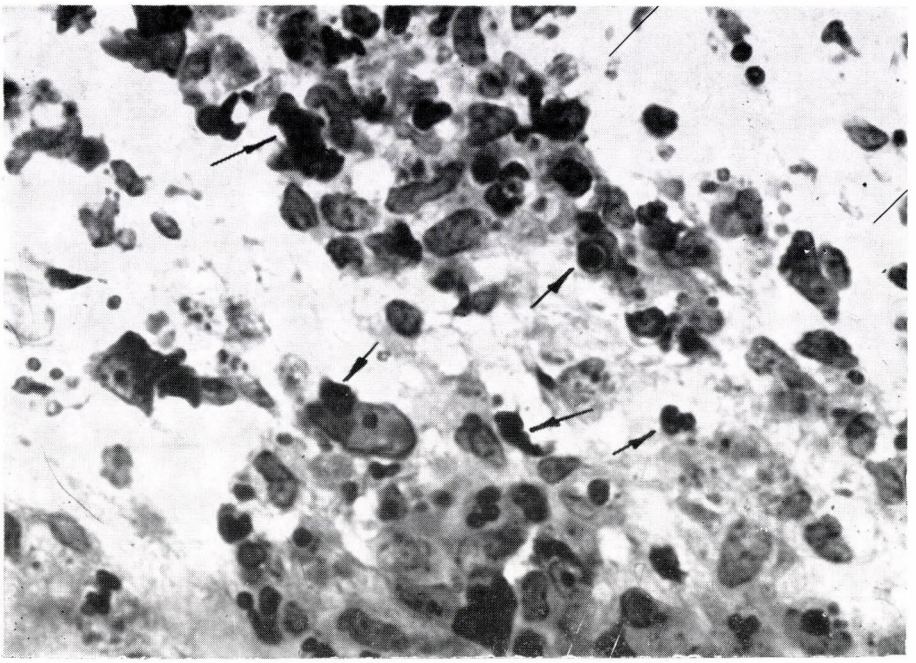

c

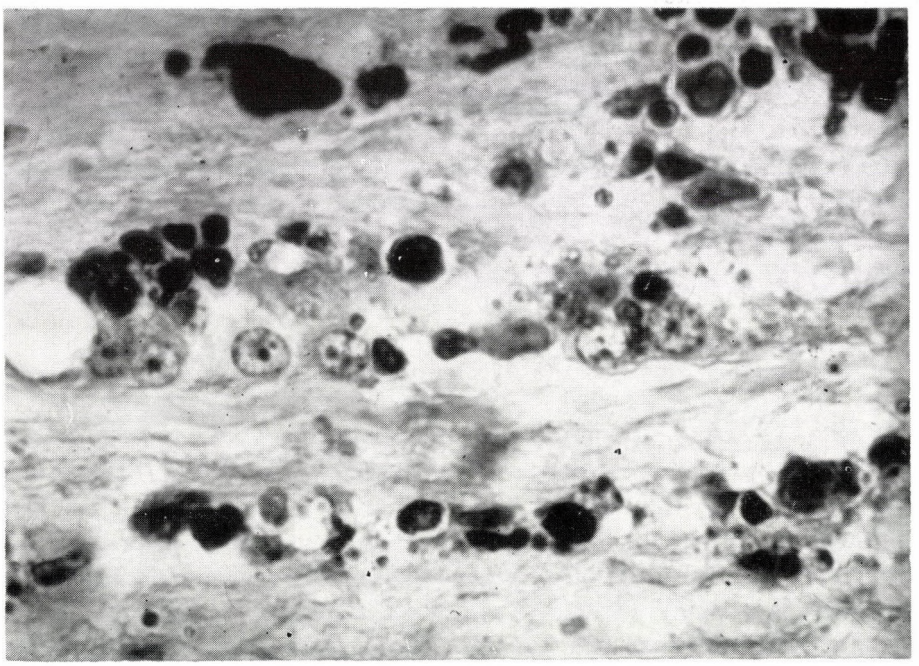

d

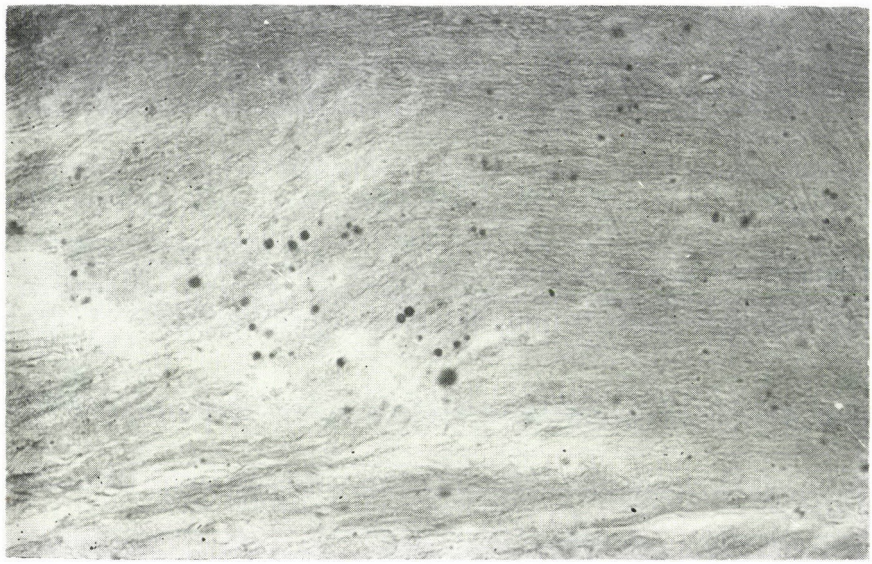

e

seen. The manifestation of demyelination could be rather essential, however, inflammatory changes were gradually decreasing. During this period the demyelination foci were revealed in the anterior and posterior funiculi of the lumbosacral segments of the spinal cord and were seen as accumulations of large (up to 40—50 and more mcm) intesively osmiophilic granules localized in the cerebral white matter among astrocytes and oligodendrocytes (Fig. 1d). Inflammatory changes during the first week of clinical recovery were manifested as a rather moderate lymphotic and monocytic infiltration in the area of the anterior and posterior longitudinal sulci in the lumbosacral segments and very seldom in the zone of the spinal cord white matter.

Structure of the demyelination foci in 3—3.5 months after EAE induction remained, as a whole, the same. Only a more diffuse arrangement of the myelin breakdown products in the white matter can be mentioned.

In 11—12 months of reconvalescence in the brain and spinal cord weakly osmiphilic, mainly small size (5—7 mcm) fragments of desintegrated myelin sheaths were found freely scattered in the white matter (Fig. 1e).

Changes connected with glial cells were not significant. Only in cases of a hyperacute course of EAE a noticeable re-arrangement (Fig. 2a) and a sharp condensation of the nuclear chromatin (Fig. 2b, c) was observed in the demyelination foci. Pathological changes in neurons were usually absent. In 3 animals, however, inoculated with BTH, lesion of the grey matter in the lumbosacral segments of the spinal cord took place as destruction and ischemic changes. Destructive changes in the neurons were acute swelling, sharp hyperchromatosis

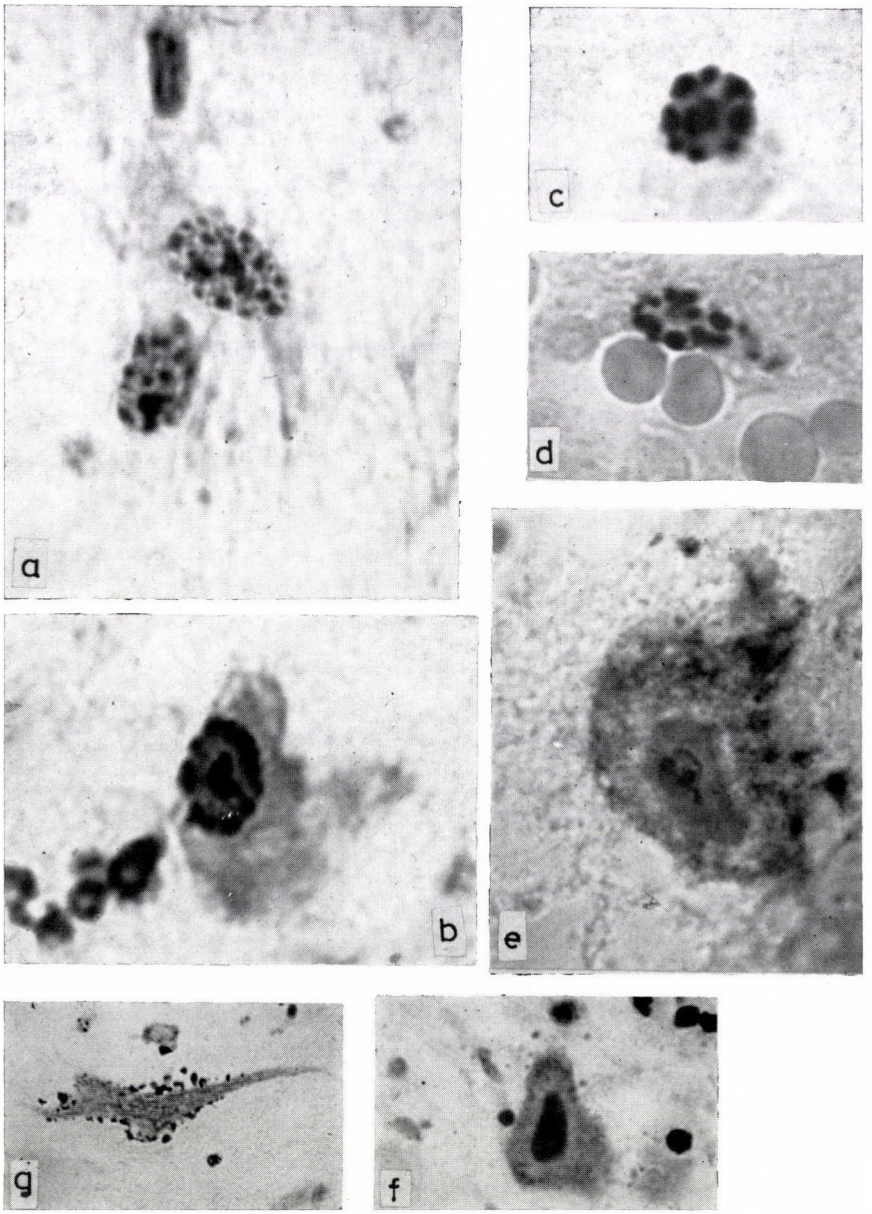

Fig. 2. Lumbosacral segment of the spinal cord (*a*—*e* — white matter, *f*—*g* — anterior horn). *a* — redistribution of chromatin in gliocytic nuclei. EAE. The 8th day after inoculation with BTH. Nissl method. ×900 *b* — intensive hypertrophy of cytoplasm and condensation of chromation in the gliocyte nucleus. EAE. The 8th day after inoculation with BTH. Nissl method. ×840. *c* — intensively manifested condensation of chromatin in a gliocyte. EAE. The 8th day after inoculation with BTH Nissl method. ×840. *d* — remnants of condensed chromatin near erythrocytes. EAE. The 8th day after inoculation with BTR. Nissl method. ×590 *e* — acute swelling with phenomena of a clumped chromatolysis nuclear hyperchromatosis and hypertrophy of the nuclear apparatus in the neuron. EAE. The 8th day after inoculation with BTH. Nissl method. ×480 *f* — ischemic alteration of the neuron. EAE. The 8th day after inoculation with BTH. Nissl method. ×320 *g* — pericellular incrustation of the neuron. EAE. The 8th day after inoculation with BTH. Nissl method. ×280

of the nucleus with hypertrophy of the nucleolar apparatus (Fig. 2d). The signs of hypoxia were pyknotic nuclei, their form copying the contours of cytoplasm (Fig. 2e). Pericellular incrustation of the bodies of the nerve cells with calcium salts (Fig. 2f) indicated ischemic changes. It should be noted that the pathological changes described were detected in the brain and the spinal cord of all animals with neurological disorders which appeared after the BTH inoculation as well as in 60 per cent of guinea pigs with EAE, induced by BPF. The CNS lesions were predominant in the spinal cord in 31 per cent and in the brain in 9 per cent of the affected animals sensitized with BPF. Demyelination and cellular inflammatory infiltration in the CNS of animals inoculated with BPF were considerably less pronounced than after the BTH inoculation (Fig. 3a, b). Therefore, on the black and white photo the myelin breakdown products are hardly discernible in the foci of early demyelination being masked by granulocyte nuclei fragments (Figs 3b, 1b). After the BTH inoculation the demyelination foci became so extensive that they could be seen when using low magnification (Fig. 3c). The myelin breakdown products in such animals were found not only along the periphery of the white matter of the spinal cord (as in EAE induced by BPF) but also in its depth and even among the nerve cells of the grey matter (Fig. 3d).

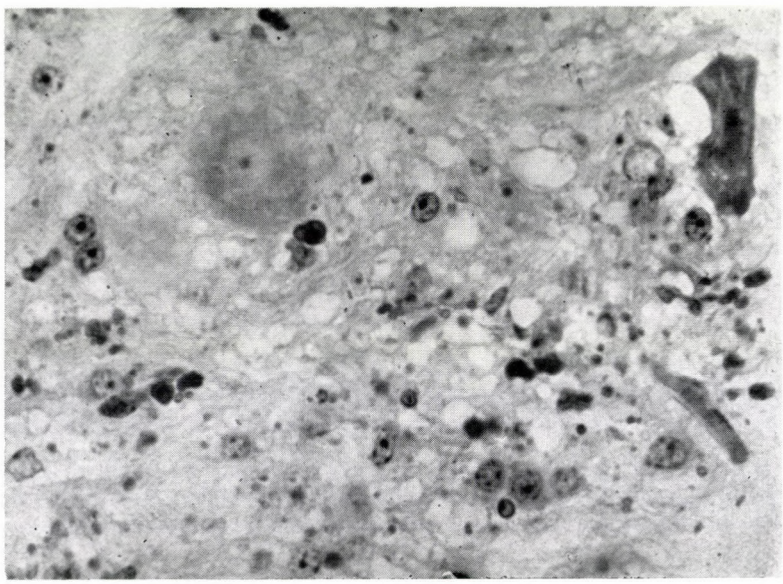

a

Fig. 3. Lumbar segment of spinal cord. White matter (*a*, *b*, *c*). Grey matter (*d*). Marchi's modified method with toluidin blue staining. *a* — widespread cell infiltration and clearly visible myelin breakdown products (arrows). EAE. 11th day after inoculation with BTH. ×90 *b* — moderate cell infiltration. Small and scattered myelin break down products hardly differ from granulocytes nuclear fragments (arrows) in the foci of moderate demyelination. EAE. 11th day after inoculation with BPF. ×120 *c* — extensive demyelination in the peripheral areas. EAE. 17th day after inoculation with BTH. ×22 *d* — myelin breakdown products in the grey matter. EAE. 17th day after inoculation with BTH. ×290

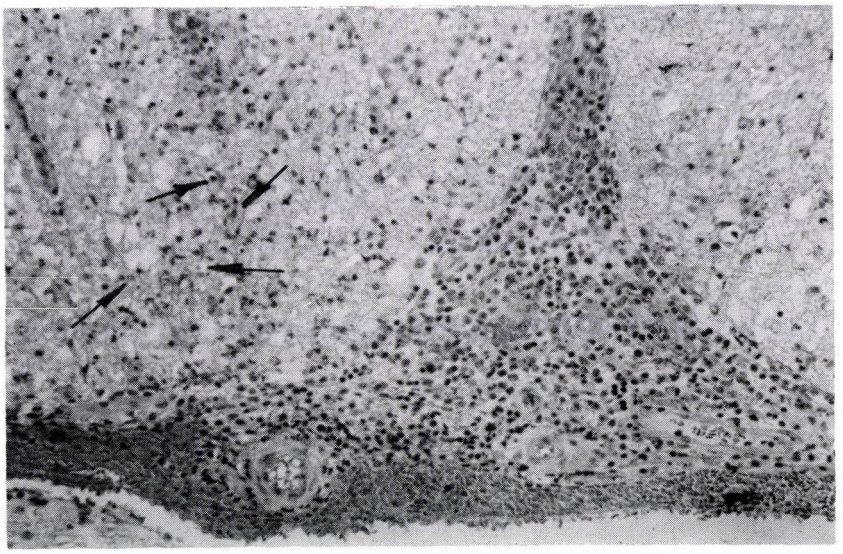

b

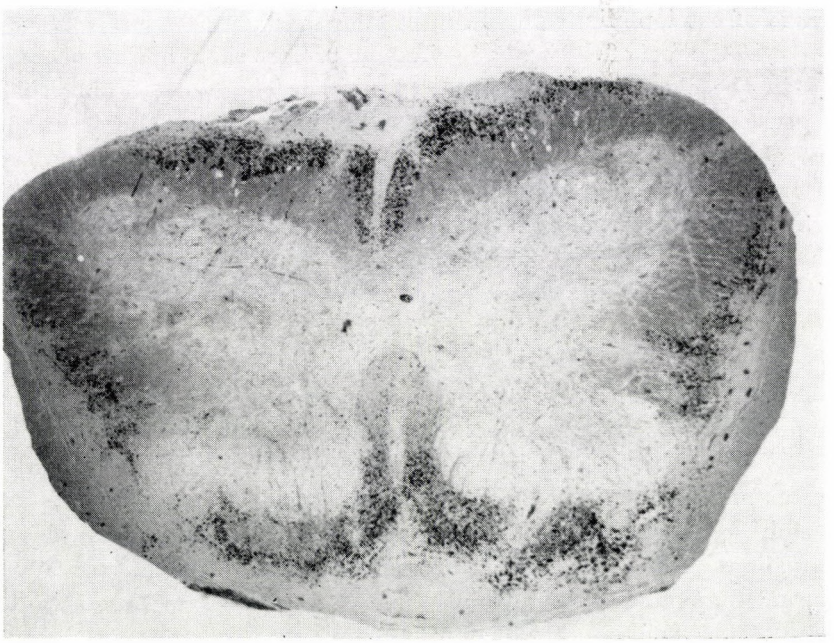

c

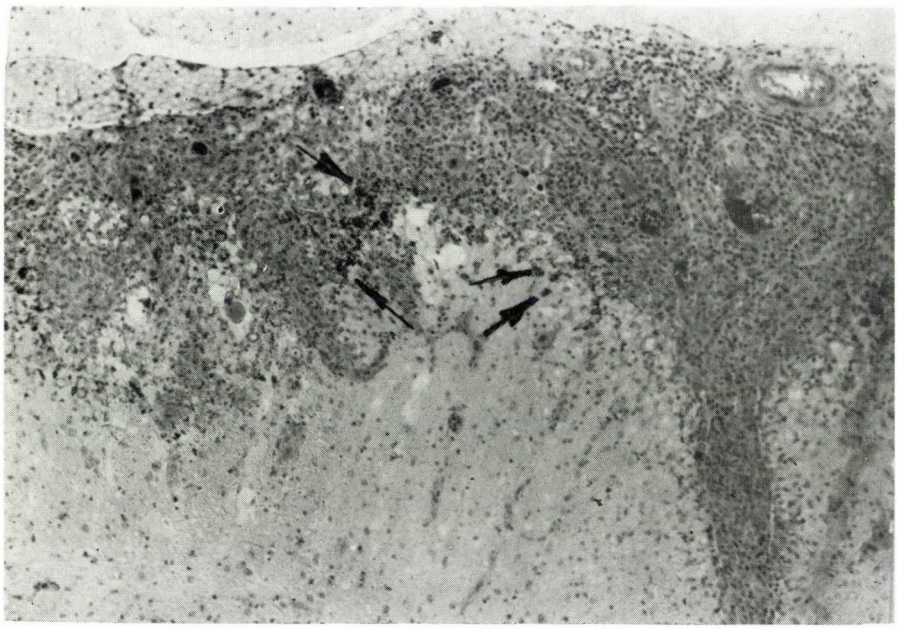

d

Discussion

As demonstrated, a specific feature of the EAE morphological picture is the change of osmiophilia in the desintegrated fragments of the myelin sheaths. Evidently, in the foci of the initial periaxonal process there are not yet essential changes in the chemical composition of myelin. Therefore, during the EAE latent period in the CNS almost exclusively poor osmiophilic granularity is revealed, and at advanced stages of the disease the intesitiy of osmiophilia of the myelin breakdown products increases essentially; this depends on their aggregation and digestion by haematogenic and glial elements. Decreasing affinity of the desintegrated fragments of the myelin sheaths to osmium at far-off stages of clinical recovery, undoubtedly, demonstrates that the processes of the myelin breakdown products digestion with glial cells have come to their end.

Demyelination, not connected with the haematogenic elements, has not been observed. Inflammatory infiltrates consisting of lymphocytes and haematogenic macrophages were the most frequent findings in the pathomorphology of the EAE latent period. In immunological reactions T-killers are known to perform damaging action to the tissue-targets without any assistance of antibodies and the complement, but in cooperation with macrophages [11]. When speaking about the immunological phenomenon of the delayed type hypersensitivity, macrophages and lymphocytes act as a single lympho-macrophageal system [8]. Thus, the data obtained make it possible to suppose that develop-

ment of early stages of the periaxonal process in the CNS can be resulted from cooperative action of lymphocytes and haematogenic macrophages.

Contrary to the data of some authors, who have stated the absence of demyelination in places of accumulation of neutrophilic granulocytes in the CNS [12], our investigation demonstrates that initial stages of the myelin sheath destruction are accompanied with the appearance of neutrophilic granulocytes in these areas. This discrepancy can be caused by insufficiently sensitive staining method with Luxol (the Luxol method) applied by other authors for revealing initial demyelination.

The lymphoid cells are demonstrated in this work to determine mainly in the white matter areas with minimal damage of the myelinated fibers and they are absent in the initial demyelination foci, where predominant elements are macrophages and neutrophilic granulocytes. This observation makes possible to consider in a new way the participation of cells in the infiltrations during the EAE development and suggests that polymorphonulcear neutrophils and macrophages evidently, possess not only phagocytic but also non-specific myelinotoxic activity. Certain dependence between the number of neutrophilic granulocytes and manifestation of periaxonal changes can be considered also as reactions of these haematogenic elements to preformed lesions in the CNS.

The data presented suggest that in the EAE morphodynamics the degree of the osmiophilic changes, size of the myelin breakdown products and cellular composition of the demyelination foci, where certain type of cellular reactions corresponds to each stage of the periaxonal changes (Table I), are the most

Table I

Periaxonal changes and cellular reactions in the EAE dynamics

Periods of EAE	Structure of periaxonal changes	Cell elements in the demyelination zones
Latent	Single, small (0.5—1.5 mcm) slightly osmiophilic fragments of myelin sheaths	Lymphocytes and haematogenic macrophages
	Focal accumulations of small slightly osmiophilic myelin breakdown products	Haematogenic macrophages and neutrophilic granulocytes
Neurological manisfestations	Focal accumulation of fragments of destroyed myelin sheaths varying in size and degree of osmiophilia	Haematogenic macrophages with admixture of astrogliocytes
Convalescence	Accumulation of mainly large (20—50 mcm) and highly osmiophilic granules	Astrocytes and macrophages of microglial origin
Remote time of convalescence	Diffuse accumulation of predominantly slightly osmiophilic, small (5—8 mcm) the myelin breakdown products	Astrocytes with intensively hypertrophied processes

important. Thus, in the dynamics of the EAE development between the demyelination processes and inflammation there exists a close interaction that determines the structure of the demyelination foci at various stages of the disease.

REFERENCES

1. Colover J: A new pattern of spinal cord demyelination in guinea pigs with acute experimental allergic encephalomyelitis mimicking multiple sclerosis. Brit J Exp Pathol 61: 390, 1980
2. Khoruzhaya TA, Bardachachyan EA: Electron microscopic investiagetion of the experimental allergic encephalomyelitis in dogs. Communication II. Peculiarities of ultrastructural alterations in the central nervous tissue depending on severity of the course. Mechanism of allergic demyelination. Cytol Gen 13: 16, 1979 (Russian)
3. Howell G, Kidd M: An electron microscopical comparison of primary and secondary demyelination in the rat central nervous system. Virchows' Archiv Abt B Zellpath 2: 181, 1969
4. Khizhnyak MG: The method of nervous tissue staining on histological sections. Bull Inventions No. 44 (authors certificate No. 1273769) 1986
5. Mayansky AN, Mayansky DN: Essays on Neutrophil and Macrophage. Nauka, Novosibirsk, 1983 (Russian)
6. Mayansky AN, Galiulin AN: Neutrophil Reactivity. University Press, Kazan, 1984 (Russian)
7. Moore C, Traugott U, Farog M, Norton W, Raine C: Experimental autoimmune encephalomyelitis. Augmentation of demyelination by different myelin lipids. Lab Invest 51: 416, 1984
8. Pigarevsky VE: Polymorphonuclear leucocyte and macrophage in inflammatory and hypersensitivity reactions. Arch Pathol 45: 14, 1983 (Russian)
9. Raine C, Traugott U, Farog M, Bornstain M, Norton W: Augmentation of immuno-mediated demyelination by lipid haptens. Lab Invest 45: 174, 1981
10. Raine C, Traugott U: The pathogenesis and therapy of multiple sclerosis is based upon the requirement of a combination of myelin antigens for autoimmune demyelination. J Neuroimmunol 2: 83, 1982
11. Serov VV: Inflammation and immunity, hypersensitivity. Arch Pathol, 45: 3, 1983 (Russian)
12. Vacenic J, Grcevic M, Vitale B: Correlative study of immunological and pathological events involved in experimental allergic encephalomyelitis. Period Biologorum 79: 91, 1977
13. Zhabotinsky Yu M, Ioffe VI: Experimental Allergic Demyelinating Diseases of the Nervous tissue. Meditsina, Leningrad, 1975 (Russian)
14. Zhitnukhin Yu L, Pleskov VM: Isolation and analysis of encephalitogenic fractions of the spinal cord proteins. Problems Med Chem. 1: 57, 1978 (Russian)

Acta Morphologica Hungarica, 36 (3—4), pp. 167—175 (1988)

ULTRASTEREOLOGIC STUDIES ON THE MYOCARDIAL MITOCHONDRIA IN EXPERIMENTAL HYPOTHYROIDISM

P. Błoch, A. Kulig

DEPARTMENT OF PATHOMORPHOLOGY INSTITUTE OF DIAGNOSTICS, MILITARY MEDICAL ACADEMY, ŁÓDŹ, POLAND

(Received 19 November 1987)

Ultrastereologic studies were performed on myocardial mitochondria in experimental hypothyroidism induced by the excision of the thyroid gland. Studies were carried out using accepted methods in stereology according to Weibel et al. [15].

Mitochondrial membrane surface areas and relative volumes of individual membranes and compartments were calculated by means of Weibel's grid and square grid.

Quantitative studies disclosed that in hypothyrotic animals mitochondrial matrix volume increased, while mitochondrial external compartment volume was reduced, which reflected lowered energy production by mitochondria and its transfer to other subcellular structures of myocardial fibers.

The studies allowed to evaluate energy state of mitochondria and enabled to examine the course bioenergetic disturbances within myocardial fibers, the effect of which was progressive heart hypodynamism and failure.

Keywords: Hypothyroidism, myocardium, ultrastereologic analysis of mitochondria

Introduction

A series of experimental studies [1, 2, 3] on chronic hypothyroidism induced by surgical excision of the thyroid gland enabled to evaluate dynamics of morphological changes in the myocardium. They were expressed as small scars and areas of congelative necrosis. Their cause was ascribed to impaired vascular perfusion associated with developing atherosclerosis, which, consequently, led to myocardial hypodynamism. Simultaneously performed electrocardiographic investigations confirmed diffuse damage to the myocardium, but they did not explain the reason for hypodynamism.

A new insight was provided by electron microscopic studies [2]. It was found that in the development of damage to the myocardium in the course of hypothyroidism an important part is played by disturbances in energetic processes reflected by mitochondrial alterations. Results of this studies prompted us to analyze further mitochondrial bioenergetics of the myocardium, the more so as the explanation of morphologic basis of myocardial alterations in the course of hypothyroidism has not been attempted as yet.

Send offprints requests to: P. Błoch, M. D. Dept. of Pathomorphology Inst. of Diagnostic, Military Acad. 90—549 Łodż, Zeromskiego Str. 113 Poland

Materials and methods

The studies were performed on 4 rats subjected to surgical excision of the thyroid gland (group E). Detailed description of the procedure was presented in our previous paper [2]. The control group consisted of 7 Sham-operated rats (group C).

The animals were operated by thoracotomy under ether anaesthesia. The heart was taken for investigations following 32 weeks of the experiment.

After thoracotomy a needle was introduced inside the left ventricle and the heart was perfused with approximately 100 ml of 5% glutaraldehyde in cacodylate buffer. Myocardial samples were taken from identical 4 points of the left ventricle. Samples were additionally fixed in the perfusion solution for 3 h. Then, they were washed in 0.13 M cacodylate buffer for 14 h, and post-fixed in 1% osmium tetrocxide for 2 h at 4°C. The material was then embedded in Araldite and cut with an LKB III ultramicrotome. Semithin sections were stained with 1% toluidine blue. Ultrathin sections were contrasted with uranyl acetate and lead citrate. The examinations were performed using a Philips EM 300 electron microscope.

Stereologic analysis of myocardial mitochondria was performed according to Weibel et al. [7, 13, 14, 15]. Ultrathin sections were photographed in constant initial magnification of $\times 27\,000$ taking 6—8 electronograms from each block [4,5]. To minimalize underestimation of parameters concerning mitochondrial internal membrane, a special method of selection was applied, as described previously [11, 13], therefore, only those mitochondria were photographed, which had the areas of the transversely cut cristae as large as possible and were free of artifacts (Fig. 1). A total 514 mitochondrial profiles were analyzed from the experimental group and 1.066 ones from the control group. In order to calculate mitochondrial membrane surface area per unit of volume the Weibel's network with 15 test lines ($z = 0.494\mu m$) was placed 17×23 cm electromicrograph with final magnification of $\times 81\,000$. Data for measurements of relative volumes of individual mitochondrial membranes and compartments were obtained from a square network of density of 53.8 points/μm^2. Points falling over mitochondrial profile (P_{mit}), matrix (P_{mat}), internal membrane plus cristae (P_c) and external compartment (P_{ec}) (intermembrane space plus intracristal space) were counted. The following parameters were calculated:

Relative volume of the mitochondrial external membrane (V_{em}):

$$V_{em} = \left(1 - \frac{P_{mat} + P_c + P_{ec}}{P_{mit}}\right) \times 100\%$$

Relative volume of the internal membrane (V_{im}):

$$V_{im} = \frac{P_c}{P_{mit}} \times 100\%$$

Relative volume of the matrix (V_{mat}):

$$V_{mat} = \frac{P_{mat}}{P_{mit}} \times 100\%$$

Relative volume of the external compartment (V_{ec}):

$$V_{ec} = \frac{P_{ec}}{P_{mit}} \times 100\%$$

Surface area of the external membrane per unit of mitochondrial volume (S_{em}):

$$S_{em} = \frac{4\,l_{em}}{z \times l_{mit}}$$

Surface area of the internal membrane per unit of mitochondrial volume (S_{im}):

$$S_{im} = \frac{4\,l_{em} + 8\,l_{im}}{z \times l_{mit}}$$

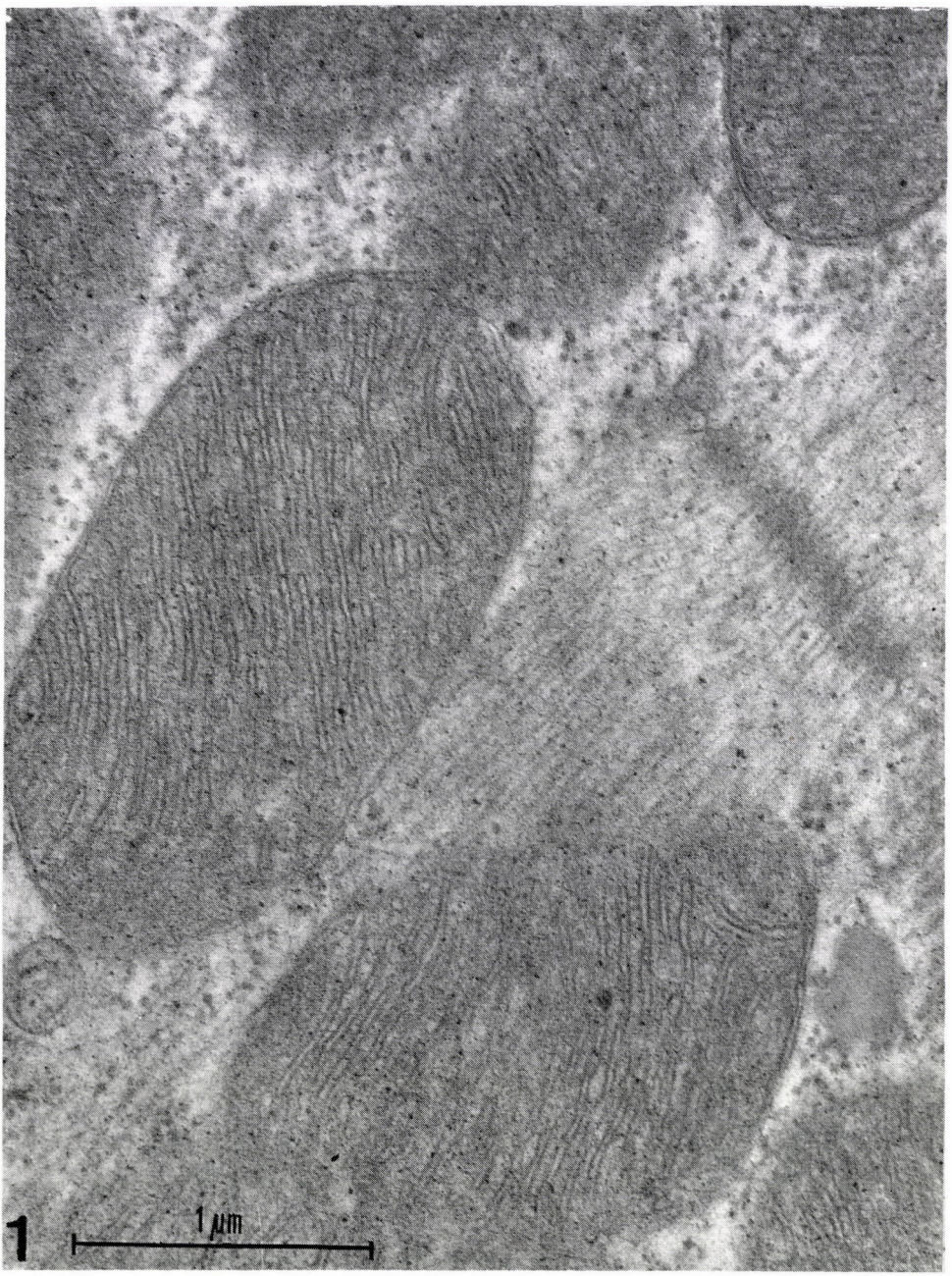

Fig. 1. Representative electron microphotograph of a longitudinal section of mitochondria from a left ventricular myocardial cell. The tissue was obtained from a hypothyroid rat. ×81 000

In order to evaluate interrelationships between compartment volumes and internal membrane surface area, partition coefficients were calculated [5, 12]:

$$E_{mat} = \frac{V_{mat}}{S_{im}}$$

$$E_{ec} = \frac{V_{ec}}{S_{im}}$$

They determine matrix (E_{mat}) or external compartment (E_{ec}) volumes per unit of mitochondrial internal membrane surface area.

All calculations of mean values, standard deviations and standard errors of means were calculated with a special programme for an Odra 1305 computer. Statistical analysis was performed using Kruskal-Wallis rank sum test [6].

Results

External and internal membrane surface areas were found to be significantly decreased in the experimental groups (Table 1, Fig. 2).

Internal membrane to internal membrane surface area ratio was lower in the group E than that in the control group (Table 1, Fig. 3) and the difference was statistically significant.

Relative volume of the external compartment was significantly decreased in hypothyreotic rats in comparison with that in normal rats (Table 1, Fig. 4), while relative volume of the internal compartment significantly increased from 42.8 ± 0.97 in the group C to 67.9 ± 0.75 in the group E (Table 1, Fig. 4).

Relative volume of the internal membrane significantly decreased from 29.0 ± 1.1 in the group C to 11.9 ± 0.43 in the group E (Table 1, Fig. 4), while the difference in the relative volume of the external membrane between both groups was insignificant.

Partition coefficient E_{ec} was decreased in the group E (Table 1, Fig. 5), while it E_{mat} raised in the group E and the rise was significant in relation to that in the group C.

Discussion

Ultrastereologic analysis of myocardial mitochondria performed according to Weibel [14, 15], enabled to evaluate their energy states and bioenergetic disturbances in myocardial fibers in the course of hypothyroidism. Quantitative assessment revealed that at the end of the experiment hypothyrotic animals had increased matrix volume and lowered external compartment volume of their myocardial mitochondria. Changes in mitochondrial compartment volumes are morphological equivalents of disturbed bioenergetics within myocardial fibers, indicating altered ATP biosynthesis. Lowered surface area of the internal membrane, which contains respiratory chain enzymes involved in the oxydative phosphorylation, reflects impaired production of ATP necessary for normal

Table 1

Stereological characteristics of mitochondria

No	Compartment	Parameter	Symbol	Unit of measure	Control ($\bar{x} \pm SD$)	Experimental ($\bar{x} \pm SD$)	P 0.01	P 0.05	P 0.1
1	External membrane surface area per unit of mitochondrial volume	Surface Volume	S_{em} V_{em}	$\mu m^2/\mu m^3$	6.19 $\pm$0.19	4.95 $\pm$0.21	+	+	+
2	Internal membrane surface area per unit of mitochondrial volume	Surface Volume	S_{im} V_{im}	$\mu m^2/\mu m^3$	37.4 $\pm$1.04	25.7 $\pm$0.88	+	+	+
3	Internal to external membrane surface area ratio	Surface	S_{im}/S_{em}	—	6.81 $\pm$0.29	5.84 $\pm$0.44	—	+	+
4	Relative matrix volume	Volume	V_{mat}	%	42.8 $\pm$0.97	67.9 $\pm$0.75	+	+	+
5	External compartment volume relative to intracristal plus intermembrane space volumes	Volume	V_{ec}	%	24.0 $\pm$0.50	15.5 $\pm$0.57	+	+	+
6	Relative volume of internal membrane	Volume	V_{im}	%	29.0 $\pm$1.1	11.9 $\pm$0.43	+	+	+
7	Relative volume of external membrane	Volume	V_{em}	%	4.2 $\pm$0.29	4.7 $\pm$0.28	—	+	+
8	Partition coefficient of external compartment	Partition coefficient	E_{ec}	$\mu m^3/\mu m^2$	0.0070 $\pm$0.0002	0.0066 $\pm$0.0003	—	—	—
9	Partition coefficient of matrix	Partition coefficient	E_{mat}	$\mu m^3/\mu m^2$	0.012 $\pm$0.0004	0.0293 $\pm$0.0012	+	+	+

$\bar{x} \pm SD$ — mean $\pm$ standard deviation of the mean

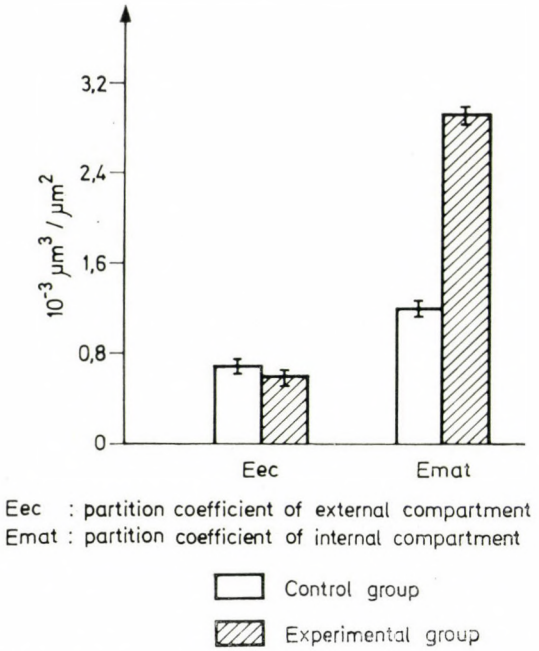

Fig. 2. Mitochondrial membrane surface areas per mitochondrial volume unit

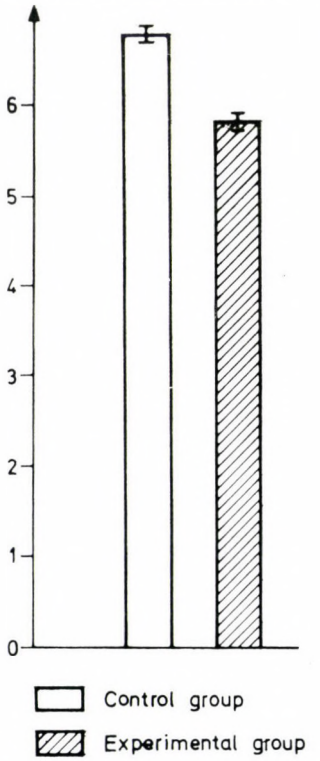

Fig. 3. Internal membrane to external membrane surface area ratio

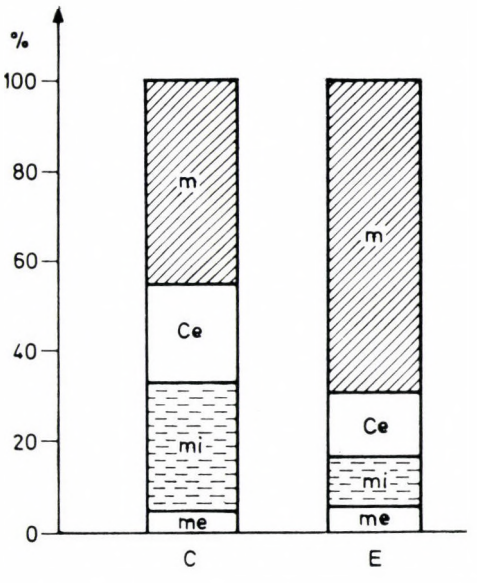

m : matrix
Ce : external compartment
mi : internal membrane
me: external membrane
C : control group
E : experimental group

Fig. 4. Relative volumes of mitochondrial membrane compartments

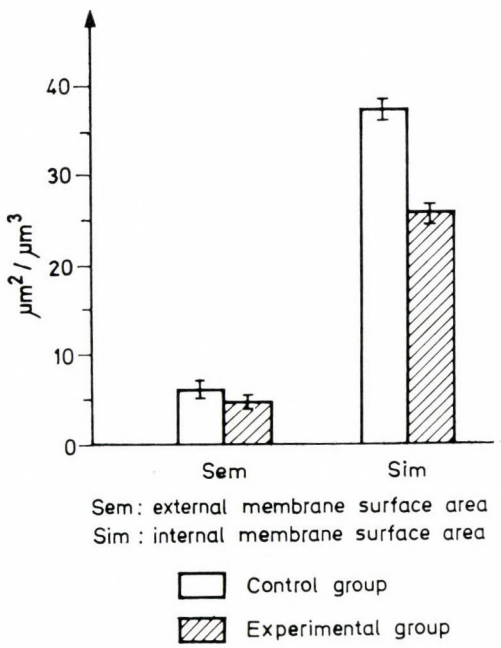

Sem: external membrane surface area
Sim : internal membrane surface area

Control group
Experimental group

Fig. 5. Partition coefficient of external and internal compartments

activity of the myocardium. This observation would explain myocardial hypodynamism with subsequent myocardial failure in the course of hypothyroidism. In turn, decreased surface area of the external compartment, normaly rich with adenylate kinase and diphosphonucleoside kinase [8, 16, 17], proves impairment of its role as a mediator in the transfer of already decreased high-energy phosphate compounds from the mitochondrium to other structures of the myocardial fibers. McCallister and Page [10], using another experimental model, described a rise in the partition of mitochondrial fraction in the fiber volume in response to thyroxine administration to rats with excised thyroid gland, which is an evidence for more dense packing of the cristae probably at the cost of the mitochondrial matrix. The latter suggestion is in agreement with our result indicating a rise in the matrix volume in animals with experimental hypothyroidism.

Direct contribution of thyroid hormones to the regulation of oxydation and energy production within mitochondria was confirmed by the detection of specific receptors on the mitochondrial internal membrane [9]. It is supposed that binding of the thyroid hormones to the receptors induces alterations in the spatial arrangement of macromolecules forming internal part of the mitochondrial membrane. Lehninger [8], who investigated electrophoretic pattern of mitochondrial proteins, found a protein of molecular weight of 54 000 within mitochondria obtained from tissues of normal rats and of rats with excised thyroid gland, receiving triiodothyronine, while this protein was lacking in the mitochondria in rats with excised thyroid gland and not receiving triiodothyronine.

Impairment of high-energy compound production affects myocardial fiber biology, induces metabolic derangements reflected by morphological abnormalities. The earliest changes at the submicroscopic level lead to myocardial dysfunction due to energy deficiency.

Stereologic studies on mitochondria according to Weibel enabled to elucidate mechanisms of energy disturbances in the myocardium in the course of hypothyroidism, which induces reduced energy production and progressive heart failure.

REFERENCES

1. Błoch P: Dynamik morphologischer Veränderungen im Herzen im Verlauf experimenteller Hypothyreose. Dissertation. Militärmed. Akademie. Łódź 1983
2. Błoch P, Kulig A: Die ultrastrukturellen Veränderungen des Myokards bei Ratten mit experimenteller Hypothyreose (im Druck) Zbl. allg. Pathol. pathol. Anat. 131: 337 1986
3. Błoch P, Kulig A: Experimental studies of morphological changes in the heart in the course of hypothyroidism. Pat Pol XXXVII: 131—144, 1986
4. Cieciura L, Rydzyński K, Klitończyk W: Stereologic Studies on mitochondrial configuration in different organs of the rat. Cell Tissue Res 196: 347 1979
5. Cieciura L, Rydzyński K, Klitończyk W, Haraźna J: Stereology of mitochondria in different metabolic states. Acta Med Pol, 18: 291 1977

6. Firkowicz Sz: Statystyczne badanie wyrobów. Wydawnictwo Nauki i Techniki, Warszawa, 1970
7. Kistler A, Waber R: A morphometric analysis of inner membranes related to biochemical characteristics of mitochondria from heart muscle and liver in mice. Exp Cell Res, 91: 326, 1975
8. Lehninger A L: The Mitochondrion. Molecular Basis of Structure and Function. WA, Benjamin, Inc, New York. 1965
9. Lutz W, Jaździewski B, Mirosław W: Wpływ hormonów tarczycy na metabolizm komórkowy. Pol Tyg Lek XXXVI: 687, 1981
10. McCallister LP, Page E: Effects of thyroxin on ultrastructure of rat myocardial cells: A stereological study. J Ultrastruct Res 42: 136, 1973
11. Rydzyński K, Cieciura L: Modification of the configurational states of mitochondria of the choroid plexus ependyma in vivo. J Ultrastruct Res 70: 118, 1980
12. Rydzyński K: Badania nad zmianami konfiguracji mitochondriów wywołanych 2,4-DPN w ependymie splotu naczyniówkowego mózgu szczura. Dissertation. Militärmed. Akademie, Łódź 1978
13. Smith HE, Page E: Morphometry of rat heart mitochondrial subcompartments and membranes application to myocardial cell atrophy after hypophysectomy. J Ultrastruct Res 55: 31, 1976
14. Weibel ER: Principles and methods for the morphometric study of the lung and other organs. Lab Invest 12: 131, 1963
15. Weibel ER, Kistler GS, Scherle WF: Practical stereological methods for morphometric cytology. J Cell Biol 30: 23, 1966
16. Wojtczak L: Transport jonów i metabolitów przez błony mitochondrialne jako czynnik regulujący współzależność metaboliczną miedzy mitochondrium a cytoplazmą. W: Monografie Biochemiczne pod red. Z Kaniugi. Utlenianie Biologiczne Warszawa, 1972
17. Wojtczak L: Enzymatyczna organizacja błon mitochondrialnych. Postepy Biochemii, 17: 209, 1971

Acta Morphologica Hungarica, 36 (3—4), pp. 177—183 (1988)

CYTOCHEMICAL EXAMINATIONS OF Ca, CYTOCHROME OXIDASE AND SUCCINATE DEHYDROGENASE ENZYMES IN ENDOMETRIUM CARCINOMATOUS TISSUE AFTER HIGH DOSE PROGESTOGEN TREATMENT

Z. SZARVAS[1], I. BALOGH[2], K. PATAI[1]

[1]SECOND CLINIC OF OBSTETRICS AND GYNECOLOGY, SEMMELWEIS MEDICAL UNIVERSITY, BUDAPEST, HUNGARY
[2]DEPARTMENT OF FORENSIC MEDICINE, SEMMELWEIS MEDICAL UNIVERSITY, BUDAPEST, HUNGARY

(Received 2 December 1987)

Authors investigated the effect of high dose progestogen in endometrium carcinomatous tissue on the distribution of calcium depots, as well as on the chemically detectable activity of cytochrome oxidase and succinate dehydrogenase. By means of electron microscopy no characteristic destructive effect could unequivocally be demonstrated; cytochemical examinations showed a very significant activity of cytochrome oxidase, and in the activity of succinate dehydrogenase a considerable decrease was observed. They found distributional alterations in plasma membranes, in mitochondria and in the ground cytoplasm. Changes between Ca depots are thought to have an effect on tumour cells also in a protective way, and can be regarded as compensatory phenomena.

Keywords: Endometrium, carcinoma, progestogen therapy, mitochondrial damage

Introduction

In our previous publications we dealt with examinations in the course of which it was observed that in mitochondria of the human endometrium carcinomatous cells, degenerative alterations showing different degrees of severity developed as a result of progestogen treatment [13, 14]. The morphological evaluation of these changes regarded as a damage is rather problematic, as one of the characteristics of mitochondria of carcinomatous cells is the wide morphological variety, and the boundaries between normal and pathological deviations cannot unequivocally be marked out. Histochemical examinations investigating the function of mitochondria in human endometrium carcinomatous tissues are hardly met with in the literature. The increase of intramitochondrial electron-dense structures following mitochondrial impairments due to the progestogen effect described by us, can be regarded as the morphological evidence of the impairment [13].

Send offprint requests to: Dr. Z. Szarvas, 2nd Clinic of Obstetrics and Gynecology, Semmelweis Medical University, 1446 Budapest, P. O. Box 429, Hungary

The aim of our present publication is to prove the mitochondrium impairments following progestogen treatment by means of enzyme-histological examinations.

Materials and methods

Five of our patients suffering from histologically proved endometrium carcinoma were, following diagnosis, given preoperatively high dose progestogen therapy with the drug Depoprovera (medroxiprogesteron-acetate). All our patients belonged histologically to the "highly differentiated" endometrium carcinoma group. Patients were treated for eight weeks with a weekly progestogen dose of 1000 mg. Other types of therapy (cytostatical or Ra-irradiation) were not applied. The control group consisted of some patients in whom the progression was limited to a clinically circumscribed extent, to areas of microscopical magnitude; for this reason also we dispensed with preoperative intracavital radiotherapy, and after histological diagnosis hysterectomy was performed. Following progestogen therapy hysterectomy was performed in the examined patients and the tissue preparations were subjected to electron microscopic enzyme-histochemical examinations. For morphological examinations the specimen was fixed in 2.5% glutaraldehide, for "routine" electron microscopic examinations in 1% ozmiumtetroxide. For histochemical examinations the tissue specimens were incubated for 45 min at room temperature. The following methods were employed: potassium-pyroantimonate *sugar of lead* method was applied to determine calcium cytochemically [3]. The composition of the incubation medium for determining succinate-dehydrogenase was as follows: 0.5 M potassium-sodium-tartrate total quantity 3 l, to which in 0.1 M Strönsen phosphate buffer (pH 7.6), 0.8 ml 1.0 M sodium-succinate, 0.7 ml 0.05 M potassium ferricicyanide were added [4]. For determining cytochromoxidase the unfixed specimen was incubated for 45 min at room temperature. The incubation solution contained 5 mg diaminobenzidin-tetrahydrochloride (DAB), 10 ml 0.05 M, in 10 ml 0.05 M hydrochloric -Tris buffer (pH 7.4) the final pH was 7.3. To the control material 0.01 M end concentration KCN was added according to the method of Seligman et al. [11].

Results

In our untreated control material characteristic structures of adenocarcinoma were observed including membrane alterations [15], well known in mitochondria. Cytochemical examinations revealed intracellular calcium in the membranes, in mitochondria and free cytoplasma (Fig. 11). The precipitate of cytochromoxidase reactions could be observed in the form of precipitate on the surface of the inner membrane (Fig. 1). The precipitate of SDH-enzyme reaction was intramitochondrially localized on the membrane (Fig. 7).

In all our treated patients the alterations were of the same tendency, so they are dealt with together.

1. The cytochromoxidase reaction as compared with the control (Fig. 1). significantly decreased, but localization of the reaction did not change, at the same time its continuity was disrupted on the mitochondrial membranes (Figs 2—6).

2. The SDH reaction in the treated material was also comparable to the control (Fig. 7) as to its localization, but the intensity of reaction significantly decreased (Figs 8—10).

3. Remarkable alterations could be observed in the intracellular distribution of calcium. As compared with the control there were signs of depletion in different calcium pools. The decrease of calcium precipitate from the plasma

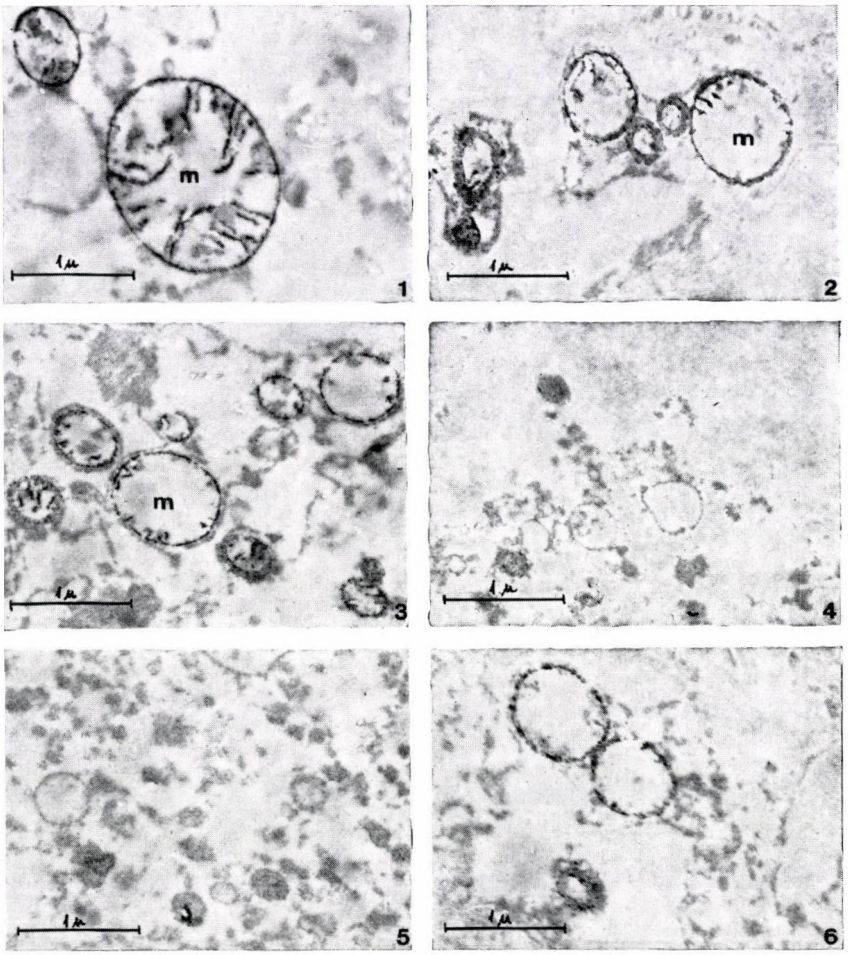

Figs 1—6 Cytochrome oxidase reaction in endometrium carcinoma. *Fig. 1* control, untreated; *Figs 2—6.* treated material; Final magnification ×24 000

membrane and from the cytoplasma was significant, while the precipitate in the mitochondria could be clearly observed, but compared with the control it also showed a decreasing tendency (Figs 12—14).

Discussion

In addition to routine histological and electron microscopic methods, succinated hydrogenase and cytochrome oxidase activities and demonstrable intercellular calcium were investigated. Succinate dehydrogenase and cytochrome oxidase were observed in intramitochondrial localizataion. The diaminobenzidine tetrahydrochloride reaction end-product corresponding to cytochrome oxidase could be observed inside the cristae as well as on the surface of the outer compartment and inner membrane.

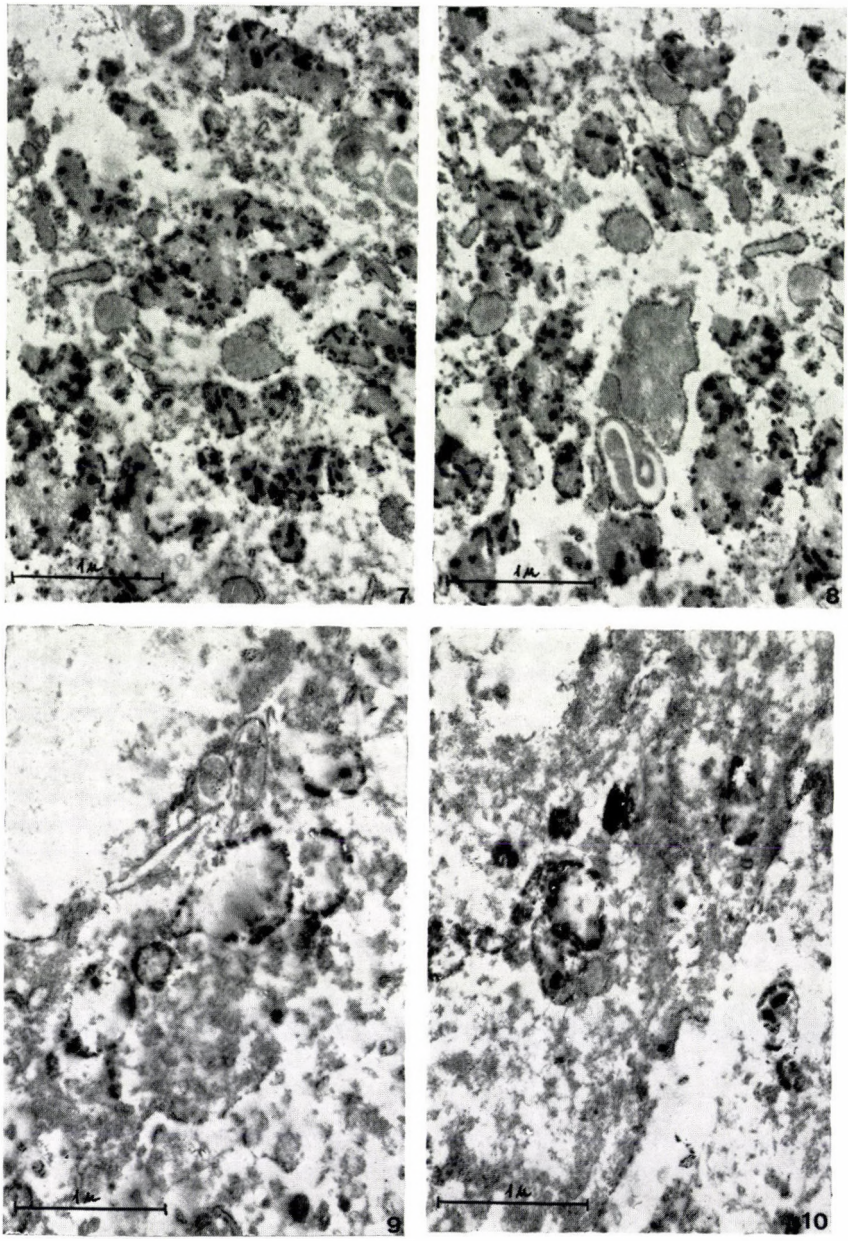

Figs 7—8 Succinate dehydrogenase reaction in endometrium carcinoma. *Fig.* 7 control, untreated; *Figs 8—10.* treated material; Final magnification ×30 000

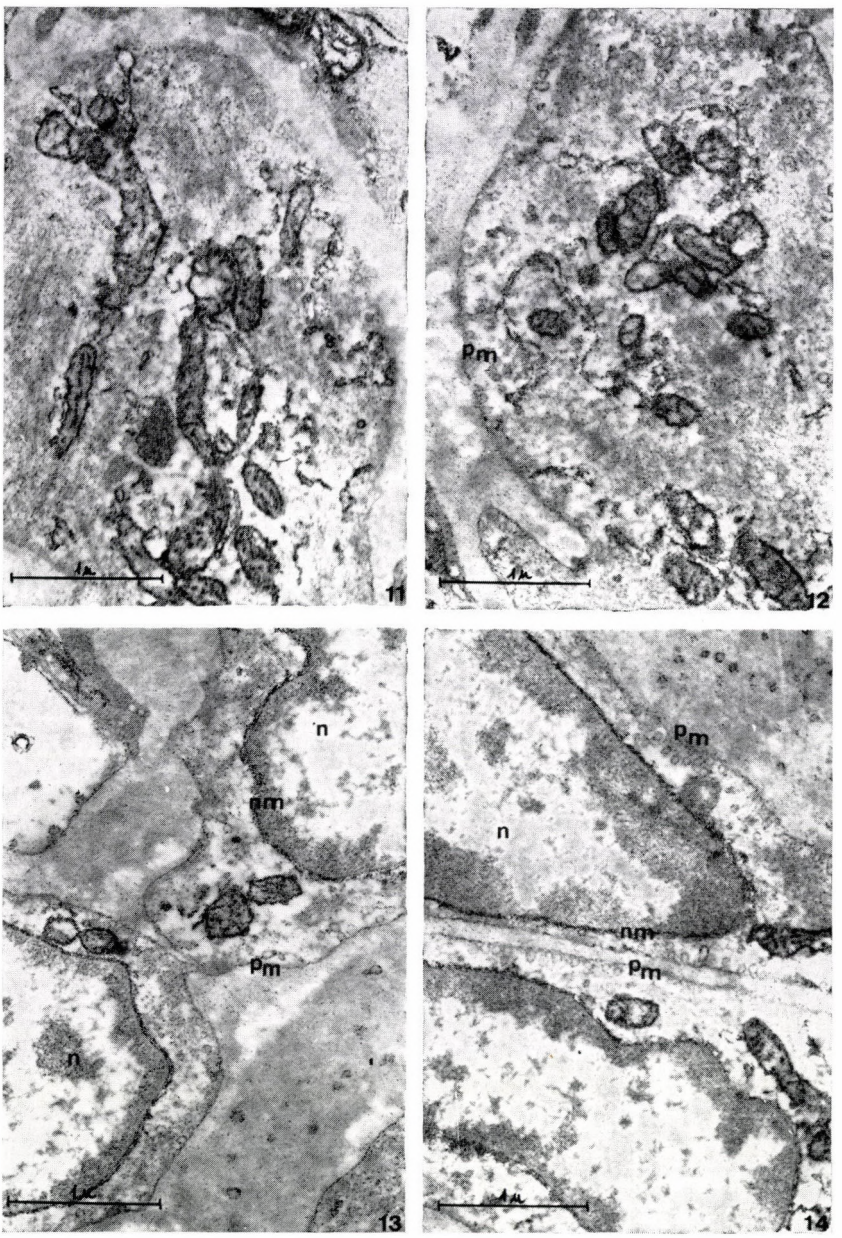

Figs 11—14 Cytochemical detection of calcium. *Fig. 11* control, untreated; *Figs 12—14* treated material; Final magnification ×30 000

This reaction is very sensitive, it responds to the slightest hypoxic, anoxic and toxic impairments and influences by decreasing the activity [2, 5, 7, 8, 11, 12]. In the present case it can be brought into connection with the effect of treatment, if we consider the fact that activity significantly decreases due to influences, or if it cannot be observed but may be supposed that in the tumour tissue, in the respiratory chain of the tumour cell even a definite impairment may develop irreversibly damaging the metabolism of the tumour cell.

Succinate dehydrogenase bound to CoQ by FAD represents another target differing from cytochrome oxidase. The cytochemical reaction of intramitochondrial character, can be seen on the inner surface of the inner membrane. The reaction as opposed to cytochrome oxidase is less sensitive, but it is extremely stable and suitable for comparison. With the help of the reaction anoxic, hypoxic and toxic alterations are detectable, and the compensatory activity increase is also perceptible. In non-necrotic tissues the cytochrome oxidase activity generally decreases upon hypoxic effect, but remains, while succinate dehydrogenase does not change, or it decreases only in a small degree. According to our experience relating to cyanide, carbonmonoxide and other toxic substances cytochrome-oxidase reacts cytochemically on toxic effects much quicker and with a total loss of activity. In some cases, however, an activity increase in the early compensatory phase may be supposed.

For the morphological examination of intracellular calcium depots we applied as a routine the parallel examination of potassium pyroantimonate, sugar of lead and oxalate reactions. According to our experience the calcium depots conditionally bound to plasma membranes, endoplasmic reticulum, mitochondria as well as in the ground cytoplasm can be visualized in the skeletal musculature and in the muscle tissue of the heart, uterus and endometrium. The joint employment of reactions and their comparison with the control are suitable for monitoring morphologically the treatment and supplementing the pharmacological examination [9, 10, 11].

The cytochemical precipitate of the intracellularly demonstrable calcium in our material can be observed partly in the cell membrane, partly in the intracellular cell-constituents, mainly in the mitochondria as well as in the so called ground cytoplasm. It is established that in the case of pathological or pathologically increased calcium metabolism an accumulation may develop in the intracellular depots. The drugs influencing calcium metabolism may possess different points of attack. Such agents can be e.g. drugs causing depletion of the plasma membrane, or the decrease of the free cytoplasmatic or mitochondrial quantity of calcium, or counteract accumulation. In our material calcium cytochemical examinations reveal the decrease of reaction precipitate in the plasma membrane as well as in the mitochondria, and the reaction precipitate can similarly decrease also in the free cytoplasm.

This fact shows the effect of the applied treatment on the metabolism of

calcium, it alters the distribution among intracellular calcium depots, which exerts by the depletion of calcium depots of increased activity, a certain protective influence hampering, — in this particular case —, the necrosis of the tumour cell.

In our material progesteron-treated and untreated carcinomatous cases were compared. Since the degree of differentation of the adenocarcinoma was identical, we thought comparison permissible corresponding to control. Though by simple electron microscopic examinations no significant destructive effect damaging tumour could be proved, at the same time — with the help of cytochemical reactions localized to mitochondria — we succeeded in confirming the tumour damaging effect of progestogens being manifested possibly through mitochondria. On the basis of all these it may be supposed that in the structures involved in the metabolism of endometrium carcinoma cells, impairments develop which can be regarded as morphologically irreversible. Progestogens exert, at the same time, an effect on the distribution of intracellular calcium as well as on the NADH and FAD dependent cytochrome oxidase and succinate dehydrogenase enzymes too. The results of our examinations may thus be regarded as an indirect morphological proof of the fact that gestagens have a hampering effect on the growth of endometrium carcinoma.

REFERENCES

1. Balogh I, Sótonyi P, Somogyi E: Effect on the heartmuscle of experimental carbon-monoxide poisoning. Acta Morph Acad Sci Hung 23: 165, 1975
2. Balogh I: Carbon-monoxide poisoned heartmuscle Cand Diss Budapest 1983, 56—58
3. Elzanowsky W, Lewartovski B, Beresewicz A, Wojtczak J: Influence of acethylcholine on intracellular distribution of calcium antimonate in the guinea pig atria. Acta Physiol Pol 27: 235, 1976
4. Kerpel-Fronius S, Hajós F: The use of ferricyanide for the light and electron microscopic demonstration of succinic dehydrogenase activity Histochemie 14: 343, 1968
5. Kerpel-Fronius S, Hajós F: A method for the electron microscopic demonstration of cytochrome oxidase in fresh and formaline-prefixed tissues Histochemie 10: 216, 1967
6. Komnick H: Histochemische Calcium-Localisation in der Skelettmuskulatur des Frosches Histochemie 18: 24, 1969
7. Litwin JA: Effect of stabilizers on diaminobenzidine reactions of mitochondria Histochemistry 44: 349, 1975
8. Ogawa K, Barrnett RJ: Electron cytochemical studies of succinic dehydrogenase and dihydronicotinamide-adenine-dinucleotide diaphorase activities J Ultrastruct Res 12: 488, 1965
9. Roels F: Cytochrome and cytochrome oxidase in diaminobenzidine staining of mitochondria J Histochem Cytochem 22: 442, 1974
10. Rubányi G, Balogh I, Kovács AGB, Somogy E, Sótonyi P: Ultrastructure and localization of calcium in uterine smooth muscle Acta Morph Acad Sci Hung 28: 269, 1980
11. Seligman AM, Karnovsky MJ, Wasserkrug HL, Hanken JS: Non-droplet ultrastructural demonstration of cytochrome oxidase activity with a polymerizing osmiophilic reagent, diamine-benzidine (DAB) J Cell Biol 38: 1, 1968
12. Sótonyi P, Somogyi E, Balogh I, Nemes A: The evaluation of electron microscopic cytochrome oxidase reaction in experimental heartmuscle hypoxia Cell Mol Biol 26: 9, 1980
13. Szarvas Z: Intramitochondrial changes in the adenocarcinoma cells of the human endometrium after progestogen treatment Morph Igazságü Orv Szemle 20: 81, 1980
14. Szarvas Z: Wirkung der Progestogene auf Endometriumkarzinom Zbl Gynekol 101: 1323, 1979
15. Szarvas Z: Peculiar alterations in the structure of mitochondria of glandular cells of adenocarcinoma of the endometrium Morph Igazságü Orv Szemle 15: 177, 1975

Acta Morphologica Hungarica, 36 (3—4), pp. 185—190 (1988)

HISTOLOGICAL EVALUATION OF PULPAL RESPONSES TO FOUR COMPOSITE RESINS IN DOG DENTAL PULPS

J. URBIZO VÉLEZ[1], R. DELGADO FERNANDEZ[1], J. A. RODRIGUEZ PALACIOS[1], JOLÁN BÁNÓCZY[2], IDA NYÁRASDY[2]

[1]DEPARTMENT OF ORAL PATHOLOGY, FACULTY OF STOMATOLOGY, HIGHER INSTITUTES OF MEDICAL SCIENCES OF HAVANA, HAVANA, CUBA
[2]DEPARTMENT OF CONSERVATIVE DENTISTRY, FACULTY OF DENTISTRY, SEMMELWEIS UNIVERSITY MEDICAL SCHOOL, BUDAPEST, HUNGARY

(Received 5 December 1987)

The pulpal responses to four composite resins — used in dentistry for anterior tooth restorations — were studied in adult dog teeth. The materials were placed in Class V. buccal cavities following the instruction of the manufacturers and their effects were evaluated after 72 h, 30 and 60 days using routine histological methods. The results indicated that a pulpal response was observed only at the 72 h time interval in all the resins investigated, and the index of this response was less than 1 for all of them

Keywords: Composite resins, pulpal response, dog-experiments

Introduction

In the recent years stomatology in general and particularly conservative dentistry has experienced a qualitative jump with the introduction of new filling materials in clinical practice, among them, composite resins. The development of these materials has greatly enhanced the ability of dentists to perform anterior restorations, and numerous clinical studies were carried out, investigating the characteristics of these materials [9, 10, 11].

Composite resins consist of an organic binder with an inorganic and/or organic filler [9]. The first used in dentistry, in the seventies, consisted of an organic binder of the BIS-GMA type with more than 70 weight % inorganic filler. Since the introduction of these first resins, microfilled composite resins have been developed. They consist of a resin system that contains smaller size particles and a lower filler content than conventional composite resins (35 to 50 weight % filler).

The international odontologic literature is rich in publications about the histological reactions to various composite resins [1, 2, 5, 6, 7, 8, 12, 13, 14, 15, 16, 17, 18]. Most of the authors pointed out that these materials caused irritation to the dental pulp and reported different degrees of pulpal damage using different methods of evaluation and different criteria.

Send offprint requests to: Prof. Dr. J. Bánóczy, Department of Conservative Dentistry, Semmelweis Medical University, Budapest, Mikszáth Kálmán tér 5. H-1088, Hungary

The aim of this work was to perform an experimental histological study to determine the effect of various resins on the dental pulp by using a standardized method of evaluation, and to establish a realistic comparison among the results obtained.

Materials and methods

This study investigated the pulpal response to four composite resins: two conventional (Evicrol and Lumicon) and two microfilled composite resins (Isopast, Isomolar). The study was carried out in 12 male dogs weighing of 6 $\pm$ 2 kg, with all their permanent teeth erupted and without caries. After being anaesthetized with sodium pentobarbital (30 mg/kg body weight) each animal received a thorough pretreatment followed by preparation of sixteen Class V cavities on the buccal surface of teeth using a 35 carbide bur in an air-turbine handpiece with air/water spray. The size of each cavity was standardized in the following manner: the cervico-occlusal dimension was 1.5 mm, the mesio-distal width was 3 mm, and the depth was 2/3 the thickness of dentin. For each material three dogs were used. The test materials were prepared following the manufacturer's instructions and using a calcium hydroxide cavity liner (Reocap) for all the resins. Eight cavities were filled with the resin to be evaluated, and of the remaining eight, four were filled with silicate cement without cavity liner (in order to establish the unacceptable extreme of pulpal inflammation due to the filling material) and four with zinc oxyde-eugenol (ZnO-E) serving as neutral controls.

The teeth were surgically removed under anaesthesia in the following three time intervals: 72 h, 30 days and 60 days. They were fixed in 10% neutral formalin, demineralized in 10% formic acid, embedded in paraffin, serially sectioned at 6 μm, and stained with haematoxylin and eosin. The microscopical evaluation was carried out by the same person with an optical microscope. The criteria used were:

A) Reduction in odontoblast population beneath the cavity

0 — No difference as compared to other sites of the pulp
1 — Reduction of less than 10% of the population
2 — Reduction between 10—50% of the population
3 — Reduction of more than 50% of the population

B) Displacement of odontoblast nuclei into dentinal tubules

0 — No displacement
1 — Less than 10% of tubules containing nuclei
2 — Between 10—50% of tubules containing nuclei
3 — More than 50% of tubules containing nuclei

C) Presence of inflammatory cells in the odontoblastic layer per 1 mm length of cavity floor

0 — Under four cells
1 — From 5 to 25 cells
2 — From 26 to 100 cells
3 — More than 100 cells
4 — Abscess formation

D) Presence of inflammatory cells in the rest of the pulp, per 1 mm length of cavity floor

0 — Under four cells
1 — From 5 to 25 cells
3 — From 26 to 100 cells
3 — More than 100 cells
4 — Abscess formation

The index of pulpal response for each material was calculated using the criteria of the B. S. I. Methods of Biological Assessment of Dental Materials [3], and were compa red.

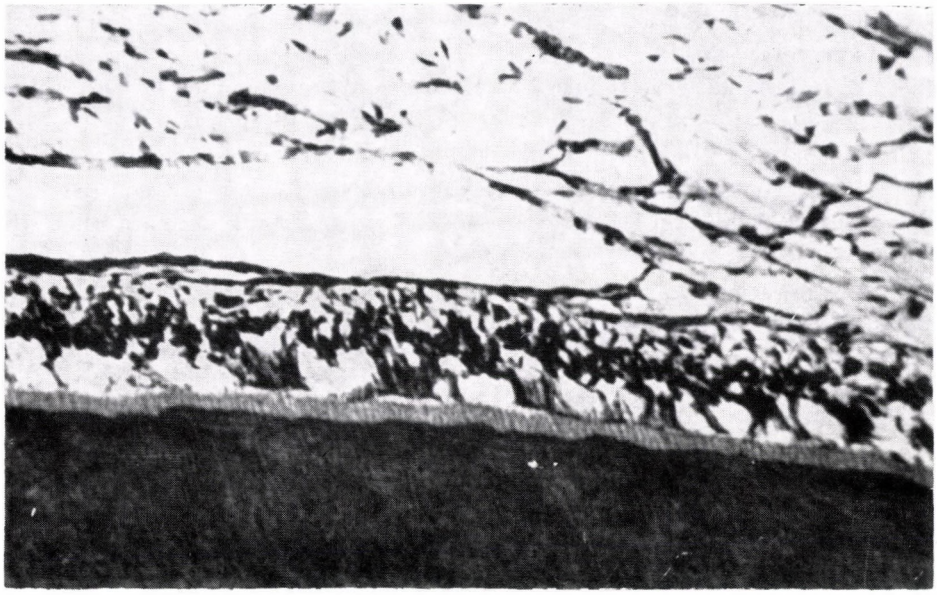

Fig. 1 Photomicrograph showing disruption of the odontoblastic layer, 72 h after filling with Evicrol. ×200 H.E.

Results

72 hours: At this period a pulpal response was observed associated with all the four resins studied, characterized by reduction in the odontoblast population below the cavity due to disruption of this layer and areas of vacuolization (Fig. 1). In all the materials the index was lower than 1 (from 0.35 to 0.90) (Table I). In the controls filled with zinc oxyde-eugenol only a slight reduction was observed in the odontoblast population after 72 h (index 0.10) while in the teeth filled with silicate cement most severe alterations could be observed (0.50 to 2.16) (Table I.).

Table I

Pulpal response index of each composite resin after three different time intervals

Material	72 h				30 days				60 days			
	A	B	C	D	A	B	C	D	A	B	C	D
EVICROL	0.41	0	0	0	0	0	0	0	0	0	0	0
LUMICON	0.35	0	0	0	0	0	0	0	0	0	0	0
ISOPAST	0.90	0	0.54	0.54	0	0	0	0	0	0	0	0
ISOMOLAR	0.41	0	0.29	0.52	0	0	0	0	0	0	0	0
SILICATE	2.16	0.50	1.11	1.60	0.25	0.25	0	0	0.11	0	0	0
ZnO-E	0.10	0	0	0	0	0	0	0	0	0	0	0

Another feature observed was vascular congestion, beïng more prominent with Isomolar (Fig. 2.).

An inflammatory response was observed in pulps under Isopast (index 0.54) and Isomolar (0.29 and 0.52). In most teeth the response consisted mainly of polymorphonuclear leukocytes and was limited to the odontoblastic layer and in some cases to the superficial pulp near the cavity (Fig. 3).

Abscess formation was a feature seen as expected only in teeth filled with silicate cement without cavity liner.

No alterations were observed either 30 or 60 days after restorations with the resins and with zinc oxyde-eugenol, (Table I.) however, they were present in the teeth filled with silicate cement.

Discussion

The results indicate that all the composite resins evaluated produced pulpal response only after 72 h of their application, mainly with reduction in odontoblast population below the cavity. Nevertheless, in all cases the index was acceptable (less than 1) according with the B. S. I. criteria. The highest index was obtained with Isopast. Lumicon was the least irritant material with an index of 0.35 followed by Evicrol with 0.41. We agree with Goto and Jordan [6], Heys [7], Langeland et al. [8], and Tobias et al. [14] in the fact that these materials initially cause irritation, but the pulpal response decreases as the post-operative interva lincreases. On the other hand, Stanley et al. [13] state that organic and macromolecular irritants of the resins may induce their maximum responses after a longer time interval, but we did not observe this in our work.

In the resins studied, no displacement of odontoblasts nuclei into dentinal tubules was observed. We only saw this feature in teeth filled with silicate cement. The results obtained in the control group demonstrated that the injury provocated by cavity preparation was minimal.

The inflammatory response in relation with the odontoblastic layer and the rest of the pulp was evident with Isopast and Isomolar. The highest index was obtained with silicate, accompanied by abscess formation in some sections.

In our study the initial pulpal reactions disappeared and a complete recovery was observed 30 and 60 days after placing the restorations. Heys et al. [7] reported pulpal reactions at the 3-day-time interval and at 5—8 weeks following treatment. This may be explained by the fact that these authors did not use either cavity liners or acid etching that might reduce pulpal inflammation. Brännström and Nordenvall [4] demonstrated that acid etching followed by a bonding agent reduced micro-leakage and the risk of bacterial invasion from

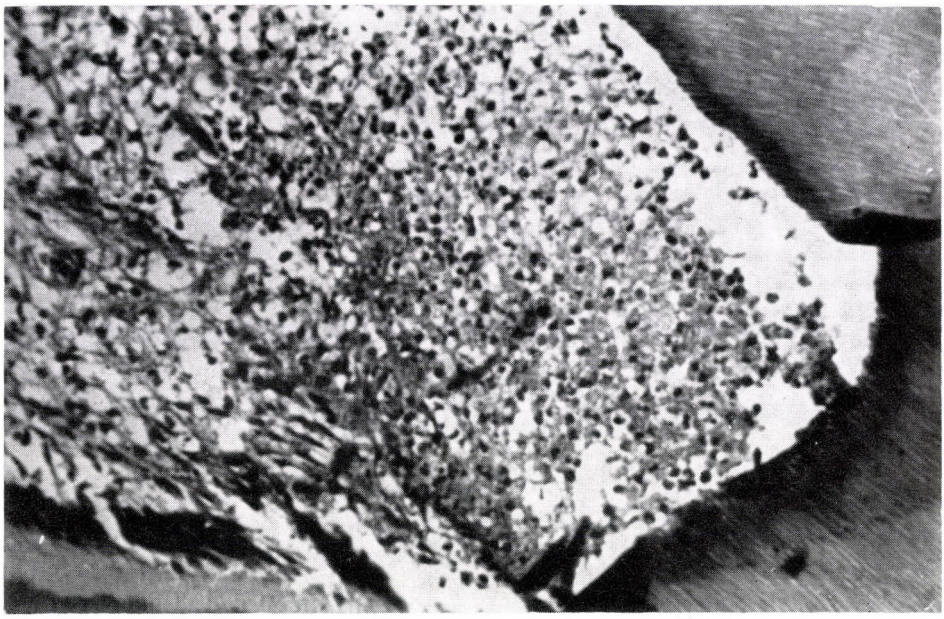

Fig. 2 Histological section of a tooth filled with Isomolar extracted after 72 h of the restoration. Note vascular congestion and areas of haemorrhage. ×200 H.E.

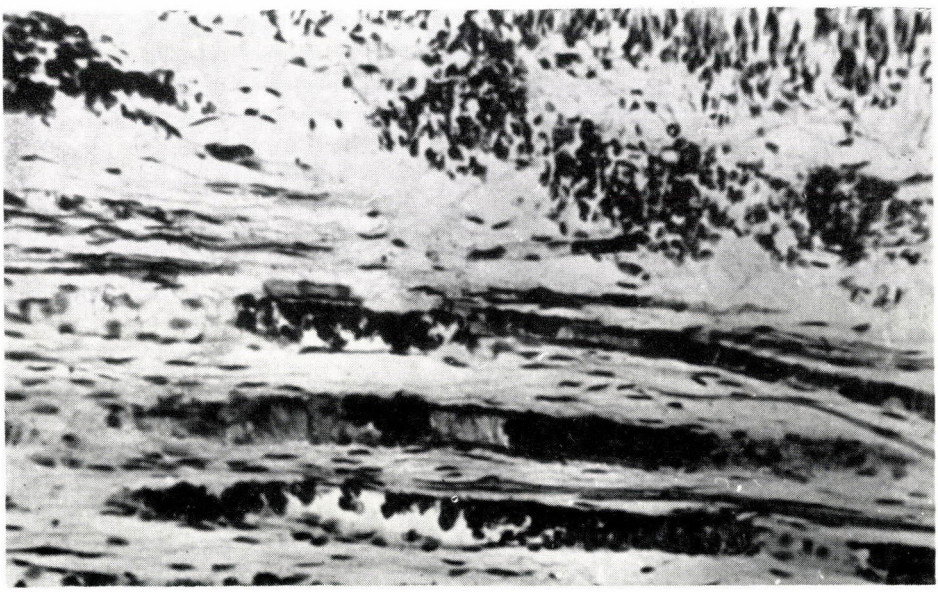

Fig. 3 Severe pulpal damage associated with a silicate cement filling, 72 h after the restoration. Observe the abscess formation with destruction of the odontoblastic layer ×200 H.E.

the surface. Moreover, the use of a cavity liner serves to occlude cut dentinal tubules avoiding the penetration of bacteria and their products. We consider very important to point to the need of using cavity liners under these materials in order to minimize their toxic effects.

Conclusions

1. A reduction in odontoblastic population below the cavity was observed in all the composits resins used.

2. Teeth treated with Isopast and Isomolar showed pulpal inilammation.

3. Pulpal reactions were limited up to 72 h after restorations.

4. The pulpal response index was lower than 1 in all the materials studied.

REFERENCES

1. Adams RJ, Lord GH: Preliminary histopathological study of a new quartz-filled composite dental restorative material. J Dent Res 50: 474, 1971
2. Adams RJ, Lord GH: Histopathological study of a quartz-filled composite dental restorative material. J Dent Res 52: 362, 1975
3. B. S. I.: Methods of biological assessment of dental materials. BS 5828, 1980, 919
4. Brännström M, Nordenvall KJ: Bacterial penetration, pulpal reaction and the inner surface of Concise Enamel Bond. Composite fillings in etched and unetched cavities. J Dent Res 57: 3, 1978
5. Eriksen HM: Pulpal response of monkeys to a composite resin cement. J Dent Res 53: 565, 1974
6. Goto G, Jordan RE: Pulpal response to composite materials. J Prost Dent 28: 601, 1972
7. Heys RJ, Heys DR, Fitzgerald M: Histological evaluation of microfilled and conventional composite resins on monkey dental pulps. Int Endod J 18: 260, 1985
8. Langeland LK, Dowden WE, Tronstad L, Langeland K: Pulp reaction to composite materials. J Dent Res 50: 260, 1971
9. Lutz F, Phillips RW, Roulet JF, Imfeld Th: Komposits-Klassifikation und Wertung. Schweiz Mschr Zahnheilk 93: 914, 1983
10. Nyárasdy I, Fehérváry E: Evicrol és Isopast tömések összehasonlító vizsgálata. Fogorv Szle 79: 374, 1986 (In Hungarian)
11. Nyárasdy I, Herczegh B, Bánóczy J: Klinische Untersuchungen von Komposit (Evicrol) Füllungen. Zahn-, Mund- Kieferheilk. 72: 244, 1984
12. Seelig A, Doyle JK: Comparison of pulpal irritation caused by three filling materials. J Dent Res 53: 193, 1974
13. Stanley HR, Boiven RL, Folio J: Compatibility of various materials with oral tissues. II. Pulp responses to composite ingredients. J Dent Res 58: 1507, 1979
14. Tobias M, Cataldo E, Shierre FR, Clark RE: Pulp reaction to a resin-bonded quartz composite. J Dent Res 52: 1281, 1973
15. Tóth A, Herczegh B, Mária M, Lovasi Zs: A Concise tömőanyag pulpakárosító hatásának vizsgálata kutyán. Fogorv Szle 68: 131, 1975 (In Hungarian)
16. Triadan H: Tierexperimentelle Kurz- und Langzeituntersuchungen der Dentin- und Pulpaverträglichkeit zweier neuen Komposit-Füllungsmaterialien. Schweiz Mschr Zahnheilk 92: 758, 1982
17. Welker VD, Katenkamp D, Neupert G: Bindegewebsreaktionen nach Implantation von Composite-Füllungsmaterial und Silikat-Zement. Dtsch zahnärztl Z. 32: 533, 1977
18. Welker VD, Neupert G, Katenkamp D: Zell- und Gewebereaktionen auf Komposite und weiterentwickelte restaurative Kunststoffe (Isosit) im biologischen Experiment. Zahn-, Mund- Kieferheilkd 68: 659, 1980

Acta Morphologica Hungarica, 36 (3—4), pp. 191—202 (1988)

THE MOSAIC OF COLOUR-SPECIFIC PHOTORECEPTORS IN THE MAMMALIAN RETINA AS DEFINED BY IMMUNOCYTOCHEMISTRY

Á. Szél, P. Röhlich

1st LABORATORY OF ELECTRON MICROSCOPY, 2nd DEPARTMENT OF ANATOMY, HISTOLOGY AND EMBRYOLOGY, SEMMELWEIS UNIVERSITY MEDICAL SCHOOL, BUDAPEST

(Received 28 January 1988)

A monoclonal antibody (OS-2) produced earlier to chicken visual pigments was found to recognize a small fraction of cones in mammalian species. Recently, these cones were shown to be blue-sensitive by the method of selective photic damage. After exposing rabbits to intense blue light, characteristic morphological changes were found in cones stained by OS-2. Another monoclonal antibody (COS-1), in turn, labelled all the intact cones which remained unstained by OS-2. The complementarity of OS-2 positive and COS-1 positive cones was demonstrated in several mammalian species, including monkey and man.

Keywords: Immunocytochemistry, colour vision, mammals, human, retinal cones

Introduction

During the past decades a considerable amount of data has been accumulated on the colour-specificity of retinal photoreceptor cells using microspectrophotometry, electrophysiology and selective degeneration or stimulation by monochromatic light [2, 5—9, 13]. These methods require living, in most cases dark-adapted retinas and sophisticated instrumentation. Recently, we developed a novel approach based on the idea that different visual pigments are responsible to recognize various colours, and the differences in the protein components of the pigments can be detected immunologically. The advantage of this approach is that visual cells can be distinguished from each other by immunocytochemistry using visual pigment-specific antibodies on sections of embedded material. This strategy proved to be successful since we could make distinction between photoreceptor cells of the chicken by antibodies produced to chicken photoreceptor membranes [17]. Subsequently, the antibodies were characterized to be specific to visual pigments [18]. The antibodies could be correlated to colour-specificity of visual cells in the gecko, a retinal system characterized both morphologically and microspectrophotometrically [19]. The question arised whether these antibodies are suitable for distinguishing colour-specific photoreceptor cells also in the mammalian retina in which morphologi-

Send offprint requests to: Dr. Ágoston Szél 2nd Department of Anatomy, Histology and Embryology, Semmelweis University Medical School Budapest, IX. Tűzoltó u. 58. H-1450 Hungary

cal differences between cone cells are hardly or not detectable. Two monoclonal antibodies (mAbs) were found to be especially useful in mammals. One of them, mAb COS-1, labelled a considerable fraction of the cones both in the avian and mammalian retinas, while the other one, mAb OS-2, recognized all photoreceptor cells in the avian retina. In mammals, however, this latter mAb was bound only to about 10% of all cones. This finding made us to assume that mAb OS-2 which behaves in the bird as a universal anti-visual pigment antibody is specific in mammals to a definite visual pigment. It is well known that blue-sensitive cones comprise about 10% of the cones [15, 16], and are arranged in the monkey in a regular pattern [4]. Since we observed the same pattern and frequency of cones stained by mAb OS-2 in the monkey retina, we assumed that OS-2 is specific to the visual pigment of blue-sensitive cones. The specificity of mAb OS-2 to the blue-sensitive cones was proven by two independent ways [20]. As the first approach the method of selective photic damage [15] was chosen. The experiment was carried out on rabbits known for containing blue-sensitive elements in the retina [3, 4]. A small fraction of cones in the retina of animals exposed to intense blue light showed characteristic morphological alterations (vacuolization of inner segments, deformation of the outer segments). Since only these rarely occurring, deformed cones were stained by mAb OS-2, the conclusion was drawn that this antibody is specific to the blue-sensitive cones [20]. Another evidence was furnished by the ground squirrel retina, where mAb OS-2 recognized exclusively the so called B cones. These cones, exhibiting larger inner segments, were proved to be blue-sensitive [1]. In the present study several different mammalian species were tested by this blue-specific antibody, together with mAb COS-1 specific to another cone sub-population.

Materials and methods

1. Animals, preparative steps

Ground squirrels (Citellus citellus). The animals, kept under normal laboratory conditions, were killed by air embolism, the posterior half of the eyes were immersed in ice-cold 0.1 M phosphate-buffered 1% glutaraldehyde fixative (pH 7.2), and the retinas were separated from the underlying pigment epithelium in one minute after death. Following one hour fixation (22 °C) the retinas were cut into small pieces, washed several times in phosphate buffer, followed by incubation in 0.1 M Tris buffer overnight (2% sucrose was added to balance the osmotic pressure). After dehydration in ethanol, the retinal pieces were embedded in Araldite. 0.5—1 μm thick radial and tangential sections were prepared for immunocytochemistry. The sections were cut on a Reichert OMU-2 ultramicrotome. The morphology of the single photoreceptor cells was studied on carefully oriented radial sections. Tangential sections were also presented to demonstrate the organization and distribution of the different photoreceptor cell types.

Bovine and pig retinas. The sources of these animals were the local sloughter-houses. The enucleation followed the death of the animals within 5 min. The eyes were cut into two parts in the equatorial plane. The posterior halves were processed as described before.

The *monkeys (Cercopithecus aethiops)* were immobilized, narcotized intravenously and exsanguinated. The enucleation was carried out about 5 min after death. The fovea was fixed separately.

The retina of a *human* patient (50-year-old woman, suffering in malignant melanoma) was also used. The retina was fixed as described above within 2 min after the operative enucleation. As the fovea was completely destroyed as a result of the tumour, only the peripheral parts of the retina could be processed for immunocytochemistry.

Rabbits, rats, hamsters and guinea pigs were also used in the experiments. Following ether narcosis, the animals were decapitated. The eyes were enucleated within 1 min after death, and the retinas were processed as described above.

The *dog* (used for another physiological experiment) was killed by an overdose of intravenous Nembutal. After enucleation, the eyes were carried to the laboratory in ice cold 0.1 M phosphate buffer. Within 20 min the eyes were cut into two parts and subsequently immersed in the fixative.

2. Immunocytochemistry

Prior to the immunoreaction the embedding resin was removed from the sections by sodium-methoxide [10]. After preincubation in 2% bovine serum albumin, the sections were reacted with the primary antibodies for 1 h at room temperature. The dilutions of the monoclonal antibodies were 1 : 10 000 for all species except for the ground squirrel where 1 : 1000 proved to be more suitable. For comparison, a polyclonal anti-rhodopsin serum was also used diluted 1 : 2000. The production and characterization of the three antibodies was described elsewhere [18]. Shortly: mice were immunized by a photoreceptor membrane suspension derived from the cone-rich chicken retina. When screening the hybridoma cell lines with light microscopic immunocytochemistry, only those clones were selected which specifically stained the photoreceptor outer segments. These cell lines were grown up, cloned repeatedly, and were characterized by immunobiochemical methods. The polyclonal anti-rhodopsin serum was produced in rats by immunizing the animals with the excised opsin bands from electrophoretically separated bovine photoreceptor outer segment proteins. The characterization was carried out by light and electron microscopic immunocytochemistry and by immunoblotting. The bound antibodies were detected by the avidin-biotin system (Vectastain, Vector, Burlingame). The biotynylated second antibodies were followed by the avidin-peroxidase complex. The immunoreaction was revealed by diaminobenzidine.

The immunocytochemistry was controlled by the omission of the primary or the secondary antibodies and by immunoreactions carried out on non-retinal tissues of the same animals.

Results

Using the three anti-visual pigment antibodies (mAb OS-2, COS-1 and anti-rhodopsin) three different photoreceptor cell types could be selectively labelled. The rod cells of all kinds of retinas, as expected, were stained by the polyclonal antirhodopsin serum. None of the cones bound this antibody. On the contrary, the cones were recognized by the two monoclonal antibodies. While OS-2 was specific to a rarely occurring cone type in all animal species, mAb COS-1 labelled the majority of cone photoreceptors (Figs 1 and 2) Consecutive serial tangential sections reacted with the different antibodies were used to decide if there are common elements of the two cone subpopulations, and if there are cones which are not recognized by any of the two cone-specific antibodies. Comparing the identical elements on serial section pairs (Figs 2 and 5) it was clearly observable that each cone was stained by either mAb OS-2 or COS-1, and no one was stained by both of them.

Calculating the ratios of the two cone types, it was evident that in all species the number of the OS-2 positive elements was falling in the range of 5 and 10%.

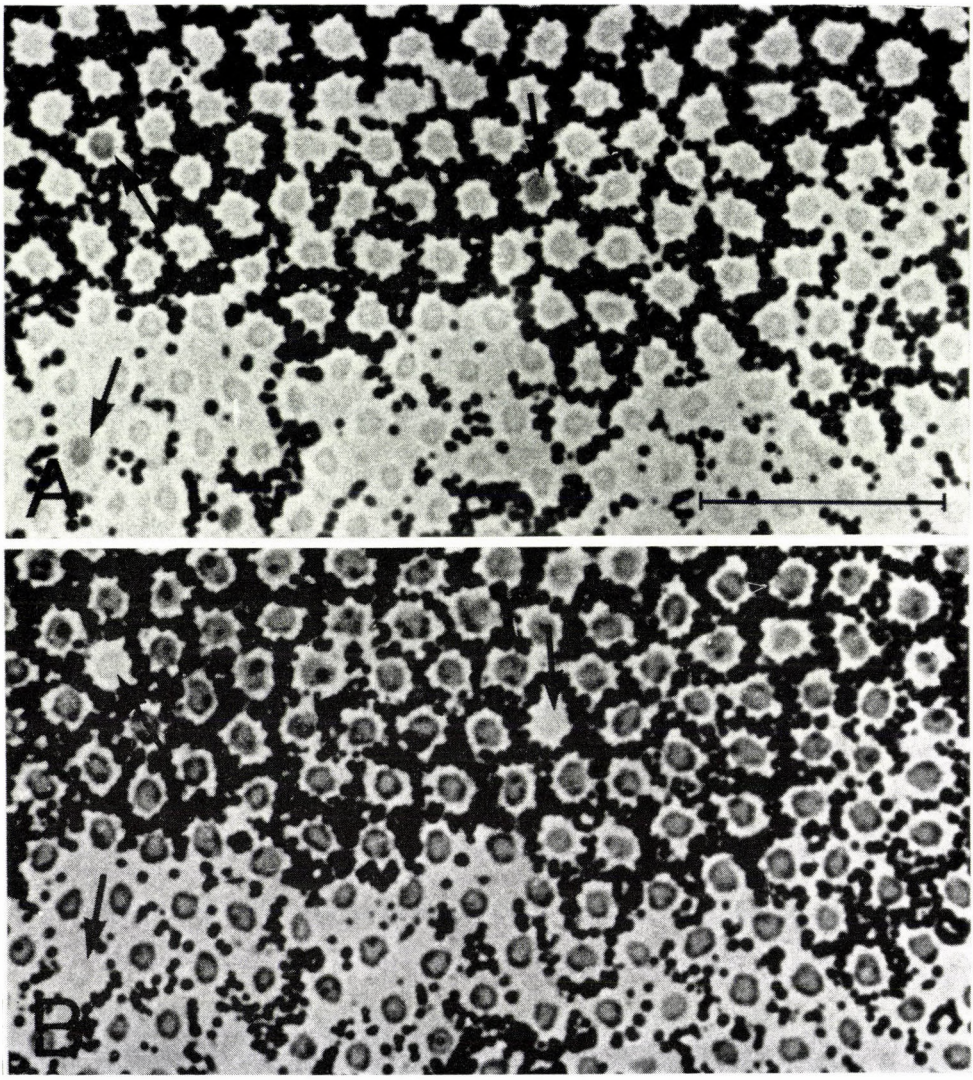

Fig. 1. A pair of adjacent tangential sections of the ground squirrel retina reacted with mAb OS-2 (A) and COS-1 (B) to show the complementarity of the two cone-specific antibodies. The cone outer segments are surrounded by the processes of the retinal pigment epithelial cells stacked with black pigment granules. Note that mAb OS-2 labelled only a few cone outer segments leaving the majority of cones unstained, which, in turn, were recognized by mAb COS-1. Some blue-sensitive cones stained by OS-2, but not by COS-1 are marked on the identical sections by arrows. Bar 10 μm

All three antibodies were absolutely specific to the photoreceptor outer segments. No other parts of the photoreceptors, or other cell types of the retinas were labelled (Figs 1 and 7C). In the controls, where no primary or secondary antibody was used, no staining could be observed.

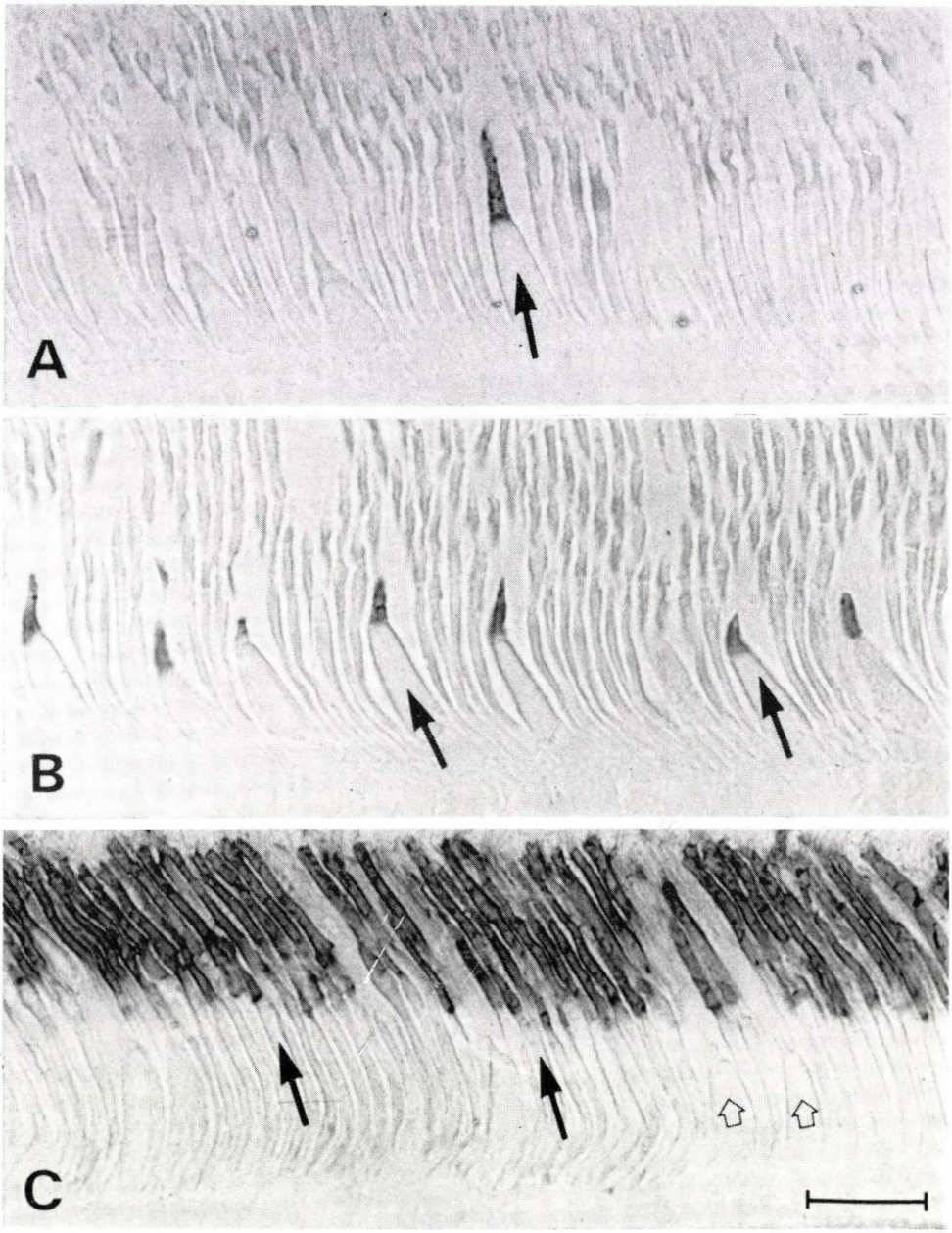

Fig. 2. Radial semithin sections of the bovine retina reacted with mAb OS-2 (A), mAb COS-1 (B) and anti-rhodopsin (C). mAb OS-2 labelled the outer segments of a rarely occurring cone type (filled arrow, A), while the majority of cones were stained by mAb COS-1 (B). Anti-rhodopsin antibody stained all the rod outer segments (filled arrows, C) leaving the cones unstained (open arrows). Note that all three antibodies recognized exclusively the outer segments, while other parts of the photoreceptors together with other retinal cell types remained unstained. Bar 10 μm

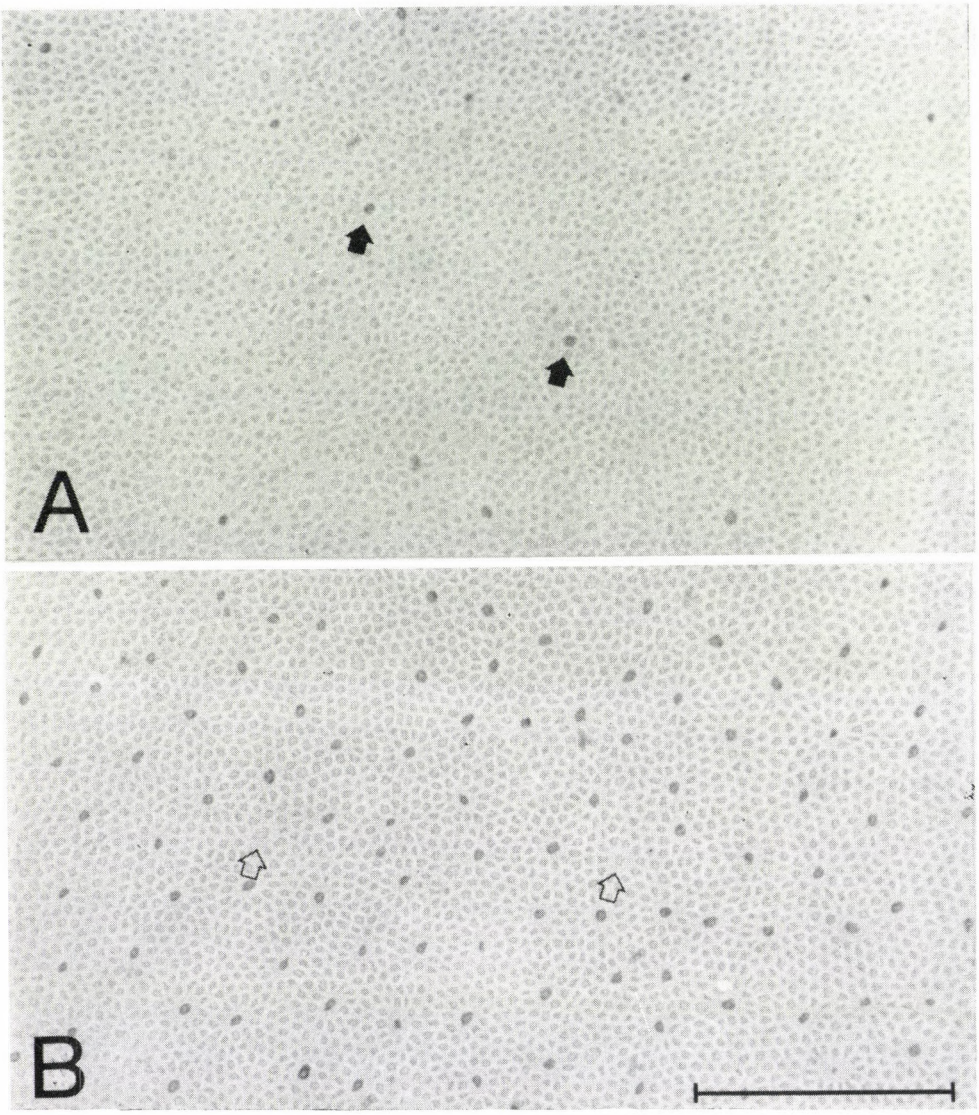

Fig. 3. Tangential sections of the human retina reacted with different cone-specific antibodies. The periphery of the primate retina is abundant in rod cells surrounding the less numerous cone photoreceptors. A rarely occurring cone type recognized by mAb OS-2 (filled arrow, A) is responsible for the blue-sensitivity. The other cones, being sensitive to the middle (green) and long (red) wavelengths are stained by mAb COS-1 (B). Note the negative blue-sensitive cones on B (open arrows). Bar 20 μm

Among the different species the following variations could be observed: Although the bovine (Fig. 1), the rabbit, the dog, the pig (Fig. 7) and the guinea pig (not shown) retinas together with the periphery of the monkey and human retinas (Figs 3 and 4) were similar as regards the ratios of the COS-1 and OS-2

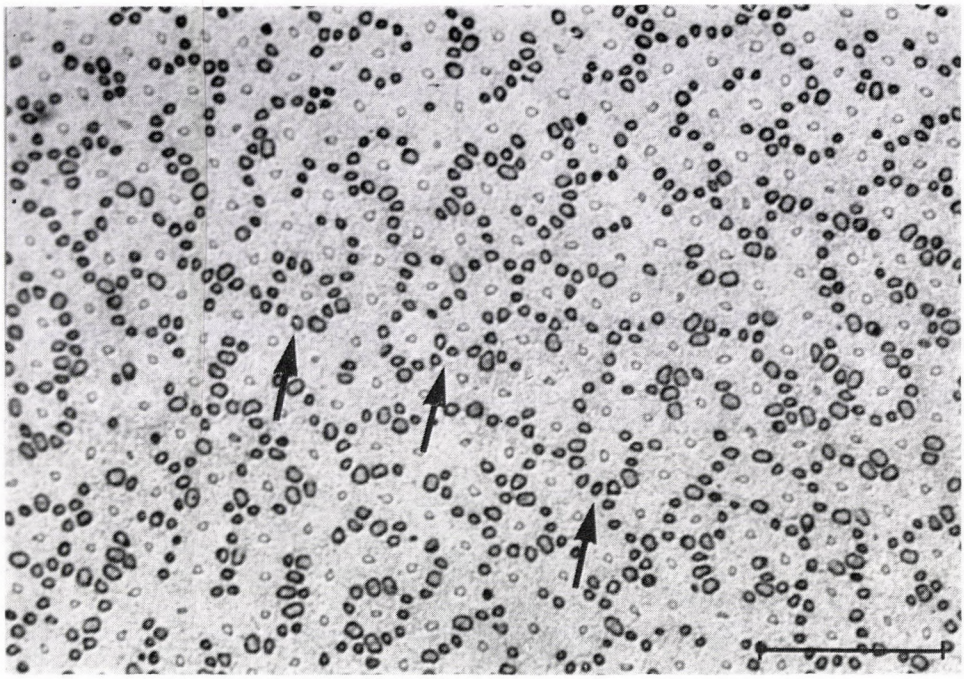

Fig. 4. Tangential section taken from the periphery of the monkey retina not far from the fovea. Note, that the rods (positively stained by anti-rhodopsin) are surrounding the unlabelled cone outer segments in a more or less regular circle. Towards the ora serrata, the retina becomes more and more abundant in rod cells. Bar 20 μm

positive elements, the distribution of the photoreceptor cells was strikingly different between the primate and non-primate retinas. While the primate cones were always surrounded by a more or less regular circle of rods, the organization of the non-primate cones and rods exhibited much less regularity (Fig. 7A and B).

The OS-2 positive cone cells were always distributed rather evenly among the other cones. Neighbouring OS-2 positive elements could be rarely detected in the retinas. In the fovea of the monkey, where no rods could be found at all, the cones were organized in a regular, hexagonal pattern (Fig. 5A and B). Away from the center, this regularity changed due to the appearing rods. Anti-rhodopsin positive rod cells were intermingled between the straight lines of the cones (Fig. 5C).

A unique feature of the hamster (not shown) and the rat retinas (Fig. 6) was the paucity of OS-2 positive cones. On radial sections they could be hardly seen. These elements could be identified in a suitable number only on tangential sections of the rat retinas. This peculiarity can be attributed to the low number of cones in this animal. The ratio of the two cone types was, neverthless, the same as described in the other species.

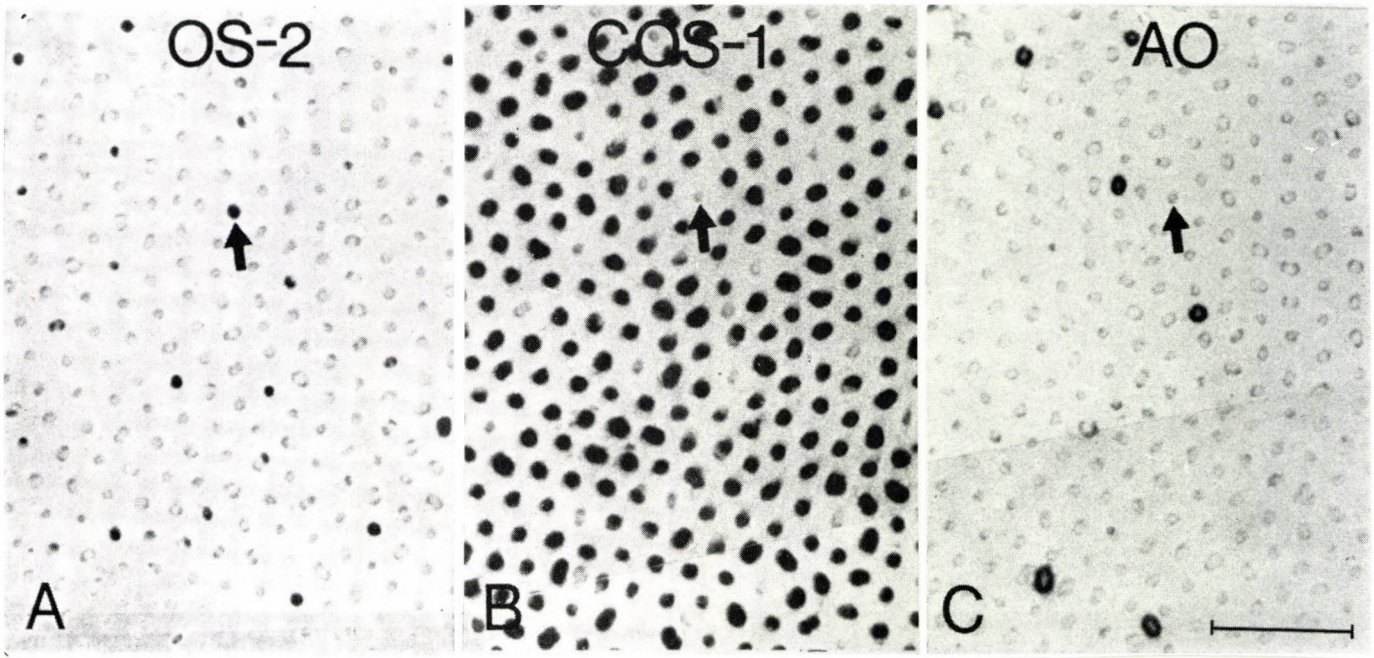

Fig. 5. Consecutive tangential sections of the monkey fovea reacted with mAb OS-2 (A), mAb COS-1 (B) and anti-rhodopsin (C). The foveal cones are organized in a relatively regular hexagonal pattern. Since the specimen is not derived from the very centre of the fovea, some rod outer segments stained by anti-rhodopsin can also be seen among the cones. The arrows show the same blue-sensitive cone outer segments on the three identical sections. Note the complete complementarity of the three antibodies. Bar 10 μm

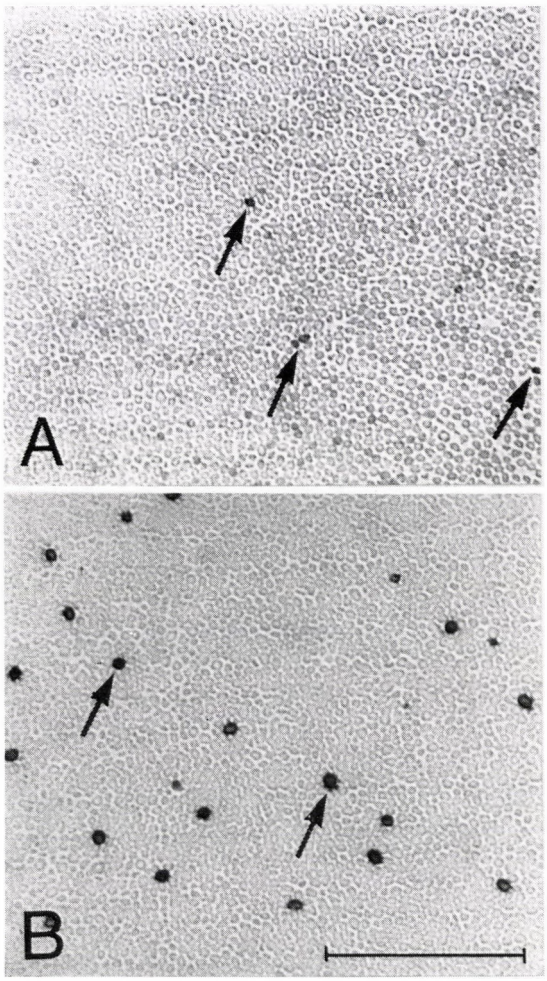

Fig. 6. Tangential sections of the rat retina reacted with mAbs OS-2 and COS-1, resp. Note the relatively small number of blue-sensitive cones (arrows, A). The control section (B) shows the distribution of the middle-to-long wavelength sensitive cone outer segments stained by mAb COS-1 (arrows, B). Bar 20 μm

In contrast to all other species, the gound squirrel retina (Fig. 2) was unique in its abundance of cones. The rods were comprising less than 3% of the total photoreceptor cell number. This animal, which was earlier thought to have a pure-cone retina, contained OS-2 positive cones in the same ratio as the others. 7% of the total cone cell number was stained by OS-2, and the other 93% was labelled by mAb COS-1.

Other species (bovine, dog, pig, guinea pig) were differing from each other exclusively in the shape and size of their photoreceptor cells. The exact description of these differences was beyond the aim of the present paper.

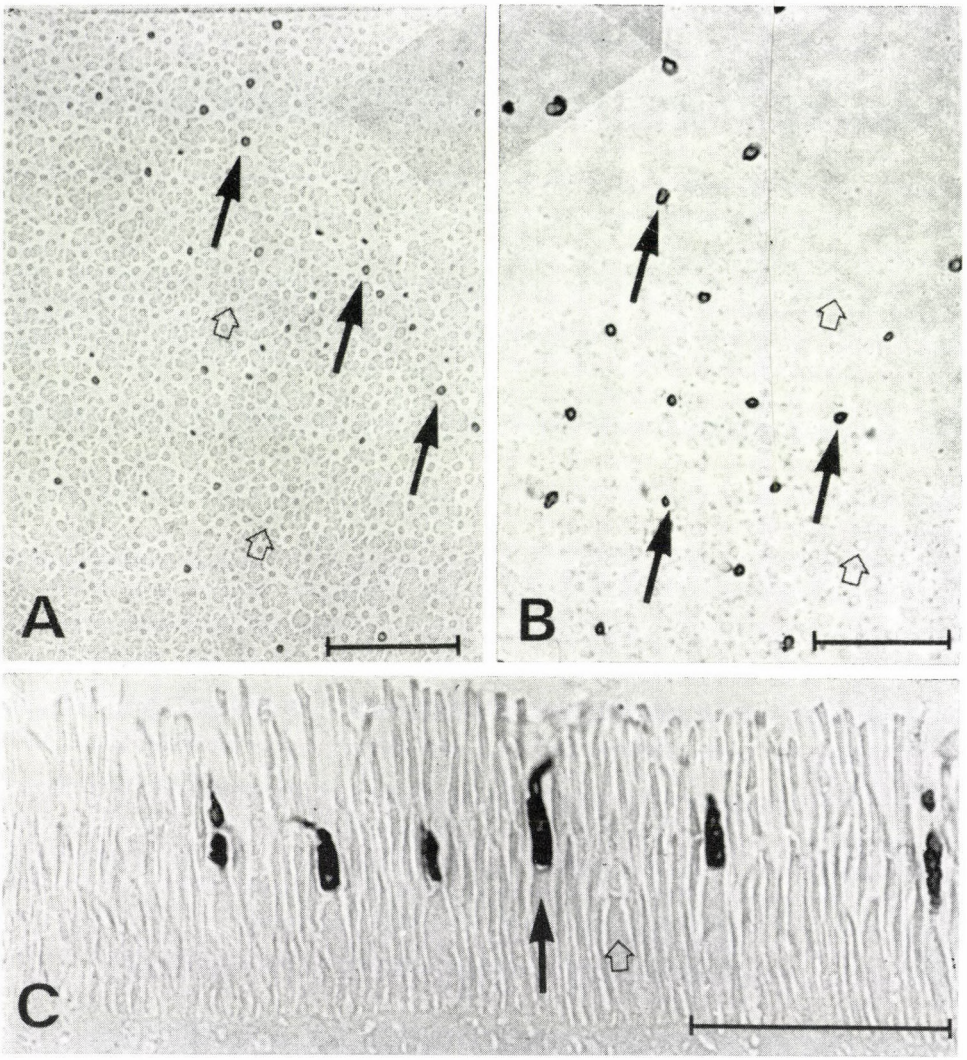

Fig. 7. Distribution of certain cone cell types in the retina of different mammalian species. (A) and (B) are tangential sections of pig and rabbit retinas, resp., reacted with mAb OS-2. Note that the blue sensitive cones stained by the antibody comprise only a minor fraction of the total cone population. The majority of cones are left unlabelled. (C) is a radial section derived from the dog retina reacted with mAb COS-1 showing the middle-to-long wavelength sensitive cones. The stained outer segments are marked with filled arrows, while the open arrows point to the unstained ones. Bar 20 μm

Discussion

Since in our earlier experiments, only those elements of the rabbit retina which were damaged by the intense blue light were recognized by mAb OS-2, the conclusion could be drawn that this antibody is specific for the blue-sensi-

tive cones [20]. Since mAb OS-2 was shown to be specific for visual pigments [18], the antibody obviously recognizes the blue-sensitive cones by binding selectively to the blue-sensitive visual pigment of the rabbit.

From the observations on the rabbit and ground squirrel retina [20], one can clonclude that the OS-2 positive cones of the other mammalian species are also blue-sensitive. This assumption is supported by the fact that the distribution pattern of the monkey blue cones [4] is the same as that of the OS-2 positive cone cells in our monkey retinas. The percentage of the blue cones in several investigated mammalian species [1, 15] is in good agreement with the quantity of the OS-2 positive elements. The molecular similarity of the blue-sensitive pigments derived from different animals is evidenced by our previous immunobiochemical results. Reacting the electrophoretically separated photoreceptor membrane proteins of different mammalian species (rabbit, pig, monkey) with mAb OS-2, one single protein band of molecular mass 36 kD falling in the visual pigment range was stained [20].

A remarkable observation of our immunocytochemical investigations was that our other anti-visual pigment antibody, COS-1, stained all the cones unlabelled by mAb OS-2. This is a convincing evidence for mAb COS-1 being specific to the middle-to-long wavelength (green and red) sensitive cones of the rabbit and the other mammalian retinas. It is not surprising that the blue-sensitive pigment can be distinguished immunologically from the middle-to-long-wave sensitive pigments, since it was shown in man [11] that these pigments exhibit only 43% mutual identity, while the red- and green-sentitive pigments are 96% identical. The 4% difference of the antigenic determinants was not enough to be detected by the monoclonal antibodies.

MAbs OS-2 and COS-1 seem to be complementary antibodies being specific to the short and middle-to-long wavelength sensitive mammalian cone cells, respectively. It seems to be reasonable to use them to detect the distribution of the two main cone types in the mammalian retinas. Taken into consideration that all animal species investigated so far, exhibited two immunologically different cone types,it can be assumed that all of them are possessing the anatomical substrates of the colour vision. Although different colour-specific primate cone cells have been much earlier described [12, 14], the question whether the non-primate animals can discriminate the different colours was debated for decades. In rodents, even the presence of the cone cells was doubtful, and the rats were considered as animals having pure-rod retinas. Our studies with cone specific antibodies furnished evidence that the duplicity theory is valid also in the rat, and at least two different kinds of cones are present in the retina of this animal. Electrophysiological experiments raised the possibility of colour-discrimination in rabbits and cats [3, 4]; the blue- and green-sensitive cones of the ground squirrel were elegantly differentiated by the nitro-blue-tetrazolium histochemical reaction [1].

Using electron microscopic immunocytochemistry distinct morphologic differences could also be established in the future between colour-specific cone cells. Another approach is to detect the morphological basis of the synthesis and intracellular transport of the different visual pigment molecules.

Our observations on the human retina raise the possibility that mAb OS-2 and COS-1 can become useful tools also in ocular pathology. The various forms of colour-blindness could be characterized by these colour-specific antibodies. Intensive investigations are in progress to produce further antibodies to discriminate the red- and green-sensitive visual pigments.

REFERENCES

1. Ahnelt PK: Characterization of the color related receptor mosaic in the ground squirrel retina. Vision Res 25: 1557, 1985
2. Bowmaker JK, Dartnall HJA, Mollon JD: Microspectrophotometric demonstration of four classes of photoreceptor in an old world primate, Macaca fascicularis. J Physiol 298: 111, 1980
3. Caldwell JH, Daw: NW New properties of rabbit retinal ganglion cells. J Physiol 276: 257, 1978
4. De Monasterio FM, Schein SJ, McCrane EP: Staining of blue-sensitive cones of the macaque retina by a fluorescent dye. Science 213: 1278, 1981
5. Govardovskii VI, Zueva LV, Lychakov DV: Microspectrophotometric study of visual pigments in five species of geckos. Vision Res 24: 1421, 1984
6. Hárosi FI: Cynomolgus and rhesus monkey visual pigments. Application of Fourier transform smoothing and statistical techniques to the determination of spectral parameters. J Gen Physiol 89: 717, 1987
7. Kaneko A, Tachibana M: Electrophysiological measurements of the spectral sensitivity of three types of cones in the carp retina. Jap J Physiol 35: 355, 1985
8. Liebman PA: Microspectrophotometry of receptors. In: Dartnall HJA (ed.) Handbook of Sensory Physiology. VII/1. Springer Verl Berlin. 1972
9. Marc R, Sperling HG: Chromatic organization of primate cones. Science 196: 454, 1977
10. Mayor HD, Hampton JC, Rosario B: A simple method for removing the resin from epoxy-embedded tissue. J Biophys Biochem Cytol 6: 909, 1961
11. Nathans J, Thomas D, Hogness DS: Molecular genetics of human color vision: the genes encoding blue, green, and red pigments. Science 232: 193, 1986
12. Nunn BJ, Schnapf JL, Baylor DA: Spectral sensitivity of single cones in the retina of Macaca fascicularis. Nature 309: 264, 1984
13. Ohtsuka T: Spectral sensitivities of seven morphological types of photoreceptors in the retina of the turtle, Geoclemys reevesii. J Comp Neurol 237: 145, 1985
14. Schnapf JL, Kraft TW, Baylor DA: Spectral sensitivity of human cone photoreceptors. Nature 325: 439, 1987
15. Sperling HG, Johnson C, Harwerth RS: Differential spectral photic damage to primate cones. Vision Res 20: 1117, 1980
16. Sperling HG: Spectral sensitivity, intense spectral light studies and the color receptor mosaic of primates. Vision Res 26: 1557, 1986
17. Szél Á, Takács L, Monostori É, Vigh-Teichmann I, Röhlich P: Heterogeneity of chicken photoreceptors as defined by hybridoma supernatants. An immunocytochemical study. Cell Tiss Res 240: 735, 1985
18. Szél Á, Takács L, Monostori É, Diamantstein T, Vigh-Teichmann I, Röhlich P: Monoclonal antibody recognizing cone visual pigment. Exp Eye Res 43: 871, 1986
19. Szél Á, Röhlich P, Govardovskii VI: Immunocytochemical discrimination of visual pigments in the retina of the nocturnal gecko Teratoscincus scincus. Exp Ey Res 43: 895, 1986
20. Szél Á, Diamantstein T, Röhlich P: Identification of the blue-sensitive cones in the mammalian retina by anti-visual pigment antibody. J Comp Neurol, 273: 593, 1988

Acta Morphologica Hungarica, 36 (3—4), pp. 203—213 (1988)

ORGANELLE DISTRIBUTION IN THE WEDGE-, SPINDLE- AND INVERTED WEDGE-SHAPED NEUROEPITHELIAL CELLS DURING CHICK EMBRYO NEURULATION

J. G. Fernandez, C. A. Chamorro, P. Paz, J. M. Villar

DEPT. OF CELLULAR BIOLOGY AND ANATOMY, VETERINARY FACULTY, UNIVERSITY LEON, SPAIN

(Received 2 March 1988)

The formation of the neural tube is a morphogenetic process involving cell-shape changes. The activity of the cytoskeletal elements of the neuroepithelial cells and the interkinetic nuclear migration affect the neuroepithelial cell shape in a way that these cells acquire three distinct conformations of wedge-shaped, spindle-shaped and inverted wedge-shaped cells. Each of them is ultrastructurally characterized in this paper with regard to the intracellular distribution of mitochondria, rough endoplasmic reticulum, yolk droplets, lipid bodies and Golgi apparatus. These distribution patterns are analyzed in relation to the role played by the neuroepithelial cells during the succesive phases of neural tube formation.

Keywords: Organelle distribution, neuroepithelial cells, chick embryo, neurulation

Introduction

Neurulation is a complex phenomenon that produces the early rudiments of the central nervous system. Various mechanisms of neurulation have been proposed [9, 16, 20], but only the changes in neuroepithelial cell shapes have gained widespread acceptance. Thus microtubules and microfilaments act in the chick neuroepithelial cells leading to the "columnarization" and "bottling" of these cells [7].

The columnarization of neuroepithelial cells is accomplished by the microtubules arranged longitudinally within neuroepithelial cells [2, 20]. Treatment with antimicrotubular agents as colchicine prevents neuroepithelial cell elongation [3, 19, 21].

Apical bands of microfilaments are present in the chick neuroepithelium [8, 10, 11, 15] leading to the bottling of neuroepithelial cells. Disruption of microfilaments with cytochalasin B inhibits neural tube formation [13, 22, 25].

During neural tube formation, and additional phenomenon is occurring and affecting neuroepithelial cell shape; i.e., interkinetic nuclear migration [12]. The position of the nucleus during this migration determines whether a particular neuroepithelial cell is wedge-shaped (nucleus at the basal side of the neu-

Send offprint requests to: J. G. Ferenandez, M. D. Dept. of Cellular Biology and Anatomy, Veterinary Faculty, University Leon, 247071 Leon, Spain

roepithelium), inverted wedge-shaped (nucleus at to apical side of the neuroepithelium), or spindle-shaped cells (nucleus neither at the apical nor basal sides of the neuroepithelium), [18].

Neuroepithelial cells show an apico-basal polarity due to the epithelial nature of the neural tube. This remarkable polarity could influence the intracellular arrangement of the cytoplasmic organelles of neuroepithelial cells. On the other hand, interkinetic nuclear migration may be associated with the specific changes in the subcellular distribution patterns showed by neuroepithelial cells [14].

In this paper the existence of organelle distribution patterns for the three cell types of neuroepithelium is investigated, considering certain organelles in these cells: mitochondria, rough endoplasmic reticulum, yolk droplets, lipid bodies and Golgi apparatus. Such ultrastructural characterization might be of interest in relation to the phases of neurulation in which each cell type is involved.

Materials and methods

Processing for transmission electron microscopy

Fertile white Leghorn eggs were incubated to stages 6, 8, 10 and 12 [5] and the midbrain regions of the embryos were collected following the criteria used by Schoenwolf and Franks [18]. The pieces were fixed directly after removal from the yolk with 2% glutaraldehyde buffered with 0.1 M cacodylate (330—360 mOs) at pH 7.4 for 1 h and rinsed in this buffer. Then, they were post-fixed with a buffered osmium tetroxide solution for 3 h and washed in buffer. Dehydration was accomplished using increasing concentrations of ethanol and finally the samples were embedded into Epon 812 resin. Semithin sections were stained with toluidin blue and ultrathin ones mounted on 200-mesh grids and contrasted with uranyl acetate and lead citrate. The grids were examined in a Jeol 100 CX transmission electron microscope operating at 60 kV.

Sampling procedures

In our study sampling problems can be overcome by using only sections cut perpendicularly to neuroepithelium [24]. To obtain a representative sample the method described by Williams [26] was used. Midbrain regions from fifteen embryos of each stage were oriented according to the cephalocaudal axis in the inclusion procedures and eight blocks were selected at each stage by using a digital random table. Three grids were obtained from each selected block and the pool of grids was observed. Thus, ten neuroepithelial cells with nuclear profile were photographed from each grid, following the method reported by Hirakow and Gotoh [6], obtaining finally 240 profiles for each stage. These cellular profiles were classified according to the position of the nucleus [18] in wedge-, spindle- and inverted wedge-shaped cells to analyze separately the organelle distribution. The micrographs were printed at magnifications of 12 000— 22 000 and analyzed for the study of organelle distribution.

Organelle distribution analysis

The analysis of organelle distribution was made in the three neuroepithelial cell shapes (wedge-shaped, spindle- and inverted wedge-shaped) considering three zones within these cells: apical, median and basal, by using the nucleus as reference. Thus two lines passing through apical and basal poles of the nucleus were drawn delimiting these zones (see Fig. 1). At each cellular zone the profiles of mitochondria, rough endoplasmic reticulum, yolk droplets and lipid bodies were quantified, and the obtained values were expressed as percentages of distribution in each zone.

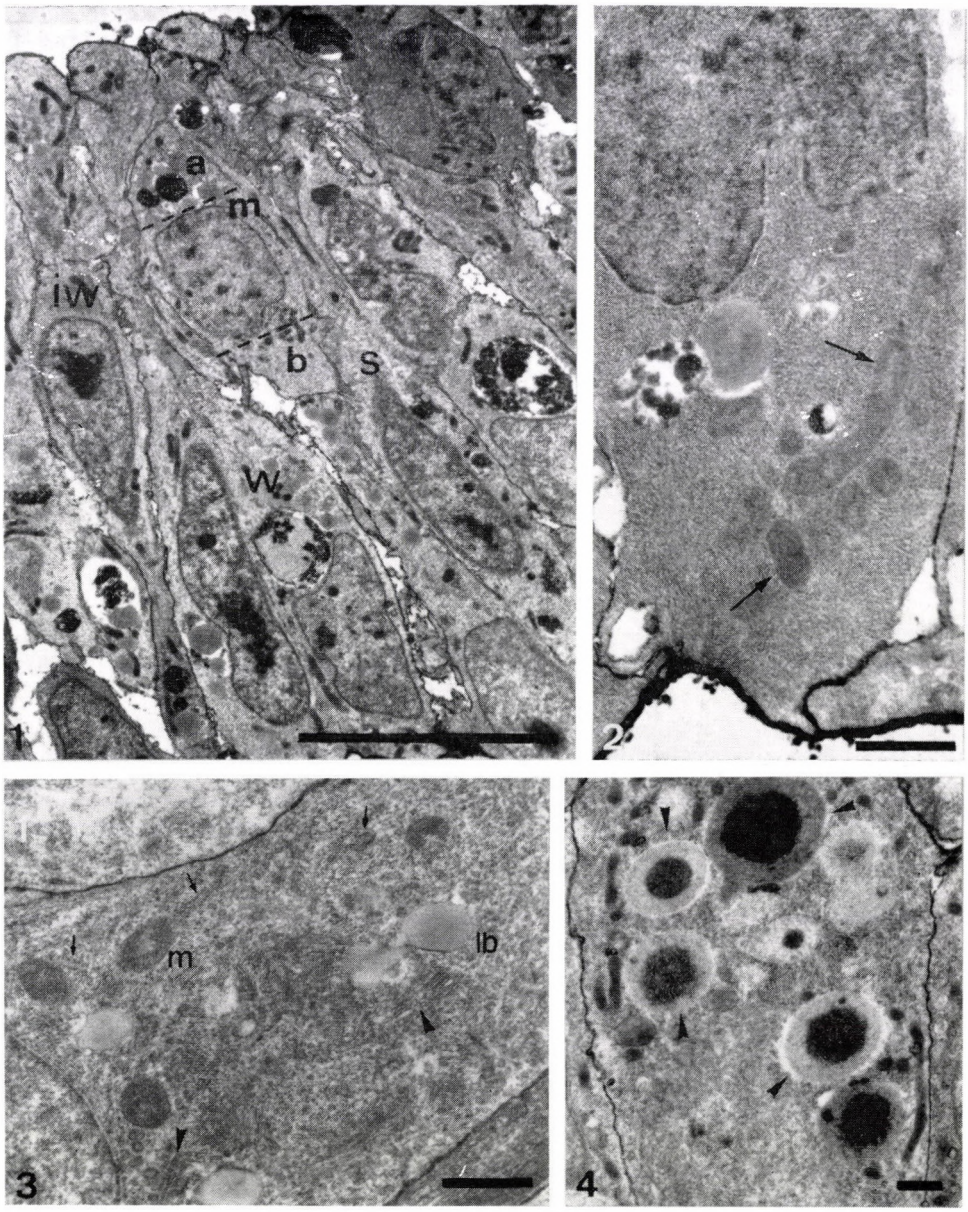

Fig .1. Transmission electron micrograph from the neuroepithelium of stage 10 chick embryos. Three cellular zones are selected for the organelle distribution analysis (a, apical; m median; b, basal). IW: inverted wedge-shaped cells, W: wedge-shaped cells, S: spindle-shaped cells. Bar: 10 μm

Fig. 2. Basal zone of a wedge-shaped cell of stage 8 neuroepithelium in which numerous mitochondria (arrows) could be seen. Bar: 1 μm

Fig. 3. Electron micrograph from the apical zone of a spindle-shaped neuroepithelial cell of stage 10 that presents Golgi elements (arrowheads), rough endoplasmic reticulum cisternae (arrows), mitochondria (m) and lipid bodies (lb). Bar: 1 μm

Fig. 4. Micrograph showing several yolk droplets (arrowheads) in the apical zone of an inverted wedge-shaped neuroepithelial cell from stage 8 embryos. Bar: 1 μm

The Golgi apparatus was analyzed as a whole, considering the cellular zone in which it appeared. Thus the percentages obtained express the cellular proportion representing the Golgi apparatus in each cellular zone (apical, median and basal).

Statistical analysis

The obtained percentages were subjected to the G-independence test [23] based on chi-square distribution by using a level of significance of $P < 0.05$. Thus the percentages of each organelle and cellular zone were compared between the three cell types to find significant differences ($P < 0.05$) between wedge-shaped, spindle-shaped and inverted wedge-shaped cells with regard to their organelle distribution patterns (see Table IV).

Results

Organelle distribution in the wedge-shaped cells (Table I)

Wedge-shaped neuroepithelial cells show their nucleus located at the basal side of neuroepithelium and an apical prolongation extending toward the apical side of neuroepithelium (see Fig. 1). Within these cells the mitochondrial profiles are more abundant in the basal zone (Fig. 2), the percentages in this zone ranging between 40—60%. Rough endoplasmic reticulum cisternae are more numerous within the apical zone of the cell at stages 6, 8 and 10, but at stage 12 the basal zone contains a 50.7% of the rough endoplasmic reticulum cisternae.

Table I

Distribution percentages of mitochondria (m), rough endoplasmic reticulum (rer), yolk droplets (yd), lipid bodies (lb) and Golgi apparatus (ga) in the wedge-shaped cells from chick neuroepithelium at stages 6,8,10 and 12

		6	8	10	12
	B	40.1	50.5	60.4	54.9
m	M	29.9	17.7	22.6	24.1
	A	30.0	31.8	17.0	21.0
	B	27.4	32.0	32.8	50.7
rer	M	30.1	22.3	25.9	22.5
	A	42.5	45.7	41.3	26.8
	B	49.4	22.0	66.7	—
yd	M	21.5	34.1	—	—
	A	29.1	43.9	33.3	100
	B	—	3.9	26.7	—
lb	M	33.3	17.3	13.3	—
	A	66.7	78.8	60.0	100
	B	—	—	—	—
ga	M	—	—	—	—
	A	100	100	100	100

B: basal zone
M: median zone
A: apical zone

Yolk droplets of the wedge-shaped cells are present in the basal zones in higher percentages than in the median and apical zones at stages 6 and 10, though stages 8 and 12 present much more yolk droplets in the apical zone of the cell. In all stages the lipid body distribution within wedge-shaped neuroepithelial cells is preferably apical, as well as the Golgi apparatus of these cells locates always in the apical zone of the cell.

Organelle distribution in the spindle-shaped cells (Table II)

Neuroepithelial cells whose nucleus is located in centrally and taper apically and basally acquire a spindle-shape (see Fig. 1). Mitochondrial distribution in these cells shows similar percentages in the basal and apical zones (30—40%) at stages 6, 8 and 10 whereas at stage 12 in the apical zone there are higher percentages than in the basal and median zones. Except at stage 6, the rough endoplasmic reticulum cisternae distribute more frequently within the apical zone of the spindles-shaped cells. Yolk droplets of the spindle-shaped cells are more abundant in the apical zone at stages 6, 10 and 12 but at stage 8 they are homogeneously distributed into basal and apical zones. A 80—100% of the

Table II

Distribution percentages of mitochondria (m), rough endoplasmic reticulum (rer), yolk droplets (yd), lipid bodies (lb) and Golgi apparatus (ga) in the spindle-shaped cells from chick neuroepithelium at stages 6,8,10 and 12

		6	8	10	12
	B	41.1	39.4	36.5	28.2
m	M	24.4	23.2	29.7	32.1
	A	34.5	37.4	33.8	39.7
	B	43.7	27.5	25.7	22.1
rer	M	15.5	30.8	27.7	34.5
	A	40.8	41.7	46.6	43.4
	B	33.3	50.0	20.0	—
yd	M	16.1	3.3	20.0	40.0
	A	50.6	46.7	60.0	60.0
	B	60.0	5.4	6.1	—
lb	M	20.0	2.7	6.0	—
	A	20.0	91.9	87.9	100
	B	—	—	—	—
ga	M	—	—	—	—
	A	100	100	100	100

B: basal zone
M: median zone
A: apical zone

lipid bodies of the spindle-shaped cells of stages 8, 10 and 12 are located within the apical zone, whilst at stage 6 the basal zone contains a 60% of these inclusions. Finally, all spindle-shaped neuroepithelial cells present their Golgi apparatus located into apical zone (Fig. 3).

Organelle distribution in the inverted wedge-shaped cells (Table III)

Inverted wedge-shaped neuroepithelial cells have their nucleus located in the apical side of neuroepithelium and a cytoplasmic portion extending toward the basal side of neuroepithelium (Fig. 1). Mitochondrial distribution patterns at the four stages studied are very different since the highest mitochondrial proportion is observed in the median zone at stages 6 and 10, in the apical zone at stage 8 and in the basal zone at stage 12. Rough endoplasmic reticulum cisternae show a similar distribution in neuroepithelial inverted wedge-shaped cells of stages 6 and 8 (25% in basal, 31% in mediuan and 43% in apical zone), whereas at stage 10 a 40% of the rough endoplasmic reticulum profiles are in the median zone and at stage 12 there is a homogeneous distribution of these profiles in the three cellular zones. Yolk droplets distribute in similar percentages in

Table III

Distribution percentages of mitochondria (m), rough endoplasmic reticulum (rer), yolk droplets (yd), lipid bodies (lb) and Golgi apparatus (ga) in the inverted wedge-shaped cells from chick neuroepithelium at stages 6, 8, 10 and 12.

		6	8	10	12
	B	24.3	19.4	37.2	39.3
m	M	41.4	27.8	37.2	30.4
	A	34.3	52.8	25.6	30.3
	B	25.0	25.0	23.7	35.6
rer	M	31.3	31.9	39.5	31.1
	A	43.7	43.1	36.8	33.3
	B	39.1	23.1	66.7	—
yd	M	21.7	19.2	—	—
	A	39.2	57.7	33.3	100
	B	—	42.9	33.4	—
lb	M	—	—	33.3	—
	A	100	57.1	33.3	100
	B	—	—	—	—
ga	M	—	—	—	—
	A	100	100	100	100

B: basal zone
M: median zone
A: apical zone

basal and apical zones at stage 6 though at stage 10 a 66.7% of the yolk droplets are in the basal zone of the inverted wedge-shaped cells. These inclusions are more abundant in the apical zone at stages 8 (57.7%), (see Fig. 4) and 12 (100%). A location preferably apical of the lipid bodies is observed in the neuroepithelial cells of stages 6, 8, and 12, but at stage 10 these inclusions are homogeneously distributed in the three cellular zones of the inverted wedge-shaped cells. The Golgi apparatus shows an apical polarity in the inverted wedge-shaped neuroepithelial cells since its location within these cells is always in the apical zone.

Discussion

The morphogenetic events occurring in the embryo induce some structural and functional changes affecting the ultrastructure of the embryonic cells. Changes occur in organelle development and intracellular distribution during morphogenesis [1].

With respect to mitochondrial distribution in the wedge- and spindle-shaped cells one can observe how in the apical zone of the wedge-shaped cells (Table I) the percentage of mitochondria is more elevated at stages 6 and 8, whereas the same zone of the spindle-shaped cells (Table II) shows similar percentages in the four stages studied. Thus in the apical zone of the wedge-shaped cells appear the highest mitochondrial percentages when the elevation and convergence of neural folds are taking place (stages 6 and 8). This fact would be related in our opinion with the local energy supply for the apical microfilament contraction. The apical bundle of microfilaments contracts actively during neural tube formation [11] and narrows the apices of neuroepithelial cells. That the spindle-shaped neuroepithelial cells maintain their apical percentages of mitochondria during the four stages suggests that spindle cells might be involved in the mechanism of neural fold fusion that starts at stage 10. Schoenwolf and Desmond [17] pointed out that neural fold fusion is accomplished by the apical prolongations of the spindle-shaped cells from the opposite folds that contact in the midline. This mechanism is also an active process that requires energy supply provided by mitochondria. Thus the apical percentages of mitochondria in the neuroepithelial spindle-shaped cells do not diminish from stage 8 to 10 yielding a suitable energy supply for neural folds fusion.

The yolk droplets and lipid body distribution in the three neuroepithelial cell shapes is markedly apical in the four stages analyzed (see Tables I, II and III). This distribution pattern of cytoplasmic vitelline inclusions would be related with the localization of the Golgi apparatus in the neuroepithelial cells that is always apical. During neurulation there is an active consumption of reserves contained in the inclusions that requires a relationship between Golgi apparatus and vitelline cytoplasmic inclusions [4]. Thus one could expect most of the inclusions distributed preferably apically.

Analysis of the cell organelle distribution patterns in the three neuroepithelial cell types (wedge-shaped, spindle-shaped and inverted wedge-shaped) of the chick embryo reveals a subcellular identity for each one. Table IV shows the statistical analysis for differences between the three cell types with regard to the organelle distribution patterns. Only the Golgi apparatus localization does not present significant differences between the three neuroepithelial cell shapes. Nevertheless mitochondria, rough endoplasmic reticulum and vitelline inclusions show an intracellular distribution that differs significantly between the three cell types at the four stages considered (Table IV). Therefore one can observe that each neuroepithelial cell type of each stage can be characterized ultrastructurally by its organelle distribution. In this respect the bottle-shaped neuroepithelial cells of *Xenopus laevis* embryo can also be identified by their intracellular organelle distributions [20].

On the basis of these results we have made schematic drawings to characterize the three neuroepithelial cell types at each stage (see Fig.5). These draw-

Table IV

Significant differences ($P < 0.05$) found for each stage (6, 8, 10 and 12), organelle (m: mitochondria, rer: rough endoplasmic reticulum, yd: yolk droplets, lb: lipid bodies, ga: Golgi apparatus) and cellular zone (B: Basal, M: Median, A: Apical) between the distribution percentages of the three neuroepithelial cell types

		6	7	10	12
	B	bc	abc	ab	abc
m	M	bc	b	b	a
	A	—	bc	abc	abc
	B	ac	—	ab	abc
rer	M	ac	ab	bc	ab
	A	—	—	c	ac
	B	ab	ac	ac	—
yd	M	—	abc	—	—
	A	abc	bc	ac	ac
	B	—	bc	ac	—
lb	M	a	a	bc	—
	A	abc	abc	abc	—
	B	—	—	—	—
ga	M	—	—	—	—
	A	—	—	—	—

a: There are significant differences between wedge-shaped and spindle-shaped cells
b: There are significant differences between wedge-shaped and inverted wedge-shaped cells
c: There are significant differences between spindle-shaped and inverted wedge-shaped cells
— : There are no significant differences

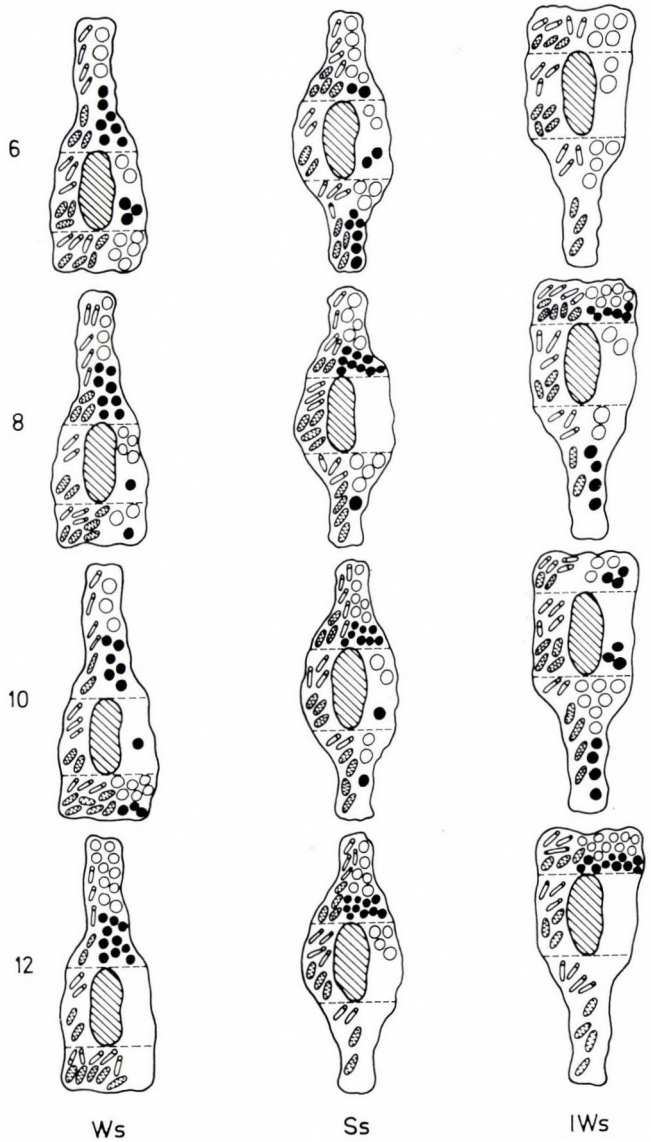

Fig. 5. Diagrammatic representation of the organelle distribution in the wedge- (Ws), spindle- (Ss) and inverted wedge-shaped (IWs) neuroepithelial cells from chick embryos at stages 6, 8, 10 and 12. The distribution and relative number of each organelle are indicative of the distribution percentages. Each profile of an organelle means a 10% of distribution percentage in a cell zone. Symbols: ovals, mitochondria; tubes, rough endoplasmic reticulum; white circles, yolk droplets; dark circles, lipid bodies, The Golgi apparatus is not represented here since its location within neuroepithelial cells is always apical

ings show a specific chronologic evolution of the organelle distribution patterns in the three neuroepithelial cell types. Wedge-shaped, spindle-shaped and inverted wedge-shaped cells differentiate progressively as neurulation proceeds, in a way that stage 12 neuroepithelial cells present organelle distribution percentages distinct for each cell type (Fig. 5.) Moreover, the statistical analysis (TableIV) reveals that the significant differences between organelle distribution percentages of the three neuroepithelial cell types are more remarkable in stage 12 than in the other stages. Distribution of the mitochondria and rough endoplasmic reticulum cisternae differs significantly between the three cell types at stage 12 embryos (Table IV). These facts strongly suggest that wedge-shaped and inverted wedge-shaped neuroepithelial cells have well-defined organelle arrangement. Whether the intracellular arrangement described for the three morphological states of the neuroepithelial cells is only a consequence of each particular cell type, arises as a question to be analyzed. In further studies we will study the effects of treatment with microtubule and microfilament inhibitors.

REFERENCES

1. Burgess DR, Schroeder TE: The cytoskeleton and the cytomusculature. An overview. In: Jasmin C, Cantin M (eds) Methods and Achievements in Experimental Pathology. Karger, Basel 1979, 171
2. Burnside B: Microtubules and microfilaments in amphibian neurulation. Amer Zool 13: 989, 1973
3. Fernandez JG, Paz P, Chamorro CA: Effects of colchicine on the shape of chick neuroepithelial cells during neurulation. Anat Rec 219: 296, 1987a
4. Fernandez JG, Paz P, Chamorro CA, Fernandez M, Villar JM: Intracellular distribution of yolk droplets, lipid bodies and Golgi apparatus in the chick neuroepithelial cells during neurulation. Cytobiol 51: 25, 1987b
5. Hamburger V, Hamilton HL: A servies of normal stages in the development of the chick embryos. J Morph 88: 49, 1951
6. Hirakow R, Gotoh T: A quantitative ultrastructural study on the developing rat heart. In: Liberman M, Sano T (eds) Developmental and Physiological Correlates of Cardiac Muscle, Raven Press, New York 1975, 75
7. Jacobson AG: Morphogenesis of the neural plate and tube. In: Connelly TG et al. (eds) Morphogenesis and Pattern Formation, Raven Press, New York 1981, 233
8. Karfunkel P: The activity of microtubules and microfilaments in neurulation in the chick. J Exp Zool 181: 289, 1972
9. Karfunkel P: The mechanisms of neural tube formation. Int Rev Cytol 38: 245, 1974
10. Lee HY, Nagele RG: Studies on the mechanisms of neurulation in the chick. — Interrelationship of contractile proteins, microfilaments and the shape of neuroepithelial cells. J Exp Zool 235: 205, 1985
11. Lee H, Kosciuk MC, Nagele RG, Roisen FJ: Studies on the mechanisms of neurulation in the chick: possible involvement of myosin in elevation of neural folds. J Exp Zool 225: 449, 1983
12. Martin A, Langman J: The development of the spinal cord examined by autoradiography. J Embryol Exp Morph 14: 25, 1965
13. Morriss-Kay GM, Tuckett F: The role of microfilaments in cranial neurulation in the rat embryos: effects of short-term exposure to cytochalasin D. J Embryol Exp Morph 88: 333, 1985
14. Nagele RG, Lee HY: Ultrastructural changes in cells associated with interkinetic nuclear migration in the developing chick neuroepithelium. J Exp Zool 210: 89, 1979
15. Nagele RG, Lee HY: Studies on the mechanism of neurulation in the chick: microfilament-mediated changes in cell shape during uplifting of neural folds. J Exp Zool 213: 391, 1980

16. Schoenwolf GC: On the morphogenesis of the early rudiments of the developing central nervous system. Scanning Electron Microsc, t 1: 289, 1982
17. Schoenwolf CG, Desmond ME: Descriptive studies of occlusion and re-opening of the spinal canal of the early chick embryo. Anat Rec 209: 251, 1984
18. Schoenwolf GC, Franks MV: Quantitative analysis of changes in cell shapes during bending of the avian neural plate. Dev Biol 105: 257, 1984
19. Schoenwolf GC, Powers ML: Shaping of the chick neuroepithelium during primary and secondary neurulation: role of cell elongation. Anat Rec 218: 182, 1987
20. Schroeder TE: Neurulation in *Xenopus laevis*. An analysis and model based upon light an electron microscopy. J Embryol Exp Morph 23: 427, 1970
21. Smith JL, Schoenwolf GC: Cell cycle and neuroepithelial cell shape during bending of the chick neural plate. Anat Rec 218: 196, 1987
22. Smits-Van Prooije A, Poelmann R, Dubbeldam J, Mentink M, Vermeij-Keers C: The formation of the neural tube in rat embryos, cultured in vitro, studied with teratogens. Acta Histochem (Suppl) XXXII: 41, 1986
23. Sokal RR, Rohlf FJ: Biometry. WH Freeman and Co., San Francisco 1969
24. Weibel ER: Stereological Methods, Vol 1, Practical Methods for Biological Morphometry. Academic Press, New York (1979)
25. Wiley MJ: The effects of cytochalasins on the ultrastructure of neurulating hamster embryos "in vitro". Teratology 22: 59, 1980
26. Williams MA: Stereological techniques. In: Practical Methods in Electron Microscopy. Vol 6, Quantitative Methods in Biology, Glamert AM, North-Holland, Amsterdam, 1977, 5

Acta Morphologica Hungarica, 36 (3—4), pp. 215—225 (1988)

INTERMEDIATE FILAMENT TYPING IN TUMOUR DIAGNOSTICS — AN AID IN HISTOGENETIC CLASSIFICATION?

L. LANGBEIN, H. KOSMEHL, D. KATENKAMP

INSTITUTE OF PATHOLOGICAL ANATOMY, FRIEDRICH-SCHILLER-UNIVERSITY, JENA, GDR

(Received 29 June 1987)

It is commonly accepted, that a histogenetic correlation can be established between tumour and mother tissue by means of intermediate filament typing. Recent results concerrning the co-expression of different intermediate filaments within one cell, the occurrence of epithelial-specific intermediate filaments in soft tissue tumours, and the modulation of intermediate filament type expression caused by some bioactive substances and viral infections cast doubts on the general acceptance of the histogenetic classification of human tumours by intermediate filament typing. Its characterization determines only the actual morphological differentation of the neoplastic cells and represents a valuable tool for the diagnostic assessment of the tumour under the viewpoint of the functional differentiation of its cells. A doubtless conclusion concerning the mother tissue of the neoplasia (histogenetic origin) is therefore not possible.

Keywords: Tumour classification, intermediate filaments, histogenesis, immunohistochemistry

The cytoskeleton of human and animal cells is composed of three main components: microfilaments and microtubules with associated proteins and intermediate filaments [12, 25, 38, 79]. While microfilaments and tubules seem principally to be correlated to more dynamic and function-related activities, the system of intermediate filaments has its basic task in the maintenance of cellular integrity, cellular shape and internal structure of cells [9, 16, 37, 39].

Because they are pertinent to essential cellular constituents for primitive and ontogenetically old cell functions, intermediate filaments are considered, to be stable molecular-biological formations [5, 70, 71, 73].

The intermediate filaments are morphologically characterized by their diameter of 10 nm and their cellular arrangement. They can be distinguished by biochemical and immunological methods into five filament classes: keratin-filaments (19 polypeptides; 40—70 kD), neurofilaments (3 polypeptides; 63-145, and 200 kD), glial filaments (53 kD), desmin filaments (52 kD), and vimentin filaments (54 kD) [21, 59, 60]. These types of intermediate filaments are expressed in adult, non-neoplastic, and in situ growing cells regularly in tissue specific manner (48):

— keratin filaments in epithelial cells
— vimentin filaments in many types of mesenchymal cells

Send offprint requests to: Dr. L. Langbein, Institute of Pathological Anatomy, Friedrich-Schiller-University, DDR-6900 Jena, Ziegelmühlenweg 1

— desmin filaments in skeletal, heart and most smooth muscle cells
— glia filaments in astrocytes and some ependymal cells
— neurofilaments in neural cells.

The classification of human tumours into carcinomas and sarcomas, tumours of the haematopoetic and lymphatic system as well as neoplasias of the central nervous system is based on their origin from distinct mother tissues and is designated as histogenetic classification.

Intermediate filaments, as primitive and phylogenetically old structures, can be identified in well-differentiated or undifferentiated tumours by means of immunochemical methods [60] — despite the lack of other tumour cell characterizing features. Labelling of the same intermediate filament type in both neoplastic and corresponding normal tissue leads to the concept of the histogenetic classification of human tumours by intermediate filament typing [50, 56, 57, 63].

The distribution of keratin is particularly investigated in detail, because these filaments may be considered to be of the greatest diagnostic value. Particular importance of the keratin demonstration lies in the identification of undifferentiated carcinomas and/or their distinction from other undifferentiated tumours [3, 64].

Using polyclonal or monoclonal antibodies to keratin or cytokeratin polypeptides, demonstration of epithelial origin is possible not only for cells of epidermoid carcinomas (Fig. 1) [28, 49], but also for cells of simple non-stratified carcinomas of parenchymal organs, for example adenocarcinomas [2, 62], urothelial carcinomas [56], thyroid carcinomas [81] and neuroendocrine carcinomas [10, 54, 60].

Investigations with monoclonal antibodies against different keratin polypeptides or with 2-dimensional gel electrophoresis showed that during the process of differentiation of non-neoplastic epithelial cells in vivo [6, 30] and in vitro [36], the intermediate filament pattern shows variations. Also during experimental carcinogenesis variations of keratin pattern between carcinoma and the original tissue were observed [19, 19, 28, 53]. Furthermore, there appears to be a qualitative and quantitative heterogeneity in cellular keratin expression also in a distinct tumour [17, 68; Fig. 1].

Regarding these results one has to question the common view, that a cell expresses only one single cell-type-specific intermediate filament.

It is known for a longer time, that most cells isolated from the tissue, for example cells in cultures and ascites, co-express vimentin in addition to their original intermediate filament type [23, 61; Fig. 2]. After re-integration of the cells into the tissue, the vimentin disappears [52].

An additional expression of vimentin filaments to keratin filaments [21], neurofilaments [8], glia filaments [67] or desmin filaments [31, 56] is known to take place in embryonic tissues.

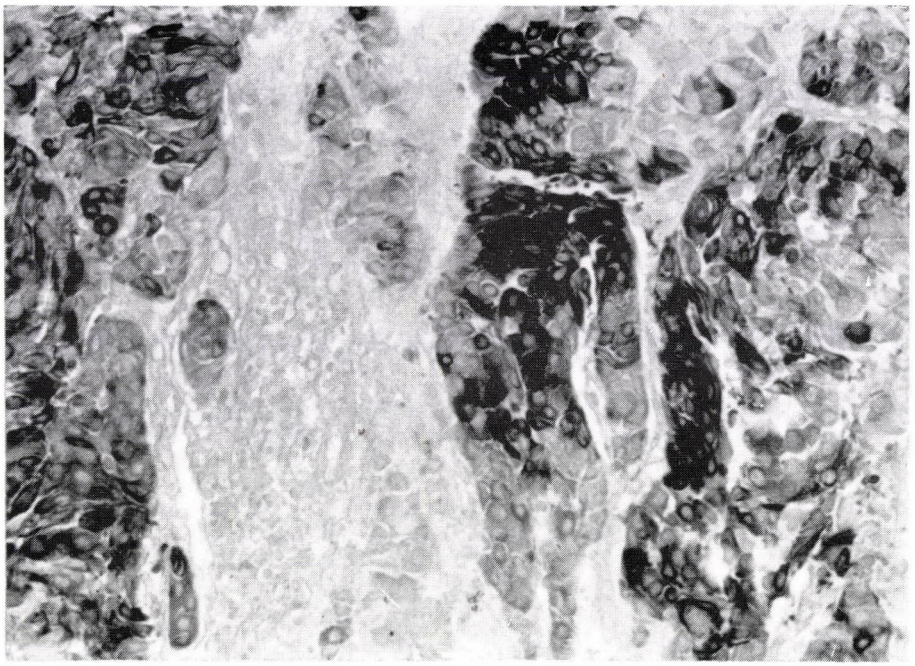

Fig. 1. Demonstration of keratin in an epidermoid carcinoma of the lung. Note the heterogeneous expression of keratin in different cell groups of the carcinoma; (polyclonal antikeratin antibodies, indirect peroxidase technique. ×190)

A number of malignant tumours develop different types of intermediate filaments within the same cell (cf. Table I; Figs 3, 4). Three different intermediate filament types could be identified within one neoplastic cell [1, 65, 80]. Another important fact; keratin filaments, characteristic for epithelial differentiated cells, can be demonstrated in soft tissue tumours — synovial sarcomas [18], epitheloid sarcomas [15, 51] and malignant mesotheliomas [17, 78], which are derived from a mesenchymal stem cell [32].

Alterations of intermedite filament expression can also be achieved by several bioactive substances. Vitamine A [24, 33] and some hormones [35, 43, 66, 76] may influence the keratin polypeptide pattern or the intermediate filament type (cf. 65). After viral infections such alterations are possible, too [7, 69].

These results cast some doubts on the general acceptance of the concept of histogenetic classification of human tumours by intermediate filament typing [cf. 26]. Conclusions on the histogenesis of cells, based on the determination of intermediate filament types should be considered only with limitations, because the intermediate filament pattern is obviously determined primarly by the functional state at the time of investigation and not so far by the cellular origin. This is underlined by the occurrence of keratin-positive cells in soft tissue tumours or by the co-expression of different intermedite filament types

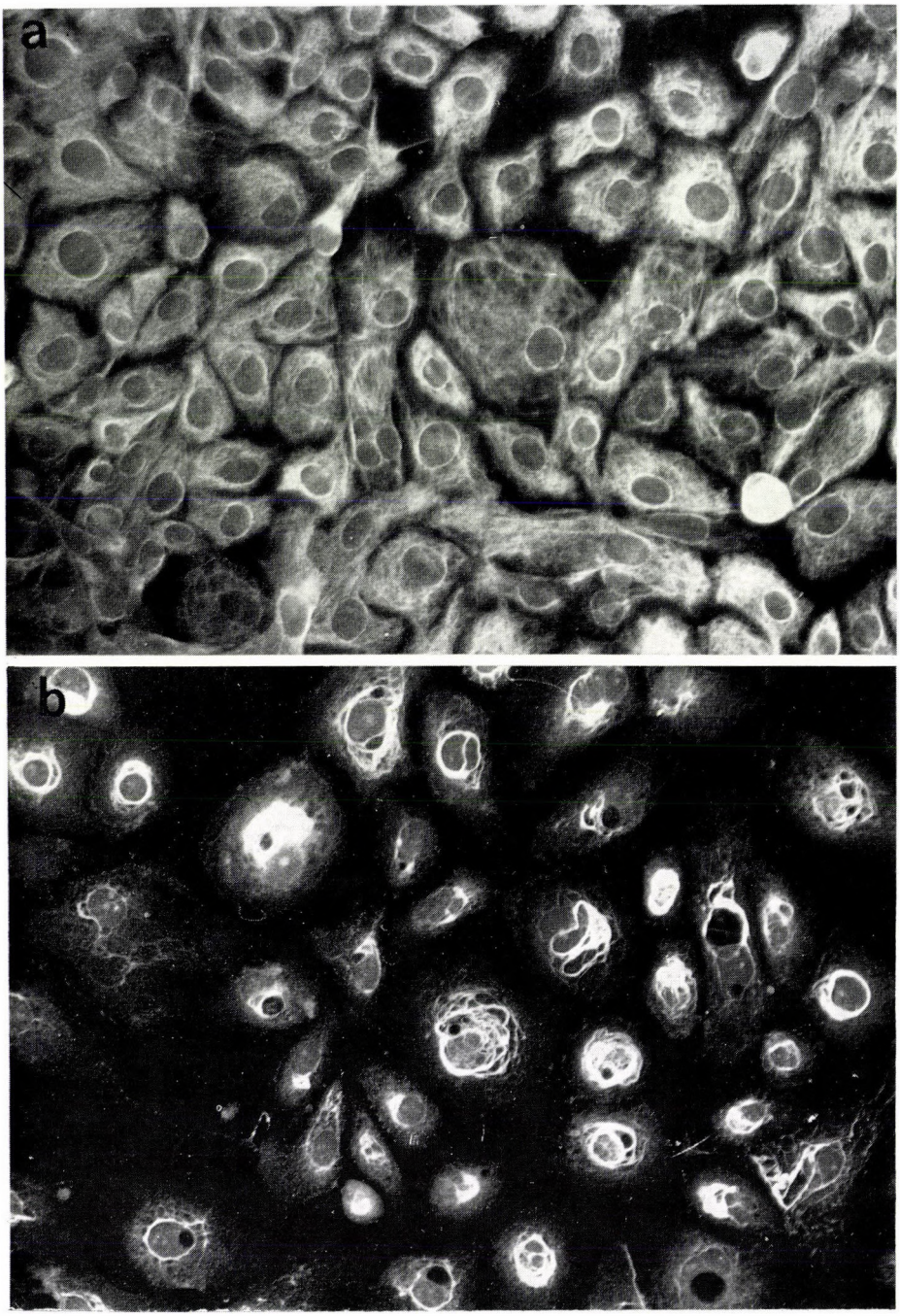

Fig. 2. Co-expression of vimentin filaments (a) and keratin filaments (b) in cells of an established epitheloid rat liver cell line; (polyclonal anti-vimentin antibodies, polyclonal antikeratin antibodies, indirect immunofluorescence technique. ×420)

Table I

Co-expression of intermediate filaments in different human tumours (selected from literature)

Tumour	Keratin	Vimentin	Desmin	Glia fila.	Neuro-fila.	Authors
Renal cell carcinomas	+	+				Waldherr *et al.* 1985
Adenocarcinomas (lung)	+	+				Upton *et al.* 1986
Thyreoid carcinomas (follicular, papillar)	+	+				Miettinen *et al.* 1984
Thyreoid carcinomas (medullar)	+	+			+	Schröder *et al.* 1986
Pleomorph adenomas	+ +	+ +		 +		Caselitz *et al.* 1981 Achtstätter *et al.* 1986
Adenocarcinomas (parotis)	+	+	+			Sato *et al.* 1985
Oat-cell cercinomas (lung)	+				+	Lehto *et al.* 1983
Merkel cell carcinomas	+				+	Gould *et al.* 1985
Islet cell tumour	+				+	Miettinen *et al.* 1985
Carcinoid	+				+	Lehto *et al.* 1985
Leiomyosarcomas		+/-	+			Miettinen *et al.* 1984
Rhabdomyosarcomas		+	+			Altmannsberger *et al.* 1982
Gliomas (astrocytomas)		+		+/-		Herpers *et al.* 1986
Rhabdoid tumours	+	+/-				Tsuneyoshi *et al.* 1986
Meningiomas	+	+		+/-		Tsuneyoshi *et al.* 1986 Budka 1986

within one cell (cf. Table I). Therefore, the demonstration of keratin filaments in the adenomatoid tumours of the genital tract, for example, only permits to designate these neoplasias as epithelially or mesothelially differentiated and does not permit an unambiguous conclusion as to an epithelial or mesothelial origin (histogenesis) of these tumours [34] (Figs 4, 5). On the other hand, in cases of co-expression of keratin- and neurofilaments in neuroendocrine carcinomas [46], one is not able to decide, if the stem cell has an epithelial or neural nature.

Therefore, the co-expression of different intermediate filament classes within the same cell, especially in neoplasias, means that these cells may express some features of different kind of tissues. Labelling of only one intermediate filament type using a single intermediate filament antiserum describes the possible tumour differentiation in a limited manner.

With respect to tumour diagnosis the labelling of different intermediate filament types gives a useful contribution to the actual functional differentiation of neoplastic cells and thereby can be considered as an essential contribution to tumour biology.

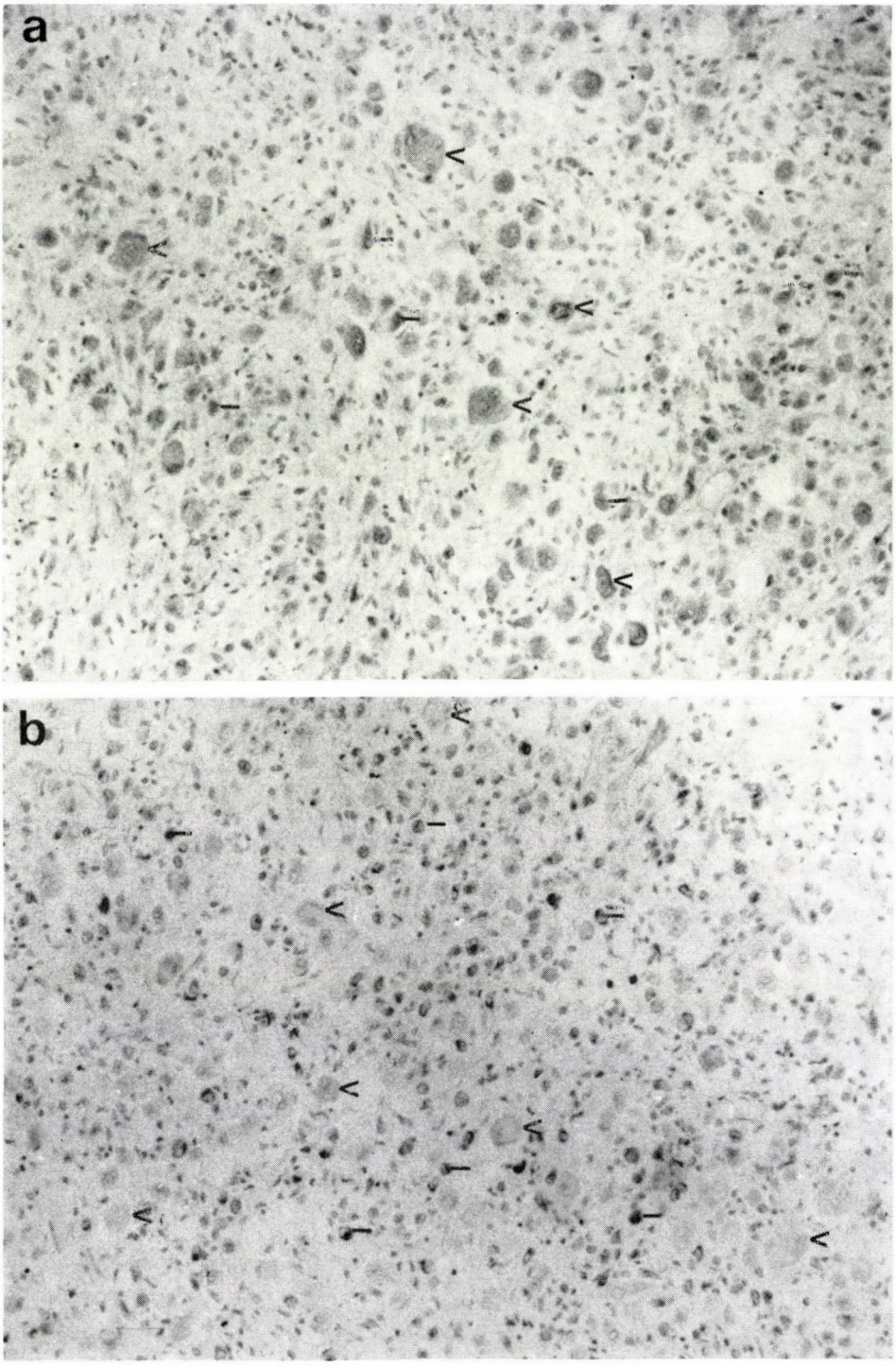

Fig. 3. Expression of desmin (a) and vimentin (b) in the cells of an experimental methylcholanthrene-induced murine rhabdomyosarcoma. Medium-sized tumour cells are decorated by vimentin and desmin antibodies as well (—). Giant tumour cells only express desmin (<) and are failing in vimentin staining (<); (monoclonal anti-desmin antibodies, polyclonal anti-vimentin antibodies, PAP-technique, heamatoxylin counterstaining. ×190)

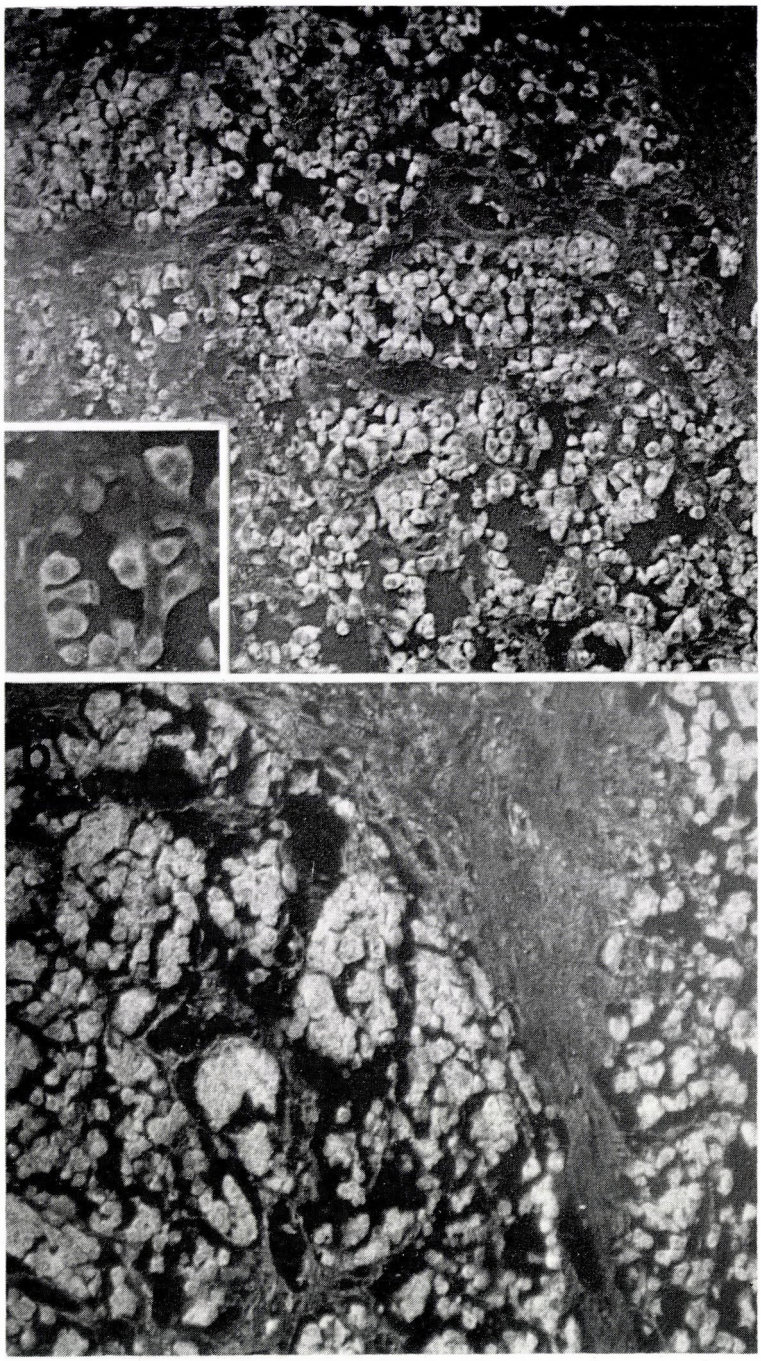

Fig. 4. Expression of keratin (a) and vimentin (b) in the cells of a human hepatocellular carcinoma; (polyclonal anti-vimentin antibodies, polyclonal antikeratin antibodies, indirect immunofluorescence technique. ×190, inset ×460)

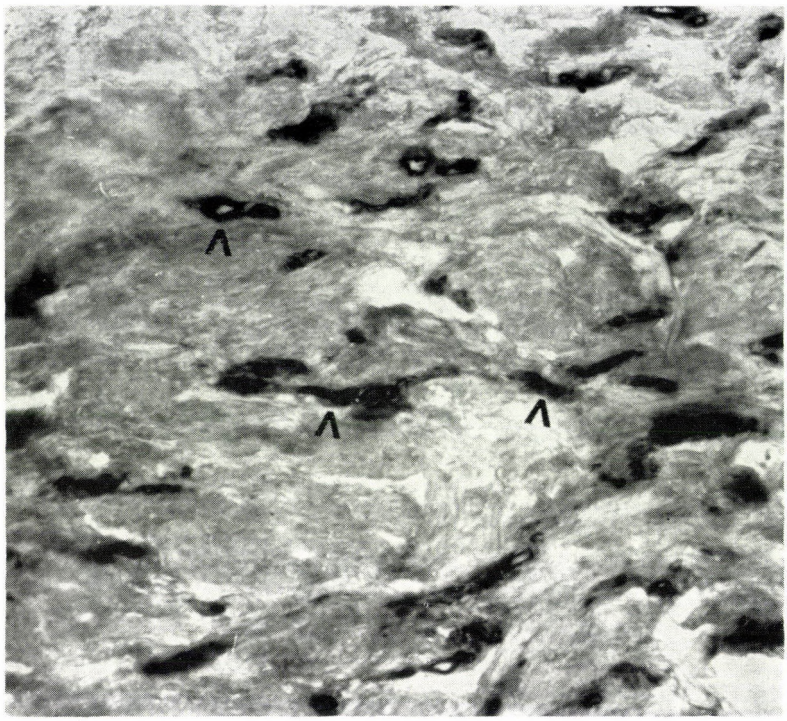

Fig. 5. Expression of keratin in the tumour cells (<) of a human epididymal adenomatoid tumour indicates an epithelial or mesothelial differentiation; (polyclonal anti-keratin antibodies, indirect peroxidase technique. ×200)

REFERENCES

1. Achtstätter T, Moll R, Anderson A, Pitz S, Schwechheimer K, Franke WW: Expression of glial filament protein (GFP) in nerve sheaths and non-neural cells re-examined using monoclonal antibodies, with special emphasis on the co-expression of GFP and cytokeratin in epithelial cells of human salivary gland and pleomorphic adenomas. Differentiation 31: 206, 1986
2. Altmannsberger M, Osborn M, Hölscher A, Schauer A, Weber K: The distribution of keratin-type intermediate filaments in human breast cancer. An immunohistochemical study. Virchow's Arch Cell Pathol 37: 277, 1981
3. Altmannsberger M, Osborn M, Schauer A, Weber K: Antibodies to intermediate filament proteins. Cell-type specific markers on paraffin-embedded human tissues. Lab Invest 45: 427, 1981
4. Altmannsberger M, Osborn M, Treuner J, Hölscher A, Weber K, Schauer A: Diagnosis of human childhood rhabdomyosarcoma by antibodies to desmin, the intermediate filament protein of muscle specific intermediate filaments. Virchow's Arch Cell Pathol 39: 203, 1982
5. Anderton BH: Intermediate filaments. A family of homologous structures. J Muscle Res Cell Motil 2: 141, 1981
6. Banks-Schlegel SP: Keratin alterations during embryonic epidermal differentiation. A presage of adult epidermal maturation. J Cell Biol 93: 551, 1982
7. Banks-Schlegel SP, Rhim JS: Keratin expression of both chemically and virally induced human epidermal keratinocyte during the process of neoplastic conversion. Carcinogenesis 7: 153, 1986

8. Bignani A, Raju T, Dahl D: Localization of vimentin, the non-specific intermediate filament protein in embryonal glia and early differentiating neurons. In vivo and in vitro immunofluorescence study of the rat embryo with vimentin and neurofilament antisera. Develop Biol 91: 286, 1982
9. Birchmeyer W: Cytoskeleton. Structure and function. TIBS 9: 192, 1984
10. Blobel GA, Gould VE, Moll R, Lee I, Huzar M, Geiger B, Franke WW: Co-expression of neuroendocrine markers and epithelial cytoskeletal proteins in bronchopulmonary neuroendocrine neoplasm. Lab Invest 52: 39, 1985
11. Blobel GA, Moll R, Franke WW, Kayser KW, Gould VE: The intermediate cytoskeleton of malignant mesotheliomas and its diagnostic significance. Amer J Pathol 121: 235: 985
12. Brinkley BR: The cytoskeleton. A perspective. Meth Cell Biol 24: 1, 1982
13. Budka H: Non-glial specifities of immunohistochemistry for the glial fibrillary acidic protein (GFAP). Triple expression of GFAP, vimentin and cytokeratins in papillary meningioma and metastasizing renal carcinoma. Acta Neuropathol 72: 43, 1986
14. Caselitz J, Osborn M, Seifert, G, Weber K: Intermediate filament proteins (prekeratin, vimentin, desmin) in the normal parotid gland and parotid gland tumors. Immunofluorescence study. Virchow's Arch Pathol Anat 393: 273, 1981
15. Chase D, Enzinger FM, Weiss SW, Langloss JM: Keratin in epitheloid sarcoma. An immunohistochemical study. Amer J Pathol 8: 435, 1984
16. Cohen C: Cell architecture and morphogenesis. I. Cytoskeletal proteins. TIBS 4: 73, 1979
17. Cooper D, Schermer A, Sun TT: Biology of disease. Classification of human epithelia and their neoplasms using monoclonal antibodies to keratins. Strategies, applications and limitations. Lab Invest 52: 243, 1985
18. Corson JM, Weiss LM, Banks-Schlegel SP, Pinkus GS: Keratin proteins in synovial sarcoma. Amer J Surg Pathol 7: 107, 1985
19. Czernobilski B, Moll R, Franke WW, Dallenbach-Hellweg, G, Hellweg-Maljert P: Intermediate filaments of normal and neoplastic tissues of female genital tract with emphasis on problems of differential tumor diagnosis. Path Res Pract 179: 31, 1984
20. Erlandson RA: Diagnostic immunohistochemistry of human tumors. An interim evaluation. Amer J Surg Pathol 8: 615, 1986
21. Franke WW, Grund C, Kuhn C, Jackson BW, Illmensee K: Formation of cytoskeletal elements during mouse embryogenesis. III. Primary mesenchymal cells and their first appearance of vimentin filaments. Differentiation 23: 43, 1982
22. Franke WW, Schmid E, Osborn M, Weber K: Different intermediate-sized filaments distinguished by immunofluorescence. Proc Natl Acad Sci USA 75: 5034, 1978
23. Franke WW, Schmid E, Winter, E, Osborn M, Weber K: Widespread occurrence of intermediate-sized filaments of the vimentin type in cultured cells from diverse vertebrates. Exp Cell Res 123: 25, 1979
24. Fuchs E, Green H: Changes in keratin expression during terminal differentiation of the keratinocyte. Cell 19: 1033, 1981.
25. Goldman RD, Milsted A, Schloss JA, Starger J, Yerna MJ: Cytoplasmic fibers in mammalian cells. Cytoskeletal and contractile elements. Ann Rev Physiol 41: 703, 1979
26. Gould VE: Histogenesis and differentiation. A re-evaluation of these concepts as criteria for the classification of tumors. Human Pathol 17: 212, 1986
27. Gould VE, Moll R, Moll I, Lee I, Franke WW: Biology of disease. Neuroendocrine (Merkel) Cells of the skin. Hyperplasias, dysplasias, and neoplasms. Lab Invest 52: 334, 1985
28. Grace MP, Kim KH, True LD, Fuchs E: Keratin expression in normal esophageal epithelium and squamous cell carcinoma of the esophagus. Canc Res 45: 841, 1985
29. Herpers MJHM, Ramaekers FCS, Aldeweireldt J, Moesker O, Sloof J: Co-expression of glial fibrillary acidic protein- and vimentin-type intermediate filaments in human astrocytomas. Acta Neuropathol 70: 333, 1986
30. Holthöfer H, Miettinen M, Lehto V-P, Lehtonen E, Virtanen I: Expression of vimentin and cytokeratin types of intermediate filament proteins in developing and adult human kidneys. Lab Invest 50: 552, 1984
31. Holtzer H, Bennett GS, Tapscott SJ, Croop JM, Toyama Y: Intermediate-sized filaments. Changes in synthesis and distribution in cells of myogenic and neurogenic lineages. Cold Spr Harb Symp Quant Biol 46: 317, 1982
32. Katenkamp D, Raikhlin NT: Stem cell concept and heterogeneity of malignant soft tissue tumor — a challange to reconsider diagnosis and therapy? Exp Pathol 28: 3, 1985
33. Kim KH, Schwartz F, Fuchs E: Differences in keratin synthesis between normal epithelial cells and squamous cell carcinomas are mediated by vitamine A. Proc Natl Acad Sci USA 81: 4280, 1984
34. Kosmehl H, Langbein L, Katenkamp D: Adenomatoid tumors—mesotheliomas or not?

An histochemical and immunohistochemical light and electron microscopic (TEM/REM) study. Arch Geschwulstforsch. 57: 141, 1987
35. Kronenberg MS, Clark JH: Changes in keratin expression during the estrogen-mediated differentiation of rat vaginal epithelium. Endocrinology 117: 1480, 1985
36. Langbein L, Neupert G: Modulation of expression of intermediate filaments during the development of established rat liver cell lines. Acta Histochem 80: 149, 1986
37. Lazarides E: Intermediate filaments as mechanical integrators of cellular space. Nature 283: 249, 1980
38. Lazarides E, Intermediate filaments. A class of chemically heterogeneous, developmentally regulated proteins. Ann Rev Biochem 51: 219, 1982
39. Lazarides E, Revel JP: The molecular basis of cell movement. Sci Amer 240: 88, 1979
40. Lee J, Blobel GA, Franke WW, Gould VE: Bronchopulmonary carcinoid co-expressing neuroendocrine markers and cytokeratin. Ultrastruct Pathol 9: 331, 1985
41. Lehto VP, Miettienen M, Virtanen I: A dual expression of cytokeratin and neurofilaments in bronchial carcinoid cells. Int J Canc 35: 412, 1985
42. Lehto VP, Stenman, S, Miettinen M, Dahl D, Virtanen I: Expression of neural type of intermediate filaments as a distinguishing feature between oat cell carcinoma and other lung carcinomas Amer J Pathol. 110: 113, 1983
43. Leroux-Nicolet, J, Noel M, Baribault H, Goyette R, Marceau N: Selective increase in cytokeratin synthesis in cultured rat hepatocytes in response to hormonal stimulation. Biochem Biophys Res Comm 114: 556, 1983
44. Miettinen M, Franssila K, Lehto V-P, Paasivuo R, Virtanen I: Expression of intermediate filament proteins in thyroid gland and thyroid tumors. Lab Invest 50: 262, 1984
45. Miettinen M, Lehto V-P, Badley RA, Virtanen I: Expression of intermediate filaments in soft tissue tumors. Int J Canc 30: 541, 1982
46. Miettinen M, Lehto V-P, Dahl D, Virtanen I: Varying expression of cytokeratin and neurofilament in neuroendocrine tumors of human gastrointestinal tract. Lab Invest 52: 429, 1985
47. Miettinen M, Lehto V-P, Virtanen I: Keratin in epithelial cells of classical biphase synovial sarcoma. Virchow's Arch Cell Pathol 40: 157, 1982
48. Miettinen M, Lehto V-P, Virtanen I: Antibodies to intermediate filament proteins in the diagnostic and classification of human tumors. Ultrastruct Pathol 7: 83, 1983
49. Miettinen M, Lehto V-P, Virtanen I: Antibodies to intermediate filaments. The differential diagnosis of ncutanous tumours. Arch Dermatol 121: 736, 1985
50. Miettinen M, Partanen S, Lehto V-P, Virtanen I: Mediastinal tumors. Ultrastructural and immunohistochemical evaluation of intermediate filaments as diagnostic aids. Ultrastruct Pathol 4: 337, 1983
51. Mills SE, Fechner RE, Bruns DE, OíHara MF: Intermediate filaments in eosinophilic cells of epitheloid sarcoma. A light microscopic, ultrastructural and electrophoretic study. Amer J Surg Pathol 5: 195, 1981
52. Molencraft VF, Ramaekers FCS, Jap P, Vooijs P, Mungyer G: Changing intermediate sized filament pattern in metastatic hepatocellular carcinoma cells of the guinea pig. Virchow's Arch Cell Pathol 51: 285, 1986
53. Moll R, Franke WW, Schiller DL, Geiger B, Krepler R: The catalog of human cytokeratin patterns of expression in normal epithelia, tumors and cultured cells. Cell 31: 11, 1982
54. Moll R, Moll I, West W: Changing in the pattern of cytokeratin polypeptides in epidermis and hair follicles during skin development in human fetuses. Differentiation 23: 170, 1982
55. Nathrath WBJ, Arnholt H, Wilson PD: Keratin, luminal epithelial antigen and carcinoembryonic antigen in human urinary bladder carcinomas. An immunohistochemical study. Path Res Pract 175: 299, 1982
56. Osborn M: Intermediate filaments as histologic markers. An overview. J Invest Dermatol 81: 104, 1983
57. Osborn M, Altmannsberger M, Debus E, Weber K: Intermediate filaments as markers for determinating the histogenetic origin of human tumors. J Submicrosc Cytol 16: 149 1984
58. Osborn M, Caselitz J, Weber K: Heterogeneity of intermediate filament expression in vascular smooth muscle. A gradient in desmin positive cells from the rat aortic arch to the level of the arteria iliaca communis. Differentiation 20: 196, 1981
59. Osborn M, Geisler N, Shaw G, Sharp G, Weber K: Intermediate filaments. Cold Spr Harb Symp Quant Biol 46: 413, 1982
60. Osborn M, Weber K: Biology of disease. Tumor diagnosis by intermediate filament typing: A novel tool for surgical pathology. Lab Invest 48: 372, 1983

61. Ramaekers FCS, Haag D, Kant A, Moesker O, Jap PHK, Vooijs GP: Co-expression of keratin- and vimentin-type intermediate filaments in human metastatic carcinoma cells. Proc Natl Acad Sci USA 80: 2618, 1983
62. Ramaekers FCS, Huysman A, Moesker O, Kant A, Jap P, Herman C, Vooijs P: Monoclonal antibodies to keratin filaments, specific for glandular epithelia and their tumors. Use in surgical pathology. Lab Invest 49: 353, 1983
63. Ramackers FCS, Puts JJG, Moesker O, Kant A, Huysman A, Haag D, Jap PHK, Herman CJ, Vooijs P: Antibodies to intermediate filament proteins in the immunohistochemical identification of human tumors. An overview. Histochem J 15: 691, 1983
64. Said JW: Immunohistochemical localization of keratin proteins in human tumor diagnosis. Human Pathol 14: 1017, 1983
65. Sato M, Hayashi Y, Yanagawa T, Yoshida H, Yura Y, Azume M, Ueno A: Intermediate-sized filaments and specific markers in a human salivary gland carcinoma cell line and its nude mouse tumors. Canc Res 45: 3878, 1985
66. Schmid E, Schiller DL, Grund C, Franke WW: Tissue type specific expression of intermediate filament protein in a culture epithelial cell line from bovine mammary gland. J Cell Biol 96: 37, 1983
67. Schnitzer J, Franke WW, Schachner M: Immunochemical demonstration of vimentin in astrocytes and ependymal cells of developing and adult mouse nervous system. J Cell Biol 90: 435, 1981
68. Schröder S, Bockhorn-Dworniczak B, Kastendiek H, Böcker W, Franke WW: Intermediate filament expression in thyroid gland carcinomas. Virchow's Arch Pathol Anat 409: 751, 1986
69. Steinberg ML, Defendi V: Altered pattern of keratin synthesis in human epidermal keratinocyte transformed by SV 40 viruses. J Cell Physiol 123: 117, 1985
70. Steinert PM, Jones JCR, Goldman RD: Intermediate filaments. J Cell Biol 99: 22, 1984
71. Steinert PM, Steven AC, Roop DR: The molecular biology of intermediate filaments. Cell 42: 411, 1985
72. Summerhayes JC, Cheng Y-SE, Sun TT, Chen BL: Expression of keratin and vimentin intermediate filaments in rabbit bladder epithelial cells at different stages of benzo(a) pyrene-induced neoplastic progression. J Cell Biol 90: 63, 1981
73. Traub P: Intermediate Filaments. Springer Verl, Heidelberg—New York—Tokyo, 1985
74. Tsuneyoshi M, Daimaru I, Hashimoto H, Enjoji M: Malignant soft tissue neoplasms with the histologic features of renal rhabdoid tumors. An ultrastructural and immunohistochemical study. Human Pathol 16: 1235, 1986
75. Upton MP, Hirohashi S, Tome Y, Miyazawa N, Suemasu K, Shimasato Y: Expression of vimentin in surgically resected adenocarcinomas and large cell carcinomas of the lung. Amer J Surg Pathol 10: 560, 1986
76. Venetianer A, Schiller DL, Magin T, Franke WW: Cessation of cytokeratin expression in a rat hepatoma cell line lacking differentiated functions. Nature 305: 730, 1983
77. Waldherr R, Schwechheimer K: Co-expression of cytokeratin and vimentin intermediate-sized filaments in renal cell carcinoma. A comparative study of the intermediate-sized filament distribution in renal cell carcinomas and normal human kidney. Virchow's Arch Pathol Anat 408: 15, 1985
78. Warhol MJ: The ultrastructural localization of keratin proteins and carcinoembryonic antigen in malignant mesotheliomas Amer J Pathol 116: 385, 1984
79. Weber K, Osborn M: Cytoskeleton, structure and gene regulation. Path Res Pract 175: 128, 1982
80. Wiedenmann B, Franke WW, Kuhn C, Moll R, Gould VE: Synaptolysin: a marker protein for neuroendocrine cells and neoplasms. Proc Natl Acad Sci USA 83: 3500, 1986
81. Wilson NW, Pambakian H, Richardson TC, Stokoe MR, Makin CA, Heyderman E: Epithelial markers in thyroid carcinoma. An immunoperoxidase study. Histopathology 10: 815, 1986

Acta Morphologica Hungarica, 36 (3—4), pp. 227—234 (1988)

THE EFFECTS OF HYPERTENSION ON THE WALL OF THE LARGE INTRACRANIAL ARTERIES WITH SPECIAL REFERENCE TO THE CHANGES OF SOME CONNECTIVE TISSUE ELEMENTS

KATALIN HEGEDŰS

DEPARTMENT OF NEUROLOGY AND PSYCHIATRY UNIVERSITY OF DEBRECEN, MEDICAL SCHOOL, DEBRECEN, HUNGARY

(Received 1 October 1987)

The effect of hypertension on the wall of the major cerebral arteries of 62 patients was investigated at the light microscopical level. This series does not include patients with atherosclerosis of the large intracranial arteries. In hypertensive individuals the intracranial arteries showed concentric intimal thickening. Furthermore, the collagenous fibers occurred in the media as early as in the third decade of life in place of reticular fibers. On the basis of literary data and our findings one may suppose that under permanent mechanical influence the arterial smooth muscle cells synthetize predominantly collagenous fibers instead of reticular fibers.

Keywords: Arterial wall, connective tissue, hypertension

Introduction

Most of the authors do not make distinction between the changes of the large cerebral arteries induced by hypertension and those caused by atherosclerosis [2, 3, 4, 16, 18]. According to Cervós-Navarro [2] the causal link between hypertension and atherosclerosis cannot be denied, however, the hypertensive vascular changes have to be regarded as a distinct nosological entity on the basis of the following facts:

1. The hypertension plays undoubtedly an important role in the development of atherosclerosis, however, the hypertension by itself also causes characteristic vascular abnormalities.

2. The hypertensive vascular changes are restricted mainly to the arterioles, while the atherosclerotic process affects predominantly the larger arteries.

3. The pathological features of these two vascular diseases also differ from each other, moreover, they can develop separately.

4. The complications of hypertensive vascular abnormalities are also different from those of atherosclerosis.

Abbreviations: L = lumen, I = intima, M = media, A = adventitia

Send offprint requests to: Katalin Hegedűs, M. D. Dept. of Neurology and Psychiatry University of Debrecen, Medical School, 4012 Debrecen, Hungary

The vascular abnormalities which are characteristic for hypertension — thickening of the muscular layer, hyalinosis, and development of miliary aneurysms — are predominantly limited to the arterioles. The thickening of the media of the larger arteries is also a consistent feature in hypertension. However, this alteration can generally be observed in the arteries of younger individuals.

The thickening of the media is considered as an adaptive response to compensate for the increased wall tension [1, 2] because the thickness of the arterial wall is directly related to the tangential tension in it, a result of pressure and radius [1]. It is still under debate whether the thickening of the media is caused by the hypertrophy of the smooth muscle cells (SMCs) or by their hyperplasia. The data having been published recently support the former view [3].

After the 5th—6th decades of life the thickening of the muscular layer can commonly no longer observed because the wall of the larger arteries dilates. The damage of the internal elastic lamina (IEL) and the accumulation of collagenous fibers in the media are most probably the cause of dilation of the larger arteries in patients with a long history of hypertension [2].

Hypertension induces also the thickening of the intima [3]. Under experimental conditions the hypertension enhances the permeability of the intima to a variety of substances [4, 11, 12, 19]. The thickening of the intima in hypertension is also attributable to the accumulation of both cellular and extracellular elements [3, 11].

The purpose of the present paper is to demonstrate the effect of hypertension on the wall of the large intracranial arteries with special reference to the changes of connective tissue elements. From this point of view little attention has been paid till now to the events taking place in the major cerebral arteries under the effect of chronic hypertension.

The discussion of pathological changes affecting the arterioles in hypertensive patients is beyond the scope of the present paper.

Materials and methods

The large intracranial arteries of 62 patients with a history of hypertension more than 5 years were investigated microscopically. In each case the general autopsy revealed left ventricular hypertrophy which is characteristic of hypertension. The revelant clinical data of patients investigated are summarized in Table I. This series does not include patients with macroscopically visible atherosclerosis of the intracranial arteries.

The brains were fixed in 10% formaldehyde solution for a week.

Under the age of 40 from all the large intracranial arteries (internal carotid, anterior cerebral, middle cerebral, basilar, and vertebral) samples were taken at a branching point and at least 4—6 mm away from them. Over the age of 40, the basilar and left or right middle cerebral arteries were subjected to microscopical examination in the same way mentioned above.

The sections were 7 μm thick and they were stained with hematoxylin-eosin, elastic van Gieson, orcein, trichrome, periodic acid Schiff, and Gömöri's method for reticulin.

Table I

Age years)	Total	Sex		Hemorrhage				Softening	No cerebrovascular disorders
		M	F	total	hemisphere	thalamus	brain stem		
20—30	3	2	1	2	2	—	—	—	1
31—40	5	3	2	5	5	—	—	—	—
41—50	12	7	5	10	8	1	1	2	—
51—60	20	9	11	14	9	3	2	4	2
61—70	9	3	6	7	6	1	—	2	—
71—80	9	4	5	6	4	1	1	3	—
81—90	4	1	3	2	2	—	—	2	—
Total	62	29	33	46	36	6	4	13	3

Abbreviations: M = male, F = female

Results

On macroscopical inpsection the walls of the large intracranial arteries were thickened and less transparent than those of normotensive individuals without cerebrovascular disorders. The thickening of the arterial wall became more prominent with increasing age.

Microspical examination revealed concentric intimal thickening in segments away from the branching points (Fig. 1A, B). At the branching sites the intimal thickening was somewhat larger.

The next consistent microscopical feature was that the collagenous fibers occurred in the media of the large intracranial arteries as early as in the third decade (Fig. 2) while they became visible generally in the 6th decade in patients without cerebrovascular diseases [10]. It is worth of mention that the intimal thickening having developed in arteries of hypertensive patients never narrowed the lumen markedly because of the gradual dilation of the arteries (Figs 1, 2).

In the continuity of IEL small gaps could always be found. Extensive defects of the IEL were encountered only in two young patients who died of cerebral haemorrhage. The case report of one of the patients was published in 1982 [5].

We found partial lack of reticular fibers in three patients (Fig. 3). They died in the age of 33, 76 and 29 years. The first patient died of cardiac arrest and had no cerebrovascular disturbances. The second suffered from thalamic haemorrhage, and the third from hemispherial bleeding. The media of the large intracranial arteries in the other cases contained a dense network of reticular fibers until the time when the collagenous fibers began to replace the reticular fibers (Fig. 4).

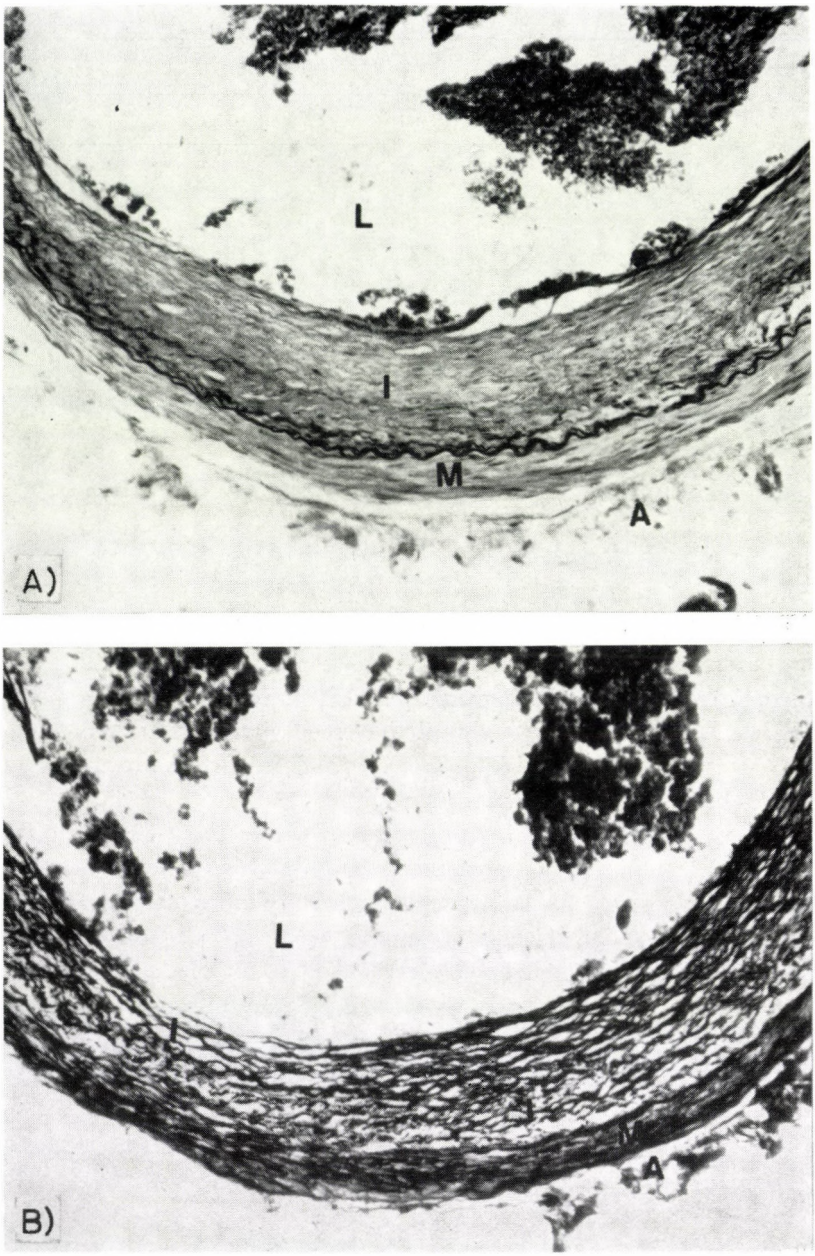

Fig. 1. The right internal carotid artery of a 45-year-old woman with a history of hypertension of 15 years. (A): orcein; ×100, B Gömöri's method for reticulin; ×100. (A): The intima is uniformly thickened and the artery is dilated. (B): The media contains thick fibers and the thickened media comprises thinner fibers. The former correspond to the collagenous fibers and the latter to the reticular fibers

Fig. 2. The left anterior cerebral artery of a 61-year-old man with 20-year-long history of hypertension. Gömöri's method for reticulin; ×400. The reticular fibers are replaced by collagenous fibers in the media. In the thickened intima reticular fibers are seen

In the concentrical intimal thickening the reticular fibers were localized close to the lumen forming a cell-rich layer. Under this layer the collagenous fibers were the principal connective tissue elements in the thickened intima.

Discussion

Our results confirm the hypothesis held by some authors [2] that the hypertension by itself induces pathological alterations of the large intracranial arteries. In the studies concerning the effect of hypertension, there is generally no mention about this fact, they discuss the abnormalities of arterioles.

The hypertension causes concentric intimal thickening of the large cerebral arteries in contrast to atherosclerosis and aging. In the latter two conditions the intimal thickening is generally eccentric. The concentric intimal thickening leads most probably to the loss of the transparent appearance of arteries in

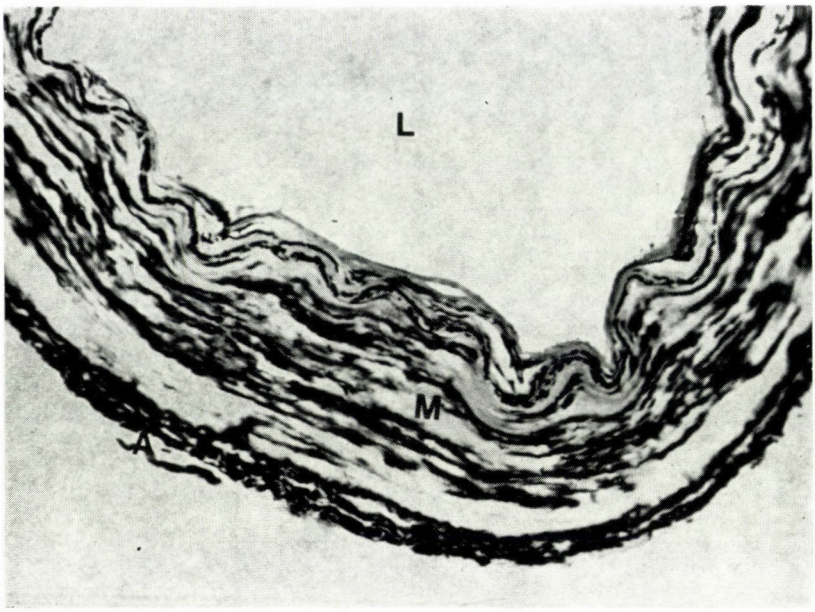

Fig. 3. The right middle cerebral artery of a 76-year-old hypertensive woman who died of thalamic haemorrhage. Gömöri's method for reticulin; ×160. The media is poorly supplied by reticular fibers

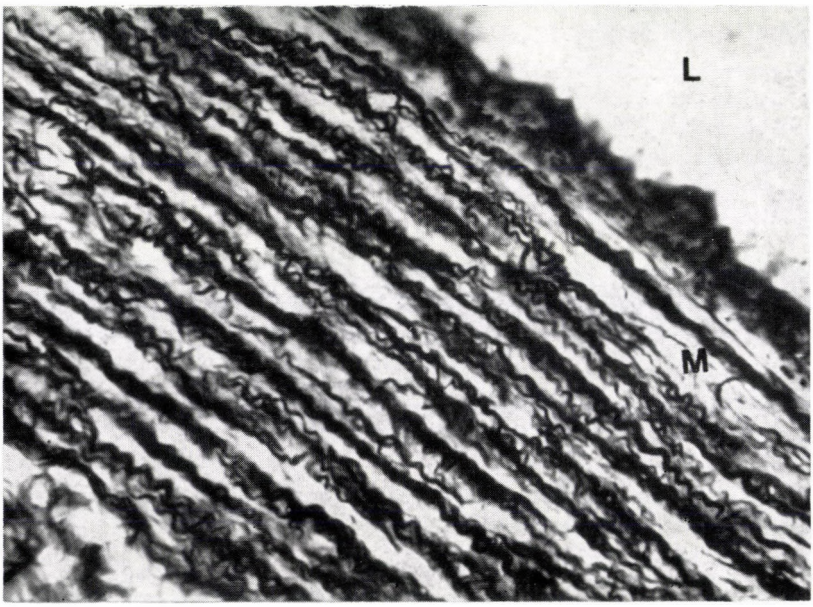

Fig. 4. The right anterior cerebral artery of a 27-year-old woman who suffered from hypertension for 7 years. Gömöri's method for reticulin; ×400. The reticular fibers form a dense network in the media (normal pattern)

hypertensive patients. It seems to be obvious that the first step in the development of hypertensive vascular changes is the same that in atherosclerosis and aging ,i.e., the damage of the endothelium. This induces enhanced proliferation of SMCs of the arterial wall, the migration of SMCs from the media into the intima and the increased rate of collagen synthesis [18].

Hypertension generally does not influence the density of reticular fibers in the media of the major intracranial arteries, however, collagenous fibers occur earlier than in the arteries of patients without vascular diseases [6, 8]. Experimental data support this observation. Stretching of arterial SMCs in culture stimulates their collagen synthesis [13, 14]. Moreover, in the blood vessels of spontaneously hypertensive rats the synthesis of collagen also increases [16] and their arteries become more rigid than those of normotensive animals [1]. Therefore, it might be assumed that the increased mechanical stress induced by hypertension constitutes a direct stimulus for collagen synthesis [18].

It is well-known that the classical collagen fibers contain Type I collagen and Type III collagen constitutes the classical reticular fibers. In the arterial wall both types of collagen are synthetized by SMCs. The ratio of collagen Type I to Type III in the normal arterial wall is approximately 3 : 7 [15]. In patients without vascular diseases the reticular fibers form a dense network around the SMCs of the media and the collagenous fibers confine to the adventitia [6]. With increasing age the collagenous fibers may occur also in the media and in the thickened intima [6]. Under pathological circumstances — such as atherosclerosis [8] — the ratio of collagen Type I to Type III can change in the arterial wall [15].

Our findings indicate that the permanent mechanical stress promotes mainly the enhanced synthesis of collagenous fibers (i.e. — that of Type I collagen) not only in the thickened intima but also in the media. The effect of hypertension on the arterial wall presented in this paper is very important because in the literature there is no mention about the type of collagen which predominates in hypertension.

In hypertensive individuals the reticular fiber deficiency has obviously to be regarded as an accidental finding on the basis discussed above. Partial lack of reticular fibers proved to be a consistent pathological feature in patients with the following disorders: unexplained subarachnoid hemorrhage [9], dissecting aneurysm [7], and berry aneurysms [6, 8]. In the latter condition the reticular fiber dificiency was confirmed recently also by quantitative measurements [17].

The present observations do not contradict the widely accepted view that the hypertension causes mainly the damage of the arterioles and its consequences — predominantly the bleeding — is also the result of the pathological alterations of arterioles.

Further detailed investigations are needed to confirm the presented observations and to clarify their importance.

REFERENCES

1. Berry C: Mechanical vascular changes and hypertension: pathological consequencies. Path Res Pract 180: 336, 1985
2. Cervós-Navarro J: Gefässerkrankungen und Durchblutungsstörungen des Gehirns. In: Ule G, (ed) Pathologie des Nevenssystems I. Durchblutungsstörungen und Gefässerkrankungen des Zentralnervensystem. Springer Verl Berlin—Heidelberg—New York, 1980, 318
3. Chobanian AV, Prescott MF, Haudenschild CC: Recent advances in molecular pathology. The effects of hypertension on the arterial wall. Exp Mol Pathol 41: 153, 1984
4. Gabbiani G, Badonnel M, Róna G: Cytoplasmic contractile apparatus in aortic endothelial cells of hypertensive rats. Lab Invest 32: 227, 1975
5. Hegedűs K, Fekete I: Defects of elastic lamina in middle cerebral artery. A possible cause of a primary intracerebral hemorrhage in a young woman. Arch Psychiat Nervenkr 232: 515, 1982
6. Hegedűs K: Some observations on reticular fibers in the media of the major cerebral arteries. A comparative study of patients without vascular diseases and those with ruptured berry aneurysms. Surg Neurol 22: 301, 1984
7. Hegedűs K: Reticular fiber deficiency in the intracranial arteries of patients with dissecting aneurysm and a review of the possible pathogenesis of previously reported cases. Eur Arch Psychiat Neurol Sci 234: 395, 1985
8. Hegedűs K: Ectasia of the basilar artery with special reference to possible pathogenesis. Surg Neurol 24: 463, 1985
9. Hegedűs K: Pattern of reticular fibers of the major cerebral arteries in cases of unexplained subarachnoid hemorrhage. J Neurol 233: 44, 1986
10. Hegedűs K, Molnár P: Az intracranialis nagy artériák rácsrostjainak és egyéb kötőszövetes elemeinek az életkor előrehaladásával összefüggő változásai. Ideggy Szle 39: 305, 1986
11. Hüttner I, Boutet M, Róna G, More RH: Studies of protein passage through arterial endothelium. III. Effect of blood pressure levels on the passage of fine structure protein tracers through rat arterial endothelium. Lab Invest 29: 536, 1973
12. Jellinek H, Nagy Z, Hüttner I: Investigations of the permeability changes of the vascular wall in experimental malignant hypertension by means of a colloidal iron preparation. Brit J Exp Pathol 50: 13, 1969
13. Knierim HJ, Kao VC, Wissler RW: Actomycin and myosin and the deposition of lipids and serum proteins. Arch Pathol 84: 119, 1967
14. Leung DYM, Glagov S, Mathews HB: Cyclic stretching stimulates synthesis of matrix components by arterial smooth muscle cells in vitro. Science 1981: 475, 1976
15. Mc Cullagh KA, Balian: Collagen characterization and cell transformation in human atherosclerosis. Nature 258: 73, 1975
16. Newman RA, Langner RO: Age related changes in the vascular collagen metabolism of the spontaneously hypertensive rat. Exp Geront 13: 83, 1978
17. Østergaard JR, Reske-Nielsen E, Oxlund H: Histological and morphometric observations on reticular fibers in the arterial beds of patients with ruptured intracranial saccular aneurysm. Neurosurgery 20: 554, 1986
18. Pietilä K, Nikkari T: Role of arterial smooth muscle cell in the pathogenesis of atherosclerosis. Med Biol 61: 31, 193
19. Wiener J, Latter RG, Meltzer AB, Spiro D: The cellular pathology of experimental hypertension. IV. Evidence for increased vascular permeability. Amer J Pathol 54: 187, 1969

Acta Morphologica Hungarica, 36 (3—4), pp. 235—240 (1988)

THE BIPHASIC NATURE OF A HUMAN AMELANOTIC MELANOMA TUMOUR LINE HT-18

BHANU IYENGAR[1], J. TÍMÁR[2], B. SZENDE[2]

[1]INSTITUTE OF PATHOLOGY, NEW DELHI, INDIA, [2]1st INSTITUTE OF PATHOLOGY AND EXPERIMENTAL CANCER RESEARCH, BUDAPEST, HUNGARY

(Received 12 November 1987)

The morphological features of a human amelanotic melanoma tumour line, HT-18 was studied in vitro. Primary cultures show that the tumour cells are biphasic with respect to their differentiation as revealed by light microscopy, SEM and TEM. Most of the cells show numerous processes resembling neuronal dendrites. The cytoplasm contains stage I and II melanosomes, occasionally melanosomes showing irregular pigmentation. According to these observations it appears that the HT-18 cells are at an earlier phase of differentiation showing both melanogenic and neurogenic activity.

Keywords: Amelanotic melanoma, melanogenesis, neurogenesis, morphology

Introduction

Epidermal melanocytes are derived from the neural crest cells during embryogenesis. In vitiliginous skin in a large proportion of cases, the marginal melanocytes show neural differentiation [1]. The melanocytes may proliferate and give rise to a malignant tumour, the melanoma, which may or may not show pigmentation. In the present work the growth characteristics and the morphology of the human amelanotic melanoma tumour line, HT-18 have been studied to assess the nature of their differentiation.

Materials and methods

All studies were performed on primary cultures of a human amelanotic melanoma tumour line xenografted on immuno-suppressed CBA mice [9]. Cells were mechanically dissociated and separated with 0.08% Difco trypsin. The cells were suspended in H-MEM medium with 10% Flow FCS. They were allowed to adhere to plastic for 1 1/2 h, then washed with phosphate-buffered saline (PBS), and were resuspended in Nunc and Linbro multi-dishes (24 wells). Each well started with 5×10^5 cells. Flask cultures were made in Greiner T25 flask with 5 to 10×10^6 cells. These were incubated at 37 °C in 7.5% CO_2 atmosphere.

Cultures were viewed daily to study growth characteristics. The established monolayers were cut out and mounted on slides. These were stained by Sevier Munger stain [2] for dendritic processes and melanin. The monolayers were fixed in 2% glutaraldehyde

Send offprint requests to: Bhanu Iyengar, M. D. Institute of Pathology (ICMR), Safdarjang Hospital, P. O. Box 4909, New Delhi 110 029, India

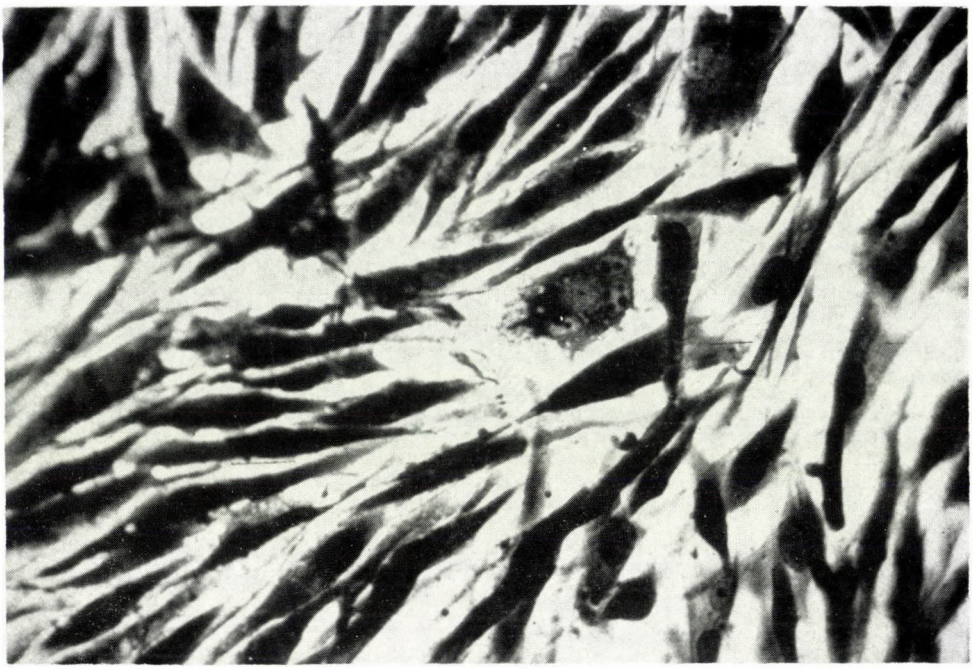

Fig. 1. Light microscopy of the primary culture of HT-18 showing dendritic and axon-like processes stained with silver. In the centre a polygonal cell shows pigment granules in the cytoplasm (Sevier-Munger ×25)

(PBS pH = 7.2) for 1 h, washed and post-fixed in 1% O_SO_4 (PBS). After dehydration in the case of SEM studies, the monolayer was left in situ and critical point dried (Balzer), coated with gold and viewed in a TESLA BS-300 stereoscan, while in the case of TEM it was floated off by propylene oxide, embedded into Polybed 812, "ultracut" and examined in a JEOL-100B transmission electron microscope.

Results

Light microscopy

Cultured the cells have a dendritic appearance. The nuclei are large and vesicular, the cytoplasm is abundant and is thrown into processes of varying lenghts. These processes are covering other cells. A few cells appear rounded without dendritic processes (Fig. 1).

On silver stained preparations (Fig. 1) a few melanosomes are seen scattered within the cytoplasm of the dendritic cells. These granules are more prominent within the rounded cells. The dendritic processes are stained with silver as with axis cylinders and arborise on distant cells.

Scanning electron microscopy

The tumour cells are flat, bi- or multipolars. They show long axon-like processes (Fig. 2) interlacing with each other. There are numerous smaller dendritic processes running from the surface. These end sometimes in knob-like structures. These processes appear to arborise on polygonal cells. In scanning SEM pictures the cells appear almost like nerve cells.

Transmission electron microscopy

As shown by TEM, the cells vary in size and shape. Most cells have abundant cytoplasm which is thrown into numerous dendritic processes, occasionally into axon-like projections which extend to a considerable distance (Fig. 3).

The cytoplasm contains melanosomes. The Golgi vesicles appear dilated with early formation of laminated structures typical for the earliest melanosome stages (Fig. 4). Occasional laminated structures are evident which are partially separated. Most of the melanosomes are of stage I or II, with little melanization. The internal structure of these organelles shows convoluted lamellae, the melanosomes being round, oval or markedly elongated. The matrix shows pigment in occasional melanosomes. Several cells contain vacuoles within the cytoplasm. The dendritic and axon-like processes do not contain any melanosomes. The internal structure shows longitudinal filaments as seen in neurites (Fig. 5).

Discussion

From the present study it appears that the tumour cells in amelanotic melanoma HT-18 have neuroid characteristics. The presence of melanosomes within them and silver staining confirm the melanoma origin of the cell line. The interesting features of dendritic processes and their contacts with other cells is indicated by scanning and transmission EM, by histology and growth characteristics.

The epidermis shows three varieties of dendritic cells, the melanocytes, the Langerhans cells and the Merkel cells [3, 4]. The characteristic feature of the melanocyte is the presence of melanosomes which can be seen in a fairly large number in the HT-18 cells. The stage II melanosomes are in abundance. The level of melanin formation is low in this tumour line. The melanosomes vary considerably in size and configuration as seen in EM micrographs. In the epidermal melanocytes the dendritic processes contain melanosomes which are pinched off by the process of apocopation. By this process the pigment granule is passed into the neighbouring basal cells and prickle cells. In the HT-18 cells the dendrites and axon-like processes are on the neighbouring cells almost as in

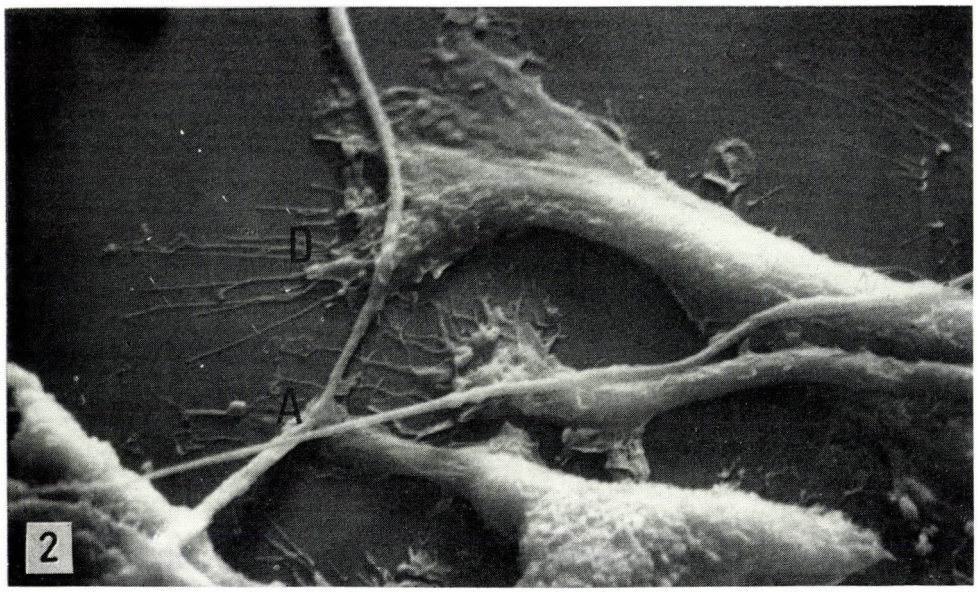

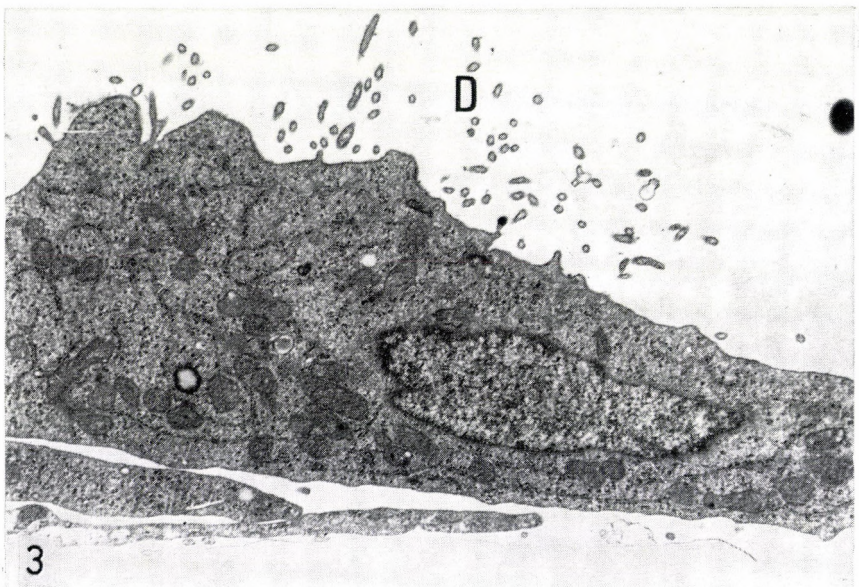

Fig. 2. Scanning EM of HT-18 cells highlighting mostly bipolar flat tumour cells with long axon-like processes (A) and shorter dendritic ones (D) (×3000)

Fig. 3. Transmission electron microscopy of a HT-18 cell showing numerous surface projections (D). The cytoplasm contains endoplasmic reticulum, mitochondria and nucleus (×36 000)

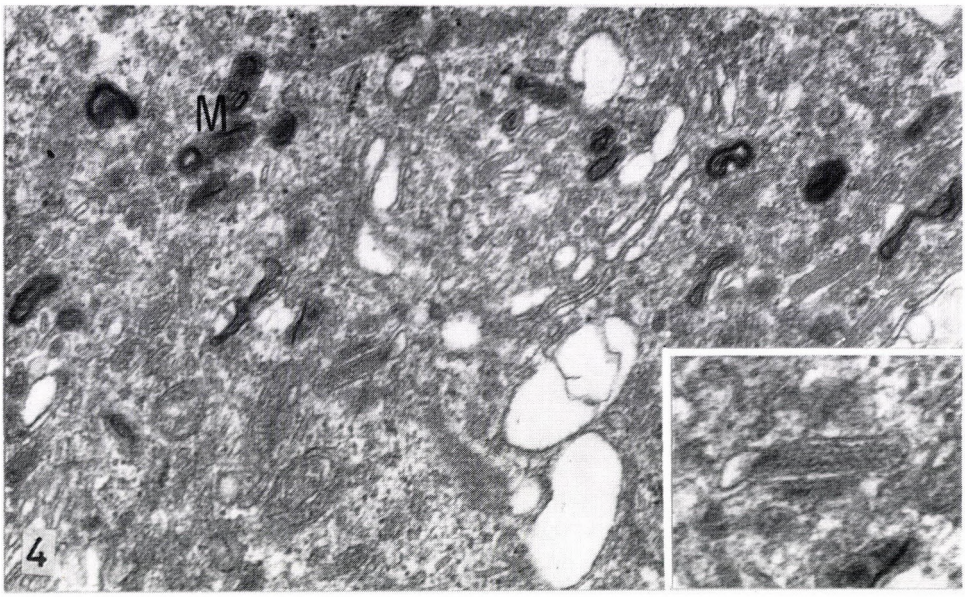

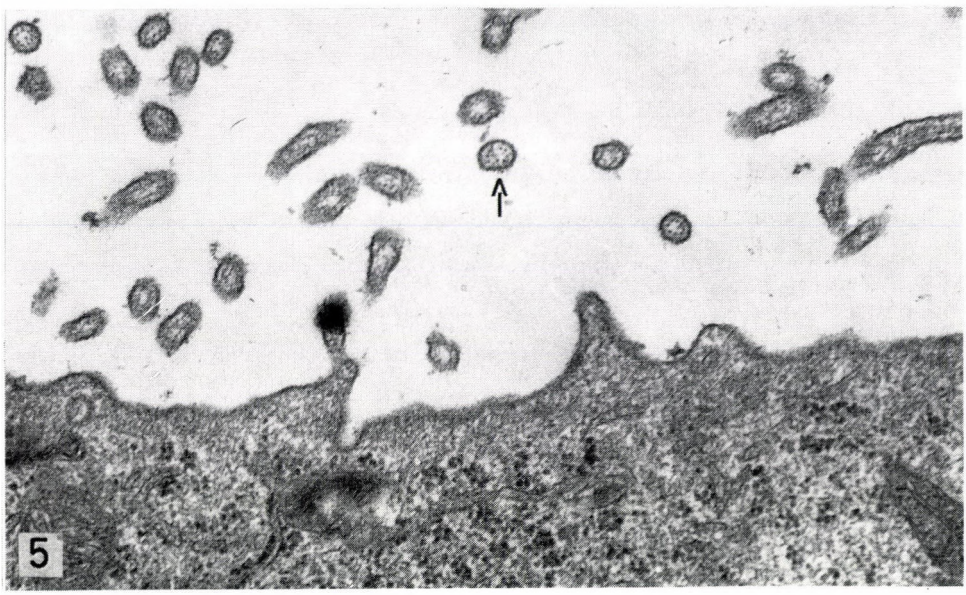

Fig. 4. Cytoplasm of HT-18 melanocyte shows partly pigmented and abnormal melanosomes (M). The inset demonstrates laminated structure of an early stage melanosome (×48 000)

Fig. 5. TEM picture at high magnification of a dendritic process to show the internal structure consisting of microfilaments resembling the structure of neurites (↗) (×96 000)

synaptic endings. No melanosomes are present within these processes, the internal structure which is like that of neurites [8]. The staining characteristics of these structures are also similar to those of neurites (as seen by silver staining). This feature has been observed by Moellmann et al. [8], and similar finding was noted in mouse melanoma cultures [6, 7].

The Birbeck granules typical of the Langerhans cells and neurosecretory granules seen in Merkel cells are absent in the tumour cells [4, 5].

It can be concluded that the melanotic melanoma cells have a neuroid appearance and the melanosomes show a low level of pigment production. The granules do not move into the dendritic processes which extend from the cell surface. Thus, these cells show an early biphasic stage of melanocyte differentiation as also seen in the dendritic melanocytes of vitiligo.

Acknowledgement

This work was supported by the INSA-HAS scientist exchange programme in the framework of which Dr. Bhanu Iyengar (Institute of Pathology-ICMR, New Delhi) visited the Ist Institute of Pathology and Experimental Cancer Research, Semmelweis Medical University, Budapest, Hungary.

REFERENCES

1. Iyengar B, Misra RS: Neural differentiation of melanocytes in vitiliginous skin. Acta Anat, 1987 (In press)
2. Luna LG (ed.): Manual of Histologic Staining Methods of the Armed Forces Institute of Pathology. (3rd Ed.), Mc Graw Hill Book Co, N.Y. 1968
3. Lever WF, Schaumburg Lever G: Histopathology of the Skin (5th Ed.), J.B. Lippincott Co, Philadelphia, Toronto 1975, 16,
4. Zelickson AS, Mottaz JH, Minneapolis ES: Epidermal dendritic cells. Arch Derm 98: 652, 1968
5. Winkelmann RK, Breathnach AS: The Merkel cell. J Invest Derm 60: 2, 1973
6. Pawekel J, Wong G, Sansone M, Morowitz J: Molecular controls in mammalian pigmentation yale. J Biol Med 46: 430, 1973
7. Lee TH, Lee MS, Lu MY: Effects of MSH on melanogenesis and tyrosinas of B-16 melanoma. Endocrin 91: 1180, 1972
8. Moellman G, Mcguire J, Lerner AB: Intracellular dynamics and fine structure of melynocytes. Yale. J Biol Med, 46: 337, 1973
9. Kopper L, Steel GG: The therapeutic response of three human tumor lines maintained in immun-suppressed mice. Cancer Res, 35: 2704, 1976

Acta Morphologica Hungarica, 36 (3—4), pp. 241—251 (1988)

GLYCOSAMINOGLYCAN CONTAINING FAT-STORING CELLS IN HEPATIC FIBROGENESIS

B. Szende, K. Lapis, J. Timár, Zs. Schaff, K. Simon, A. Jeney, A. Divald, S. Paku, F. Timár

Ist INSTITUTE OF PATHOLOGY AND EXPERIMENTAL CANCER RESEARCH
SEMMELWEIS MEDICAL SCHOOL, BUDAPEST, HUNGARY

(Received 12 September 1988)

Male F-344 rats were treated for 10 weeks either with CCl_4 (0.2 ml/kg, per os, twice a week) or with CCl_4 (same as above) and phenobarbital (0.2 g/l in drinking water). Liver fibrosis and cirrhosis developed in both treated groups, and was confirmed histologically. Cirrhosis was more frequent after the CCl_4 + phenobarbital treatment. The collagen content of the liver, measured by morphometry and biochemically, was significantly higher in the animals of the group treated with CCl_4 + phenobarbital than in the animals treated only with CCl_4. Specially altered fat-storing cells (Ito cells) were found in the periportal and septal fibrotic areas in direct proportion to the amount of fibrosis and cirrhosis. They were identified as altered fat-storing cells by their desmin content and Vitamin A storing capability. This study demonstrated that these cells were enlarged and contained neutral fat, lipofuscin and PAS-positive material. The potential role of GAG-containing FSC in fibrogenesis is discussed.

Keywords: Fat-storing cells, Ito cells, glycosaminoglycans, liver, fibrogenesis

Introduction

The development of fibrosis is the most common and most serious event in chronic liver disease.

Collagen and other extracellular matrix formation in liver cirrhosis has been studied extensively in the last decade [25, 28, 29]. A series of in vitro studies showed that macromolecules of the extracellular matrix such as collagen I—III—IV, laminin, fibronectin and glycosaminoglycans (GAG) can be produced by hepatocytes [6, 7, 10, 11, 14, 22, 34]. Other cells found in the liver, Kupffer cells and macrophages, produce fibronectin in culture [1, 26].

An increase in concentration and a pathologic distribution of extracellular matrix molecules were found in hepatic cirrhosis [25, 26, 29]. These changes are always connected with the presence of inflammatory cells, such as lymphocytes,

Abbreviations: FER: rough surfaced endoplasmic reticulum; HID: high iron diamine; H and E: hematoxylin and eosin; GAG: glycosaminoglycans; CHS: chondroitin sulphate; DS: dermatan sulphate; MA—FAF: macrophage fibroblast proliferation stimulating factor; cAMP: cyclic adenosine monophosphate; FSC: fat-storing cells; CCl_4: carbon tetrachloride; PAS: periodic acid Schiff reaction; IU: international unit

Send offprint requests to: Dr. B. Szende, Ist Institute of Pathology and Experimental Cancer Research, Semmelweis Medical University, H-1085 Budapest, Üllői út 26, Hungary

macrophages and mast cells [20, 35, 38]. Besides producing fibronectin [1], macrophages also produce a so-called fibroblast proliferation stimulating factor (MA-FAF). This factor also modulates the production of cAMP and prostaglandin by fibroblasts and in this way it plays a role in the regulation of collagen synthesis [15, 36, 38].

Lymphocytes are also sources of humoral factors which active macrophages and stimulate fibroblast migration and proliferation [15, 24, 37, 38]. The role of mast cells in fibrosis and cirrhosis is presently not well understood [20].

The role of Ito cells [12] or fat-storing cells (FSC) in the production of collagen, has been discussed [13, 16, 17, 18, 39]. The histogenesis of FSC is closely related to that of fibroblasts and myofibroblasts. Recently Yokoi and co-workers [40] have shown a close relationship between the degree of hepatic fibrosis in an experimental model and the number of FSC in the fibrotic areas. These authors also demonstrated that FSC contain desmin, and that they belong to the myogenic cell line which is able to develop to myofibroblasts producing collagen. Burt and co-workers [3] observed an increased number of desmin-containing stellate cells in experimental rat liver injury. They concluded that these cells were identical to FSC. Recently, Verhoeven and Buyssens [33] suggested that FSC are modified pericytes. They argued that desmin positivity supported the concept of FSC as pericytes with a special function in Vitamin A storage and collagen synthesis.

In the present study, different degrees of hepatic fibrosis and cirrhosis were produced either by treatment with CCl_4 or whith CCl_4+phenobarbital treatment according to the method of McLean [19]. The *in vivo* localization and biosynthesis of extracellular matrix compounds was studied to reveal the source of the newly formed extracellular matrix components. The number and morphology of FSC were investigated in relation to the degree of fibrosis and cirrhosis. New features of activated FSC, their GAG content and phagocytic capacity were demonstrated.

Materials and methods

The experimental groups consisted of 20, 8-week-old male F-344 rats. Animals of the *first group* were treated for 10 weeks with 0.2 ml/kg CCl_4 dissolved in oleum helianthi, each was given 0.5 ml solution by gastric tube twice a week. Members of the *second group* were treated with CCl_4 in the same way as group one while receiving phenobarbital (0.2 g/l in drinking water). In one of the control groups *(group three)* animals received oleum helianthi (0.5 ml per animal, by gastric tube, twice a week). In the other control group *(group four)* only phenobarbital (0.2 g/l in drinking water) was given. At the 71st day of the experiment all animals were sacrificed.

The liver was observed macroscopically, one part of each lobe was preserved for biochemical studies, the other parts were fixed in 8 per cent buffered formalin for histology. Small pieces of the livers of 5 animals from each group were fixed in glutaraldehyde-O_8O_4 for electron microscopy. Oil red-O staining was done using formalin-fixed frozen sections. Paraffin-embedded material was used for H.E., PAS, Picrosirius red, alcian blue, toluidine blue, Ziehl-Nielsen, Prussian blue, and pH 2.0 and pH 4.0 iron colloid [30] staining. Immunohistochemical

procedures were done for desmin (anti-desmin serum: Stravigen B-SA, BioGenex Laboratories, Dublin. CA., USA). GAG were identified ultrastructurally after application of high iron diamine (HID) reaction after Spicer et al. [31].

Testicular hyaluronidase (Hyaluronidase Sigma, UK) was dissolved in sodium acetate buffer, pH 5.6, at a concentration of 2000 U/ml. The sections were incubated for 1 h at 37 °C. The controls were incubated in buffer alone.

Ultrathin sections were contrasted with uranyl acetate and examined using a JEM 100 B electron microscope. Morphometry to quantitate the percentage of collagen in the slides stained with Picrosirius was performed by means of a Quantimet videodensitometer (Cambridge Instruments, U.K.). GAG-containing cells (blue cytoplasm after Fe-colloid staining) were counted in 5 μ thick sections and their number was given per cubic millimeter liver tissue. Student's t test was used for statistical analysis.

Carrageenan Iota, (Sigma) was administered i. p. 5 mg/animal in 0.01 ml PBS one day before sacrificing the animals to label the phagocytic cells in the liver parenchyme. Carrageenan was identified in tissue using the method of Gangolli et al. [8].

Biochemical studies

The amount of collagen was determined by the measurement of hydroxyproline in the cellular proteins after hydrolysis under nitrogen in 6 M HCl at 105 °C for 24 h [2].

The uronic acid content of the glycosaminoglycans was quantitated according to the method of Noesser [23].

Vitamin A injection

Two animals receiving the CCl_4 + phenobarbital treatment were injected i.p. with 50 000 IU of Vitamin A, 24 h before sacrifice. Frozens sections of liver were investigated using a fluorescent microscope (Olympus BTHU, reflected light, Y 550 filter).

Results

1. *Liver fibrosis-cirrhosis*

Macroscopically, the surface of the liver was uneven in different degrees in the animals treated with CCl_4 or CCl_4+phenobarbital. True atrophic cirrhosis was also observed in 18 animals in the group treated with CCl_4+phenobarbital.

Under the light microscope, fibrosis (two cases) or cirrhosis (eighteen cases) were observed in all livers from animals treated with CCl_4+phenobarbital. Treatment with CCl_4 alone resulted in various degrees of septal and periportal fibrosis. With morphometry, the red-stained areas amounted to 5—12 % of the areas of the sections. Table I. shows the percentage of red-stained col-

Table I

The ratio of red areas (collagen fibres) in Picrosirius-stained liver sections of CCl_4, CCl_4+phenobarbital, oleum helianthi and phenobarbital-treated P-344 male rats

Treatment	Per cent of collagen fibres
1. CCl_4	5.14±2.40
2. CCl_4+phenobarbital	12.26±7.38
3. Oleum helianthi	2.23±1.56
4. Phenobarbital	1.77±1.13

(Significance between group 2. and 1.: $p < 0.01$ and between group 1. and groups 3. and 4.: $p < 0.01$)

lagen fibres. Whereas the average content of collagen in the livers of the animals treated with CCl_4 was 5.14 ± 2.38 %, treatment with CCl_4+phenobarbital resulted in a collagen content of 12.25 ± 7.38 % ($p < 0.01$).

The control groups had these collagen contents (oleum helianthi 1.77 ± 1.13% and phenobarbital 2.23 ± 1.56%), which were not elevated above normal.

Biochemically, the amounts of collagen and GAG were increased in the livers of animals treated either with CCl_4 alone or CCl_4+phenobarbital. It is noteworthy that in the animals treated with CCl_4+phenobarbital treated animals the amounts of these biopolymers were significantly higher than in the livers of the group treated with CCl_4 alone (Table II).

Table II

Hydroxyproline* and uronic acid** content of the liver of CCl_4, CCl_4+phenobarbital, oleum helianthi and phenobarbital-treated F-344 male rats

Treatment	Hydroxyproline (μg/g wet mass)	Uronic acid (μg/g wet mass)
1. CCl_4	443 ± 233	95 ± 51
2. CCl_4+phenobarbital	$619 + 391$	$116 + 70$
3. Oleum helianthi	$286 + 120$	66 ± 37
4. Phenobarbital	202 ± 49	64 ± 27

(Significance between group 2. and group 1.: $p < 0.05$ and between group 1. and groups 3. and 4.: $p < 0.05$)
* Protein bound
** GAG associated

2. *GAG-containing cells*

In the portal areas and along the connecetive tissue tracts forming thickened septa or surrounding the pseudolobules, a number of relatively large (20—30μ in diameter) cells were seen (Fig. 1). The cells had abundant cytoplasm and round nuclei with medium chromatin content. Their cytoplasm showed a faint basophilic staining with H.E., and was PAS positive even after amylase digestion. The iron colloid method at pH 2.0 resulted in medium to dark blue staining of the cytoplasm (Fig. 2a) indicating GAG content. Oil red O staining showed fat droplets in the cytoplasm of these cells (Fig. 2b). The same result was obtained with alcian blue staining. These cells also showed a week desmin positivity (Fig. 2c). Serial sections showed that the GAG, oil red O and desmin positive cells were identical.

Small amounts of native brown, Prussian blue-negative pigment were present in the cytoplasm of nearly all these cells. Twenty four hours after Carrageenan administration, these GAG-containing cells were filled with granules showing purple metachromasia after staining with toluidine blue. This demon-

strated the uptake of Carrageenan into the cytoplasm (Fig. 3). No such cells were found in the control groups.

The Fe-colloid staining at light microscopy level was compared in sections from testicular hyaluronidase-treated and control samples at pH 2.0. In the control samples, strong blue staining of the cytoplasm indicated the presence of GAG (Fig. 5a), but this was diminished dramatically in cells treated with testicular hyaluronidase (Fig. 5b). This demonstrated the presence of chondroitin sulphate in these cells.

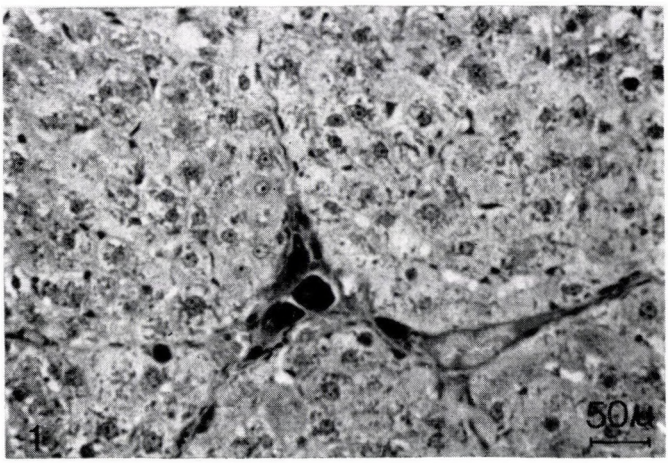

Fig. 1. Enlarged, specially altered fat-storing cells (Ito cells) in the portal area and in the septa (arrows) of cirrhotic rat liver (alcian blue, ×200)

Using the *fluorescent microscope*, the GAG containing cells of the livers of the aminals treated with Vitamin A showed enlargement and a marked light green fluorescence indicating to the uptake of Vitamin A by these cells (Fig. 2d). In the fibrotic or cirrhotic livers of rats not treated with Vitamin A, only the light yellow autofluorescence of lipofuscin was observed.

Table III. shows the quantitative distribution of the GAG-containg cells. The average number in the CCl_4 treated group amounted to $62.51 \pm 17.38/mm^3$ whereas in the CCl_4+phenobarbital treated group the average number was $145.50 \pm 28.80/mm^3$. This difference was significant at the level $p < 0.005$.

No GAG-containg cells were found in the the livers of the controls.

Ultrastructure

The large cells in the portal areas contained phagolysosomes, cholesterin crystals, well developed rough endoplasmic reticulum and Golgi bodies in their cytoplasm (Fig. 4). The most important feature of these cells was the HID

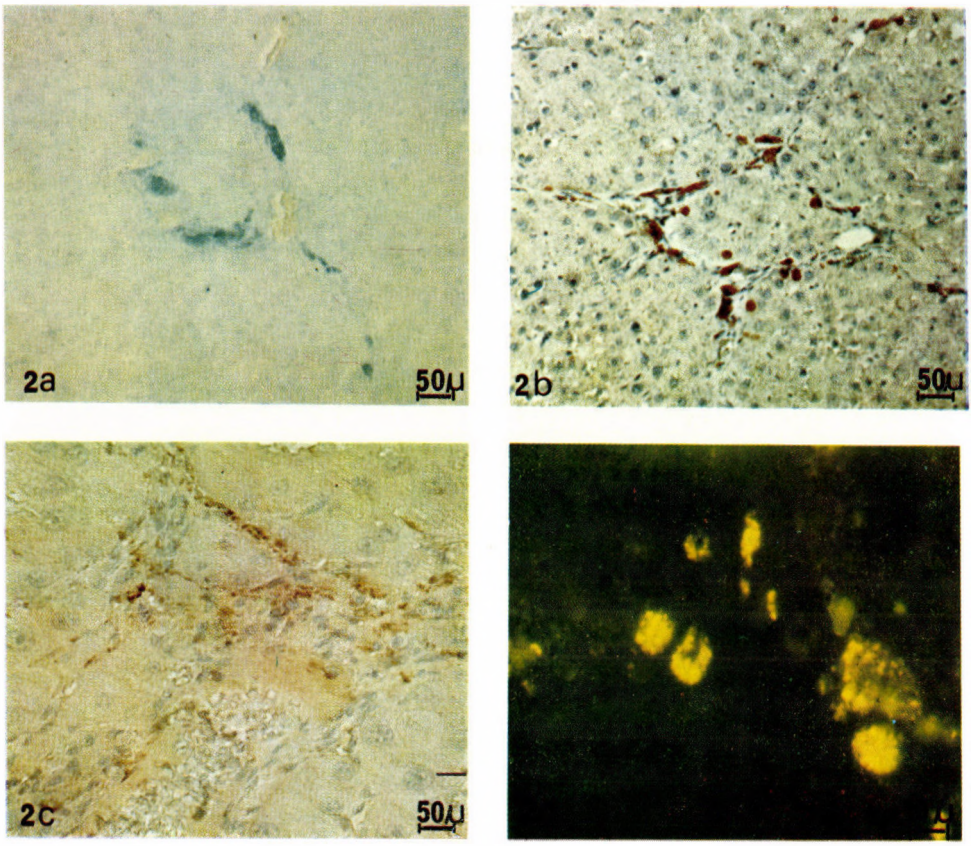

Fig. 2a. Fat-storing cells containing glycosaminoglycans in cirrhotic rat liver (pH 2.0 iron colloid, ×200). *b.* Fat-storing cells containing neutral fat in cirrhotic rat liver (oil red O, ×200). *c.* Fat-storing cells showing desmin positivity in cirrhotic rat liver (anti-desmin immunohistochemical reaction, ×200). *d.* Vitamin A fat-storing cells in cirrhotic rat liver (autofluorescence of frozen section, ×800)

staining of the cytoplasmic granules and weaker diffuse HID-positivity in the cytoplasm, indicating sulphated GAG (Fig. 4, insert).

Other mesenchymal cells

Elongated perisinusoidal cells with desmin positivity (unaltered FSC) were observed around the sinusoids in a density not different from the controls. The Kupffer cells did not show significant qualitative or quantitative alterations in either of the experimental groups. Only a few lymphocytes were seen in the portal regions of the animals treated with CCl_4 or CCl_4+phenobarbital. In livers with fibrosis or cirrhosis, scattered mast cells were demonstrated with Ziehl-Nielsen staining in the periportal regions and along the collagen fibres.

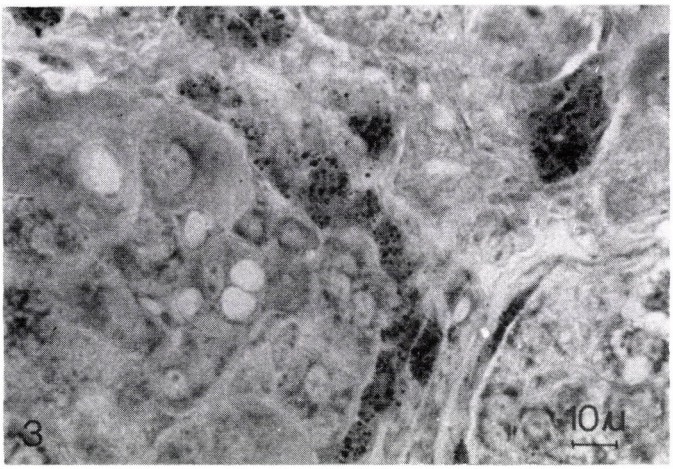

Fig. 3. Demonstration of Carrageenan taken up by portal fat-storing cells. Carrageenan appeared as metachromatic purple material in the cytoplasm of fat-storing cells (tolouidine blue, ×600)

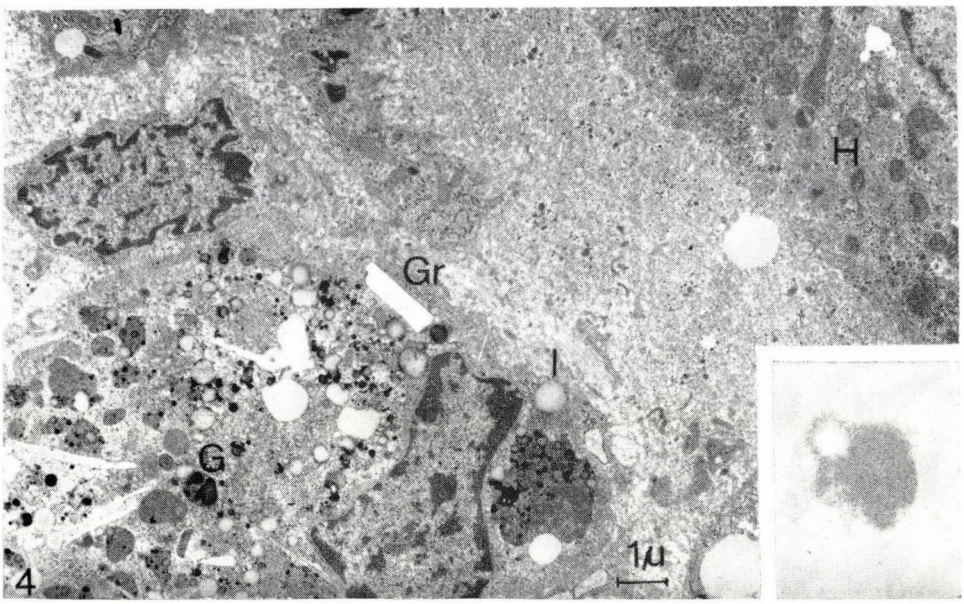

Fig. 4. Portal area in cirrhotic liver at ultrastructural level. Note the presence of a large cell in the extracellular matrix, with abundant cytoplasm containing medium electrondense granules (G), cholesterin crystals (Cr) and some lipid droplets (l). H = hepatocyte, L = lymphocyte. N: 173905, ×7200

Fig. 4. Insert: Detection of sulphated GAG in fat-storing cell with HID stain at ultrastructural level. Note strong positivity in cytoplasmic granules. N: 173518, ×20000

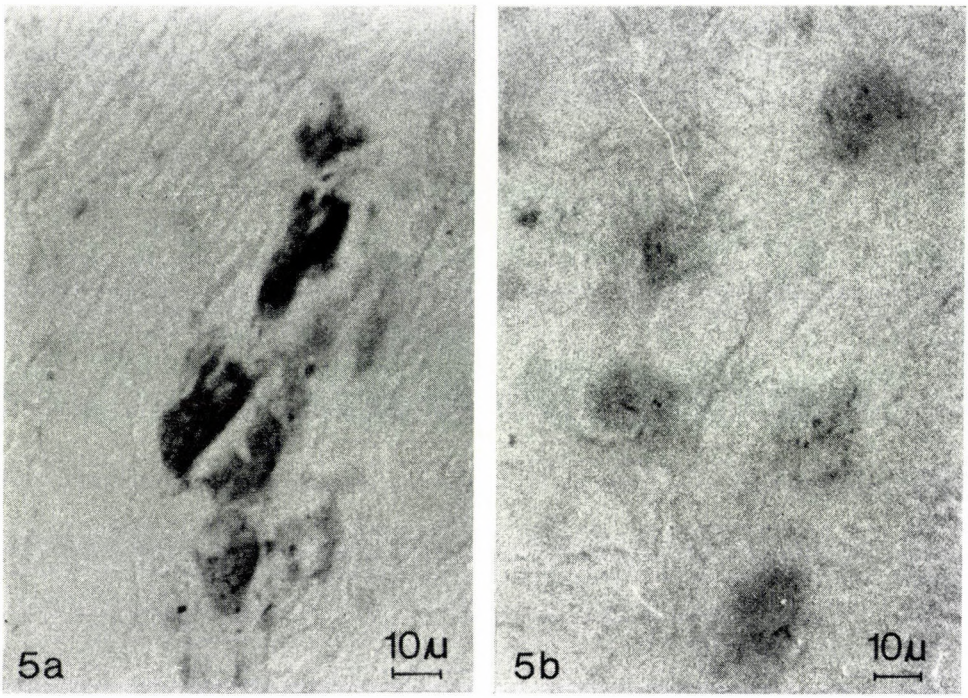

Fig. 5a. Detection of GAG in portal fat-storing cells of cirrhotic rat liver. *b* Detection of GAG in portal fat-storing cells of cirrhotic rat liver after testicular hyaluronidase pre-treatment. Note the dramatically decreased reaction. (Fe-colloid stain at pH = 2. ×800)

Table III

Number of GAG containing fat-storing cells per cubic millimeter in the liver of CCl_4, CCl_4+phenobarbital, oleum helianthi and phenobarbital-treated F-344 male rats

Treatment	Cells/mm³
1. CCl_4	62.51±17.38
2. CCl_4+phenobarbital	145.50±28.80
3. Oleum helianthi	n. d.
4. Phenobarbital	n. d.

Section thicness: 5μ
n. d.: tested but not detected
(significance between group 2. and group 1.: $p < 0.005$)

Discussion

In agreement with the results of McLean [19], we found that treatment with CCl_4+phenobarbital resulted in a more severe fibrotic change in the rat liver than treatment with CCl_4 alone. This allowed us to compare chronic liver

injuries of two degrees of severity. The most interesting result of our present study was that the number of mesenchymal cells containing GAG increased in parallel with the extent of hepatic fibrosis and cirrhosis. These findings were confirmed by our biochemical results, showing the parallel elevation of the concentrations of collagen and GAG in the liver.

The morphological studies, demonstrated that the GAG-containg cells are desmin positive, and take up and store Vitamin A. These observations indicate that they really are modified FSC. These cells also contain a considerable amount of neutral lipid, lipofuscin and PAS-positive material. Due to these the cytoplasm of the modified FSC is more extended than that of normal FSC. Ultrastructurally, the cells appear to be of mesenchymal origin and show some characteristics of macrophages based also on the Carrageenan phagocytosis.

Although the macrophage function of FSC has not been described till now, we may presume, that these mesenchymal cells can acquire phagocytic capacity under the circumstances of chronic liver poisoning with CCl_4.

These characteristics point to the fact that these cells are FSCs which have migrated into the portal areas as well as into the septa which contain the newly formed collagen fibres. These FSCs show significant morphological changes compared to the FSCs in normal liver. The FSCs in damaged liver are enlarged and contain a considerable amount of GAG. Whether the GAG is synthesized or taken up by the FSC is unknown. According to Schafer et al. [27] however, fat-storing cells are able to synthesize GAG *in vitro*, especially chrondroitin sulfate and dermatan sulfate which are the dominant GAG species in cirrhotic liver [21, 32]. The FSC may also synthesize hyaluronic acid *in vitro* [9].

The present study confirms the positive correlation between the amount of collagen and the number of FSC recently described by Matsuzaki et al. [17], Yokoi et al. [39, 40]. Furthermore the study demonstrates that these cells contain large amounts of GAG. It has been shown *in vitro* that FSCs are able to produce both collagen [5] and GAG [27]. We suggest based on the HID positivity in the Golgi zone that they are able to do the same *in vivo*.

We consider the most important result of our study that we were able to localize a cell type in cirrhotic liver which can be responsible for the elevated GAG content. The production of GAG components may facilitate the formation and packaging of connective tissue ground substance. In vivo studies using labeled GAG precursors are in progress to confirm the origin of the intracellular GAG.

REFERENCES

1. Alitalo K, Hovi T, Vaheri A: Fibronectin is produced by human macrophages. J Exp Med 151: 602, 1980
2. Bitter T, Muir HM: A modified uronic acid carbazole reaction. Anal Biochem 4: 330, 1962
3. Burt AD, Robertson JL, Hair J, McSween RNM: Desmin-containing stellate cells in rat liver: distribution in normal animals and response to experimental acute liver injury. J Pathol 150: 29, 1986
4. Burt AD, McSween RNM: Desmin-containg stellate cells in the rat liver: author's reply. J Pathol 154: 288, 1988
5. De Leeuw AM, McCarthy SP, Geerts A, et al: Purified rat liver fat-storing cells in culture divide and contain collagen. Hepatology 4: 392, 1984
6. Diegelmann RF, Cohen JK, Guzelian PS: Rapid degradation of newly synthesized collagen by primary cultures of adult rat hepatocytes. Biochem Biophys Res Commun 97: 819, 1980
7. Foidart JM, Berman JJ, Paglia L, Rennard SL, Abe S, Peratoni A, Martin GR: Synthesis of fibronectin, laminin, and several collagens by a liver-derived epithelial cell line. Lab Invest 42: 525, 1980
8. Gangolli SP, Wright MG, Grasso P: Identification of Carrageenan in mammalian tissues: an analytical histochemical study. Histochem J 5: 37, 1973
9. Gressner AM, Haarmann R: Hyaluronic acid synthesis and secretion by rat liver fat-storing cells (parisinusoidal lipocytes) in culture. Biochem Biophys Res Commun 151: 222, 1988
10. Guzelian PS, Qureshi GD, Diegelmann RF: Collagen synthesis by primary cultures of parenchymal cells from adult rat liver. Collagen Rel Res 1: 83, 1981
11. Guzelian PS, Diegelmann RF: Localization of collagen prolyl-hydroxylase to the hepatocytes. Exp Cell Res 123: 269, 1979
12. Ito T: Structure and function of the fat-storing cell (FSC) in the liver. Acta Anat Nippon 53: 393, 1978
13. Kent G, Gay S, Inou T et al.: Vitamin A-containing lipocytes and formation of type III collagen in liver injury. Proc Natl Acad Sci USA 73: 3719, 1976
14. Langness U, Udenfriend S: Collagen biosynthesis in non-fibroblastic cell lines. Proc Natl Acad Sci USA 71: 50, 1974
15. Leibovich SJ, Ross R: A macrophage-dependent factor stimulates the proliferation of fibroblasts in vitro. Am J Pathol 84: 501, 1976
16. Mak KM, Leo MA, Lieber CS: Alcoholic liver injury in baboons: transformation of lipocytes to transitional cells. Gastroenterology 87: 188, 1984
17. Matsuzaki Y, Kuroda H: Changes of Ito cells (fat-storing cells) by administration of carbon tetrachloride with reference to hepatic fibrosis. Acta Hepatol Jap 26: 1472, 1985
18. McGee JOD, Patrick RS: The role of perisinusoidal cells in hepatic fibrosis. An electron microscopic study of acute carbon tetrachloride liver injury. Lab Invest 26: 429, 1972
19. McLean EK: An improved method for producing cirrhosis of the liver in rats by simultaneous administration of carbon tetrachloride and phenobarbitone. Br J Exp Path 50: 502 1969
20. Murata K, Okudaira M, Akashia K: Mast cells in human liver tissue. Acta Dermatovener (Stockholm) (Suppl) 73: 157, 1973
21. Murata K, Ochiai Y, Akashio K: Polydispersita of acidic glycosaminoglycan components in human liver and the changes at different stages in liver cirrhosis. Gastroenterology 89: 1248, 1985
22. Ninomiya Y, Hata R, Nagal Y :Glycosaminoglycan synthesis by liver parenchymal cell clones in culture and its change with transformation. Biochim Biophys Acta 629: 349, 1980
23. Noesser JE: The determination of hydrocyproline in tissue and protein samples containing small proportions of this amino acid. Arch Biochem Biophys 92: 440, 1961
24. Postlethwaite AE, Keski-Oja J, Balian G, Kang AH: Induction of fibroblast chemotaxis by fibronectin. J Exp Med 153: 494, 1981
25. Rojkind M, Giambrone MA, Bienyica L: Collagen types in normal and cirrhotic liver. Gastroenterology 76: 710, 1979
26. Rojkind M, Ponce-Noyola P: The extracellular matrix of the liver. Collagen Rel Res 2: 151, 1982
27. Schafer S, Zerbe O, Gressner AM: The synthesis of proteoglycans in fat-storing cells of rat liver. Hepatology 7: 680, 1987
28. Seyer JM, Hutcheson ET, Kang AH: Collagen polymorphism in normal and cirrhotic human liver. J Clin Invest 59: 241, 1977

29. Seyer JM: Interestitial collagen polymorphism in rat liver with CCl_4-induced cirrhosis. Biochim Biophys Acta 629: 490, 1980
30. Spicer SS: Diamine methods for differentiating mucosubstances histochemically. J Histochem Cytochem 13: 211, 1965
31. Spicer SS, Hardin JH, Senser ME (1978): Ultrastructural visualisation of sulphated complex carbohydrates in blood and epithelial cells with the high iron diamine procedure. Histochem J 10: 435, 1978
32. Stuhlsatz HW, Vierhaus S, Gressner AM: The distribution pattern and structural differences of the glycosaminoglycans in normal and cirrhotic human liver. In: Popper H, Reutter W, Gudat F (eds), Structural Carbohydrates in the Liver. MPT Press, Ltd. Lancester, England, 1983, 650—651
33. Verhoeven D, Buyssens N: Desmin-containing stellate cells in the rat liver. Letter to the Editor. J Pathol 154: 287, 1988
34. Voss B, Allam S, Reuterberg J, Ullrich K, Gieselmann V, von Figura K: Primary cultures of rat hepatocytes synthesize fibronectin. Biochem Biophys Res Commun 90: 1348, 1979
35. Wahl LM, Olsen CE, Sandberg AC, Mergenhagen SE: Prostaglandin regulation of macrophage collagenase production. Proc Natl Acad Sci USA 74: 4955, 1977
35. Wahl SM, Wahl LM, McCarthy JB: Lymphocyte mediated activation of fibroblast proliferation and collagen production. J Immunol 121: 942, 1978
37. Wahl SM, Wahl LM: Modulation of fibroblast growth and function by monokines and lymphokines. In: Pick E, (ed.:): Lmypholines, 2. Academic Press, New York, 1981, 179—201
38. Wahl SM, Tsukamoto Y, Obrist R, McCarthy JB, Mergenhagen SE: Stimulation of fibroblast activity by soluble mediators. In: Popper H, Gerlach H, Kühn K (eds): Proceedings of Connective Tissue of the Normal and Fibrotic Human Liver. Georg Thieme Verlag, Stuttgart, 1981
39. Yokoi Y, Matsuzaki K, Miyazaki A, et al: Distribution and morphometric determination of fat-storing cell (Ito cell) in hepatic fibrosis. In: Kim A, Knook DL (eds), Cells of the Hepatic Sinusoid. The Kupffer Cell Foundation, The Netherlands, 1986, 267—268,
40. Yokoi Y, Namikisa T, Matsuzaki K, Miyazaki A, Yamaguchi Y: Distribution of Ito cells in experimental hepatic fibrosis. Liver 8: 48, 1988

Acta Morphologica Hungarica, 36 (3—4), pp. 253—254 (1988)

Book reviews

K. BRODMANN: *Vergleichende Lokalisationslehre der Grosshirnrinde in ihren Prinzipien dargestellt auf Grund des Zellenbaues.* Johann Ambrosius Barth, Leipzig, 1909. DM 65,—

This book is a reprint edition of Dr. Korbinian Brodmann's classic book on the comparative cytoarchitectonic of the cerebral cortex, published in 1909. The basic work of Brodmann, the 52 areas of the cerebral cortex he distinguished and designated on the basis of the morphology of the cortex are well known all over the world, and many figures of his cytoarchitectionic atlas can be found in most neuroanatomical or neurophysiological textbooks.

In the preface, Brodmann mentions that the original goal of his research was to perform a topographical analysis of the human cerebral cortex concerning the cell structure. But during his studies he had been faced with the question how the structure of the cortex develops during ontogenesis and what kind of differences might exist in the morphology of the cerebral cortex of the animal kingdom, particularly in mammals. This has extended his studies and resulted in a very complex comparative analysis of the cytoarchitectonics of the cerebral cortex. This book is a very thorough, concise, well-written and illustrated summary of his observations. It is divided in three sections. In the first section principles of comparative cytoarchitectonics are described. The second section deals with the principles of the comparative areas on the surface of the cerebral cortex. The third section represents the synthetic part: it is an attempt to find a morphological, physiological and pathological cortex organology. The book ends with a recent postscript by E. Winkelman and K. Seidel. This provides a brief curriculum vitae of Brodmann and comments on his cytoarchitectonic work. Brodmann did not receive too much recognition for his contribution during his life. As an example, the Medical Faculty of the University in Berlin did not approve his "Habilitationschrift". Everybody interested in neuroscience will find this classic book, which has also a significant historic value, to be interesting to read.

B. HALÁSZ

I. KÖRNYEI (ed.): *Neuropathologia*
Akadémiai Kiadó Budapest, 1987. (417 pages, 345 partly coloured illustrations.) Ft 312. —

The edition of this book is an outstanding achievement of Hungarian medical literature. The brilliant spirit of the Nestor of Hungarian neuropathology, István Környei, is reflected in this issue. The best representatives of neuropathology in Hungary contributed to the book, compiling the experience of several decades. Out of the 27 chapters, 12 are dealing with the problems of general neuropathology, i.e. the basic alterations in the neurocytes, neural fibres and glia cells due to degeneration, inflammation, hypoxia. The special neuropathology is systematically described pointing out the inflammatory and heredodegenerative diseases as well as the tumours of the central and peripheral nervous system. A separate chapter describes the most important muscular diseases. An excellent survey on liquor cytology is also given.

This book can be used as a textbook by pathologists, neuropathologists, and neurologists. The authors give a description of the macroscopic and microscopic alterations in a most didactive style. The methods of electron microscopy and immunohistochemistry as well as neurochemistry are also described when the application of this methods is necessary for the correct diagnosis.

The correlations between neuropathology and other disciplines is clearly expressed in this comprehensive study. The book can be recommended for pathologists, neuropathologists, neurologists and to the best of medical students.

We are looking forward to see the English or German edition of this book.

B. SZENDE

A. KRESS and J. MILLIAN: *The female genital tract of the shrew Crocidura russula.*

Advances in Anatomy, Embryology and Cell Biology Vol. 101, Springer Verlag; Berlin, Heidelberg, New York, London, Paris, Tokyo, 1987. pp. 76 : 31 figs. DM 63,—

The anatomy and histology of the mammalian reproductive system have been studied primarily in humans and in laboratory animals (rat, mouse, hamster). Thus, knowledge on wild animals, and especially on Insectivora, is rather imcomplete. Nowadays, such information is important both in reproductive biology and also in taxonomical studies, when the external morphological features are insufficient for the classification of a given taxon. This book sets out to fill the above-mentioned gap by describing the findings of up-to-date electron microscopic studies, and there is no doubt that this approach is a correct and worthwhile one. The authors have performed systematic electron microscopic examinations of all anatomical areas of the female genital tract of the shrew. A marked difference was revealed in the fine structural organization of the wall of the bursa ovarica as compared to higher mammalian species. A primitive mammalian characteristic was also found; the bursa ovarica completely envelops the ovary. The presence of the complete epoophoron and paraophoron in the genital tract of *Crocidura* species is a conspicuous feature, because this part is usually absent in adult humans. The authors additionally describe the fine structural characteristics of the uterine tuba, the uterus, the cervix and the vagina. The text is illustrated with 31 figures; all the micrographs are of excellent quality. Detailed discussions follow the results, and finally a concluding discussion is also presented. More than 160 references are given. In conclusion, this book is very well written, referenced and illustrated. The work can strongly be recommended to those interested in reproductive biology and taxonomy.

I. BENEDECZKY

MAJOR NEW CHEMICAL AND PATENT MEETING ANNOUNCED FOR 1989

INFONORTICS LTD has announced a major new international conference and exhibition to cover electronic information in chemical, pharmaceutical and patent information. The meeting and exhibition will take place in the Convention Centre, Montreux Switzerland, 26—28 September 1989, and will be arranged in conjuction with London-based IBC Technical Services.

Information can be obtained from Harry Collier (INFONORTICS LTD, 9a High Street, Calne, Wiltshire, SN11 OBS, U.K.) or from Helen Conry (IBC House, Canada Road Byfleet, Surrey KT14 7JL, U.K.).

The Johns Hopkins University School of Medicine offers the 30th ANNUAL POSTGRADUATE INSTITUTE FOR PATHOLOGISTS IN CLINICAL CYTOPATHOLOGY

The Institute begins in February 1989. Application and completed preregistration must be accomplished before 24th of March, 1989. For details, contact: John K. Frost, M. D. The Johns Hopkins Hospital, Baltimore, MD 21205, USA.

The entire course is given in English.

PRINTED IN HUNGARY

Akadémiai Kiadó és Nyomda Vállalat, Budapest

INSTRUCTIONS TO AUTHORS

Form of manuscript

Contributors are requested to supply two complete copies of the manuscript including all tables and illustrations. Manuscripts should be typed double-spaced with margins of at least 4 cm. Pages should be numbered consecutively.

The *headline* should include the title of the paper, authors' names, and name and short postal address of the institute where the work was done.

An *abstract* of not more than 200 words should be supplied typed before the text. It should briefly describe the purpose of the investigations, the methods utilized, the results obtained, and the authors' principal conclusions.

Abbreviations and symbols

Abbreviations should be spelled out when first used in the text or, alternatively, a list of abbreviations might be given. The *International System of Units (SI)* should be used for all measurements. Symbols for physical quantities are to be printed in italics and should, therefore, be underlined in the manuscript. Unusual symbols should be identified on the margin.

References

References should be numbered in alphabetical order, and these numbers only should be inserted in the text (in parentheses). In the reference list each item should include the names and initials of all authors; the title of the article; the title of the journal abbreviates according to the style used in *Index Medicus* (a list of the journals indexed is printed annually in the January issue): the volume number; the first page number; and the year of publication.

Kaplan AP, Kay AB, Austen KF: A pre-albumin activator of prekallikrein. J Exp Med 135:81, 1972

Titles of books should be followed by the publisher: place of publication; and the year.

Oláh I, Röhlich P, Törő I: Ultrastructure of Lymphoid Organs. Akadémiai Kiadó, Budapest 1975

Halász B: The endocrine effects of isolation of the hypothalamus from the rest of the brain. In: Frontiers in Neuroendocrinology. eds Ganong WF, Martini L, Oxford University Press, Oxford 1969, p. 307

Tables and illustrations

Tables should be comprehensible to the reader without reference to the text. The headings should be typed above the table. Tables should be numbered with Roman and illustrations with Arabic numerals.

Figures should be identified by number and authors' name written lightly in pencil on the back. The top should be indicated on the back of prints. The letters a, b etc. should be placed in the lower left-hand corner of prints. Staining techniques and the original magnification of photomicrographs should be stated. Figure captions should be typed on a separate sheet. The approximate place of figures and tables in the text should be indicated in the manuscript on the left-hand margin.

Proofs and reprints

Reprints and proofs will be sent to the first author unless otherwise indicated. A hundred reprints of each paper will be supplied free of charge.

Periodicals of the Hungarian Academy of Sciences are obtainable at the following addresses:

AUSTRALIA
C.B.D. LIBRARY AND SUBSCRIPTION SERVICE
Box 4886, G.P.O., *Sydney N.S.W. 2001*
COSMOS BOOKSHOP, 145 Ackland Street
St. Kilda (Melbourne), Victoria 3182

AUSTRIA
GLOBUS, Höchstädtplatz 3, *1206 Wien XX*

BELGIUM
OFFICE INTERNATIONAL DES PERIODIQUES
Avenue Louise, 485, *1050 Bruxelles*
E. STORY-SCIENTIA P.V.B.A.
P. van Duyseplein 8, *9000 Gent*

BULGARIA
HEMUS, Bulvar Ruszki 6, *Sofia*

CANADA
PANNONIA BOOKS, P.O. Box 1017
Postal Station "B", *Toronto, Ont. M5T 2T8*

CHINA
CNPICOR, Periodical Department, P.O. Box 50
Peking

CZECHOSLOVAKIA
MAD'ARSKA KULTURA, Národni třida 22
115 66 Praha
PNS DOVOZ TISKU, Vinohradská 46, *Praha 2*
PNS DOVOZ TLAČE, *Bratislava 2*

DENMARK
EJNAR MUNKSGAARD, 35, Nørre Segade
1370 Copenhagen K

FEDERAL REPUBLIC OF GERMANY
KUNST UND WISSEN ERICH BIEBER
Postfach 46, *7000 Stuttgart 1*

FINLAND
AKATEEMINEN KIRJAKAUPPA, P.O. Box 128
00101 Helsinki 10

FRANCE
DAWSON-FRANCE S.A., B.P. 40, *91121 Palaiseau*
OFFICE INTERNATIONAL DE DOCUMENTATION ET LIBRAIRIE, 48 rue Gay-Lussac
75240 Paris, Cedex 05

GERMAN DEMOCRATIC REPUBLIC
HAUS DER UNGARISCHEN KULTUR
Karl Liebknecht-Straße 9, *DDR-102 Berlin*

GREAT BRITAIN
BLACKWELL'S PERIODICALS DIVISION
Hythe Bridge Street, *Oxford OX1 2ET*
BUMPUS, HALDANE AND MAXWELL LTD.
Cowper Works, *Olney, Bucks MK46 4BN*
COLLET'S HOLDINGS LTD., Denington Estate,
Wellingborough, Northants NN8 2QT
WM DAWSON AND SONS LTD., Cannon House
Folkstone, Kent CT19 5EE
H. K. LEWIS AND CO., 136 Gower Street
London WC1E 6BS

GREECE
KOSTARAKIS BROTHERS INTERNATIONAL BOOKSELLERS, 2 Hippokratous Street, *Athens-143*

HOLLAND
FAXON EUROPE, P.O. Box 167
1000 AD Amsterdam
MARTINUS NIJHOFF B. V.
Lange Voorhout 9-11, *Den Haag*
SWETS SUBSCRIPTION SERVICE
P.O. Box 830, 2160 Sz Lisse

INDIA
ALLIED PUBLISHING PVT. LTD.
750 Mount Road, *Madras 600002*
CENTRAL NEWS AGENCY PVT. LTD.
Connaught Circus, *New Delhi 110001*
INTERNATIONAL BOOK HOUSE PVT. LTD.
Madame Cama Road, *Bombay 400039*

ITALY
D. E. A., Via Lima 28, *00198 Roma*
INTERSCIENTIA, Via Mazzè 28, *10149 Torino*
LIBRERIA COMMISSIONARIA SANSONI
Via Lamarmora 45, *50121 Firenze*
SANTO VANASIA, Via M. Macchi 58
20124 Milano

JAPAN
KINOKUNIYA COMPANY LTD.
Journal Department, P.O. Box 55
Chitose, *Tokyo 156*
MARUZEN COMPANY LTD., Book Department
P.O. Box 5050 Tokyo International, *Tokyo 100-31*
NAUKA LTD., Import Department
2-30-19 Minami Ikebukuro, Toshima-ku, *Tokyo 171*

KOREA
CHULPANMUL, *Phenjan*

NORWAY
TANUM-TIDSKRIFT-SENTRALEN A.S.
Karl Johansgata 43, *1000 Oslo*

POLAND
WĘGIERSKI INSTYTUT KULTURY
Marszalkowska 80, *00-517 Warszawa*
CKP I W, ul. Towarowa 28, *00-958 Warszawa*

ROUMANIA
D. E. P., *Bucuresti*
ILEXIM, Calea Grivitei 64-66, *Bucuresti*

SOVIET UNION
SOYUZPECHAT — IMPORT, *Moscow*
and the post offices in each town
MEZHDUNARODNAYA KNIGA, *Moscow G-200*

SPAIN
DIAZ DE SANTOS Lagasca 95, *Madrid 6*

SWEDEN
ESSELTE TIDSKRIFTSCENTRALEN
Box 62, *101 20 Stockholm*

SWITZERLAND
KARGER LIBRI AG, Petersgraben 31, *4011 Basel*

USA
EBSCO SUBSCRIPTION SERVICES
P.O. Box 1943, *Birmingham, Alabama 35201*
F. W. FAXON COMPANY, INC.
15 Southwest Park, *Westwood Mass. 02090*
MAJOR SCIENTIFIC SUBSCRIPTIONS
1851 Diplomat, P.O. Box 819074,
Pallas, Tx. 75381-9074
READ-MORE PUBLICATIONS, INC.
140 Cedar Street, *New York, N. Y. 10006*

YUGOSLAVIA
JUGOSLOVENSKA KNJIGA, Terazije 27, *Beograd*
FORUM, Vojvode Mišića 1, *21000 Novi Sad*

Index: 26.017